

**The role of human and *Drosophila* NXF proteins
in nuclear mRNA export**

Dissertation zur Erlangung des
naturwissenschaftlichen Doktorgrades
der Bayerischen Julius-Maximilians-Universität Würzburg

vorgelegt von
Andrea Herold
aus
Würzburg

Würzburg, 2003

Eingereicht am: **18.02.2003**

Mitglieder der Prüfungskommission:

Vorsitzender: Prof. Dr. Rainer Hedrich

1. Gutachter: Prof. Dr. Ulrich Scheer

2. Gutachter: Dr. habil. Matthias Hentze

Tag des Promotionskolloquiums: **28.05.2003**

Doktorurkunde ausgehändigt am:

This thesis describes work carried out in the laboratory of Dr Elisa Izaurralde at the European Molecular Biology Laboratory (EMBL) in Heidelberg under the supervision of Prof. Dr Ulrich Scheer (Department of Cell and Developmental Biology/Zoology I, Bayerische Julius-Maximilians-Universität Würzburg). This work was completed between September 1999 and February 2003 and was supported by an EMBL predoctoral fellowship.

The thesis is organized as a paper dissertation ("kumulative Dissertation").
The following publications are presented in the thesis:

1. Herold, A., Suyama, M., Rodrigues, J. P., Braun, I.C., Kutay, U., Carmo-Fonseca, M., Bork, P., and Izaurralde, E. (2000) TAP (NXF1) belongs to a multigene family of putative RNA export factors with a conserved modular architecture. *Mol Cell Biol* **20**, 8996-9008.
2. Jun, L., Frints, S., Duhamel, H., Herold, A., Abad-Rodrigues, J., Dotti, C., Izaurralde, E., Marynen, P., Froyen, G. (2001) NXF5, a novel member of the nuclear RNA export factor family, is lost in a male patient with a syndromic form of mental retardation. *Curr Biol* **11**, 1381-1391.
3. Herold, A., Klymenko, T., and Izaurralde, E. (2001) NXF1/p15 heterodimers are essential for mRNA nuclear export in *Drosophila*. *RNA* **7**, 1768-1780.
4. Herold, A., Teixeira L., and Izaurralde, E. (2003) Genome-wide analysis of mRNA nuclear export pathways in *Drosophila*. *Submitted*.
5. Braun, I.C., Herold, A., Rode, M., Conti, E., and Izaurralde, E. (2001) Overexpression of TAP/p15 heterodimers bypasses nuclear retention and stimulates nuclear mRNA export. *J Biol Chem* **276**, 20536-20543.
6. Braun, I. C., Herold, A., Rode, M., and Izaurralde, E. (2002) Nuclear export of mRNA by TAP/NXF1 requires two nucleoporin binding sites but not p15. *Mol Cell Biol* **22**, 5405-5418.
7. Lange, B.M.H., Rebollo, E., Herold, A., and Gonzalez, C. (2002) Cdc37 is essential for chromosome segregation and cytokinesis in higher eukaryotes. *EMBO J* **21**, 5364-5374.

Acknowledgements

First of all, I want to thank Dr Elisa Izaurralde for giving me the opportunity to work in her lab. I would like to thank her for excellent scientific guidance and all her enthusiasm and constant support throughout the last years. She was always there to listen to problems, discuss results and cheer me up when things were not working in the way they should.

I am very grateful to Prof. Dr Ulrich Scheer for the supervision of this thesis as a member of the Faculty of Biology of the University of Würzburg. He and Dr Iain Mattaj were members of my thesis advisory committee at EMBL. I would like to thank them for their interest in my work, and for many critical discussions and good suggestions. I would also like to thank Dr Matthias Hentze for readily agreeing to evaluate this thesis.

A special "thank you" goes to all past and present members of the Izaurralde lab. In particular, I would like to thank all the current lab members Daniel Forler, Kerstin Gari, David Gatfield, Andreas Lingel, Michaela Rode, Leonie Unterholzner and Wei Yao for creating such a good working atmosphere with many interesting discussions and great fun. I would also like to acknowledge Isabelle Braun for many fruitful collaborations, and Leonie and Kerstin for comments on this thesis.

Many thanks to the EMBL photolab and the EMBL computer and networking group for the friendly assistance with various layout and software problems.

Mein größter Dank gilt jedoch meiner Familie. Meine Eltern haben mich stets in allem, was ich getan habe, mit allen Kräften unterstützt. Mein Bruder Jens hat mir in wissenschaftlichen und privaten Angelegenheiten mit Rat und Tat zur Seite gestanden. Vielen Dank dafür! Vielen Dank auch an Michael, der mich in den letzten Jahren bei Höhenflügen begleitet und vor Sturzflügen bewahrt hat.

Table of Contents

| | |
|--|-----------|
| Summary | 1 |
| Zusammenfassung | 4 |
| | |
| 1 Introduction | 7 |
| 1.1 Nucleocytoplasmic transport: an overview | 7 |
| 1.1.1 Why is there so much traffic? | 7 |
| 1.1.2 Principles of nucleocytoplasmic transport | 7 |
| 1.1.3 The nuclear pore complex | 8 |
| 1.1.4 The importin β -like family of transport receptors | 9 |
| 1.1.5 The RanGTPase system: how directionality is achieved..... | 9 |
| 1.2 The nuclear export of RNAs | 11 |
| 1.2.1 Nuclear export of tRNAs | 11 |
| 1.2.2 Nuclear export of rRNAs..... | 12 |
| 1.2.3 U snRNA export | 13 |
| 1.2.4 Nuclear export of mRNAs | 14 |
| What is the export signal?..... | 14 |
| The role of hnRNP proteins in mRNA export..... | 16 |
| Identification of an mRNA export receptor | 16 |
| A heterodimeric export receptor for mRNAs in human and yeast: TAP:p15 and Mex67p:Mtr2p..... | 17 |
| The NXF family | 19 |
| Association of the heterodimeric mRNA export receptor with cellular mRNAs: the role of REF proteins and UAP56/Sub2p..... | 21 |
| Nuclear mRNA export is coupled to other processes: efficient recruitment and quality control..... | 23 |
| Other factors implicated in mRNA export | 26 |
| Regulated mRNA export | 28 |
| The role of Crm1 in mRNA export | 30 |
| 1.3 Objectives of this study | 31 |
| 1.3.1 What was known at the beginning of this study? | 31 |
| 1.3.2 Goals and techniques | 32 |
| | |
| 2 Results/Publications | 33 |
| 2.1 The nuclear export factor family: characterization of human NXF proteins | 34 |
| 2.1.1 Paper 1 TAP (NXF1) belongs to a multigene family of putative RNA export factors with a conserved modular architecture..... | 34 |

| | | |
|------------|--|------------|
| 2.1.2 | Paper 2: NXF5, a novel member of the nuclear RNA export factor family, is lost in a male patient with a syndromic form of mental retardation | 49 |
| 2.2 | Role of <i>Drosophila</i> NXFs, p15 and UAP56 in nuclear mRNA export..... | 62 |
| 2.2.1 | Paper 3: NXF1/p15 heterodimers are essential for mRNA nuclear export in <i>Drosophila</i> | 62 |
| 2.2.2 | Paper 4: Genome-wide analysis of mRNA nuclear export pathways in <i>Drosophila</i> | 78 |
| 2.3 | Functional analysis of TAP/NXF1 domains | 117 |
| 2.3.1 | Paper 5: Overexpression of TAP/p15 heterodimers bypasses nuclear retention and stimulates nuclear mRNA export | 117 |
| 2.3.2 | Paper 6: Nuclear export of mRNA by TAP/NXF1 requires two nucleoporin binding sites but not p15..... | 127 |
| 2.4 | Role of Cdc37 in chromosome segregation and cytokinesis | 143 |
| 2.4.1 | Paper 7: Cdc37 is essential for chromosome segregation and cytokinesis in higher eukaryotes | 143 |
| 3 | Discussion and Perspectives | 156 |
| 3.1 | The NXF:p15 heterodimer acts as a functional unit in mRNA export..... | 156 |
| 3.2 | NXF1:p15 and UAP56 define a single mRNA export pathway in <i>Drosophila</i>..... | 159 |
| 3.3 | Cotranscriptional surveillance might account for decreased mRNA levels after export inhibition | 161 |
| 3.4 | A role for Crm1 and NXF proteins in mediating alternative mRNA export pathways? | 163 |
| 3.5 | RNAi and microarrays: novel approaches to study mRNA export <i>in vivo</i> | 169 |
| | References | 171 |
| | Abbreviations..... | 181 |
| | Curriculum vitae..... | 183 |
| | Publications..... | 184 |

Summary

A distinguishing feature of eukaryotic cells is the spatial separation of the site of mRNA synthesis (nucleus) from the site of mRNA function (cytoplasm) by the nuclear envelope. As a consequence, mRNAs need to be actively exported from the nucleus to the cytoplasm. At the time when this study was initiated, both human TAP and yeast Mex67p had been proposed to play a role in this process.

Work presented in this thesis (section 2.1) revealed that TAP and Mex67p belong to an evolutionarily conserved family of proteins which are characterized by a conserved modular domain organization. This family was termed nuclear export factor (NXF) family. While the yeast genome encodes only one NXF protein (Mex67p), the genomes of higher eukaryotes encode several NXF proteins. There are two *nx*f genes in *C. elegans* and *A. gambiae*, four in *D. melanogaster*, and at least four in *H. sapiens* and *M. musculus*. It was unclear whether, apart from TAP and Mex67p, other members of this family would also be involved in mRNA export.

In the first part of this thesis (2.1), several human NXF members were tested for a possible function in nuclear mRNA export. They were analyzed for their interaction with RNA, nucleoporins and other known TAP partners *in vitro*, and tested for their ability to promote nuclear export of a reporter mRNA *in vivo*. Using these assays, human NXF2, NXF3 and NXF5 were all shown to interact with the known NXF partner p15. NXF2 and NXF5 were also found to bind directly to RNA, but only NXF2 was able to bind directly to nucleoporins and to promote the nuclear export of an (untethered) reporter mRNA. Thus NXF2 possesses many and NXF3 and NXF5 possess some of the features required to serve as an export receptor for cellular mRNAs. As NXF2 and NXF3 transcripts were mainly found in testis, and the closest orthologue of NXF5 in mouse has the highest levels of expression in brain, these NXF members could potentially serve as tissue-specific mRNA export receptors.

In the second part of this work (2.2), the role of different *Drosophila* NXF proteins and other export factors in mRNA export was investigated using double-stranded RNA interference (RNAi) in *Drosophila* Schneider cells. Three of the four predicted *Drosophila* NXF members (NXF1-3) were found to be expressed in this cell line and could be targeted by RNAi. Depletion of endogenous NXF1 inhibited growth and resulted in the nuclear accumulation of polyadenylated RNA. Fluorescence *in situ* hybridization revealed that export of both heat shock and non-heat shock mRNAs, including intron-containing and intronless mRNAs, was inhibited. Depleting endogenous NXF2 or NXF3 had no apparent phenotype. These results suggested that NXF1 (but not NXF2-NXF4) mediates the export of bulk mRNA in *Drosophila* cells.

We and others have shown that human NXF proteins function as heterodimers bound to the small protein p15. Accordingly, silencing of *Drosophila p15* resulted in a block of mRNA export which was indistinguishable from the export inhibition seen after targeting NXF1. These observations indicated that neither NXF1 nor p15 can promote export in the absence of the other subunit of the heterodimer.

NXF1:p15 heterodimers are implicated in late steps of mRNA export, i.e. in the translocation of mRNP export cargoes across the nuclear pore complex. The mechanism by which NXF1:p15 dimers are recruited to the mRNA is unclear. A protein that is thought to play a role in this process is the putative RNA helicase UAP56. Similar to NXF1 and p15, UAP56 was shown to be essential for mRNA export in *Drosophila*. UAP56 is recruited cotranscriptionally to nascent transcripts and was suggested to facilitate the interaction of NXF1:p15 with mRNPs.

Even though both NXF1:p15 heterodimers and UAP56 had been implicated in general mRNA export, it was unclear whether there are classes of mRNAs that require NXF1:p15, but not UAP56 or *vice versa*. It was also unclear what fraction of cellular mRNAs is exported by NXF1:p15 dimers and UAP56, and whether mRNAs exist that reach the cytoplasm through alternative routes, i.e. by recruiting other export receptors.

To address these issues we performed a genome-wide analysis of nuclear mRNA export pathways using microarray technology (2.2.2). We analyzed the relative abundance of nearly half of the *Drosophila* transcriptome in the cytoplasm of *Drosophila* Schneider cells depleted of different export factors by RNAi. We showed that the vast majority of transcripts were underrepresented in the cytoplasm of cells depleted of NXF1, p15 or UAP56 as compared to control cells. Only a small number of mRNAs were apparently not affected by the depletions. These observations, together with the wide and similar effects on mRNA levels caused by the depletion of NXF1, p15 or UAP56, indicate that these proteins define the major mRNA export pathway in these cells. We also identified a small subset of mRNAs which appeared to be exported by NXF1:p15 dimers independently of UAP56.

In contrast, no significant changes in mRNA expression profiles were observed in cells depleted of NXF2 or NXF3, suggesting that neither NXF2 nor NXF3 play an essential role in mRNA export in *Drosophila* Schneider cells.

Crm1 is a transport receptor implicated in the export of a variety of non-mRNA and protein cargoes. In addition, human Crm1 has been suggested to be involved in the export of a specific mRNA species, serving as a "specialized" mRNA export receptor. A role of human Crm1 in the export of bulk mRNA is considered unlikely. We analyzed the role of *Drosophila* Crm1 in mRNA export by inhibiting Crm1 with the drug leptomycin B in Schneider cells. Subsequent microarray analysis demonstrated that the inactivation of

Crm1 resulted in decreased cytoplasmic levels of less than 1% of all mRNAs, indicating that Crm1 is indeed not a major mRNA export receptor.

The genome-wide analysis also revealed a feedback loop by which a block to mRNA export triggers the upregulation of genes involved in this process.

This thesis also includes two sections describing projects in which I participated during my Ph.D., but which were not the main focus of this thesis. In section 2.3, the role of the different TAP/NXF1 domains in nuclear mRNA export is discussed. Section 2.4 describes results that were obtained as part of a collaboration using the RNAi technique in Schneider cells to study the function of Cdc37.

Zusammenfassung

Bedingt durch die räumliche Trennung von Transkription und Translation müssen mRNAs in eukaryotischen Zellen aktiv vom Kern in das Cytoplasma transportiert werden. Zu Beginn dieser Arbeit war bekannt, dass das menschliche Protein TAP und Mex67p aus Hefe an diesem Prozess beteiligt sind.

Mit Hilfe von Datenbankrecherchen konnte in dieser Arbeit gezeigt werden (Kapitel 2.1), dass TAP und Mex67p zu einer Proteinfamilie von verwandten Proteinen gehören, deren Mitglieder sich durch eine konservierte, modulartige Domänenstruktur auszeichnen. Dieser bis dahin unbekanntes Familie wurde die Bezeichnung "Nuclear Export Factor (NXF)"-Familie zugewiesen. Während das Hefegenom für nur ein NXF-Protein (Mex67p) kodiert, finden sich in den Genomen höherer Eukaryoten mehrere *nxf*-Gene. So konnten in *C. elegans* und *A. gambiae* zwei *nxf*-Gene und in *D. melanogaster*, *H. sapiens* und *M. musculus* vier *nxf*-Gene identifiziert werden. Es war jedoch unklar, ob diese bis dahin uncharakterisierten NXF-Proteine - ähnlich wie TAP und Mex67p - an mRNA-Exportprozessen beteiligt sind.

Daher wurde im ersten Teil dieser Arbeit (2.1) untersucht, inwieweit verschiedene menschliche NXF-Proteine die typischen Charakteristika von mRNA-Exportrezeptoren aufweisen. Hierzu wurde analysiert, ob die einzelnen humanen NXF-Proteine in der Lage sind, mit RNA, Kernporenproteinen und anderen schon bekannten TAP-Interaktoren *in vitro* zu interagieren. Zudem wurden verschiedene menschliche NXF-Proteine auf ihre Fähigkeit getestet, den Export einer Reporter-mRNA *in vivo* zu stimulieren. Mit Hilfe dieser Experimente konnte nachgewiesen werden, dass NXF2, NXF3 und NXF5 in der Lage sind, mit dem TAP-Interaktor p15 zu interagieren, aber nur NXF2 und NXF5 direkt an RNA binden können. Ausschließlich NXF2 war in der Lage, direkt an Kernporenproteine zu binden und den Export der getesteten Reporter-mRNA zu stimulieren. NXF2 besitzt also die typischen Eigenschaften eines mRNA-Exportrezeptors, während bei NXF3 und NXF5 nur einige dieser Eigenschaften nachgewiesen werden konnten. Da in Säugetieren eine gewebespezifische Expression verschiedener TAP-Homologe nachgewiesen wurde, könnte es sich bei diesen NXF-Mitgliedern um gewebespezifische Exportfaktoren handeln. So wurden z.B. humane NXF2- und NXF3-Transkripte vor allem in Hodengewebe detektiert, während das nächstverwandte Ortholog von menschlichem NXF5 in Maus am stärksten in Hirngewebe exprimiert wird.

Im zweiten Teil dieser Arbeit (2.2) wurde die mögliche Beteiligung von *Drosophila*-NXF-Proteinen an mRNA-Exportprozessen mit Hilfe von RNA-Interferenz (RNAi) in *Drosophila*-Schneiderzellen untersucht. Die Analyse wurde dabei auf nur drei der vier NXF-Proteine (NXF1-3) beschränkt, da das vierte (NXF4) in diesen Zellen nicht exprimiert ist bzw. nicht nachgewiesen werden konnte. Die Depletion von endogenem

NXF1 durch RNAi verursachte einen Wachstumsstopp der Zellen sowie eine Akkumulation von polyadenylierten RNAs im Kern. Mit Hilfe von *in-situ*-Hybridisierung konnte gezeigt werden, dass in Zellen, in denen NXF1 depletiert worden war, der Export von Hitzeschock-mRNAs und Nicht-Hitzeschock-mRNAs blockiert war. Hierbei waren sowohl intronlose, als auch intronhaltige Transkripte betroffen. Die Depletion von endogenem NXF2 oder NXF3 hatte keine offensichtlichen Auswirkungen auf den Phänotyp der Zellen. Diese Ergebnisse deuten darauf hin, dass NXF1 (nicht aber NXF2-NXF4) für den Export des Großteils von mRNAs in *Drosophila*-Schneiderzellen verantwortlich ist.

Es war postuliert worden, dass menschliche NXF-Proteine nur als Heterodimere (komplexiert mit dem Protein p15) aktiv sind. In dieser Arbeit konnte nachgewiesen werden, dass die Depletion von p15 mit Hilfe von RNAi in *Drosophila*-Schneiderzellen - ähnlich wie die Depletion von NXF1 - eine Blockierung des Exports von mRNAs zur Folge hat. Die nahezu identischen Effekte nach der Depletion von NXF1 oder p15 legen den Schluss nahe, dass keines der zwei Proteine ohne das andere mRNAs exportieren kann, die Bildung eines Heterodimers also auch in *Drosophila* essentiell ist.

NXF1:p15-Heterodimere spielen eine Rolle bei späten Vorgängen des Kernexports, da sie die Translokation von mRNPs durch die Kernpore hindurch vermitteln. Unklar ist jedoch, wie NXF1:p15-Dimere an das mRNA-Substrat binden. Es war postuliert worden, dass die RNA-Helikase UAP56 dabei eine Rolle spielt. UAP56 ist ähnlich wie NXF1 und p15 essentiell für den Export von mRNAs in *Drosophila*. Es bindet schon während der Transkription an die RNA und könnte die Interaktion von NXF1:p15 mit dem Transkript erleichtern.

Obgleich NXF1:p15 und UAP56 eindeutig als essentielle Exportfaktoren identifiziert worden waren, war die Frage, inwieweit alle mRNA-Exportvorgänge NXF1, p15 und UAP56 benötigen, noch unbeantwortet. Beispielsweise könnten mRNAs existieren, die NXF1 und p15 benötigen, nicht aber UAP56 (oder umgekehrt). Zudem könnten mRNAs existieren, die ganz ohne die Hilfe von NXF1, p15 und UAP56 exportiert werden können, z.B. indem sie andere Exportfaktoren nutzen.

Um diese Frage zu beantworten, wurde eine auf Microarrays basierende "large scale"-Analyse durchgeführt (2.2.2). Dabei wurden die relativen Häufigkeiten von etwa der Hälfte aller *Drosophila*-Transkripte im Cytoplasma von *Drosophila*-Schneiderzellen bestimmt, in denen verschiedene Exportfaktoren mit Hilfe von RNAi inhibiert worden waren. Mit diesem Ansatz konnte gezeigt werden, dass im Cytoplasma von Zellen, in denen die Expression von NXF1, p15 oder UAP56 durch RNAi inhibiert worden war, der Großteil aller Transkripte im Vergleich zu Kontrollzellen unterrepräsentiert war. Diese Ergebnisse deuten darauf hin, dass sowohl NXF1:p15 also auch UAP56 essentiell für den Export der meisten mRNAs sind. Es konnte aber auch eine geringe Anzahl von Transkripten identifiziert werden, deren Abundanz im Cytoplasma sich durch die

Depletion dieser drei Proteine nicht veränderte. Diese Transkripte könnten u.U. mit Hilfe von alternativen Exportrezeptoren in das Cytoplasma gelangen. Des Weiteren wurde eine kleine Gruppe mRNAs gefunden, die von NXF1:p15-Dimeren ohne die Hilfe von UAP56 exportiert werden.

Im Gegensatz dazu konnten keine signifikanten Änderungen der mRNA Expressionsprofile in Schneiderzellen nachgewiesen werden, in denen NXF2 oder NXF3 mit Hilfe von RNAi depletiert worden waren. Dies legt den Schluss nahe, dass weder NXF2 noch NXF3 eine essentielle Aufgabe beim Export von mRNAs in diesen Zellen haben.

Das Protein Crm1 ist ein Transportrezeptor, der am Export von einer Vielzahl von RNA- und Proteinsubstraten beteiligt ist. Menschliches Crm1 wurde als potentieller mRNA-Exportrezeptor für einzelne mRNAs mit spezifischen Eigenschaften gehandelt. Eine Beteiligung am generellen Export von mRNAs wurde aber als unwahrscheinlich angesehen. In dieser Arbeit wurde eine mögliche Beteiligung von *Drosophila*-Crm1 an mRNA-Exportprozessen untersucht (2.2.2). Durch eine Behandlung mit Leptomycin B wurde Crm1 in *Drosophila*-Zellen inhibiert. Die nachfolgenden Analysen mit Hilfe von Microarrays konnten bestätigen, dass Crm1 auch in *Drosophila* kein genereller mRNA Exportfaktor ist, da weniger als 1% aller Transkripte signifikant niedrigere Level im Cytoplasma aufwiesen. Zudem konnten bisher keine Transkripte identifiziert werden, die eindeutig von Crm1, aber ohne die Beteiligung von NXF1:p15 exportiert werden.

In der auf Microarrays basierenden Analyse konnte außerdem ein "feedback loop" nachgewiesen werden, der im Falle einer Exportinhibierung zu einer Hochregulierung von Genen führt, die eine Rolle bei Kernexportprozessen spielen.

Zudem werden in dieser Arbeit zwei Projekte beschrieben, an denen ich während meiner Doktorarbeit beteiligt war, die aber nicht das Hauptthema meiner Promotion waren. Kapitel 2.3 beschreibt die Analyse der Rolle der verschiedenen TAP/NXF1-Domänen beim mRNA-Kernexport. Kapitel 2.4 enthält Daten, die im Rahmen einer Kooperation erzielt wurden, bei der die Funktion von Cdc37 mit Hilfe von RNAi in *Drosophila*-Schneiderzellen untersucht wurde.

1 Introduction

1.1 *Nucleocytoplasmic transport: an overview*

1.1.1 Why is there so much traffic?

A distinguishing feature of eukaryotic cells is the organization into distinct nuclear and cytoplasmic compartments separated by the nuclear envelope. This double membrane segregates the site of DNA and RNA synthesis (the nucleus) from the cytoplasmic machinery for protein synthesis. While this compartmentalization provides excellent possibilities for the regulation of gene expression, it also necessitates the evolution of efficient mechanisms to transport macromolecules between the nucleus and the cytoplasm. Proteins with a nuclear function, such as transcription factors or histones, have to be imported into the nucleus. Most classes of RNAs have to be transported to the cytoplasm, either because they participate in translation (mRNAs, tRNAs, rRNAs) or because they undergo maturation (U snRNAs) (reviewed by: Cullen, 2000; Gorlich and Kutay, 1999; Ohno *et al.*, 1998). It has been estimated that more than one million macromolecules per minute are actively transported between the nucleus and the cytoplasm of a growing mammalian cell (Ohno *et al.*, 1998).

1.1.2 Principles of nucleocytoplasmic transport

Even though there are many different transport pathways for macromolecules, they are all believed to follow common principles (reviewed by: Gorlich and Kutay, 1999; Mattaj and Englmeier, 1998). First, all macromolecular transport processes occur *via* nuclear pore complexes (NPCs), which penetrate the nuclear envelope. Second, even though a single passage through the NPC does not seem to be energy-dependent, ongoing nucleocytoplasmic transport is an active process requiring energy. Third, the transport is achieved by soluble and saturable transport receptors which - directly or indirectly - recognize the cargo and mediate its translocation through the NPC. Fourth, transport processes are highly selective as usually only substrates which are transport-competent (such as fully processed mRNAs and tRNAs or proteins carrying specific transport signals) are recognized by their transport receptors. Fifth, transport occurs in a directional way, i.e. the substrate is bound by the soluble receptor in one compartment and released in the other compartment. The following sections will discuss some of these characteristics of nucleocytoplasmic transport processes in more detail.

1.1.3 The nuclear pore complex

NPCs are large proteinaceous structures perforating the nuclear envelope (see: Fahrenkrog and Aebi, 2002; Gorlich and Kutay, 1999; Ohno *et al.*, 1998; Rout and Aitchison, 2001; Vasu and Forbes, 2001; for reviews about NPC architecture, structure and function, and references therein). They form aqueous channels through which all nucleocytoplasmic transport processes occur. NPCs are freely permeable to small molecules (such as water and ions) but act as highly selective permeability barriers for larger molecules (> 40 kDa). To overcome this permeability barrier, macromolecules must carry specific signals which enable them to access the active transport machinery of the cell. During active transport (also called facilitated translocation), the aqueous channel of the NPC, which is ~ 9 nm in diameter when at rest, can expand to about 25 nm. There are about 3000-5000 NPCs in a growing mammalian cell, each allowing the translocation of more than 10-20 MDa of material per second (Ribbeck and Gorlich, 2001).

NPCs are eight-fold symmetric assemblies composed of a central core structure with extensions that form the cytoplasmic filaments and the nuclear basket (Figure 1). Vertebrate NPCs have a mass of approximately 125 MDa and are composed of 30-50 different proteins which are often collectively called nucleoporins. Nucleoporins are usually present in 8, 16 or 32 copies per NPC. Many nucleoporins contain characteristic domains featuring multiple repeats of short sequences ending in the amino acids phenylalanine and glycine (FG-repeats). These FG-repeats are thought to mediate interactions with soluble transport receptors. Some specific nucleoporins have been shown to be essential for only specific import or export pathways, suggesting that not all FG-repeats are functionally equivalent.

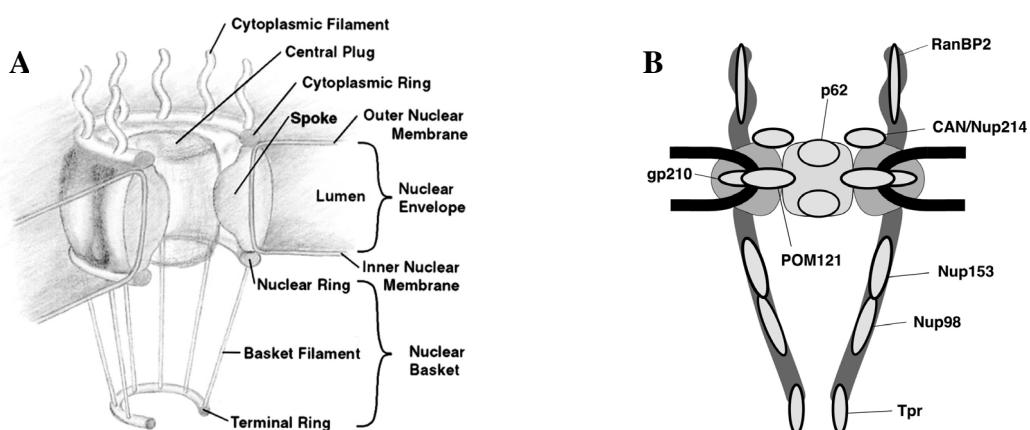


Figure 1: Schematic representation of the NPC

(A) 3D model of the NPC. The central transmembrane core as well as nuclear and cytoplasmic extensions are shown. From Ohno *et al.* (1998). (B) Localization of some vertebrate nucleoporins on the different NPC domains. The nucleoporins tested for NXF binding in paper 1 (CAN, Nup98, p62 and Nup153)(Herold *et al.*, 2000) are also represented (courtesy of Gwenael Rabut, modified from Fahrenkrog and Aebi, 2002).

1.1.4 The importin β -like family of transport receptors

The majority of nucleocytoplasmic transport processes are mediated by proteins belonging to a family of transport receptors with at least 21 members in humans, the prototype of which is importin β [see Gorlich and Kutay (1999) for a review, and references therein]. Members of this family interact with their cargo molecules directly or *via* adapter proteins, and can also bind to nucleoporins. A given transport receptor only recognizes its cargo if it has a specific transport signal, providing selectivity to the transport process. Depending on the direction in which these factors carry their substrate, they are classified as importins (cytoplasm \rightarrow nucleus) or exportins (nucleus \rightarrow cytoplasm). The common feature of these transport factors is their ability to interact with Ran in the GTP-bound state. Ran is a small ras-related GTPase that switches between a GTP- and a GDP-bound form (see below).

Some examples of importin β -like family members and their substrates are:

- **Importin β** : mediates the nuclear import of proteins containing a "classical" nuclear localization signal (NLS). The "classical" NLS is recognized by importin α , which interacts with importin β and serves as an adapter molecule. Importin β can also recognize some cargoes carrying specialized NLSs directly (e.g. HIV-1 Rev and TAT), or use other adapter proteins to import specific substrates, e.g. snurportin when importing U snRNPs;
- **Transportin-1** (also called importin β 2): imports different proteins, e.g. specific hnRNP proteins and ribosomal proteins;
- **Crm1** (also called exportin-1 or Xpo-1): serves as an export receptor for proteins containing leucine-rich (also called Rev-like) export signals. It is also involved in the nuclear export of snurportin, U snRNAs and ribosomal subunits (see 1.2.2 and 1.2.3);
- **CAS**: is a specialized exportin responsible for the export of importin- α ;
- **Exportin-t**: is an export receptor for tRNAs (see 1.2.1).

1.1.5 The RanGTPase system: how directionality is achieved

The directionality of import and export processes mediated by importin β -like receptors depends on the small RanGTPase (reviewed by: Bischoff *et al.*, 2002; Gorlich and Kutay, 1999). As Ran has very low intrinsic rates of nucleotide exchange and hydrolysis, its nucleotide state is mainly determined by guanine nucleotide exchange factors (GEFs) and GTPase activating proteins (GAPs). While the major RanGAP and its cofactors RanBP1 and RanBP2 are cytoplasmic, the major RanGEF, RCC1, is localized to the nucleus. As a consequence of this asymmetric distribution, cytoplasmic Ran is thought to exist predominantly in the GDP-bound form while nuclear Ran is largely bound to GTP.

The resulting RanGTP gradient allows directionality to importin- and exportin-mediated transport with the high nuclear RanGTP concentration serving as a nuclear marker. Importins bind their substrate in the cytoplasm in the absence of RanGTP and release it in the nucleus after binding of RanGTP. After one round of import, the importin-RanGTP complex is recycled back to the cytoplasm. Conversely, exportin-cargo complexes form only upon RanGTP binding and dissociate in the cytoplasm at low RanGTP concentrations. The empty export receptor is then recycled back to the nucleus (Figure 2).

Even though the translocation process *per se* is not directly coupled to nucleotide hydrolysis, ongoing transport is an energy-consuming task. This energy-dependence has been proposed to originate at least in part from the RanGTP gradient which requires the hydrolysis of GTP by Ran in the cytoplasm.

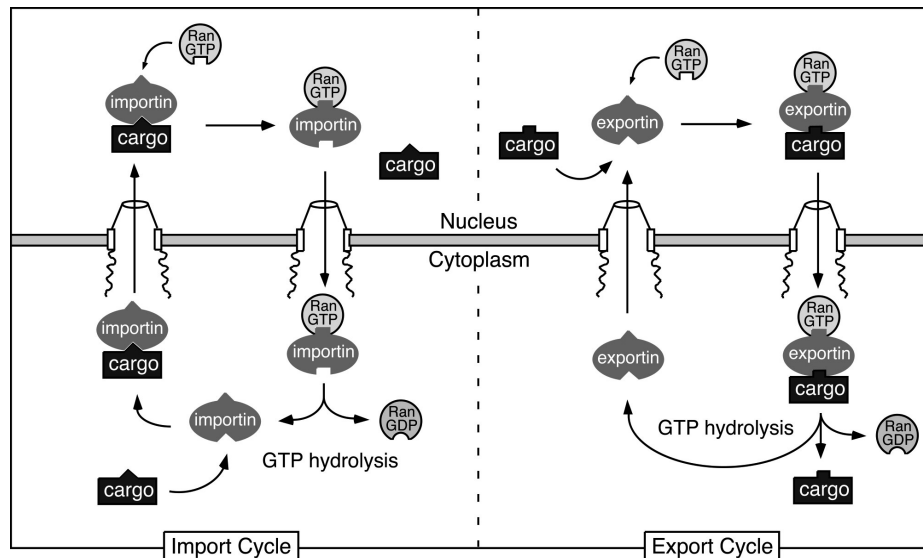


Figure 2: Nuclear import and export mediated by importin β -like transport receptors

Importins bind to cargo molecules in the cytoplasm and mediate interactions with the NPC to translocate the import complex into the nucleus. RanGTP in the nucleus binds to the importin and induces cargo release from the complex. The importin-RanGTP complex is recycled to the cytoplasm where RanGTP is displaced from the importin by RanBP1 or RanBP2, followed by RanGAP-induced GTP hydrolysis. An export cycle is similar, the crucial difference being that RanGTP induces cargo binding in the nucleus. Upon removal of RanGTP from the complex and GTP hydrolysis in the cytoplasm, the exportin dissociates from the cargo and the empty receptor recycles back to the nucleus (modified from Kuersten *et al.*, 2001).

1.2 The nuclear export of RNAs

Most classes of RNAs have to be exported to the cytoplasm after their synthesis in the nucleus. These include transcripts synthesized by RNA polymerase I (large rRNAs), RNA polymerase II (mRNAs and most U snRNAs) and RNA polymerase III (e.g. tRNAs, 5S rRNA and U6 snRNA). Microinjection experiments in *Xenopus* oocytes have shown that different classes of RNA use distinct pathways to exit the nucleus as they competitively inhibit their own export at concentrations at which they have no effect on the export of other classes of RNA (Jarmolowski *et al.*, 1994; Pokrywka and Goldfarb, 1995). This observation is based on the fact that the different classes of RNAs use different soluble transport receptors as described in the following paragraphs. While tRNAs, U snRNAs and rRNAs are exported by members of the importin β -like family, the nuclear export of mRNAs is largely independent of importin β -like family members (Figure 3). A common feature of all RNA export processes is that RNAs are generally transported as ribonucleoprotein complexes (RNPs).

1.2.1 Nuclear export of tRNAs

Two different importin β -like family members have been shown to be involved in tRNA export: exportin-t and exportin5 (Arts *et al.*, 1998a; Bohnsack *et al.*, 2002; Kutay *et al.*, 1998; reviewed by: Cullen, 2000; Gorlich and Kutay, 1999; Simos *et al.*, 2002). They are the only known members of the importin β -like family which interact directly with their RNA substrate (i.e. without the help of adapter proteins).

Exportin-t binds directly and specifically to tRNAs. This interaction is highly favored by the presence of RanGTP and therefore occurs preferentially in the nucleus (Arts *et al.*, 1998a; Kutay *et al.*, 1998). Exportin-t is believed to interact with nucleoporins allowing the translocation through the nuclear pore. The trimeric exportin-t:tRNA:RanGTP complex dissociates in the cytoplasm upon Ran removal (releasing the tRNA), and exportin-t is recycled back to the nucleus (Kutay *et al.*, 1998).

As for all other classes of RNAs, only fully processed ("mature") tRNA molecules reach the cytoplasm. The maturation of eukaryotic tRNAs includes trimming of the 3' and 5' ends of the precursors, modification of nucleosides, addition of the 3' CCA end and, in some cases, the removal of an intron (reviewed in Wolin and Matera, 1999). The maturation is generally believed to be nuclear and has been shown to be a prerequisite for export (De Robertis *et al.*, 1981; Melton *et al.*, 1980). This is in agreement with the fact that exportin-t interacts only very poorly with tRNAs lacking the mature 5' or 3' end or appropriate modifications (Arts *et al.*, 1998b; Kutay *et al.*, 1998; Lipowsky *et al.*, 1999). However, exportin-t can bind and export tRNAs containing an intron when both exportin-t and the intron-containing tRNA are injected into *Xenopus* oocytes (Arts *et al.*, 1998b;

Lipowsky *et al.*, 1999). As intron removal has been suggested to occur normally before 5' end processing, this inability to discriminate between intron-containing and intron-free tRNAs should not result in export of immature molecules under natural conditions (Lund and Dahlberg, 1998). It has also been proposed that aminoacylation facilitates nuclear export or is even a prerequisite for it (Grosshans *et al.*, 2000; Lund and Dahlberg, 1998; Sarkar *et al.*, 1999), although exportin-t can also bind to deacylated tRNAs (Arts *et al.*, 1998b; Lipowsky *et al.*, 1999). This controversy can be explained by the existence of an alternative tRNA export pathway which is aminoacylation-dependent (see below).

The functional homologue of exportin-t in *S. cerevisiae* is Los1p, which is also implicated in tRNA export. However, Los1p is not essential for viability (Hurt *et al.*, 1987), and certain tRNA species are not affected when the *LOS1* gene is disrupted (Grosshans *et al.*, 2000). This suggests that at least some tRNAs can reach the cytoplasm independently of Los1p, either by passive diffusion (as suggested by Gorlich and Kutay, 1999) or by an alternative active export pathway (as suggested by Grosshans *et al.*, 2000; Bohnsack *et al.*, 2002).

Recently, exportin5, which can form complexes with aminoacylated tRNAs in the presence of RanGTP, has been proposed to mediate tRNA export in parallel with exportin-t (Bohnsack *et al.*, 2002). Exportin5 has also been shown to mediate nuclear export of the translation elongation factor eEF1A, which binds exportin5 *via* aminoacylated tRNAs. As exportin-t and exportin5 seem to recognize different sets of tRNAs, they may fulfill complementary functions.

1.2.2 Nuclear export of rRNAs

Three of the four ribosomal RNAs (rRNAs) are produced as a single RNA polymerase I transcript which is later extensively processed and modified to yield the 18S, 5.8S and 28S rRNAs. The 5S rRNA is transcribed by RNA polymerase III and recruited separately to the assembling ribosome. About 80 ribosomal proteins associate with the primary RNA polymerase I transcript in the nucleolus to generate a pre-ribosomal particle which undergoes a series of maturation steps including the splitting into a large and a small subunit. The particles are then exported to the cytoplasm, most likely as separate precursors of the small (40S, containing the 18S rRNA) and large (60S, containing 28S, 5.8S and 5S rRNA) subunits (reviewed by: Aitchison and Rout, 2000; Lei and Silver, 2002b). The nuclear export signals are generally believed to be provided by the proteins in the ribosomal particles rather than by the RNAs themselves.

In *S. cerevisiae*, both the export of the large and the small subunit have been shown to be dependent on the RanGTPase system, suggesting that members of the importin β -like family are involved (Hurt *et al.*, 1999; Moy and Silver, 1999, 2002). Particularly, Crm1p seems to play a key role, as the drug leptomycin B (LMB) which inhibits Crm1p interferes

with the export of the large ribosomal subunit, and mutations in the *CRM1* gene interfere with the export of the small ribosomal subunit (Ho *et al.*, 2000; Moy and Silver, 1999, 2002; Stage-Zimmermann *et al.*, 2000). The non-ribosomal protein Nmd3p has been shown to act as an adapter between the 60S subunit and Crm1p (Gadal *et al.*, 2001b; Ho *et al.*, 2000). Nmd3p interacts directly with the large subunit protein Rpl10p and contains a leucine-rich nuclear export signal (NES) which allows the formation of Nmd3p:Crm1p:RanGTP complexes. Nmd3p has also been shown to shuttle between the nucleus and the cytoplasm (Gadal *et al.*, 2001b; Ho *et al.*, 2000).

Other proteins which have been implicated in the export of pre-60S and pre-40S ribosomal particles in yeast include Noc1-4p, Rix7p, Ecm1p, Nug1p and Rix1p (Bassler *et al.*, 2001; Gadal *et al.*, 2001a; Milkereit *et al.*, 2001; Milkereit *et al.*, 2002). The mechanism by which they influence nuclear export is not yet clear, and it should be noted that some of these factors also affect ribosome maturation.

1.2.3 U snRNA export

The U snRNAs U1, U2, U4 and U5 are transcribed by RNA polymerase II and acquire a monomethylated m⁷G cap structure in the nucleus. In metazoa, they are subsequently exported to the cytoplasm where they associate with Sm proteins. The cap is hypermethylated and the RNP complex is imported back into the nucleus to participate in pre-mRNA splicing.

It has been demonstrated that the m⁷G cap structure is the essential signal for U snRNA nuclear export (Hamm and Mattaj, 1990; Jarmolowski *et al.*, 1994). It is recognized by the nuclear cap-binding complex (CBC), which is composed of the two subunits CBP20 and CBP80 (Izaurralde *et al.*, 1995; Izaurralde *et al.*, 1994). Moreover, nuclear RanGTP and the export receptor Crm1 were shown to be essential for U snRNA export (Fischer *et al.*, 1995; Fornerod *et al.*, 1997; Izaurralde *et al.*, 1997b). The interaction of CBC with Crm1 is indirect and requires an adapter protein called PHAX (phosphorylated adapter for RNA export) (Ohno *et al.*, 2000). PHAX is phosphorylated in the nucleus, but dephosphorylated in the cytoplasm. As only phosphorylated PHAX can interact with Crm1, the complex of capped U snRNA:CBC:PHAX:Crm1:RanGTP can form only in the nucleus. Crm1 mediates the export of the whole complex and after reaching the cytoplasm, RanGTP hydrolysis and dephosphorylation of PHAX result in disassembly of the complex and release of the U snRNA (see Fornerod and Ohno, 2002 for a review).

In agreement with the observation that some essential components of the nucleocytoplasmic transport machinery for U snRNAs/U snRNPs cannot be found in yeast (e.g. PHAX or snurportin), it has been suggested that U snRNP assembly is nuclear in lower eukaryotes, avoiding the need for U snRNA export (Fornerod and Ohno, 2002).

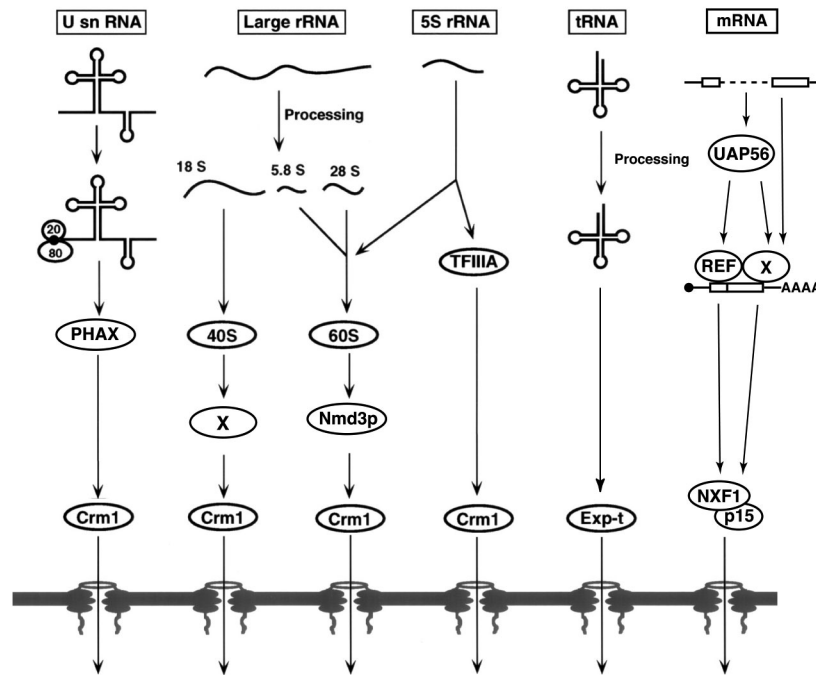


Figure 3: Schematic representation of different RNA nuclear export pathways in higher eukaryotes

Only the major pathways are shown. For example, the existence of an alternative pathway for the export of tRNAs has been reported: it is aminoacylation-dependent and does not require exportin-t, but exportin5. Similarly, alternative mRNA export pathways might exist (see text for details). The importin β -like transport factors Crm1 and exportin-t export their cargo complexed with RanGTP. It is not completely clear at which step the different adapter proteins (REF, UAP56) are recruited to the transcript in the mRNA export pathway (see 1.2.4) (modified from Cullen, 2000).

1.2.4 Nuclear export of mRNAs

What is the export signal?

Eukaryotic pre-mRNAs are also synthesized by RNA polymerase II and undergo several largely cotranscriptional processing events including the addition of an m⁷G cap at the 5' end, the removal of introns by splicing, and cleavage and polyadenylation at the 3' end. As the nuclear export of incompletely spliced mRNAs would most likely result in the synthesis of non-functional or even deleterious proteins, only fully spliced transcripts are exported to the cytoplasm and incompletely spliced precursors are actively retained in the nucleus (Chang and Sharp, 1989; Legrain and Rosbash, 1989). Although it is likely that some mRNA species are exported through alternative pathways, most mRNAs are believed to be recognized by a common set of export factors, which are largely distinct from the factors mediating tRNA, rRNA or U snRNA export.

What are the critical features committing an RNA to this mRNA export pathway? In contrast to other RNA classes whose members often have similar structural features (tRNAs) or lengths (tRNAs, U snRNAs), mRNAs are extremely heterogeneous in their appearance: different mRNAs can vary in their length from a few hundred nucleotides to up to 100,000 nucleotides (e.g. *titin* mRNA) (Labeit *et al.*, 1997). In higher eukaryotes, most pre-mRNAs undergo splicing as part of their processing, but some naturally intronless transcripts do not. As there are no common structural elements known to be present in all mRNAs apart from the 5' cap and the poly(A) tail, these two elements were good candidates to serve as the signals recognized by the mRNA export machinery. When mRNAs generated by *in vitro* transcription are injected into *Xenopus* oocytes, both the presence of a cap structure and a poly(A) tail can enhance the export, but neither is necessary or sufficient (Jarmolowski *et al.*, 1994). Nevertheless, correct 3' end formation including polyadenylation is a prerequisite for the export of cellular mRNAs (Brodsky and Silver, 2000; Custodio *et al.*, 1999; Dower and Rosbash, 2002; Eckner *et al.*, 1991; Hilleren *et al.*, 2001; Hilleren and Parker, 2001; Huang and Carmichael, 1996; Long *et al.*, 1995). However, the poly(A) tail does not provide the export signal itself, but the process of 3' end formation is required to release the RNA from the site of transcription (see also Discussion). As transcripts lacking a cap are efficiently transported in yeast (Dower and Rosbash, 2002), the presence of cap structure does not seem to be a prerequisite for mRNA export *in vivo* (Dower and Rosbash, 2002).

As splicing has been reported to enhance mRNA export in some cases (Luo and Reed, 1999), the process of undergoing pre-mRNA splicing was suggested to be used to recruit the mRNA export machinery to an RNA. However, intronless mRNAs (endogenous or artificially produced) are exported in all systems studied so far, making the process of splicing unlikely to be the only determinant for mRNA export (see also below). Furthermore, a recent study systematically investigating the identity elements discriminating an mRNA from other RNA classes demonstrated that intron-containing RNAs associate with the mRNA export machinery even when splicing is inhibited (Ohno *et al.*, 2002). Surprisingly, the insertion of (unstructured) intronic or different exonic sequences of sufficient length (~ 300 nucleotides) in a U snRNA is sufficient to recruit the mRNA export machinery to this transcript and to prevent the binding of the U snRNA export factor PHAX. Thus it seems that signals defining an mRNA are rather loosely defined. These results also suggest that the mRNA export machinery represents the default nuclear export pathway followed by unstructured RNA molecules that are either not recognized by other export factors and/or not actively retained within the nucleus because they are not yet fully processed.

Recently, it has been proposed that the mechanism by which the export machinery is recruited to a transcript depends on the nature of the transcript (Lei and Silver, 2002a).

Moreover, the process of mRNA export has also been linked to many other steps in gene expression, such as transcription and 3' end formation, reflecting that the recognition of an RNA by the mRNA export machinery might be complex and occur through diverse mechanisms (see below).

The role of hnRNP proteins in mRNA export

In higher eukaryotes, about 20 distinct, highly abundant hnRNP proteins associate with nascent pre-mRNA as it is transcribed (reviewed in Dreyfuss *et al.*, 1993). These proteins are believed to influence the fate of RNA molecules in many ways, such as appropriate folding, processing and export. It has been shown that the pattern of hnRNP proteins changes as a given RNA molecule undergoes processing and export (Daneholt, 1997; Mili *et al.*, 2001; Sun *et al.*, 1998; Visa *et al.*, 1996). Some hnRNP proteins contain nuclear retention signals and have to be removed before export (e.g. hnRNP C) (Nakielny and Dreyfuss, 1996), while others have been shown to shuttle and to accompany the mRNA to the cytoplasm (e.g. hnRNP A1 and K) (Michael *et al.*, 1997; Pinol-Roma and Dreyfuss, 1992; Visa *et al.*, 1996). These shuttling hnRNPs were suggested to bear export signals mediating the contact between the RNA and the export machinery. Specifically, hnRNP A1 has been proposed to play a role in the export of DHFR mRNA (Gallouzi and Steitz, 2001; Izaurralde *et al.*, 1997a), but a direct connection to the export machinery has not been demonstrated. Similarly, the RNA-binding protein Npl3p has been shown to be essential for general mRNA export in *S. cerevisiae*, but it is unclear whether this involvement is active and direct (Lee *et al.*, 1996). At this stage, it seems more likely that the shuttling hnRNP proteins contribute to mRNA export rather indirectly, e.g. by maintaining the structural integrity of the transcript and/or providing binding sites for the export machinery.

Identification of an mRNA export receptor

Some years ago, several studies proposed a role for the RanGTPase in the nuclear export of mRNAs, suggesting that an importin β -like protein could be involved in this process (Amberg *et al.*, 1993; Amberg *et al.*, 1992; Cheng *et al.*, 1995; Forrester *et al.*, 1992; Izaurralde *et al.*, 1997b; Kadowaki *et al.*, 1993; Kadowaki *et al.*, 1992; Petersen and Nierlich, 1978; Schlenstedt *et al.*, 1995a; Schlenstedt *et al.*, 1995b). Indeed, several members of this family were shown to be essential for bulk mRNA export, including the yeast proteins Mtr10p, Crm1p, Pse1p, Kap123p and Sxm1p (Kadowaki *et al.*, 1994; Sedorf and Silver, 1997; Stade *et al.*, 1997) and mammalian karyopherin β 2B (also called transportin-2) (Shamsher *et al.*, 2002). However, since most of these proteins are also directly involved in protein import and export, it is possible that the observed effects on

mRNA export are indirect and a consequence of impaired transport/recycling of factors required for mRNA export. Consistently, recent data obtained by microinjection experiments in *Xenopus* oocytes rather suggest that mRNA export itself does not require nuclear RanGTP (Clouse *et al.*, 2001; Ohno *et al.*, 2002). This implies that the mRNA export receptor must be different from the importin β -like family of export factors. Recently, this mRNA export receptor was identified as TAP/NXF1/Mex67p by convergence of data obtained in yeast and from studies of the simple retrovirus simian retrovirus-1 (SRV-1).

During infection, retroviruses export both fully spliced and incompletely spliced forms of the same viral RNA to the cytoplasm of the host cell. As unspliced transcripts are normally retained efficiently within the nucleus, retroviruses developed mechanisms to overcome this retention (reviewed by Cullen, 1998). In the case of SRV-1, this is achieved through the interaction of a cis-acting element on the viral RNA, referred to as constitutive transport element (CTE), with a cellular host protein. Microinjection of excess CTE RNA into *Xenopus* oocyte nuclei inhibits the export of cellular mRNAs, but does not interfere with other export pathways (Pasquinelli *et al.*, 1997; Saavedra *et al.*, 1997a). This was the first indication that the cellular cofactor for CTE function is also involved in the export of cellular mRNAs.

The cellular cofactor for the CTE was subsequently identified as the human TAP protein (also called HsNXF1). It binds the viral RNA directly through the CTE and promotes its export (Gruter *et al.*, 1998). More importantly, injection of recombinant TAP protein overcomes the mRNA export block caused by saturating amounts of CTE RNA, indicating that TAP is the limiting export factor for mRNAs under these conditions.

A role of the human TAP protein as a *bona fide* mRNA export factor was supported by studies in yeast which demonstrated that the yeast orthologue of TAP, Mex67p, is essential for poly(A)⁺ RNA export (Segref *et al.*, 1997).

By now, there is compelling evidence that TAP and its orthologues in other eukaryotic species are the key mediators of bulk mRNA export. The next section will summarize important features of this RNA export receptor.

A heterodimeric export receptor for mRNAs in human and yeast:

TAP:p15 and Mex67p:Mtr2p

Consistent with the fact that mRNA export does not depend directly on the RanGTP gradient, TAP (and presumably also Mex67p) does not interact with Ran (Fribourg *et al.*, 2001). Apart from this, TAP and Mex67p have the main features that also characterize nuclear transport receptors belonging to the importin β -like family: TAP (and presumably also Mex67p) shuttles between the cytoplasmic and nuclear compartments, both associate with their cargo (poly(A)⁺ RNA), and interact directly with FG-containing

nucleoporins mediating the export-relevant interactions between the mRNA and the NPC (Bachi *et al.*, 2000; Bear *et al.*, 1999; Katahira *et al.*, 1999; Santos-Rosa *et al.*, 1998; Segref *et al.*, 1997; Strasser *et al.*, 2000; Strawn *et al.*, 2001).

The functional and structural domain organization of TAP has been analyzed in detail. TAP can be divided in two main functional parts: an N-terminal cargo-binding domain (amino acids 1-372) and a C-terminal NPC-binding domain (amino acids 371-619; Figure 4) (reviewed by Izaurralde, 2002).

The cargo-binding domain is composed of an N-terminal fragment which contains a transportin-1-dependent NLS, an RNP-type RNA-binding domain (RBD, amino acids 119-198) and a leucine-rich repeat (LRR) domain (amino acids 203-362) (Bachi *et al.*, 2000; Liker *et al.*, 2000; Truant *et al.*, 1999). The crystal structure of a TAP fragment comprising the RBD and the LRR domain has been solved recently (Ho *et al.*, 2002; Liker *et al.*, 2000). The RBD and the LRR domain are both necessary and sufficient to mediate the interaction with CTE-containing RNAs (amino acids 102-372). In contrast to this direct binding, the specific recognition and stable association of TAP with cellular mRNAs is most likely mediated by RNA-binding proteins. Factors suggested to serve as "adapters" between TAP and the mRNAs include E1B-AP5, hGle2, members of the REF family and other proteins present in the exon-exon junction complex (EJC) (Bachi *et al.*, 2000; Kataoka *et al.*, 2001; Kataoka *et al.*, 2000; Stutz *et al.*, 2000; see also below). The interactions with these adapters have been proposed to be mediated also by the cargo-binding domain of TAP. The deletion of individual domains in the N-terminal half of TAP reduces the export activity of TAP. The removal of these domains has much weaker negative effects when TAP is directly tethered to its RNA export substrates, demonstrating the importance of these N-terminal domains for the efficient association with mRNAs (Braun *et al.*, 2001).

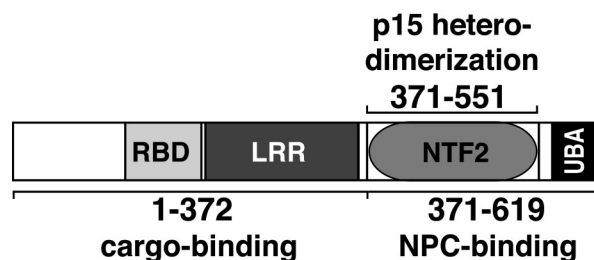


Figure 4: Structural and functional domains of human TAP

RBD: RNP-type RNA-binding domain (amino acids 119-198). LRR: leucine-rich repeat domain (amino acids 203-362). NTF2: NTF2-like domain (amino acids 371-551). UBA: UBA-like domain (amino acids 563-619). The NTF2-like scaffold formed by the TAP:p15 interaction surface harbors one nucleoporin-binding site, the UBA-like domain a second nucleoporin-binding site (modified from Herold *et al.*, 2001).

The NPC-binding domain of TAP consists of two structural domains, an NTF2-like domain related to nuclear transport factor 2 (NTF2), and a ubiquitin-associated (UBA)-like domain. Recently, the structure of both domains was solved, providing insight into the interaction of TAP with FG-repeat containing nucleoporins. Each of the two domains was shown to provide one nucleoporin-binding site on TAP (Bachi *et al.*, 2000; Fribourg *et al.*, 2001; Grant *et al.*, 2002) acting synergistically to promote translocation across the NPC (Braun *et al.*, 2002; Fribourg *et al.*, 2001; Wiegand *et al.*, 2002). As the NTF2-like domain in TAP is only functional when bound to the small protein p15 (also called Nxt1) which is also related to NTF2, the two interacting proteins are often referred to as a heterodimeric export receptor (see also Discussion).

The yeast counterpart of the TAP protein, Mex67p, has a similar domain organization overall, including an LRR, an NTF2-like and a UBA-like domain (Segref *et al.*, 1997; Izaurralde, 2002). Similar to TAP, Mex67p acts as a heterodimer. Its partner, Mtr2p is not related to human p15, but seems to be functionally analogous. This was demonstrated in complementation experiments, in which coexpression of human TAP and p15 partially rescues growth of the otherwise lethal *mex67/mtr2* double mutant, demonstrating the high degree of evolutionary conservation of the mRNA export pathway (Katahira *et al.*, 1999). The interaction with Mtr2p is also mediated by the central domain in Mex67p containing the NTF2-like domain (Strasser *et al.*, 2000). Complex formation of Mex67p and Mtr2p is required for the association of the heterodimer with the NPC and for mRNA export (Santos-Rosa *et al.*, 1998; Strasser *et al.*, 2000). Even though Mex67p has been shown to interact with nucleoporins *in vitro* in the absence of Mtr2p (Strawn *et al.*, 2001), *in vivo* studies showed that Mtr2p can associate with NPCs independently of Mex67p, whereas Mex67p requires Mtr2p for its NPC localization (Santos-Rosa *et al.*, 1998). These results suggest that, in yeast, Mtr2p might be directly involved in NPC binding. In contrast, in the human TAP:p15 heterodimer only TAP mediates interactions with nucleoporins (Fribourg *et al.*, 2001).

The NXF family

As shown in this study (Herold *et al.*, 2000), human TAP and yeast Mex67p belong to a family of proteins with a conserved modular architecture, called the nuclear export factor (NXF; sometimes also: nuclear RNA export factor) family. As the different human and *Drosophila* NXFs play a central role in this thesis, I will introduce them in the context of the whole NXF family already at this point, even though the identification of the NXF family is also part of the Results section of this thesis (2.1.1).

While the yeast genome encodes only one NXF protein (Mex67p), the genomes of higher eukaryotes encode several NXF proteins. There are two NXF family members in *C. elegans* (NXF1, NXF2) and four in *D. melanogaster* (NXF1-4) and in *H. sapiens*

(NXF1=TAP; NXF2, NXF3, NXF5) (Figure 5; [Herold *et al.*, 2001](#); [Herold *et al.*, 2000](#); [Tan *et al.*, 2000](#)). In addition, the human genome also encodes two NXF-related sequences, which are likely to represent pseudogenes (NXF4, NXF6). Phylogenetic analysis indicates that the gene duplication events leading to multiple *nxf* genes have occurred independently in several eukaryotic lineages, so that there is no clear one-to-one relationship of any isoform (Figure 5; [Herold *et al.*, 2000](#)). The overall domain organization of NXF proteins is conserved, although not all domains are present in all members (Figure 5; [Herold *et al.*, 2001](#); [Herold *et al.*, 2000](#)).

The essential roles of *S. cerevisiae* Mex67p and human TAP in mRNA export have been described above. Interestingly, although there is only one NXF protein in *S. pombe* (Mex67p), it not essential for mRNA export in this organism. Nevertheless, it has been implicated in this process, as it interacts genetically and physically with Rae1p, an essential mRNA export factor in this organism ([Yoon *et al.*, 2000](#)).

When this study was initiated, it was unclear whether apart from TAP and Mex67p, other members of this family would be involved in mRNA export. Therefore, it has been a central objective of this thesis to investigate the role of different (human and *Drosophila*) NXF proteins in mRNA export (see 1.3).

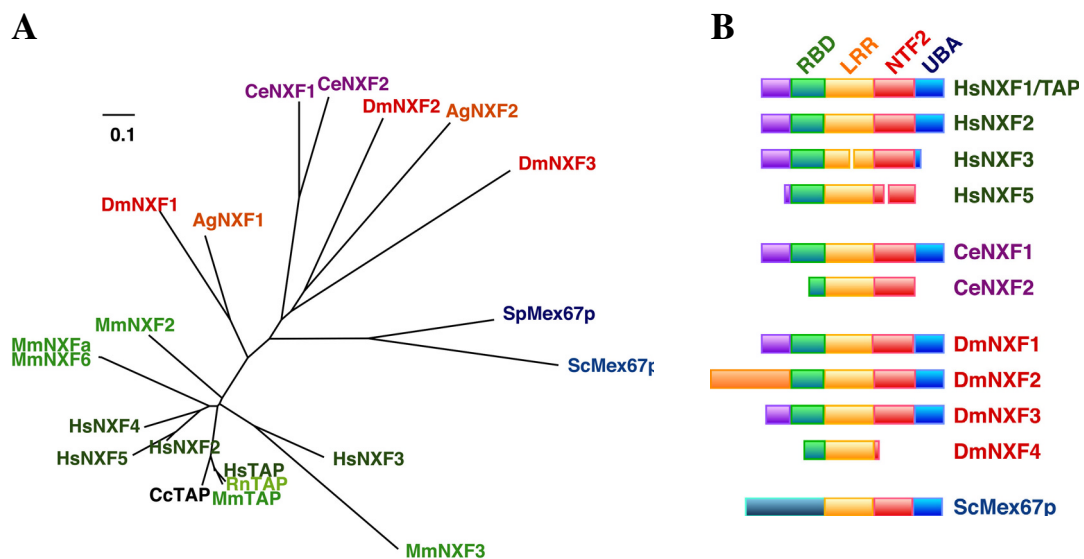


Figure 5: The NXF family

(A) Phylogenetic tree of NXF family sequences as available in June 2002. The tree was drawn by the neighbor-joining method. Only the most conserved region of NXF proteins (corresponding to amino acids 212-539 of human TAP) was considered in the analysis. DmNXF4 and HsNXF6 were excluded from the analysis as they contain few residues in this region. It is evident that in insects the gene duplication resulting in *nxf1* and *nxf2* occurred before the splitting into *Drosophila* and *Anopheles* species. No sequences related to Dm *nxf3* and Dm *nxf4* could be found in *Anopheles*, indicating that Dm *nxf3* and Dm *nxf4* might be evolved by gene duplication after speciation, or the corresponding genes were lost in *Anopheles* (courtesy of Mikita Suyama). (B) Domain organization of NXF proteins. The N-terminal domains of Mex67p and DmNXF2 do not show any similarity to TAP as indicated by the different colors. The relative sizes of the individual domains are not drawn to scale.

Abbreviations: Ag: *Anopheles gambiae*. Cc: *Coturnix coturnis* (quail). Ce: *Caenorhabditis elegans*. Dm: *Drosophila melanogaster*. Hs: *Homo sapiens*. Mm: *Mus musculus*. Rn: *Rattus norvegicus*. Sc: *Saccharomyces cerevisiae*. Sp: *Schizosaccharomyces pombe*.

Association of the heterodimeric mRNA export receptor with cellular mRNAs: the role of REF proteins and UAP56/Sub2p

As noted above, the efficient recruitment of NXF:p15 or Mex67p:Mtr2p heterodimers to cellular mRNAs is believed to depend on adapter proteins. Different RNA-binding proteins that could bridge the interaction between mRNAs and the actual export receptor have been identified. Among these are members of the conserved RNA and export factor-binding (REF) family.

The protein Yra1p, one of the two REF members in *S. cerevisiae*, was originally isolated as a protein with strong RNA-RNA annealing activity, but the relevance of this activity for Yra1p function is still obscure (Portman *et al.*, 1997). A few years later, Yra1p has been implicated in mRNA export as it interacts genetically and physically with Mex67p, and *yra1* mutants display strong defects in mRNA nuclear export. Yra1p also displays RNA-binding activity *in vitro* (Strasser and Hurt, 2000; Stutz *et al.*, 2000; Zenklusen *et al.*, 2001).

Similarly, mammalian REF proteins have been shown to bind RNA and TAP directly *in vitro* (Stutz *et al.*, 2000). Thus, REF proteins could fulfill their role as adapters by directly interacting with RNA and NXF/Mex67p, forming a bridge between the RNA substrate and its export receptor. Furthermore, REFs are shuttling proteins (Rodrigues *et al.*, 2001; Stutz *et al.*, 2000; Zhou *et al.*, 2000).

The role of mammalian REF proteins in export was demonstrated in microinjection experiments: recombinant murine REF2 can stimulate the export of mRNAs when injected into *Xenopus* oocytes. Anti-REF antibodies preventing the interaction of REFs with RNA inhibit the nuclear export of spliced and unspliced mRNAs in this system. Aly (also called REF1-I), another member of the REF family in mouse, is able to interact with Mex67p and partially complements the otherwise lethal *yra1* null mutation, showing that the function of REF proteins has been conserved throughout evolution (Strasser and Hurt, 2000). Moreover, mammalian REF is a component of the EJC whose presence on spliced mRNAs also seems to facilitate the recruitment of the nuclear export machinery (see below). As REF proteins are largely dispensable for mRNA export in *Drosophila*, other adapter proteins which are able to mediate the interaction of NXFs with mRNAs must exist in this organism (Figure 3; see also below).

Another protein implicated in the efficient recruitment of Mex67p:Mtr2p or NXF:p15 to mRNAs, is the putative RNA helicase UAP56 (called Sub2p in yeast) which had previously been implicated in spliceosome assembly (Fleckner *et al.*, 1997; Libri *et al.*, 2001). More recently, Sub2p/UAP56 was shown to be essential for bulk mRNA export in *S. cerevisiae* and *D. melanogaster*. The export defect caused by the inactivation of Sub2p/UAP56 affects intron-containing and intronless mRNAs (Gatfield *et al.*, 2001; Jensen *et al.*, 2001a; Strasser and Hurt, 2001). This is in agreement with the

observation that the association of UAP56 with the mRNP occurs cotranscriptionally and independently of splicing, as shown by immunoelectron microscopy using the *C. tetans* Balbiani ring pre-RNP as a model system (Kiesler *et al.*, 2002). The cotranscriptional association of Sub2p/UAP56 might be related to its ability to interact with a set of factors involved in transcription (see below; Strasser *et al.*, 2002).

Mammalian UAP56 interacts directly with Aly and is present together with Aly in the spliced mRNP. Furthermore, microinjection experiments in *Xenopus* oocytes showed that an excess of human UAP56 inhibits mRNA export, with a concomitant failure to recruit Aly to the spliced mRNP. This export block can be released by coinjecting high amounts of REF (Luo *et al.*, 2001). These data suggest that UAP56 interacts with REF *in vivo* and facilitates its recruitment to the mRNA.

Similarly, yeast Sub2p and Yra1p interact directly *in vivo* and *in vitro*. The function of Sub2p in mRNA export has been shown to be related to its ability to bind to Yra1p (Strasser and Hurt, 2001). This and the discovery that the interaction of Sub2p and Mex67p with Yra1p are mutually exclusive lead to the following model: Sub2p associates with the nascent mRNP during transcription and recruits Yra1p to the transcript. The interaction of Mex67p:Mtr2p with Yra1p then displaces Sub2p, rendering the mRNP export-competent (Strasser and Hurt, 2001).

By analogy to the yeast model, and as the mammalian proteins UAP56 and Aly were also shown to associate with spliced mRNPs in sequential order, it has been proposed that the function of UAP56 is to recruit Aly, which in turn recruits the heterodimeric export receptor NXF:p15.

While the above model of how the heterodimeric mRNA export receptor is recruited to the mRNP (UAP56/Sub2p recruits REF/Yra1p, REF/Yra1p recruits TAP/Mex67p) might be true in yeast, it is probably an oversimplification for higher eukaryotic systems. A study using an RNA interference (RNAi) approach in *Drosophila* cells demonstrated that the depletion of REF (and of other components of the EJC) does not lead to a complete block of nuclear mRNA export, whereas the depletion of UAP56, NXF1 or p15 does (Gatfield and Izaurralde, 2002; and this study (2.2)). These results show that the essential role of UAP56 in mRNA nuclear export is not restricted to the recruitment of REF, and that there are additional (unidentified) adapter proteins in higher eukaryotes mediating the association of NXF1:p15 heterodimers with cellular mRNAs. These experiments are supported by electron microscopic studies in *C. tetans* which demonstrate that UAP56 is present on the mRNP in exonic and intronic regions, while REF1 is restricted to regions of the transcripts in which introns have been removed (Kiesler *et al.*, 2002). This shows that the presence of UAP56 on the mRNA does not necessarily result in the recruitment of REF. In this context, it has been suggested that the role of UAP56 in mRNA could be more general. As a putative RNA-helicase, UAP56

could trigger ATP-dependent rearrangements of the mRNP. This may then facilitate the binding of different proteins which can serve as adapters for NXF:p15 heterodimers (Izaurralde, 2002).

Nuclear mRNA export is coupled to other processes: efficient recruitment and quality control

Studies over the last few years have shown that virtually all steps in gene expression are closely connected to one another (reviewed by: Maniatis and Reed, 2002; Proudfoot *et al.*, 2002). Likewise, nuclear mRNA export has been linked to transcription, splicing and 3' end formation (Figure 6). Even though the functional relevance of each of these connections is not completely clear yet, the coupling of mRNA export with splicing and 3' end formation would be one way to ensure that incompletely or improperly processed mRNAs do not reach the cytoplasm.

mRNA export and splicing

In higher eukaryotes, the majority of transcripts contain introns which have to be removed by splicing before nuclear export. Microinjection experiments in *Xenopus* oocytes demonstrated that, at least in some cases, splicing can enhance subsequent nuclear export, since spliced mRNAs are exported more efficiently than identical mRNAs that have been produced by *in vitro* transcription using the corresponding cDNA as a template (Le Hir *et al.*, 2001b; Luo and Reed, 1999). This effect was subsequently shown to depend on the deposition of a stable multiprotein-complex, the so-called exon-exon junction complex (EJC). The EJC is deposited 20-24 nucleotides upstream of exon-exon junctions, independent of the sequence there. It is approximately 335 kDa in size and minimally consists of the proteins SRm160, RNPS1, Y14, Magoh, DEK and REF (Kataoka *et al.*, 2001; Le Hir *et al.*, 2001a; Le Hir *et al.*, 2001b; Le Hir *et al.*, 2000a; Le Hir *et al.*, 2000b). Most of the EJC-components had already been directly or indirectly associated with splicing before (e.g. SRm160, DEK, RNPS1), and/or are localized in splicing speckles (e.g. REF, Y14, Magoh) (Blencowe *et al.*, 1998; Kataoka *et al.*, 2000; Le Hir *et al.*, 2001a; Mayeda *et al.*, 1999; McGarvey *et al.*, 2000; Zhou *et al.*, 2000). The EJC is thought to influence different aspects in post-splicing mRNA metabolism, such as mRNA export, translation and stability. Its function in nuclear mRNA export is supported by the fact that some of its constituents (REF, Y14 and Magoh) interact with TAP, possibly facilitating the binding of TAP:p15 heterodimers to spliced mRNPs (Kataoka *et al.*, 2001; Kim *et al.*, 2001; Le Hir *et al.*, 2001b; Stutz *et al.*, 2000). While the EJC is clearly able to promote the association with the export machinery, it is certainly not the only mechanism to recruit TAP:p15 to the mRNP. As mentioned above, the components of the EJC are dispensable for nuclear export in *Drosophila* (Gatfield and Izaurralde, 2002). Furthermore, both

naturally intronless mRNAs and intronless mRNAs which have been artificially generated from cDNA are generally exported to the cytoplasm, albeit in some cases with reduced efficiencies (especially when very short mRNAs are analyzed). In addition, a recent study in mammalian cells in which the effect of the EJC on different post-splicing steps in gene expression was systematically analyzed, demonstrated that the presence or absence of the EJC has only minor effects on nuclear export *in vivo*, while being more critical for translation (M. Moore, personal communication). Thus, under natural conditions, in addition to splicing there must be other (possibly redundant) ways to render an mRNA export-competent.

As discussed above, UAP56 has also been implicated in splicing and nuclear export of mRNA. But as it is recruited cotranscriptionally to the pre-mRNA, it is rather unlikely to play a role in the splicing-dependent recruitment of the mRNA export machinery. Another protein suggested to link splicing with mRNA export is the general splicing factor U2AF, which has been shown to interact with TAP. U2AF is able to stimulate nuclear export of an otherwise inefficiently exported mRNA, although the significance of this observation is not yet clear (Zolotukhin *et al.*, 2002).

mRNA export and transcription

It is well established that transcription and posttranscriptional events, such as capping, splicing and polyadenylation are closely linked (reviewed by: Cramer *et al.*, 2001; Maniatis and Reed, 2002). Recently, evidence has been presented that transcription might also directly promote the association of nuclear export factors with nascent mRNAs. For example, the yeast export factors Yra1p and Sub2p associate with nascent mRNAs during transcription elongation, as demonstrated by chromatin immunoprecipitation experiments (Lei *et al.*, 2001; Zenklusen *et al.*, 2002). This cotranscriptional association is thought to be mediated by the so-called THO complex whose components (Tho2p, Hpr1p, Mft1p and Thp2p) are also recruited to the transcript during transcription elongation (Strasser *et al.*, 2002; Zenklusen *et al.*, 2002). Yra1p and Sub2p have been shown to interact genetically and physically with components of this heterotetrameric complex, and their cotranscriptional recruitment requires Hpr1p, one of the THO components (Jimeno *et al.*, 2002; Libri *et al.*, 2002; Strasser *et al.*, 2002; Zenklusen *et al.*, 2002). Similarly, REF and UAP56 have been found to interact with the human counterparts of the complex (Strasser *et al.*, 2002). The THO complex is functionally and genetically linked to transcription in yeast, even though its function might be part of a cotranscriptional surveillance mechanism rather than active transcription elongation (see Discussion; Libri *et al.*, 2002; Zenklusen *et al.*, 2002). Deletion of individual THO components results in defects in nuclear mRNA export, providing a functional link between transcription and export (Libri *et al.*, 2002; Strasser *et al.*, 2002). The multiprotein-complex containing the two nuclear export factors

Sub2p and Yra1p and the different components of the THO complex, was subsequently termed TREX complex, for "transcription/export" complex (Strasser *et al.*, 2002).

While cotranscriptional (RNA polymerase II-dependent) recruitment of mRNA export factors clearly occurs *in vivo* (Kiesler *et al.*, 2002; Lei *et al.*, 2001; Zenklusen *et al.*, 2002), it is - similar to the loading of export factors facilitated by splicing - not a strict requirement for all nuclear export events. For example, mRNAs synthesized by *in vitro* transcription can be efficiently exported to the cytoplasm of *Xenopus* oocytes. This export depends on REF and UAP56, demonstrating that these factors can be loaded on the mRNA independently of transcription. Furthermore, mRNAs which are transcribed *in vivo* by bacteriophage T7 RNA polymerase in yeast are exported to the cytoplasm in a Yra1p-dependent way, even though Yra1p is not recruited to the transcript cotranscriptionally (Dower and Rosbash, 2002).

A recent study in yeast demonstrated that the mechanism by which Yra1p is recruited to a transcript is dependent on the nature of the transcript: while the association of Yra1p with an intronless mRNA was shown to occur cotranscriptionally and independently of splicing, the recruitment to a specific intron-containing pre-mRNA was splicing-dependent, and transcription alone was not sufficient to load Yra1p on this RNA (Lei and Silver, 2002a). Thus the requirements for the interaction of the mRNA export machinery with cellular mRNAs are complex and dependent on the nature of the cargo. In the case of Yra1p, the recruitment has been shown to require correct 3' end formation, regardless of the intron-status (see below; Lei and Silver, 2002a).

mRNA export and 3' end formation

3' end formation of transcripts generated by RNA polymerase II includes cleavage and polyadenylation, the latter being catalyzed by poly(A) polymerase with the assistance of poly(A)-binding protein (reviewed by Cramer *et al.*, 2001). Experiments in yeast and mammalian cells have revealed that transcripts which have not undergone these processing events are not exported to the cytoplasm (Brodsky and Silver, 2000; Dower and Rosbash, 2002; Eckner *et al.*, 1991; Huang and Carmichael, 1996; Lei and Silver, 2002a; Libri *et al.*, 2002). Transcripts whose 3' ends are generated by cis-ribozyme-directed or T7 terminator-directed cleavage fail to reach the cytoplasm (Dower and Rosbash, 2002; Eckner *et al.*, 1991; Huang and Carmichael, 1996; Libri *et al.*, 2002). Similarly, yeast strains carrying mutations in 3' end processing factors display defects in mRNA export (Brodsky and Silver, 2000; Hammell *et al.*, 2002; Lei and Silver, 2002a; Libri *et al.*, 2002). Insertion of a poly(A) stretch at the 3' end of ribozyme-cleaved transcripts does not overcome the export inhibition, indicating that the process of proper 3' end formation rather than the poly(A) tail itself allows nuclear export (Huang and Carmichael, 1996). This is in agreement with microinjection experiments in *Xenopus* oocytes using synthetic mRNAs. These

experiments revealed that the presence of a poly(A) tail does not significantly enhance the export efficiency of these transcripts (see above; Jarmolowski *et al.*, 1994).

Another link between nuclear mRNA export and 3' end formation has been made by analyzing transcripts in yeast strains defective in mRNA export. Defects in *RAT7* (Nup159), *GLE1*, *MEX67*, *RAT8* (Dbp5) or *RIP1* genes, which all result in a block to mRNA export, cause hyperadenylation of transcripts (Hammell *et al.*, 2002; Hilleren and Parker, 2001; Jensen *et al.*, 2001b). Furthermore, 3'-extended mRNAs (resulting from improper transcription termination) are frequently observed in mRNA export mutant strains (Hammell *et al.*, 2002). These 3'-extended and/or hyperadenylated mRNAs accumulate at the site of transcription. Similarly, incompletely processed transcripts also accumulate at the site of transcription in mammalian cells (Custodio *et al.*, 1999; Hilleren *et al.*, 2001; Jensen *et al.*, 2001b; Libri *et al.*, 2002). Interestingly, not all yeast mRNA export mutants show defects in 3' end formation: *yra1* or *sub2* mutants neither display termination nor polyadenylation defects (Hammell *et al.*, 2002).

Even though these data indicate a coupling between 3' end formation and mRNA export providing an efficient retention mechanism of incompletely processed transcripts, the molecular basis underlying this phenomenon remains to be established.

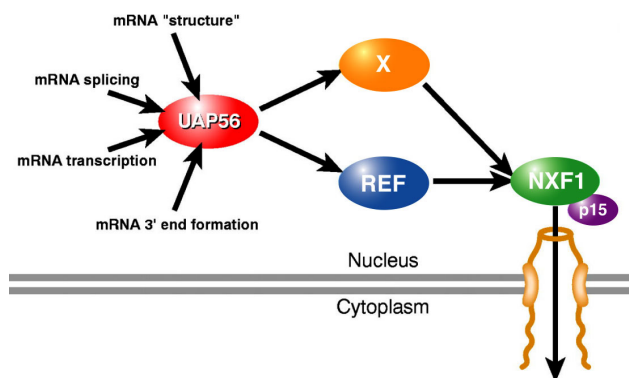


Figure 6: mRNA export is coupled to other processes

The recruitment of the mRNA export machinery can be influenced by splicing, transcription and 3' end formation. Moreover, a cotranscriptional surveillance mechanism might control mRNA "structure" before export (see also section 3.3). UAP56, NXF1 and p15 are essential for bulk mRNA export, but REF proteins are not (in *Drosophila*), indicating that other factor(s) must exist which can mediate the recruitment of the NXF1:p15 heterodimer to cellular mRNAs (modified from Cullen, 2003).

Other factors implicated in mRNA export

Apart from NXF proteins and the different factors directly implicated in their recruitment, several other proteins have been suggested to play a role in mRNA export. Amongst many others, these include different nucleoporins and the conserved proteins Gle1, Gle2 and Dbp5.

In *S. cerevisiae*, several **nucleoporins** playing a role in mRNA export have been identified, examples being Nup159p (also called Rat7p), Nup133p (also called Rat3p), Nup116p, Nup85p (also called Rat9p) and Nup145p. In mammals, the nucleoporins Nup98, Nup153, Nup133, Nup160 and TPR have been implicated in this process (reviewed by: Gorlich and Kutay, 1999; Vasu *et al.*, 2001). Inactivation of these nucleoporins does not result in a general block of all nucleocytoplasmic transport processes, but in an mRNA export defect, indicating that they might provide essential docking sites which are preferentially used by the mRNA export machinery.

S. cerevisiae **Gle1p** (also called Rss1p) is an essential protein which is concentrated at the cytoplasmic side of the NPC. Mutant strains display strong defects in mRNA export. Gle1p has been shown to contain a leucine-rich export signal which is not present in the human homologue (Del Priore *et al.*, 1996; Murphy and Wentz, 1996; Strahm *et al.*, 1999). Interestingly, human Gle1 can only complement the yeast mutant if a leucine-rich export signal is inserted (Watkins *et al.*, 1998). Human Gle1 is also concentrated at the NPC, and anti-Gle1 antibodies inhibit mRNA export (but not protein import) when injected into HeLa cells, providing evidence for a role in this process (Watkins *et al.*, 1998). However, neither human nor yeast Gle1 has been shown to shuttle or to interact with RNA.

While Rae1p is essential in *S. pombe*, its orthologue **Gle2p** is not in *S. cerevisiae* (Brown *et al.*, 1995; Murphy *et al.*, 1996). Mutations in *GLE2* or *RAE1* cause nuclear accumulation of poly(A)⁺ RNA, and both Gle2p and Rae1p are associated with the NPC. Gle2p was also shown to interact directly with the nucleoporin Nup116p (Bailer *et al.*, 1998; Murphy *et al.*, 1996). Furthermore, both Gle2p and Rae1p interact with Mex67p (Yoon *et al.*, 2000; Zenklusen *et al.*, 2001). Similarly, the human homologue hRAE1 interacts with TAP, shuttles and localizes to the NPC in a transcription-dependent manner (Bachi *et al.*, 2000; Bailer *et al.*, 1998; Pritchard *et al.*, 1999). This association is at least in part mediated by its direct interaction with the nucleoporin Nup98 (Pritchard *et al.*, 1999). hRAE1 was also shown to interact directly or indirectly with mRNPs, as it can be cross-linked to poly(A)⁺ RNA (Kraemer and Blobel, 1997). The conserved interaction between Gle2p/RAE1 and Mex67p/TAP suggests that these proteins might cooperate to export mRNAs, but the precise role of Gle2 in this process remains to be investigated.

Dbp5 belongs to the DEAD-box-containing family of RNA helicases. Dbp5 is mainly cytoplasmic, but a fraction of Dbp5 localizes to the cytoplasmic fibrils of the NPC in both yeast and mammalian cells (Schmitt *et al.*, 1999; Snay-Hodge *et al.*, 1998; Tseng *et al.*, 1998). This association with the NPC is mediated through its direct interaction with the nucleoporin CAN/Nup159p (Hodge *et al.*, 1999; Schmitt *et al.*, 1999). Yeast Dbp5p shuttles and *dbp5* mutant yeast strains display a block to poly(A)⁺ RNA export (Hodge *et al.*, 1999; Snay-Hodge *et al.*, 1998; Tseng *et al.*, 1998). Similarly, injection of anti-Dbp5

antibodies (directed against human Dbp5), or of recombinantly expressed mutant (human) Dbp5 protein inhibits mRNA export in *Xenopus* oocytes, indicating that the role of Dbp5 in mRNA export is conserved (Schmitt *et al.*, 1999). Both yeast and human Dbp5 have been shown to have ATP-dependent RNA unwinding activity *in vitro*, although this activity is dependent on the presence of other proteins ("cofactors") (Schmitt *et al.*, 1999; Tseng *et al.*, 1998). The observation that Dbp5 is located at the cytoplasmic side of the NPC has led to the proposal that it might function in the remodeling of mRNPs just after their translocation through the NPC (Schmitt *et al.*, 1999; Tseng *et al.*, 1998). Such remodeling events, which would be dependent on ATP hydrolysis by Dbp5, could confer directionality to mRNA export, and could also contribute to the energy requirements of this process. However, the essential function of Dbp5 in mRNA export does not seem to be conserved in all eukaryotic species, as Dbp5 has recently been shown to be dispensable for mRNA export in *Drosophila* (Gatfield *et al.*, 2001).

Regulated mRNA export

Nearly all steps of gene expression can be regulated in eukaryotic cells. Well-known examples for posttranscriptional regulatory events include alternative splicing, regulated polyadenylation or differential translation. Recently, evidence has been collected that nuclear mRNA export might also be subjected to regulation under certain conditions. Examples of regulated export include the preferential nuclear export of mRNAs encoding heat shock proteins induced by stress, and regulated mRNA export during development.

Cells suffering from stress quickly respond by synthesizing heat shock proteins which serve as chaperones to maintain protein stability and folding. Apart from a massive transcriptional induction of heat shock genes, paralleled by the transcriptional downregulation of non-heat shock genes, several posttranscriptional mechanisms ensure the preferential expression of heat shock factors in eukaryotes under stress.

In yeast, it has been reported that heat shock mRNAs are selectively and efficiently exported to the cytoplasm under stress, while non-heat shock mRNAs are blocked in the nuclear compartment (Saavedra *et al.*, 1996). A possible mechanism for the export inhibition of non-heat shock mRNAs involves the hnRNP-like protein Nlp3p, which is normally bound to poly(A)⁺ RNA, but dissociates from mRNAs under stress. As Nlp3p is essential for general mRNA export, this uncoupling of Nlp3p (and possibly of other RNA-binding proteins) from non-heat shock mRNAs could trigger their retention in the nucleus, rendering the RNPs export-incompetent (Krebber *et al.*, 1999). Furthermore, heat shock mRNA export was initially suggested to occur *via* a distinct pathway defined by the nucleoporin Rip1p, which is essential for heat shock mRNA export, but was proposed to be dispensable for bulk mRNA export (Saavedra *et al.*, 1997b; Stutz *et al.*, 1997). However, both the selective involvement of Rip1p in heat shock mRNA export and the general

export block of bulk poly(A)⁺ RNA under stress are discussed controversially in the field, and could not be reproduced in an independent study (Vainberg *et al.*, 2000).

In mammalian cells, heat shock induces transcription and enhances stability of mRNAs encoding heat shock proteins. Non-heat shock mRNAs are transcriptionally downregulated and not exported to the cytoplasm, resulting in their nuclear accumulation (Gallouzi *et al.*, 2000; Sadis *et al.*, 1988). Despite this export inhibition affecting bulk mRNA, heat shock mRNAs are exported to the cytoplasm, suggesting that heat shock mRNAs might have access to an export pathway which is not available to non-heat shock mRNAs (Gallouzi *et al.*, 2001). The following model has been proposed to explain these observations: Most stress-related mRNAs contain AU-rich elements (AREs), which are recognized by the HuR protein. HuR binding affects the stability of these mRNAs, and also influences their nuclear export. Under normal growth conditions HuR shuttling can occur through two separate pathways. One pathway depends on the importin β -like protein transportin-2. The other pathway is thought to be mediated by two adapter proteins (pp32 and APRIL) which contain leucine-rich export signals recognized by Crm1, another importin β -like export factor (see 1.1.4). Upon heat shock, the interaction of HuR with transportin-2 is lost, and HuR export depends solely on Crm1. As it is believed that Crm1 is not involved in the export of bulk mRNA (see below), the specific interaction of HuR with ARE-containing mRNAs might allow these mRNAs to be exported (*via* Crm1), while bulk mRNA export is inhibited (Gallouzi *et al.*, 2001; Gallouzi and Steitz, 2001). This model is in agreement with the observation that the nuclear export of transcriptionally induced *hsp70* mRNA is blocked by leptomycin B (LMB), a drug specifically inhibiting Crm1 function. In contrast, general mRNA export is not affected by LMB (Brennan *et al.*, 2000; Gallouzi *et al.*, 2001).

One example for a developmentally regulated mRNA export event involves *C. elegans tra-1* and *tra-2*, both being implicated in the terminal steps of sex differentiation. In the absence of TRA-1 protein, *tra-2* mRNA is retained in the nucleus. However, binding of TRA-1 to the 3' UTR of *tra-2* mRNA overcomes this retention and results in the export of the TRA-1 protein:*tra-2* mRNA complex to the cytoplasm. The export of this complex is dependent on Crm1 (see also Discussion; Graves *et al.*, 1999; Segal *et al.*, 2001).

Another case of regulated mRNA export occurs in *Drosophila* tendon differentiation. The transcription factor Stripe plays a key role in this process. Its expression is regulated by two distinct versions of the How protein. In tendon precursor cells, the long version [How(l)] is present, which binds *stripe* mRNA and inhibits its nuclear export, thus keeping Stripe protein levels low. In later stages of differentiation, a short form of How, How(s), is thought to compete with How(l) for binding *stripe* mRNA thus releasing the nuclear export block of *stripe* mRNA. The regulated nuclear export of *stripe* mRNA is only one of several ways to modulate Stripe activity, as the two How

proteins also differentially affect *stripe* mRNA stability (Nabel-Rosen *et al.*, 1999; Nabel-Rosen *et al.*, 2002).

In mammals, an example of regulated mRNA export has recently been reported to occur during differentiation of the nervous system in mice. The Quaking protein is required for the maturation of Schwann cells into myelin-forming cells. Different forms of the Quaking protein are generated by alternative splicing, and the balance between these different isoforms was shown to control the nuclear export of *mbp* mRNA. *mbp* encodes the "myelin basic protein" and is a major component of myelin (Larocque *et al.*, 2002). Interestingly, both How and Quaking, belong to a family of RNA-binding proteins called "signal transduction and activation of RNA" (STAR) family, suggesting that conserved features found in STAR family members might enable them to regulate nuclear export of specific mRNAs by a similar mechanism (Larocque *et al.*, 2002; Nabel-Rosen *et al.*, 1999).

These examples illustrate that the tightly controlled export of specific mRNAs can regulate differentiation. However, the precise molecular mechanisms underlying these observations e.g. how the nuclear retention of specific mRNAs is achieved, remain to be investigated.

The role of Crm1 in mRNA export

As described above, Crm1 is essential for the export of U snRNAs, ribosomal subunits and proteins containing leucine-rich NESs (see 1.1.4, 1.2.2 and 1.2.3). Crm1 is also involved in the nuclear export of late mRNAs of some retroviruses (e.g. HIV-1), but is believed to play a rather limited role in the nuclear export of cellular mRNAs (Cullen, 2003)

In yeast, a temperature-sensitive mutant of *CRM1* shows a strong nuclear accumulation of poly(A)⁺ RNA within 15 minutes after the shift to the non-permissive temperature. This observation first led to the proposal that Crm1p is also an essential and general export receptor for mRNAs (Stade *et al.*, 1997). However, subsequent experiments using a *S. cerevisiae* strain in which Crm1p function can be inhibited with LMB showed that the nuclear accumulation poly(A)⁺ RNA following LMB treatment occurs with a significant delay compared to the effect on NES-mediated export. Moreover, LMB treatment did not result in a marked decrease of protein synthesis, arguing against a role of Crm1p in general mRNA export (Neville and Rosbash, 1999). This does not exclude a role for Crm1p in the nuclear export of specific mRNAs.

In vertebrates, the following observations argue against a role for Crm1 in general mRNA export: first, injection of leucine-rich NES into *Xenopus* oocytes competes with U snRNA export, but not with mRNA export (Fischer *et al.*, 1995; Fornerod *et al.*, 1997). Similarly, high amounts of NES peptide inhibit Crm1-dependent protein export in mammalian cells, but not bulk mRNA export (Gallouzi and Steitz, 2001). Second, LMB

efficiently blocks U snRNA export in oocytes or mammalian cells, but does not result in nuclear poly(A)⁺ RNA accumulation (Fornerod *et al.*, 1997; Wolff *et al.*, 1997). Third, overexpression of a truncated form of the nucleoporin CAN that interacts with Crm1 and hence titrates it, inhibits Rev-dependent gene expression but does not affect cellular mRNA export (Bogerd *et al.*, 1998; Guzik *et al.*, 2001). Thus, a role for Crm1 in general nuclear mRNA export in higher eukaryotes is unlikely. However, Crm1 has been suggested to play a role in the export of specific mRNAs. Its potential role in the export of heat shock mRNAs has been discussed above. Furthermore, Crm1 was shown to be implicated in the export of other mRNAs containing AREs, such as *c-fos* or *cox-2* mRNA (Brennan *et al.*, 2000; Jang *et al.*, 2002).

Thus, Crm1 (and other export receptors, e.g. proteins of the NXF family; see Discussion) could serve as an alternative export receptor for mRNAs whose export needs to be regulated independently of bulk mRNA export mediated by NXF1:p15 or Mex67p:Mtr2p.

1.3 Objectives of this study

1.3.1 What was known at the beginning of this study?

When this work was initiated, the nuclear export pathway for mRNAs was poorly characterized and many factors implicated in this process (e.g. REF/Yra1p or UAP56/Sub2p) had not been described. The human TAP protein was known to be the cellular cofactor promoting the nuclear export of retroviral RNAs containing the CTE. TAP had also been proposed to serve as an export receptor for cellular mRNAs, as it was known that these viral RNAs use the same pathway as cellular mRNAs. p15 had just been identified as a TAP binding partner, but its role was unclear, as were the mechanisms of how TAP interacts with nucleoporins or RNPs. Mex67p, the orthologue of TAP in *S. cerevisiae*, had been proven to be essential for mRNA export in yeast. The TAP:p15 complex had been demonstrated to be able to functionally replace Mex67p:Mtr2p, indicating a high degree of functional conservation. Database searches performed by Peer Bork's group at EMBL, just when I started my Ph.D. work, indicated that TAP and Mex67p belong to an evolutionarily conserved family of proteins having more than one member in *H. sapiens*, *C. elegans* and *D. melanogaster*. We called this the NXF family, for nuclear export factor family. It was unclear whether apart from TAP and Mex67p other members of this family would also play a role in mRNA nuclear export.

1.3.2 Goals and techniques

The central objective of my Ph.D. project was to investigate the role of different human and *Drosophila* NXF members in nuclear mRNA export (sections 2.1, 2.2 and 2.3).

In the first part of this project (section 2.1), I cloned and characterized two human NXF proteins, NXF2 and NXF3, mainly using biochemical approaches. I analyzed their interaction with RNA, nucleoporins and other known TAP partners *in vitro*, and used reporter-gene assays to test these human TAP homologues for CTE-dependent and general RNA export activity in cultured cells (2.1.1). I have also contributed to the biochemical characterization of human NXF5 (2.1.2).

In the second part of this work (section 2.2), I investigated the function of the different NXF members and other mRNA export factors in *D. melanogaster*. We have used *Drosophila* Schneider cells in which the expression of endogenous proteins can be efficiently silenced by means of double-stranded RNA interference (RNAi), providing an excellent tool to analyze the function of the individual (potential) export factors *in vivo*. Three (NXF1-3) of the four NXF members were found to be expressed in this cell line and could be studied.

First, a combination of "classical" biochemical and cell biological techniques, such as RNA localization by *in situ* hybridization and metabolic labeling was applied to analyze the effects caused by the depletion of different NXF members and their heterodimeric interaction partner p15 (2.2.1).

Subsequently, a genome-wide analysis of different mRNA export pathways using a combination of RNAi and microarray technology was performed (2.2.2). Apart from screening for potential mRNA substrates of NXF2, NXF3 and Crm1, I also analyzed the effects caused by depleting the essential export factors NXF1, p15 or UAP56. The following questions were addressed in this large-scale analysis: what fraction of mRNAs is affected when NXF1:p15 or UAP56 function is abolished? Are there mRNAs which are still exported despite the general mRNA export block? Can we identify mRNAs requiring NXF1:p15, but not UAP56 function, or *vice versa*?

I also participated in the analysis of the role of the different TAP/NXF1 domains in nuclear mRNA export (section 2.3). To study the human TAP protein, two different mRNA export assays in mammalian cells (both based on CAT reporter mRNAs) were used (2.3.1 and 2.3.2). RNAi in Schneider cells was used to investigate the role of the NTF2- and the UBA-like domain of *Drosophila* NXF1 in mRNA export *in vivo* (2.3.2).

The last part of this thesis (section 2.4) describes results that were obtained as part of a collaboration using the technique of RNAi in Schneider cells to study the function of Cdc37 (2.4.1).

2 Results/Publications

In the following sections, the results obtained during my Ph.D. are presented in the form of journal articles. Each paper is preceded by a short introduction and a summary of results and conclusions. My contribution to each publication is also indicated.

The papers are organized into four sections:

2.1 The nuclear export factor family: characterization of human NXF proteins

Paper 1:

TAP (NXF1) belongs to a multigene family of putative RNA export factors with a conserved modular architecture

Herold, A., Suyama, M., Rodrigues, J. P., Braun, I., Kutay, U., Carmo-Fonseca, M., Bork, P., and Izaurralde, E. (2000) *Mol Cell Biol* **20**, 8996-9008.

Paper 2:

NXF5, a novel member of the nuclear RNA export factor family, is lost in a male patient with a syndromic form of mental retardation

Jun, L., Frints, S., Duhamel, H., Herold, A., Abad-Rodriguez, J., Dotti, C., Izaurralde, E., Marynen, P., Froyen, G. (2001) *Curr Biol* **11**, 1381-1391.

2.2 Role of *Drosophila* NXFs, p15 and UAP56 in nuclear mRNA export

Paper 3:

NXF1/p15 heterodimers are essential for mRNA nuclear export in *Drosophila*

Herold, A., Klymenko, T., Izaurralde, E. (2001) *RNA* **7**, 1768-1780.

Paper 4:

Genome-wide analysis of mRNA nuclear export pathways in *Drosophila*

Herold, A., Teixeira L., and Izaurralde, E. (2003) *Submitted*.

2.3 Functional analysis of TAP/NXF1 domains

Paper 5:

Overexpression of TAP/p15 heterodimers bypasses nuclear retention and stimulates nuclear mRNA export

Braun, I.C., Herold, A., Rode, M., Conti, E., and Izaurralde, E. (2001) *J Biol Chem*, **276**, 20536-20543.

Paper 6:

Nuclear export of mRNA by TAP/NXF1 requires two nucleoporin binding sites but not p15

Braun, I. C., Herold, A., Rode, M., and Izaurralde, E. (2002) *Mol Cell Biol* **22**, 5405-5418.

2.4 Role of Cdc37 in chromosome segregation and cytokinesis

Paper 7:

Cdc37 is essential for chromosome segregation and cytokinesis in higher eukaryotes

Lange, B.M.H., Rebollo, E., Herold, A., and Gonzalez, C. (2002) *EMBO J* **21**, 5364-5374.

Wherever one of these publications is cited in the thesis, the citation is underlined to indicate that the citation refers to results obtained and presented in this thesis.

2.1 The nuclear export factor family: characterization of human NXF proteins

2.1.1 Paper 1

TAP (NXF1) belongs to a multigene family of putative RNA export factors with a conserved modular architecture

Herold, A., Suyama, M., Rodrigues, J. P., Braun, I., Kutay, U., Carmo-Fonseca, M., Bork, P., and Izaurralde, E. (2000) *Mol Cell Biol* **20**, 8996-9008.

Context

The human protein TAP and its yeast orthologue Mex67p have both been implicated in the nuclear export of mRNAs. Both TAP and Mex67p act as heterodimers together with a small cofactor called p15 in humans and Mtr2p in yeast. The fact that overexpression of TAP and p15 in *S. cerevisiae* partially restores growth of the otherwise lethal *mex67/mtr2* double knockout, suggests that the mRNA export pathway mediated by TAP/Mex67p has been conserved throughout eukaryotic evolution (Katahira *et al.*, 1999). As both proteins show significant homology and share a similar domain organization (Segref *et al.*, 1997), we hypothesized that if other proteins with similarity to TAP existed, they might also play a role in mRNA export. To identify such putative mRNA export factors, we performed an extensive search for TAP and p15 homologues in higher eukaryotes and combined this with a functional characterization of selected human TAP and p15 homologues.

Summary of results and conclusions

In this study we identified two TAP-related sequences in the *C. elegans* genome, four in the *Drosophila* genome and, in addition to TAP itself, five in the human genome (of which one might be, and a second one certainly is a pseudogene). This conserved family of TAP homologues was termed NXF (nuclear export factor) family. We showed that the overall domain organization and residues critical for p15 or nucleoporin binding are conserved in most predicted family members. Two human homologues (NXF2 and NXF3) were cloned and characterized in more detail. We demonstrated that, like TAP, NXF2 interacts with the RNA-binding proteins E1B-AP5 and REF1-II, as well as with RNA *in vitro*, while NXF3 binds only to E1B-AP5. In contrast to TAP, neither NXF2 nor NXF3 interacts with the CTE of simian retrovirus type 1 *in vitro*. Accordingly neither of them promotes the nuclear export of a CTE-containing reporter RNA in quail cells. NXF2 and NXF3 were also tested for their capability to bind nucleoporins *in vitro* using pull-down assays. In agreement with the truncation of the predicted nucleoporin-binding domain in NXF3, only NXF2 was found to interact efficiently with CAN. NXF2 was also

shown to interact with several other FG-repeat containing nucleoporins (CAN, Nup154 and p62), and residues critical for this interaction were identified. These *in vitro* data were confirmed by determining the localization of GFP-tagged versions of the proteins. Both NXF2 and NXF3 were found to be mainly nuclear, and a fraction of NXF2 (but not of NXF3) localized to the nuclear rim. Furthermore, NXF2 mutants, which do not interact with nucleoporins *in vitro* were not detected at the nuclear envelope.

We also performed database searches to identify genes with similarity to human p15 (also called Nxt). We identified one *nxt* gene in *Drosophila* and *C. elegans* and two in the human genome (*p15-1* and *p15-2*). Both derivatives of p15 were shown to bind directly to TAP, NXF2 and NXF3 as demonstrated in a combined coexpression/pull down assay. The subcellular localization of p15-2 was similar to that of the previously identified p15-1 with a fraction of both proteins being localized to the nuclear envelope.

To functionally test the RNA export activity of the isolated NXF and p15 proteins we used a reporter assay in cultured human cells, which relies on the intrinsic ability of the NXF protein to recognize the reporter mRNA (see also [Braun *et al.*, 2001](#); section 2.3.1). Using this assay, three important observations were made. First, TAP and NXF2 both stimulated the nuclear export of the reporter RNA, while NXF3 did not. Secondly, the cotransfection of either p15-1 or p15-2 resulted in higher steady-state expression levels of the NXF proteins and a significant stimulation of the export activity. Third, TAP or NXF2 mutants impaired in nucleoporin binding also displayed a reduced export activity in this assay.

In this manuscript we have shown that TAP and Mex67p belong to the evolutionarily conserved NXF family of putative RNA export factors. Our results indicate that the TAP:p15-mediated export pathway has diversified in higher eukaryotes, as all tested genomes of higher eukaryotes encode multiple NXF proteins. The functional characterization of two selected human TAP homologues and the two human p15 homologues presented in this study suggest that human NXF2, p15-1 and p15-2 have the potential to act as nuclear mRNA export factors.

Contribution

I cloned the human NXF2 and NXF3 cDNAs and performed most of the *in vitro* protein- and RNA-binding studies. I also contributed to establishing the reporter mRNA export assay and performed the CTE export assay in quail cells. My work includes all experiments presented in Figures 4A-F, 5F, 6A-C and 7B and C. Furthermore, I constructed all NXF2 and NXF3 mutants/plasmids used in this study. The equal significance of the biocomputational predictions (Figures 1-3, Figure 5A-C) carried out by Mikita Suyama in Peer Bork's group and the experimental characterization presented in this paper justified a shared first authorship. My contribution to this paper is about 40%.

TAP (NXF1) Belongs to a Multigene Family of Putative RNA Export Factors with a Conserved Modular Architecture

ANDREA HEROLD,¹ MIKITA SUYAMA,¹ JOÃO P. RODRIGUES,² ISABELLE C. BRAUN,¹ ULRIKE KUTAY,³
MARIA CARMO-FONSECA,² PEER BORK,¹ AND ELISA IZAURRALDE^{1*}

European Molecular Biology Laboratory, D-69117 Heidelberg, Germany¹; Institute of Histology and Embryology, Faculty of Medicine, University of Lisbon, 1699 Lisbon Codex, Portugal²; and Institute of Biochemistry, Swiss Federal Institute of Technology, CH-8092 Zürich, Switzerland³

Received 12 July 2000/Returned for modification 15 August 2000/Accepted 6 September 2000

Vertebrate TAP (also called NXF1) and its yeast orthologue, Mex67p, have been implicated in the export of mRNAs from the nucleus. The TAP protein includes a noncanonical RNP-type RNA binding domain, four leucine-rich repeats, an NTF2-like domain that allows heterodimerization with p15 (also called NXT1), and a ubiquitin-associated domain that mediates the interaction with nucleoporins. Here we show that TAP belongs to an evolutionarily conserved family of proteins that has more than one member in higher eukaryotes. Not only the overall domain organization but also residues important for p15 and nucleoporin interaction are conserved in most family members. We characterize two of four human TAP homologues and show that one of them, NXF2, binds RNA, localizes to the nuclear envelope, and exhibits RNA export activity. NXF3, which does not bind RNA or localize to the nuclear rim, has no RNA export activity. Database searches revealed that although only one *p15 (nxt)* gene is present in the *Drosophila melanogaster* and *Caenorhabditis elegans* genomes, there is at least one additional p15 homologue (p15-2 [also called NXT2]) encoded by the human genome. Both human p15 homologues bind TAP, NXF2, and NXF3. Together, our results indicate that the TAP-p15 mRNA export pathway has diversified in higher eukaryotes compared to yeast, perhaps reflecting a greater substrate complexity.

mRNAs are exported from the nucleus as large ribonucleoprotein complexes (mRNPs). To date, proteins directly implicated in this process include several nucleoporins and RNA binding proteins (hnRNPs), an RNA helicase of the DEAD-box family (Dbp5), and the nuclear pore complex (NPC)-associated proteins Gle1p, TAP and Mex67p, and RAE1 (also called Gle2p) (reviewed in references 22, 28, and 32). Mex67p is essential for mRNA export in *Saccharomyces cerevisiae*, while RAE1 is essential for mRNA export in *Schizosaccharomyces pombe* (9, 27, 36). Their vertebrate homologues, TAP and RAE1, have also been implicated in the export of cellular mRNAs (6, 8, 12, 15, 20, 31).

We identified TAP as the cellular factor which is recruited by the constitutive transport element (CTE) of simian type D retroviruses to promote nuclear export of their genomic RNAs (12). In *Xenopus* oocytes, titration of TAP with an excess of CTE RNA prevents cellular mRNAs from exiting the nucleus (12, 30, 33). This suggests a role for this protein in the export of cellular mRNA.

Considerable progress has been made in defining TAP structural and functional domains (see Fig. 1) and in identifying its binding partners. TAP partners include various nucleoporins (4, 17); p15 (also called NXT1), a protein related to nuclear transport factor 2 (NTF2) (7, 17); transportin, which mediates TAP nuclear import (4); and several mRNP-associated proteins, such as E1B-AP5, RAE1 (4), and members of the Yra1p/REF family of proteins (37, 39). Binding of TAP to these mRNP-associated proteins is mediated by its N-terminal domain (residues 1 to 372) (4, 39). This domain includes a non-canonical RNP-type RNA binding domain (RBD) and four

leucine-rich repeats (LRRs) and exhibits general RNA binding affinity and specific binding to the CTE RNA (8, 12, 24).

TAP heterodimerizes with p15 via its NTF2-like domain (residues 371 to 551) (4, 40). Nucleoporin binding by TAP in vitro and in vivo is mediated by a domain located at the very C-terminal end of the protein (residues 508 to 619) (4, 5). The similarities of this domain to the ubiquitin-associated (UBA) domain allowed the prediction that residues located in a conserved loop were implicated in TAP-nucleoporin interaction (40).

In this study, we identify TAP homologues in *Homo sapiens*, *Caenorhabditis elegans*, and *Drosophila melanogaster*. The overall domain organization of these proteins, including residues important for p15 and nucleoporin interaction, is conserved. Two of four putative human TAP homologues, NXF2 and NXF3, have been characterized in detail. These proteins show 57 and 44% sequence identity to TAP. Neither binds specifically to the CTE RNA, indicating that they may exhibit different substrate specificities. Both proteins are localized within the nucleoplasm, but only NXF2 associates with the nuclear envelope and exhibits detectable RNA export activity. In addition, a human homologue of p15 (p15-2 [also called NXT2]) was characterized. p15-2 binds to TAP, NXF2, and NXF3 with affinities similar to those of p15. Like p15-1, a fraction of p15-2 localizes to the nuclear envelope. Both human p15 homologues participate in RNA nuclear export. Together, our results indicate that the TAP-p15-mediated export pathway has diversified in higher eukaryotes and in humans includes at least two p15 proteins and multiple TAP-like putative mRNA export factors.

MATERIALS AND METHODS

Homology searches and sequence analysis. Homologues of TAP and p15 were retrieved in expressed sequence tag (EST) databases, human genomic DNA, and the *Drosophila* and *C. elegans* genomes, as well as in various protein sequence databases, using the BLAST suite of programs (3). Multiple sequence alignments were constructed by using CLUSTAL W (42) and manually refined on the SEAVIEW alignment editor (11). To predict the genomic structure of TAP and

* Corresponding author. Mailing address: EMBL, Meyerhofstrasse 1, D-69117 Heidelberg, Germany. Phone: 0049 6221 387 389. Fax: 0049 6221 387 518. E-mail: izaurrealde@embl-heidelberg.de.

p15 homologues in various organisms, the Genewise program (<http://www.sanger.ac.uk/Software/Wise2/>) was employed. If cDNA and/or EST sequences were available, the BLASTN program for genomic sequences was also used to determine genomic structures.

Plasmids. Full-length human NXF2, NXF3, p15-2a, and p15-2b cDNAs were amplified by PCR using the human testis Marathon-Ready cDNA library (Clontech) as a template and primers introducing the appropriate restriction sites. The 3' primers were designed according to the predicted cDNAs and included stop codons. The 5' primers were designed using sequence information obtained after performing 5' rapid amplification of cDNA ends reactions with the same human testis cDNA library and oligonucleotides lying in the p15-2a, p15-2b, NXF2, and NXF3 coding region that is represented in the corresponding human genomic sequences or I.M.A.G.E. Consortium cDNA clones. The NXF2 sequence is represented in the IMAGp998P054498Q2 and IMAGp998C234110Q2 clones. NXF3 is represented in the IMAGp998M08574Q2 clone ([see http://www.rzpd.de](http://www.rzpd.de) for further information). The p15-2a and p15-2b cDNAs are represented in the genomic sequence AL031387. The complete NXF2 and NXF3 cDNA was cloned into pGEMT-easy (Promega) and sequenced. p15-2a cDNA was directly cloned in pGEXCS (29) and sequenced. The cDNAs present in these plasmids were used for all further subcloning steps.

To generate a plasmid for in vitro translation, NXF2 cDNA was excised from pGEM T-easy with *Bam*HI and *Hind*III and inserted into the same restriction sites present in pBSpALTER, a derivative of pALTER-Ex1 (Promega). NXF3 was excised with the enzymes *Nco*I and *Bam*HI and cloned into the *Nco*I/*Bam*HI sites of pBSSK-HA, a derivative of the pBSSK(+) vector (Stratagene) with the β -globin 5' untranslated region inserted between the *Hind*III and *Eco*RI sites. For the coexpression assay (see Fig. 5F), p15-1 and p15-2a cDNAs were cloned in the *Nco*I/*Not*I or *Nco*I/*Bam*HI sites of vector pET28c (Novagen), respectively.

Plasmids allowing the expression of glutathione *S*-transferase (GST) fusions of full-length NXF2 and NXF3 in *Escherichia coli* were generated by inserting the coding sequences into the *Bam*HI and *Not*I sites of pGEX4T-1 (NXF2) (Pharmacia) or the *Nco*I and *Bam*HI sites present in pGEXCS (NXF3). The NXF2 point mutants E598R, W599A, and N600A and the triple alanine substitution 3xAla598 were generated by using an oligonucleotide-directed in vitro mutagenesis system from Stratagene (Quick-change site-directed mutagenesis) in the context of pGEX4T-1-NXF2. The mutation 3xAla598 introduces a *Not*I site into the coding sequence of NXF2. Plasmid pGEX4T-1-NXF2 Δ 598-626 was made by digesting pGEX4T-1-NXF2 3xAla598 with *Ppu*MI and *Not*I and inserting the released fragment into pGEX4T-1-NXF2 cut with the same enzymes. Constructs encoding GST fusions of the NXF2 amino acids 1 to 377 and 102 to 203 (RBD) were generated by inserting the corresponding PCR products into pGEX4T-1 digested with *Bam*HI and *Not*I. A plasmid encoding a GST fusion of NXF3 amino acids 90 to 192 (RBD) was generated by inserting the corresponding PCR product into pGEXCS digested with *Nco*I-*Bam*HI. All PCRs were performed with the Expand high-fidelity PCR system (Roche). The integrity of the PCR products was confirmed by sequencing.

For expression of GFP fusions in mammalian cells, NXF2 and NXF3 cDNAs were excised from the pGEMT-easy clones with the restriction enzymes *Bam*HI/*Hind*III (NXF2) or *Eco*RI/*Bam*HI (NXF3) and inserted into the vector pEGFP-C1 (Clontech) digested with *Bgl*II/*Hind*III or *Eco*RI/*Bam*HI, respectively. pEGFP-N3 (Clontech) derivatives encoding *Staphylococcus aureus* protein A (zz) fusions of p15-1 and p15-2a were constructed in two steps: first, p15-1 and p15-2a cDNAs were cloned into the vector pRN3zz using the *Nco*I/*Bam*HI restriction sites. Then, fragments encoding the zz tag fusions were released by digesting the corresponding plasmids with *Hind*III/*Not*I and inserted into pEGFP-N3 cut with the same enzymes. Additional plasmids used in this study were previously described (4, 8, 24, 39).

In vitro translation and expression of recombinant proteins. For generation of ³⁵S-labeled in vitro-translated proteins, the combined in vitro transcription-translation (TnT) kit from Promega was used following the instructions of the manufacturer. Translation was checked by sodium dodecyl sulfate-polyacrylamide gel electrophoresis (SDS-PAGE) and subsequent autoradiography. *E. coli* BL21(DE3) was used when proteins were expressed with the pGEX vectors, while *E. coli* M15[pREP4] was used for expressing proteins cloned into the pQE vectors. Recombinant proteins were purified as previously described (12).

GST pull-down and in vitro RNA binding assays. Gel retardation assays and GST pull-down assays were performed as previously described (4, 8, 39). For in vitro synthesis of a 43-nucleotide RNA probe, pBluescribe was linearized with *Bam*HI and transcribed with T3 RNA polymerase. The amounts of unlabeled competitor RNAs used per binding reaction are indicated in the figure legends.

Ran binding assays. The expression and purification of NTF2 and the expression of importin fragments have been described previously (21). Wild-type Ran or zzRanQ69L was immobilized on immunoglobulin G (IgG)-Sepharose in the presence of the Rna1 or RCC1 and energy-regenerating system, respectively. *E. coli* lysates (250 μ l) supplemented with equal amounts (5 μ M) of purified NTF2, p15-1, or p15-2a, and a lysate from *E. coli* expressing importin β (fragment 1-452) were subjected to binding to 15 μ l of IgG-Sepharose beads coated with RanGDP or RanQ69L-GTP. Binding was performed for 4 h at 4°C in a final volume of 1.5 ml of binding buffer (50 mM HEPES [pH 7.6], 200 mM NaCl, 2 mM magnesium acetate). After being washed three times with binding buffer, the bound protein was eluted with 1.5 M MgCl₂ and precipitated with isopropanol.

The starting material and the bound fractions were analyzed by SDS-PAGE and Coomassie blue staining.

Immunofluorescence. HeLa cells were transfected with FuGENE6 (Roche). Approximately 20 h after transfection, the cells were fixed with 3.7% formaldehyde for 10 min and subsequently permeabilized with 0.5% Triton X-100 for 15 min or were extracted first with 0.5% Triton X-100 for 1 min on ice and then fixed in formaldehyde. Indirect immunofluorescence assays were performed as previously described (2). The zz fusion proteins were visualized with a rabbit polyclonal anti-protein A antibody (Sigma) (dilution, 1:1,000 in phosphate-buffered saline supplemented with 5% fetal calf serum and 0.05% Tween 20) and a secondary Cy3-coupled anti-rabbit IgG antibody (diluted 1:4,000). Coverslips were mounted in VectaShield medium (Vector Labs).

DNA transfection and CAT assays. Human 293 cells were transfected by the calcium phosphate method. The cells were transfected at 50% confluency in 6-cm-diameter dishes with a plasmid DNA mixture. This mixture consisted of 0.5 μ g of pDM138 (13, 14), 1 μ g of pEGFP-C1 plasmid encoding green fluorescent protein (GFP)-tagged versions of TAP or TAP homologues, and 1 μ g of pEGFP-N3 derivatives encoding zz-tagged versions of p15-1 or p15-2a. The total amount of plasmid DNA transfected in each sample was held constant by adding the appropriate amount of the corresponding parental plasmids without an insert. The transfection efficiency was determined by including 0.5 μ g of pCH110 plasmid (Pharmacia) encoding β -galactosidase (β -Gal), as β -Gal expression from this vector is not affected by increasing levels of TAP expression. Quail QT6 cells were transfected using Lipofectamine Plus (Life Technologies). The cells were transfected at 50% confluency in six-well dishes with a plasmid DNA mixture. This mixture consisted of 0.5 μ g of pCH110, 0.1 μ g of pDM138 or pDM138-CTE, 0.5 μ g of pEGFP-C1 plasmids encoding GFP-tagged versions of TAP or TAP homologues, 0.5 μ g of pEGFP-N3zzp15-1, and 0.8 μ g of pBSIISK. The cells were harvested 40 h posttransfection, and chloramphenicol acetyltransferase (CAT) activity was measured as described previously (26). Protein expression levels were analyzed by Western blotting with anti-GFP antibodies kindly provided by Patrick Keller.

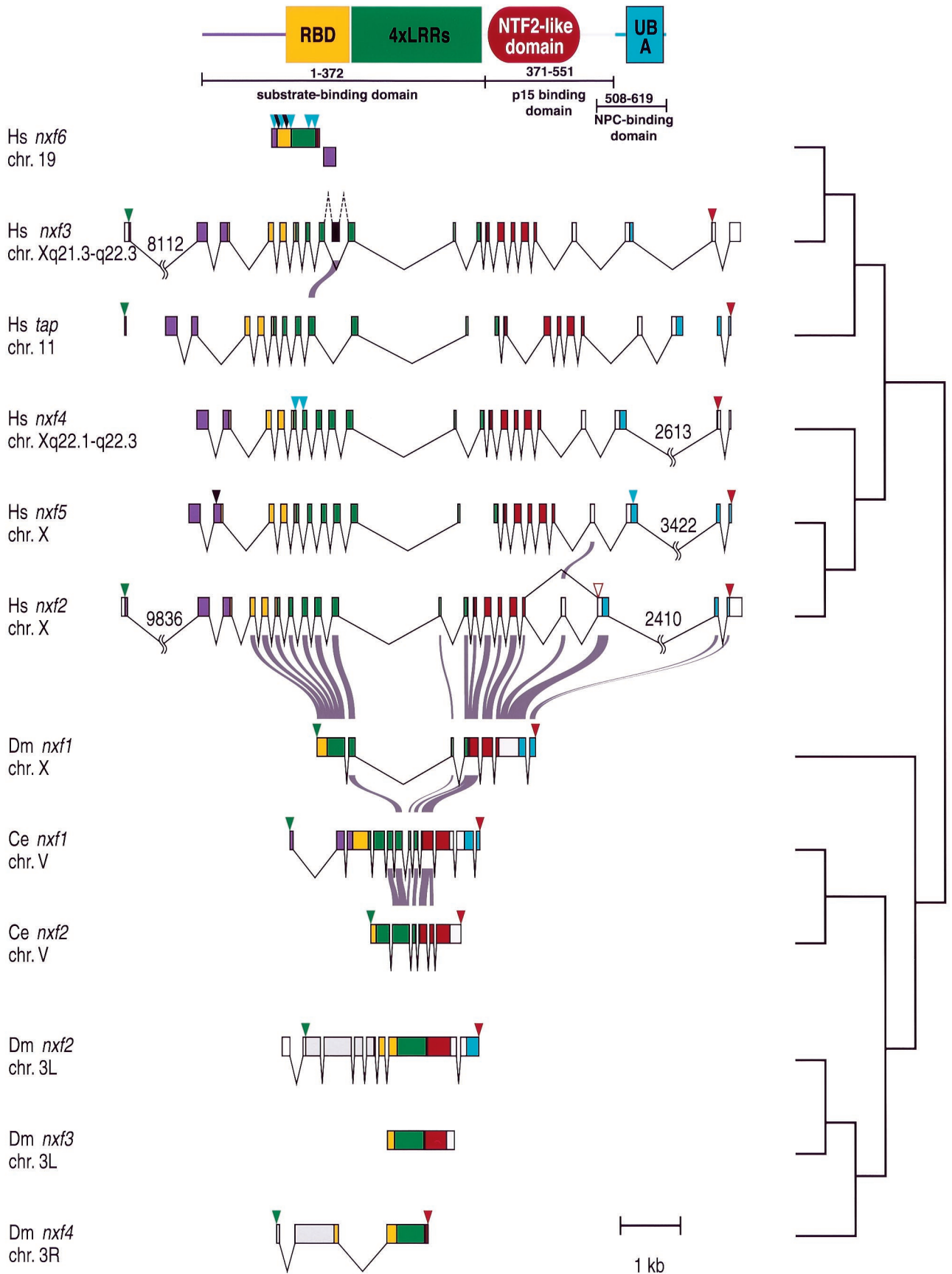
Nucleotide sequence accession numbers. The NXF2, NXF3, p15-2a, and p15-2b sequence data have been submitted to the EMBL database under accession numbers AJ277526, AJ277527, AJ277591, and AJ278323.

RESULTS

TAP belongs to a multigene family of evolutionarily conserved proteins. We performed an extensive search for TAP homologues. Using BLAST searches (3), we identified two homologues in the *C. elegans* genome, four in the *Drosophila* genome, and, in addition to TAP itself, four putative homologues in the human genome, including the two previously identified (5) (Fig. 1). In agreement with the Human Genome Nomenclature Committee, genes encoding TAP-like proteins in higher eukaryotes were named *nxf* (for nuclear export factor). To avoid confusion, we will call human NXF1 TAP.

In *C. elegans*, the two TAP-like genes were annotated only as hypothetical proteins (10). In *Drosophila*, three sequences were predicted genes (*nxf1*, *nxf2*, and *nxf4*) that show partial similarity to TAP, while the fourth sequence (*nxf3*) was detected in a portion of the genome for which no genes were predicted (1). In the human genome, several ESTs and regions in genomic DNA showed high similarity to TAP. These could be assembled into six nonidentical cDNA fragments and were found to correspond to four distinct TAP homologues when full-length inserts of various EST clones were sequenced. TAP cDNA sequence and sequences from the fragments were used to scan human genomic DNA to identify coding exons. Using the Genewise program, the genomic structure of the four human candidate TAP homologues, in addition to those of TAP itself and of a pseudogene, were predicted (Fig. 1). TAP mapped on chromosome 11. An intronless region corresponding to *nxf6* was located on chromosome 19. Due to its fragmentary nature and the multiple frameshifts and stop codons (Fig. 1), *nxf6* is likely to be a pseudogene. All four of the other homologous candidate genes were located on the X chromosome (Fig. 1).

When the predicted gene structures are compared, all human *nxf* genes show similar intron-exon patterns, with the exception of *nxf6* (Fig. 1). In spite of the presence of frameshifts and in-frame stop codons (Fig. 1), *nxf5* and *nxf4* have



retained this genomic structure. cDNAs encoding various alternative splice forms of *nxf5* have recently been isolated (Y. Lin, S. Frints, G. Froyen, and P. Marynen, submitted for publication), and at least one EST (accession number, AI150002) that corresponds to *nxf4* was identified, indicating that some splice forms of these genes are expressed. Thus, the genes might be subjected to alternative splicing, thereby avoiding the frameshifted exons. Alternative splicing seems to be an important mechanism in this gene family, as ESTs representing multiple alternative spliced forms exist in the database. Furthermore, multiple splice forms were cloned by reverse transcription-PCR (data not shown; Lin et al., submitted; A. S. Zolotukhin and B. K. Felber, personal communication), suggesting that multiple protein variants may result from the expression of human *nxf* genes.

Multiplication of *nxf* genes has occurred independently in different lineages. Phylogenetic analysis of the NXF protein family indicates that separate gene duplication events have occurred in several eukaryotic lineages (Fig. 2). Thus, although higher eukaryotes have several TAP homologues, they have evolved independently, so there is no clear one-to-one relationship of any isoforms.

Comparison of the deduced amino acid sequences of the TAP-like proteins in all species, including yeast, indicates that the overall domain organization of the protein family has been evolutionarily conserved (40) (Fig. 1 and 3), although, due to alternative splicing, not all domains are always expressed. At the genomic level, the LRRs are present in all members of the family; however, ESTs representing *H. sapiens* NXF3 and the cDNA we have isolated lack exon 9 (Fig. 1) and, as a consequence, part of the LRRs (Fig. 3). With the exception of *D. melanogaster nxf4*, the NTF2-like domain is also present in all *nxf* genes, including yeast *mex67*; however, in some forms of *H. sapiens nxf2*, exon 18 is skipped, resulting in an internal deletion within this domain and the introduction of a premature stop codon downstream of the skipped exon (Fig. 1). The UBA-like domain is absent in *D. melanogaster nxf3* and *nxf4* and *C. elegans nxf2* but is present in all human *nxf* genes. Nevertheless, the presence of premature stop codons in the *H. sapiens* NXF3, NXF4, and NXF5 genes (Fig. 3) results in proteins lacking part of this domain.

Characterization of the substrate binding domain of NXF2 and NXF3. cDNAs encoding human NXF2 and NXF3 were cloned by reverse transcription-PCR and sequenced (Fig. 3). To investigate whether these proteins interact with E1B-AP5 or the REF proteins and exhibit RNA binding activity, we performed *in vitro* binding assays.

[³⁵S]methionine-labeled NXF2 and NXF3 were synthesized *in vitro* in rabbit reticulocyte lysates and assayed for binding to glutathione agarose beads coated with either GST-E1B-AP5, GST-REF1-II, or GST. Binding of TAP to the recombinant proteins was tested in parallel. Figure 4A shows that TAP, NXF2, and NXF3 could be selected on glutathione agarose beads coated with E1B-AP5 (lane 3) but not on beads coated

with GST (lane 2). TAP and NXF2 bound to full-length REF1-II (fragment 1–163 [lane 6]) and to its C-terminal domain (fragment 103–163 [lane 5]) but not to its RBD (fragment 14–102 [lane 4]). In contrast, NXF3 did not interact with REF1-II. None of these interactions was affected by the presence of RNase A, indicating that they were not RNA mediated (data not shown; see reference 39 for TAP).

RNA and CTE binding activities were assayed by electrophoretic gel mobility retardation assays. To test general RNA binding affinity, a 43-nucleotide-long ³²P-labeled RNA probe was incubated with purified recombinant N-terminal domain of NXF2 (residues 1 to 377) fused to GST, and the resulting complexes were resolved in a native polyacrylamide gel and visualized by autoradiography (Fig. 4B). As a control, binding of GST-TAP (1 to 372) to the RNA probe was tested in parallel. The N-terminal domains of TAP and NXF2 bound to the RNA probe (Fig. 4B, lanes 2 and 6). Formation of both protein-RNA complexes was competed by the addition of increasing amounts of tRNA (Fig. 4B, lanes 3 to 5 and 7 to 9), suggesting that the proteins exhibit similar RNA binding affinities. The N-terminal domain of NXF3 could not be expressed in *E. coli*; however, full-length NXF3 coexpressed with p15-2a (see below) did not bind RNA (data not shown). The N-terminal domain of TAP contains a noncanonical RBD that exhibits general RNA binding activity (24). This domain is conserved in all vertebrate NXF proteins (24) (Fig. 1 and 3). Figure 4C shows that while the isolated RBDs of TAP and NXF2 bind RNA, the corresponding domain of NXF3 did not exhibit detectable RNA binding activity.

Binding to the CTE RNA probe was tested using *in vitro*-translated proteins. To assess the specificity of the interaction, the binding reactions were supplemented with increasing amounts of unlabeled CTE RNA or M36 RNA, a CTE derivative which does not bind TAP (12). Under conditions in which TAP bound specifically and with high affinity to the CTE RNA (Fig. 4D, lanes 3 to 6), neither NXF2 nor NXF3 interacted with the CTE probe (Fig. 4D, lanes 7 and 8). Moreover, recombinant NXF2 and NXF3, coexpressed in *E. coli* with p15-1 or p15-2a, did not show specific CTE binding (data not shown).

Next, we tested the abilities of NXF2 and NXF3 to promote CTE-dependent export of a precursor mRNA in quail cells. In this assay, TAP and TAP-like proteins were cotransfected with the reporter plasmid pDM138 (14) and its derivative pDM138-CTE. These plasmids harbor a single intron containing the CAT coding sequence, which is excised when the RNA is spliced (Fig. 4E). Cells transfected with the pDM138 plasmid express only the spliced transcripts in the cytoplasm and thus yield only trace levels of CAT enzyme activity (14). The presence of the CTE in the intron (pDM138-CTE) allows nuclear retention to be bypassed and export of the unspliced transcripts to be promoted (15). In quail cells, CTE-mediated export of this precursor mRNA requires coexpression of human TAP (15), which leads to an increase in CAT activity (Fig. 4F). This activation can be abolished by preventing TAP-nucleo-

FIG. 1. Intron-exon structure of the *nxf* genes. The domain organization of human TAP is indicated at the top. Hs, *H. sapiens*; Dm, *D. melanogaster*; Ce, *C. elegans*. When known, the chromosomal (chr.) locations are indicated below the gene names. Exons are colored according to the domains: purple, N-terminal portion found only in human homologues and *C. elegans nxf1*; yellow, RBD; green, LRR; red, NTF2-like domain; pink, linkers upstream and downstream of NTF2-like domain; cyan, UBA domain. 5' and 3' untranslated regions present in the ESTs or cDNA sequences are indicated by open boxes. Exons having no similarity to human TAP are gray. Introns are depicted as lines. The intron-exon structures are drawn to scale except for the long introns, which have breaks in the middle with the lengths indicated by numbers. An alternative splicing pathway is shown by lines above the gene (*nxf2*). A skipped exon is shown in black and connected by dotted lines (*nxf3*). Some characteristics of the sequences are indicated above the exon by filled triangles: green, initiation codon; red, termination codon; black, in-frame stop codon; cyan, frameshift. In *nxf2*, a stop codon created by alternative splicing is indicated as a red open triangle. On the complementary strand of *nxf6*, there is a region showing weak similarity to other TAP gene sequences; this region is shown in shift vertically. Some introns for the human TAP and NXF5 genes are not shown because the genes are mapped on distinct fragments of the genome sequences and the lengths of the introns are not clear. On the right, a simplified phylogenetic tree (not to scale) is shown.

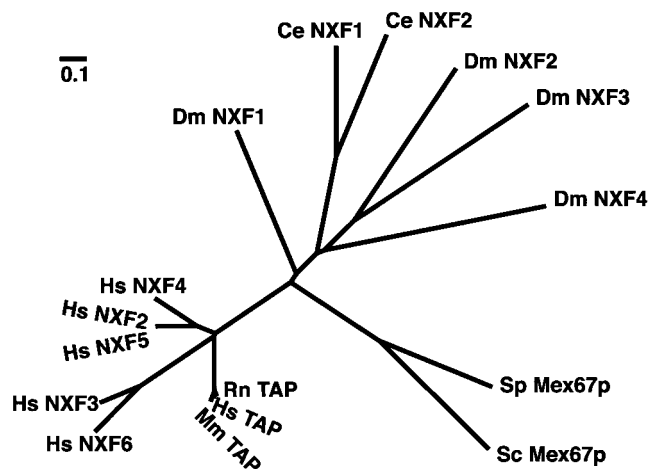


FIG. 2. Phylogenetic tree of NXF family sequences. The tree was drawn by the neighbor-joining method (34). Abbreviations (other than those in Fig. 1): Mm, *Mus musculus*; Rn, *Rattus norvegicus*; Sc, *S. cerevisiae*; Sp, *S. pombe*.

porin interaction (15) (Fig. 4F, TAP Δ NPC) or by deleting the RBD required for CTE binding (24). In contrast to TAP, neither NXF2 nor NXF3 could promote specific CTE-dependent export (Fig. 4F), although these proteins were expressed at comparable levels (data not shown).

Thus, NXF2 displays general affinity for RNA as reported previously for TAP and Mex67p (12, 17, 35, 39) and interacts with E1B-AP5 and Ref1-II, whereas NXF3 only interacts with E1B-AP5 and does not exhibit detectable RNA binding activity. Neither protein specifically interacts with the CTE RNA or mediates CTE-dependent export.

p15-2, a human p15 homologue that interacts with TAP and localizes to the nuclear rim. The NTF2-like domain of TAP heterodimerizes with p15 and is conserved in most members of the NXF family. Searches for p15 homologues revealed one *nxt*-like gene in *Drosophila* and *C. elegans* and two in available human genomic sequences (Fig. 5A). The additional human *nxt* gene was named *nxt2*. The proteins encoded by these human genes will be referred to as p15-1 and p15-2, respectively. *nxt2* is located on the X chromosome, and its genomic structure more closely resembles those of the homologues in other species than does the intronless *nxt1* gene on chromosome 20 (Fig. 5A). Human EST sequences include two alternative splice variants of *nxt2* (p15-2a and p15-2b) which differ in their 5' exons (Fig. 5A). The predicted p15-2 forms were confirmed by cloning and sequencing the corresponding cDNAs. Alignment of the deduced amino acid sequence of p15-2a with known homologues and phylogenetic analysis suggest that the two human *nxt* genes are the result of a recent duplication in the *nxt* lineage (Fig. 5B and C).

The subcellular localization of p15-2a fused to two IgG-binding units of protein A from *Staphylococcus aureus* (zz tag) was analyzed in transfected HeLa cells. Figure 5D shows that p15-2a was evenly distributed in the nucleoplasm and was excluded from the nucleolus. Furthermore, a fraction of the protein was detected in the cytoplasm. To investigate whether

p15-2a associates with the nuclear envelope, transfected HeLa cells were extracted with Triton X-100 prior to fixation (Fig. 5D, +Triton X-100). Under these conditions, most of the nucleoplasmic and cytoplasmic pools of the protein were solubilized. However, a fraction of p15-2a was resistant to detergent extraction and was clearly visualized in a rim at the nuclear periphery. Similar results were obtained when p15-2a was fused to GFP (data not shown). Thus, the subcellular localization of p15-2a is similar to that previously reported for p15-1 (7, 17).

p15-1 interacts with TAP and is closely related to NTF2 (Fig. 5C) (7, 17, 40). We therefore investigated whether p15-2a could interact with TAP or Ran. Lysates from *E. coli* supplemented with equimolar amounts of recombinant purified p15-1, p15-2a, or NTF2 were incubated with IgG-Sepharose beads coated with purified zzRanGDP, zzRanQ69L-GTP, or zzTAP. The RanQ69L mutant is GTPase deficient and remains in the GTP-bound form (19). In contrast to Black et al. (7), but in agreement with Katahira et al. (17), we could not observe binding of p15-1 or p15-2a to Ran (Fig. 5E, lanes 7, 8, 11, and 12). However, both proteins were selected on immobilized TAP (Fig. 5E, lanes 15 and 16), suggesting that they were properly folded. In addition, we could not detect binding of TAP-p15 heterodimers to RanGDP or to RanGTP (data not shown). Under the same conditions, NTF2 bound to RanGDP (Fig. 5E, lane 6), while the Ran binding domain of Importin β (fragment 1-452) bound RanQ69L-GTP (Fig. 5E, lane 13). Thus, both p15-1 and p15-2a directly interact with TAP but not with Ran.

Next, we tested whether the p15 proteins could also interact with NXF2 or NXF3. Untagged p15-1 and p15-2a were coexpressed in *E. coli* along with TAP, NXF2, or NXF3 fused to GST. The bacterial lysates were incubated with glutathione agarose beads, and after extensive washes, the bound proteins were eluted with SDS-sample buffer. Both p15-1 and p15-2a were copurified with TAP, NXF2, and NXF3 but not with GST (Fig. 5F). Moreover, coexpression of the NXF2 and NXF3 proteins with p15-1 or p15-2a significantly increased their stability, as full-length NXF3 could not be expressed in *E. coli* in the absence of p15 (data not shown).

NXF2, but not NXF3, binds to nucleoporins and localizes to the nuclear rim. To test nucleoporin binding of NXF2 and NXF3, we immobilized bacterially expressed GST-CAN (fragment 1690-2090) or GST on glutathione agarose beads. The beads were then incubated with in vitro-translated TAP, NXF2, or NXF3. Both TAP and NXF2 bound CAN, while no significant binding was observed for NXF3 (Fig. 6A). In order to determine whether NXF2 could interact with other FG-repeat containing nucleoporins, pull-down assays were performed with recombinant NXF2 or TAP fused to GST and in vitro-translated CAN (fragment 1690-1894), Nup153 (fragment 895-1475), or full-length Nup98 and p62. The TAP mutants W594A and D595R were used as negative controls (40). With the exception of Nup98, the nucleoporins tested bound to NXF2 with efficiencies similar to those with TAP (Fig. 6B, lane 6 versus lane 3).

Residues located at positions 593 to 595 in the TAP sequence (NWD [Fig. 3]) have been implicated in nucleoporin

FIG. 3. Multiple sequence alignment of NXF family sequences. First column, species names (Hs, *H. sapiens*; Dm, *D. melanogaster*; Ce, *C. elegans*); second column, protein names; third column, positions of the first aligned residues in each of the sequences. The positions conserved in 80% of the sequences are indicated in the consensus line: a, aromatic (FHXY); c, charged (DEHKR); h, hydrophobic (ACFGHIKLMRTVWY); l, aliphatic (LIV); o, hydroxyl (ST); p, polar (CDEHKRQST); s, small (ACDGNPSTV); t, turnlike (ACDEGHKRNQRST); u, tiny (AGS). The assigned domains are indicated below the consensus line. Highly conserved residues are indicated by colored boldface characters: orange, polar; light green, tiny; dark green, hydrophobic; blue, proline; light blue, hydroxyl; purple, cysteine. Exon boundaries are indicated by red marks.

Hs NXF6 1 -----SLPSGHTIGTVTKVTFQKVEQDVGLQRSSNWSKPVSA-GMYRSSHQWQDGLLAMHGL---TVRYTPCAI----R
Hs NXF3 1 -----MSLPSGHTTCHTDQVVRQRARCWDIYQRRFSSRSEPVNPG---MHSSSHQQDGDAAHGAHMDSPVRYTPYITSPVNRK
Hs TAP 1 -----MADEGKYSIEHDDERVNFPRQRKKGGRPFWRKYEGENRRSRRGGSGIRSSRLLEDQGDVAMSDAQDGPVRVYRNPYTRPNNRRG
Hs NXF4 1 -----QISEHSDGSSSP-QGKNKGGSSQGNFGEKLNLEHDEHGYELPPPHLQKVDENVEVGVHEDDPQIRNPNSTLQDPSRS
Hs NXF5 1 -----IAECRICSSSTF-QRRKKGSHFQGNFDRKRNCHYEHGGYELLPSRCQENDGSMEMRDVHKDRQLRHITPVRTQCNRKL
Hs NXF2 1 MCSTLKKCGTYRTEYAECHDHGSTF-QGRKKGSSFRDNFDRKRSCHYEHGGYERPPSHCQENDGSMEMRDVHKDRQLRHITPVRTQCNRKL
Dm NXF1 0
Ce NXF1 1 -----MERDQCFNGCWLRRRWEKSPMNRKGGFGRDAKQLSRRTKRNFRALDDPDTQSRVEDDPAVVPYR
consensus/80%hc.ct.....ht.t.....t...h..stph..ctp.ththt.....R.ps.t.....
domain(Hs TAP)

Hs NXF6 70 GTCHKQDQTHVNTKXQKPEKRTGPNRDRTLGSCXFKICIX-----NEKWLNLNLIQSQCXNPFLLIQFRYE-KMQAHIFVENASIA
Hs NXF3 78 GSFRRQDQTHVNMEREQKPPERRMEGNMDDGLTGSW-FKITVFP-FGIKYNEKWLNLNLIQNECVSPVFPVDFHYE-NMHSFFVENASIA
Hs TAP 77 DTWHDRDRRHIVTVRRDRAPPERRGGAGTSQDGTSKNW-FKITVFP-YGRKYDKAWLLSMIQSKCSVPVFPVDFHYE-NTRAOFFVEDASTAS
Hs NXF4 84 VKCHSE-----YDRIPPEREVEKNTQNGDPGTW-FKITVFP-YGIKYDKSWIVNSIQSHCSVPVFPVDFHYE-NKRAHFFIQDASAC
Hs NXF5 76 VKXHSEDOHTHTIWRNRKPPERRKMRNTQDENMRKW-FKITVFP-YGIKYDKAWLLSMIQSNCSVPVFPVDFHYE-NRACFFVQVSAAS
Hs NXF2 90 KW-HSEDEIRITTWRRNKPEPKMSQNTQDGYTRNW-FKITVFP-YGIKYDKAWLLSMIQSHCSVPVFPVDFHYE-NRACFFVQVSAAS
Dm NXF1 1 MSPHVFIPOVYRVE-RNCVIFFTDDYEA
Ce NXF1 64 ASLTSASSRRGGSSRGFQSAASIANTVGNADIV-YKCRATGAAKKVDKWLKQL-NQIIEFNKPLLWTDNARGDFEYVREDDETAS
consensus/80% ...ppt.....p.ths.ptt..ts..st..t.h.akhph.....sttWlhp.l.spss.sPhPl.a+h..p.pspaFlpstshA.
domain(Hs TAP)<---[RBD]---

Hs NXF6 153 ALKNVSGKIRDEDNKMSIFVNP--TXYPLOQRKLEKAKQIKLMVKKRCDSSQSSLDLQRLPFDPDLVTSDSKTASKP--RKCMAAFLH
Hs NXF3 165 ALKNVSGKIWEDNEKISIFVNPAGIPHFVHRELKSEKVEQIKLQAMNQCDVSEALDIQRLPFDPDLVTSDSKTASKP--RKCMAAFLH
Hs TAP 171 ALKAVNYKILDRNRRLSIIINSSAPPHTILNELKPEQVEQLKILMSKRYDGSQQALDLKGLRSDPDLVAQNDIVVNNR--RSCMAAFLH
Hs NXF4 157 ALKKNVCKIHEDEENQKIFVFNLSLTKPQSIQKMLKPKEMXIAKADPEQYDVSQQALDLQRLPFDPDLVTKHHDIDILNQ--RNYMAATLK
Hs NXF5 163 ALKDVSYKLYDDENQKICIFVSHFTAPYSVKNLKPQGMEMLEKLTMNKRYNVVQQALDLQRLPFDPDLVTKHHDIDILNQ--RNCMAAFLH
Hs NXF2 176 ALKDVSYKLYDDENQKICIFVSHFTAPYSVKNLKPQGMEMLEKLTMNKRYNVVQQALDLQRLPFDPDLVTKHHDIDILNQ--RNCMAAFLH
Dm NXF1 30 RIQHLGKNGHLDPGYRLMPRVRSGLPLVAIDAKF---EKMKVTMAKRYNIQTKALDLS--RFHADPDLKQVDFCLPFR--QNVMGAAID
Ce NXF1 152 TIRANRRRVVHKEGSTRVEFYTSKVPAPWMLKRE--TEIIRVVDKRRHNAENRVLDS--NFHEDEEFKAKDMMNLTKGNVMLTVLD
consensus/80% sl+tlsh+lhcc-st+h..hls..h...lppthK...hc.hKhhpphsspppLDlp...FcsD..hphhchh.p...ppsMuAsLc
domain(Hs TAP)<---[LRRs]---

Hs NXF6 239 VLQDNMPE-----AESVGMQDRGKQWS-QETCADRNFLS-TTFPDKSSNITSIILELFP
Hs NXF3 253 VHEENIPIT-----VMSAGEMDKWKIEPEKCADRSPVC-TTFSD-TSSNINISILELFP
Hs TAP 259 IIEENIPITLLSLNLSNNRRLYRLDDMSIVQKAPNLKILNLSGNELKSERELDKIKGLKLEELWLDGNSLC-DTFRD-QSTYIIRERFP
Hs NXF4 245 IIERNFPPITLLSLNLCNKLKLYHLGLDGLDIEKAPKVKTLNLSKNNLESAWELGKVKGLKLEELWLEGNPLC-STFSD-QSAYVSIIRERFP
Hs NXF5 251 IIERNFPPITLLSLNLCNKLKLYHLGLDGLDIEKAPKVKTLNLSKNNLESAWELGKVKGLKLEELWLEGNPLC-STFSD-QSAYVSIIRERFP
Hs NXF2 264 IIERNFPPITLLSLNLCNKLKLYHLGLDGLDIEKAPKVKTLNLSKNNLESAWELGKVKGLKLEELWLEGNPLC-STFSD-QSAYVSIIRERFP
Dm NXF1 112 IMCDDNIPLEALNLDNSISSMEAFKGVKRLPNLKIYLGDNKIPLSLHLVLRNLSILELVLKNNP-CRSRYKD-SQOIFIEVRRKFP
Ce NXF1 238 HIDDKYGNIVALSLSNRRIRHLDYASALVSIKFMVLELDSHNIHISTEKELEKFAQLPVERFFEGNPVVESPTQR--AAYIYIHQSFP
consensus/80% lhpcNhPp.....l.S.hchs+hGlp..tEhhh-tNsls.opapD.pus.lo.lthcFP
domain(Hs TAP)

Hs NXF6 291 KLLCLDGGQSPRPTLCGIEAXSRLPTCKGSPFGCDMLQNLLOFLQ-----GDRQGLLSAYHDE-ACFSLSIFFNPEDSAFSS
Hs NXF3 305 KLLCLDGGQSPRATLCGTEAHKRLPTCKGSPFGSEMKNLVLQFLQYLYIYDS---GDRQGLLSAYHDE-ACFSLSIFFNPEDSAFSS
Hs TAP 347 KLLRLDGHLEPPPIAFDVEAPTTLPPCKGSPFGTEMLKSLVLFHFLQYLYIYDS---GDRQGLLSAYHDE-ACFSLSIFFNPEDSAFSS
Hs NXF4 333 KLLCLDGGQELASPIIIGIEAPELIKPKCKGSETIKSLVLFHFLQYLYIYDS---EDRTGLLSYHDK-ACFSLITLNPEDPEFSS
Hs NXF5 339 KLLRLDGRLELAPVIVDIDSSETMKPCENFTGSETLKHVLVLFHFLQYLYIYDS---GDRQGLLSAYHDE-ACFSLAIFFDPKDSAFSS
Hs NXF2 352 KLLRLDGRLELAPVIVDIDSSETMKPCENFTGSETLKHVLVLFHFLQYLYIYDS---GDRQGLLSAYHDE-ACFSLAIFFDPKDSAFSS
Dm NXF1 200 KLVKIDGGETLEPQITFDLSEQRLLLETKASYLCDVAGAEVVRQFLDQYFRIFDS---GNRQALLDAYHEK-AMLSISMPASQAGHLNS
Ce NXF1 326 RCNMLDGVVQPLVVGPDLDIHDAMPFRAGYYPNPQIRVLVEFVTSYFDYFDGPDGQRTRRNLHNAIDADASTFSLTIEHLRGSSEHARH
consensus/80% KLLpLDGpp...hhshps.pph.ssKtsahss..lppLVhQFLppYa.haDu...tsRpsLhssYctt.uhhSlsh...tsst..p
domain(Hs TAP) ----->.....<---[NTF2-like domain]-----

Hs NXF6 336 -----FCFKFKDSRNKIKLKDPLRGELLKHTKL---DIVDLSALPKTQHDLSFLVDMWYQTEWMLCFSVNGVFKIEGQSQG-----
Hs NXF3 390 -----LAEYFKDSRNKIKLKDPLRFRLLKHTRL---NVVAFNLKPKTQHDVNSFVVDISAQTSTLCCFSVNGVFKIEGQSQG-----
Hs TAP 432 -----LEKYFKDSRNKIKLKDPLRIQLLKHTRK---EIVDLSVLPRTQHDLSYVVDLICIQTERRMLVFSVNGVFKIEGQSQG-----
Hs NXF4 418 -----NLCKYFKDSRNKIKLKDPLQRLLKHTRKCP---RNVDSLALPKTQHDFTSILVDMWYQTEWMLCFSVNGVFKIEGQSQG-----
Hs NXF5 424 -----LCKYFKDSRNKIKLKDPLKGLLKHTRK---DIVDLSALPKTQHDLSILVDMWYQTEWMLCFSVNGVFKIEGQSQG-----
Hs NXF2 437 -----FWKFNRLRLLNGEENRNLKYGRL---ACVSTLDEWPKTQHDRRTFTVDTIYINSMVFTVTLGFLKDLNDETNNPASEML
Dm NXF1 285 HND-ECFAQYAGVSHNVLKQERFARHARSARGAMDIIVALSKLPTSSHMRTFIVDVFLQSNLDLGFVFCGDLDTQTP
Ce NXF1 416h...shshp.lhp...thph..+..th...t.ss.Ls.hppopH.phohVdH.h.sp.hhsFoVpG1Fp-hp..p.s.....
consensus/80%h...shshp.lhp...thph..+..th...t.ss.Ls.hppopH.phohVdH.h.sp.hhsFoVpG1Fp-hp..p.s.....
domain(Hs TAP) ----->.....<---[NTF2-like domain]-----

Hs NXF6 336 -----SVLAFTRTFIATPGSSSLCIVNDELFRDTSHQG-----
Hs NXF3 467 -----SLRAFTRTFIATPGSSSLCIVNDELFRDTSHQG-----
Hs TAP 509 -----SVLAFTRTFIATPGSSSLCIVNDELFRDTSHQG-----
Hs NXF4 495 -----SDLAFMWTFITSGRNSSLCIVNDELFRDTSHQG-----
Hs NXF5 503 -----SVLAFTRTFIATPGSSSLCIVNDELFRDTSHQG-----
Hs NXF2 514 -----SVLAFTRTFIATPGSSSLCIVNDELFRDTSHQG-----
Dm NXF1 366 YDVRHFARITYVVPQNN-GFCIRNETFITVNAHEQVREFKRSQHQPAPGAMPSTSSAVTSPQAGAAAGLQGRNLNAGVATGPVAILSGD
Ce NXF1 499 -----SPSFRSRLVSPRENDSVAVISDQLFITVNAHEQVREFKRSQHQPAPGAMPSTSSAVTSPQAGAAAGLQGRNLNAGVATGPVAILSGD
consensus/80% ..s..hf.hoalhss.ts.shhls-dlhitlpsso.pl.....
domain(Hs TAP) ----->.....<---[NTF2-like domain]-----

Hs NXF6 336 -----TQSALFLVTPAFSSVPAFSQEQ-----QKMLPS-----
Hs NXF3 502 -----IQRAFAMPAPTPSSVPVTLSPQEQ-----QEMLQAFSTQSGMNLWSQEQCLQDNWDTYTRSAQAFTHLKAKEIPEVAFMK-----
Hs TAP 544 -----TQSALFIPVPAFSSVPAFSQEQ-----QEMLQAFSTQSGMNLWSQEQCLQDNWDTYTRSAQAFTHLKAKEIPEVAFMK-----
Hs NXF4 530 -----TQSALFIPVPAFSSVPAFSQEQ-----QEMLQAFSTQSGMNLWSQEQCLQDNWDTYTRSAQAFTHLKAKEIPEVAFMK-----
Hs NXF5 538 -----TQSALFIPVPAFSSVPAFSQEQ-----QEMLQAFSTQSGMNLWSQEQCLQDNWDTYTRSAQAFTHLKAKEIPEVAFMK-----
Hs NXF2 549 -----TQSALFIPVPAFSSVPAFSQEQ-----QEMLQAFSTQSGMNLWSQEQCLQDNWDTYTRSAQAFTHLKAKEIPEVAFMK-----
Dm NXF1 455 PLAATAFVNSGSAAISTTAVAPGAQDES-TKQMIEMASQSQMNVIWSRQCLEETNWFNHAAFVFEKLPKKNIPPEAFMK-----
Ce NXF1 551 -----VQVSAVQIAQIGVNGMGFDGAPALPTREEMIKAMCQSGMIPPFSKELADCAWNPFAQCFKN--EIKSVPAEAFMK-----
consensus/80%hpts.....st...sss.s.u.t.....pml.s.....
domain(Hs TAP) ----->.....<---[UBA domain]-----



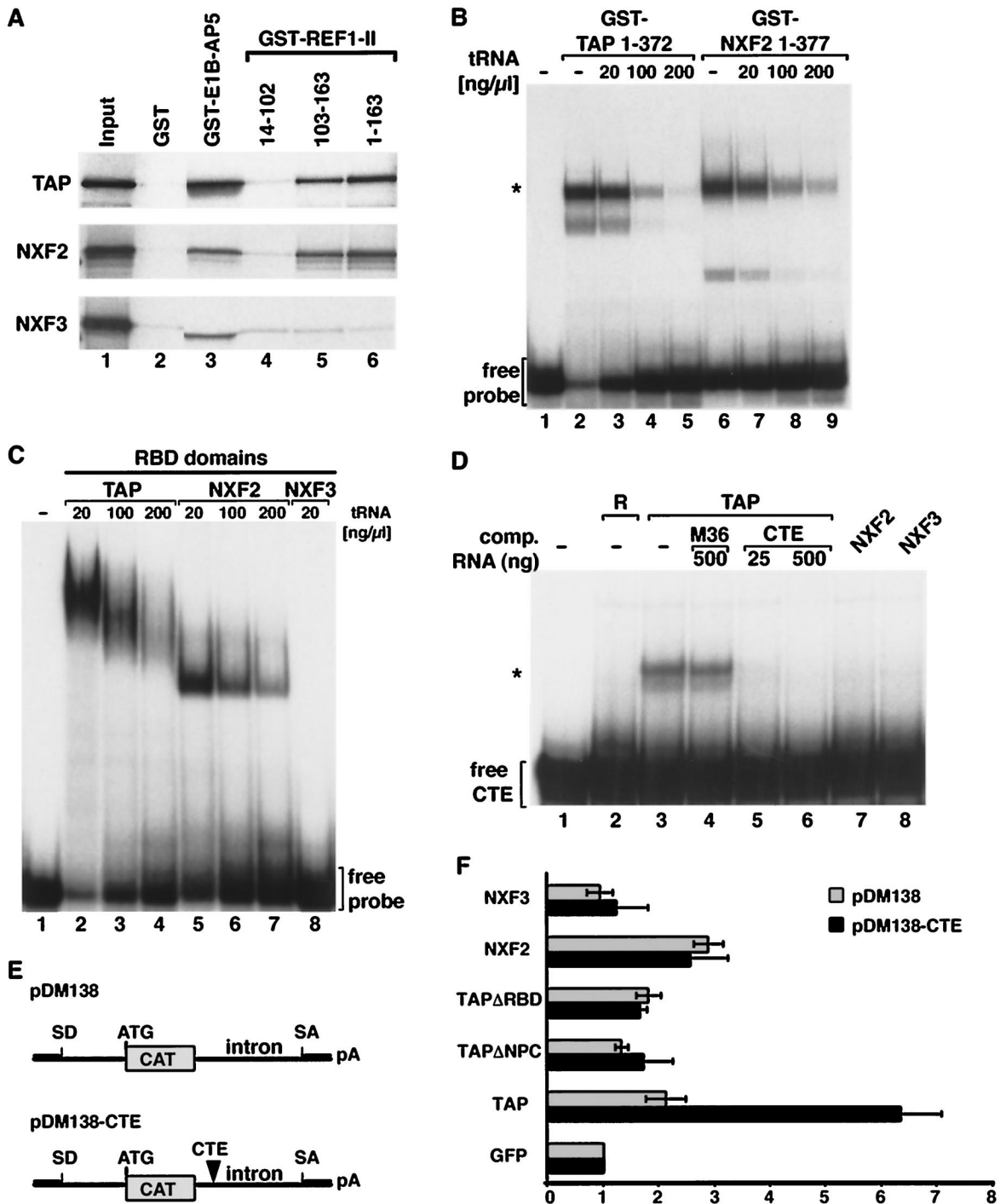


FIG. 4. Characterization of the N-terminal domains of NXF2 and NXF3. (A) GST pull-down assays were performed with [35 S]methionine-labeled TAP, NXF2, NXF3, and the recombinant proteins indicated above the lanes. Lanes 2, background obtained with glutathione agarose beads coated with GST; lanes 3, proteins selected on immobilized GST-E1B-AP5 (fragment 101–453); lanes 4 to 6, binding to GST-REF1-II or fragments of this protein as indicated. In all panels, 1/10 of the inputs (lanes 1) and 1/3 of the bound fractions (lanes 2 to 6) were analyzed on SDS-PAGE followed by fluorography. Supernatant fractions were analyzed in parallel in order to confirm that the absence of binding was not due to protein degradation (data not shown). (B and C) Gel mobility retardation assays were performed using a radiolabeled RNA probe derived from pBS polylinker and purified recombinant proteins fused to GST. (B) TAP or NXF2 N-terminal fragments (50 ng) were used; (C), 1.5 μ g of the corresponding RNA binding domains were used. Unlabeled competitor tRNA was added as indicated above the lanes. The position of the free RNA probe is indicated. The asterisk indicates the positions of the RNA-protein complexes. (D) A gel mobility retardation assay was performed with reticulocyte lysates unprogrammed (R) or programmed with cDNAs encoding TAP, NXF2, or NXF3. In lane 4, unlabeled M36 competitor RNA was added, while in lanes 5 and 6, CTE competitor RNA was included in the reaction mixtures. The amounts of the competitor RNAs are indicated above the lanes. The position of the free RNA probe is indicated on the left. (E) Schematic representation of pDM138 and pDM138-CTE vectors (14). (F) Quail cells were transfected with plasmids pDM138 or pDM138-CTE along with various plasmids encoding either GFP alone or fused to the N termini of TAP, NXF2, NXF3, or the TAP mutants indicated on the left. TAP Δ NPC has a deletion of residues 541 to 613. The cells were collected 40 h after transfection, and CAT activity was determined. Data from three separate experiments were expressed relative to the activities measured when GFP alone was coexpressed with pDM138 with or without CTE. The data are means \pm standard deviations.

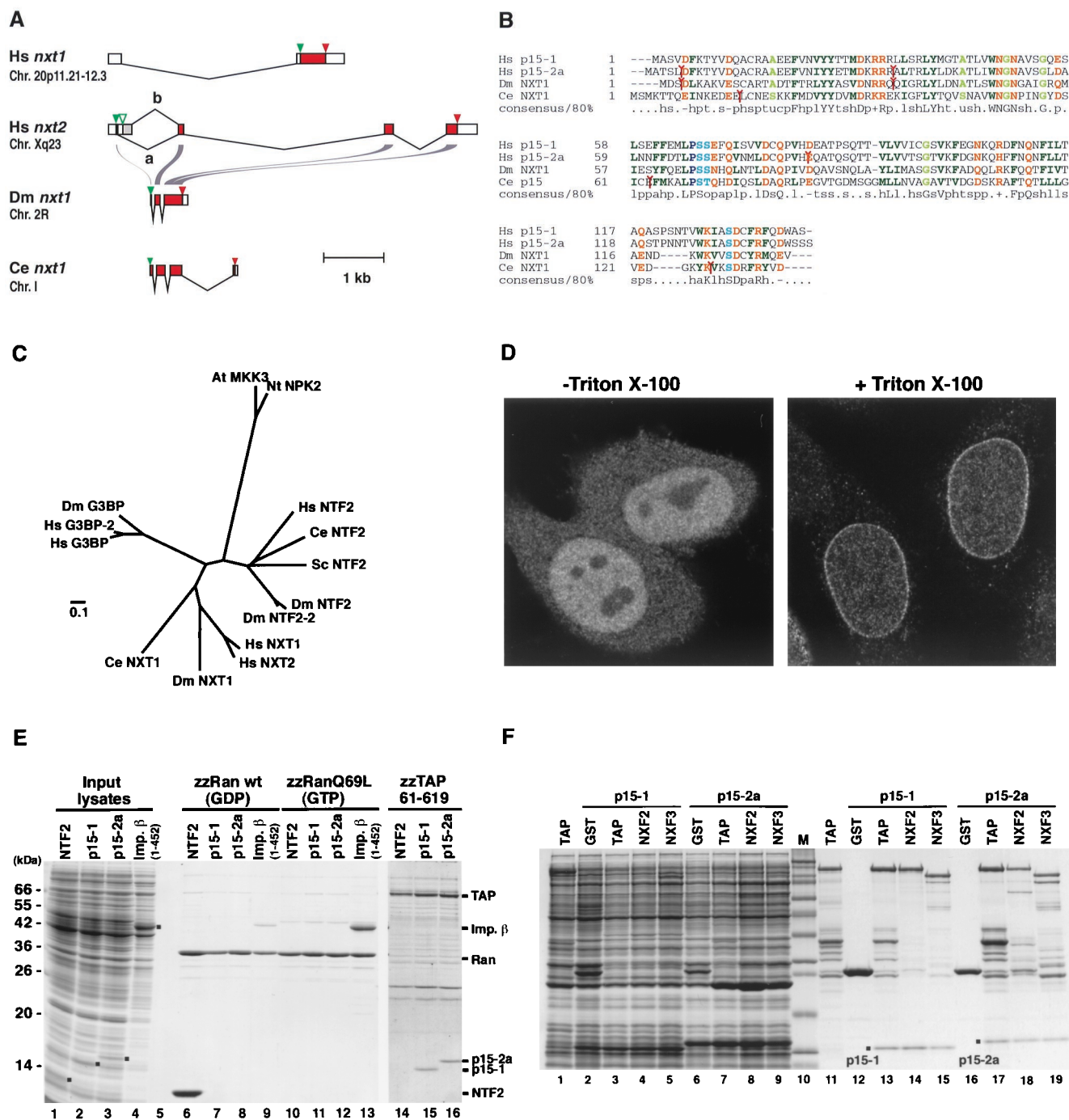


FIG. 5. p15-2a, a human p15-1 homologue, interacts with TAP and localizes to the nuclear rim. (A) Intron-exon structures of p15 family sequences. Protein coding regions and untranslated regions are colored red and white, respectively. The positions of initiation and termination codons are indicated by green and red triangles, respectively. For human p15-2a and -b, the alternative splicing pathway is shown by lines above the gene. The 5' exon of the p15-2a gene contains an open reading frame of five amino acids, while p15-2b gene 5' exon sequences contain an in-frame stop codon but no in-frame ATG. Therefore, translation of this mRNA may generate a truncated protein starting at methionine 29 in the p15-2a sequence. Alternatively, translation may start at the GTG codon (green open triangle), resulting in an open reading frame (gray), since this region does not show any similarity to the other p15 sequences. (B) Multiple sequence alignment of p15 family sequences. The symbols are as in Fig. 3. (C) Phylogenetic tree of the NTF2 family sequences. The tree was drawn by the neighbor-joining method (34). Abbreviations (other than those in Fig. 1 and 2): *At*, *Arabidopsis thaliana*; *Nt*, *Nicotiana tabacum*; G3BP, Ras-GAP SH3 domain binding protein; MKK3, MAP kinase 3; NPK2, a tobacco protein kinase. (D) Subcellular localization of p15-2a. HeLa cells were transfected with a pEGFP-N3 plasmid derivative expressing a zz fusion of p15-2a. The fusion protein was detected throughout the nucleoplasm and cytoplasm and was excluded from the nucleolus (left). On the right, HeLa cells were extracted with (+) Triton X-100 prior to fixation. A punctate labeling pattern was visible at the nuclear periphery for the p15-2a protein. (E) Lysates from *E. coli* expressing the Ran binding domain of Importin β (fragment 1-452) or supplemented with equimolar amounts of NTF2, p15-1, or p15-2a were incubated with IgG-Sepharose beads coated with purified zzRanGDP, zzRanQ69L-GTP, or zzTAP (fragment 61-619). After extensive washes, the bound proteins were eluted. One-hundredth of the inputs (lanes 1 to 4) and 1/10 of the bound fractions (lanes 6 to 16) were analyzed by SDS-PAGE followed by Coomassie blue staining. (F) Lysates from *E. coli* expressing GST fusions of TAP, NXF2, or NXF3 together with untagged versions of p15-1 or p15-2a were incubated with glutathione agarose beads. After extensive washes, the bound proteins were eluted with SDS sample buffer and analyzed by SDS-PAGE followed by Coomassie blue staining. Lanes 1 to 9, input lysates; lanes 11 to 19, bound fractions; lane 10, molecular mass markers (116, 97, 84, 66, 55, 45, 36, 29, 24, 20, and 14.2 kDa).

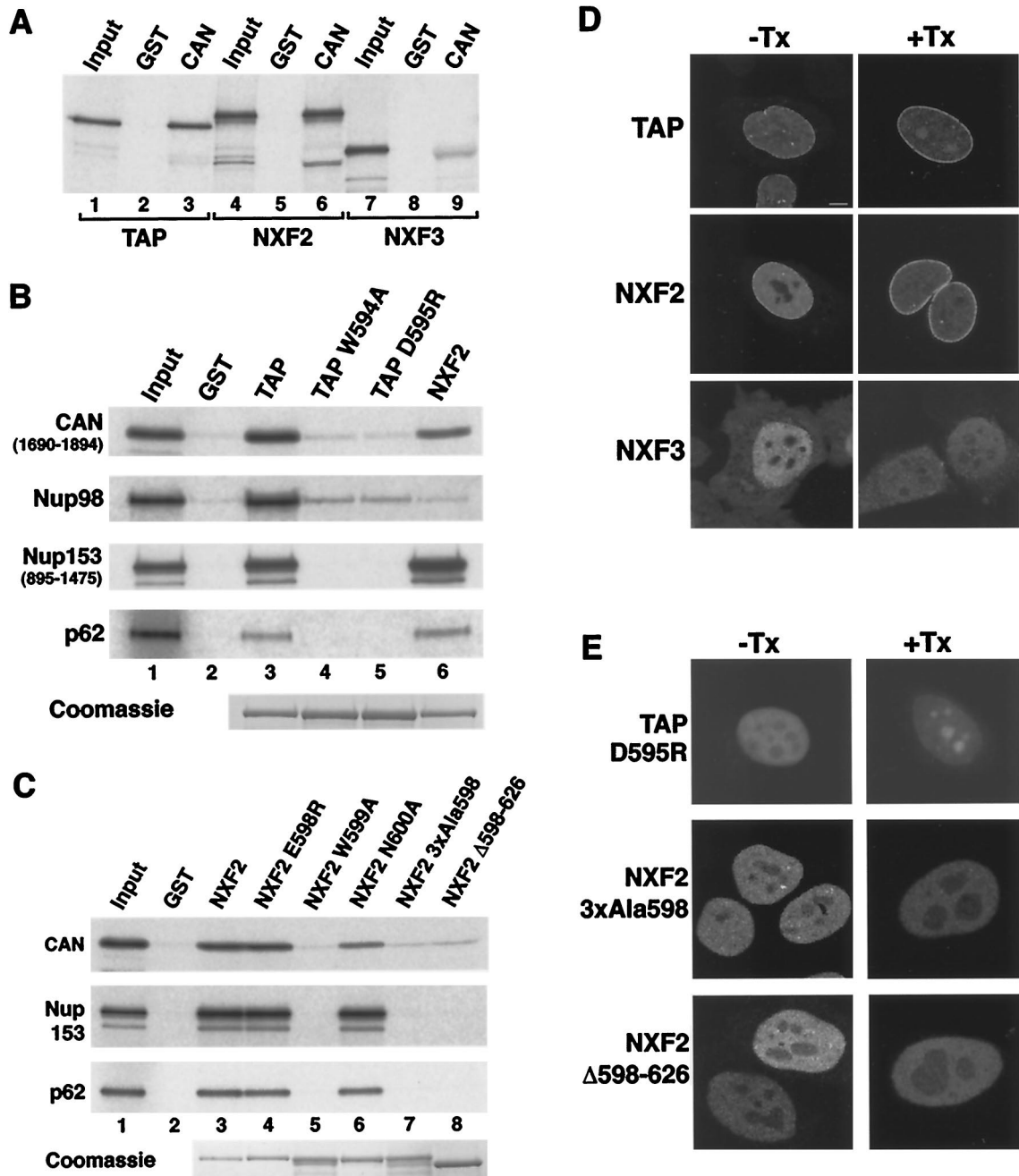


FIG. 6. A fraction of NXF2 localizes to the nuclear rim. (A) GST pull-down assays were performed with [³⁵S]methionine-labeled TAP, NXF2, or NXF3, and the recombinant proteins indicated above the lanes. One-tenth of the inputs (lanes 1, 4, and 7) and one-third of the bound fractions (lanes 2, 3, 5, 6, 8, and 9) were analyzed by SDS-PAGE followed by fluorography. (B) NXF2 interacts with multiple components of the NPC. GST pull-down assays were performed with the [³⁵S]methionine-labeled nucleoporins indicated on the left of the panels and recombinant GST or TAP, TAP W594A, TAP D595R, or NXF2 fused to GST, as indicated above the lanes. One-tenth of the input (lane 1) and one-third of the bound fractions (lanes 2 to 6) were analyzed on SDS-PAGE followed by fluorography. (C) GST pull-down assays were performed with the [³⁵S]methionine-labeled nucleoporins indicated on the left of the panels and recombinant GST, GST-NXF2, or various NXF2 mutants as indicated above the lanes. Samples were analyzed as indicated for panel A. (D and E) HeLa cells were transfected with pEGFP-C1 plasmid derivatives expressing GFP fusions of TAP, NXF2, and NXF3 or various TAP or NXF2 mutants as indicated on the left. Approximately 20 h after transfection, the cells were fixed in formaldehyde, permeabilized with Triton X-100, and directly observed with a fluorescence microscope. For all proteins, the GFP signal was detected throughout the nucleoplasm (-Tx). Cytoplasmic staining was also detected for NXF3. On the right (+Tx), HeLa cells were extracted with Triton X-100 prior to fixation. A punctate labeling pattern was visible at the nuclear periphery for TAP and NXF2, while in cells transfected with NXF3, TAP D595R, or the NXF2 mutants, no GFP signal was detected at the nuclear rim.

binding (40). We tested the effect of replacing the three loop residues of NXF2 with alanines. This substitution (3xAla598) disrupts nucleoporin binding in vitro as efficiently as the deletion of the entire NXF2 C-terminal domain (Δ598-626) (Fig. 6C,

lanes 7 and 8). As is the case for TAP, a single substitution of alanine for W599 was sufficient to disrupt nucleoporin binding (Fig. 6C, lane 5), while substitution of alanine for N600 or of arginine for E598 had no significant effect (Fig. 6C, lanes 4 and 6).

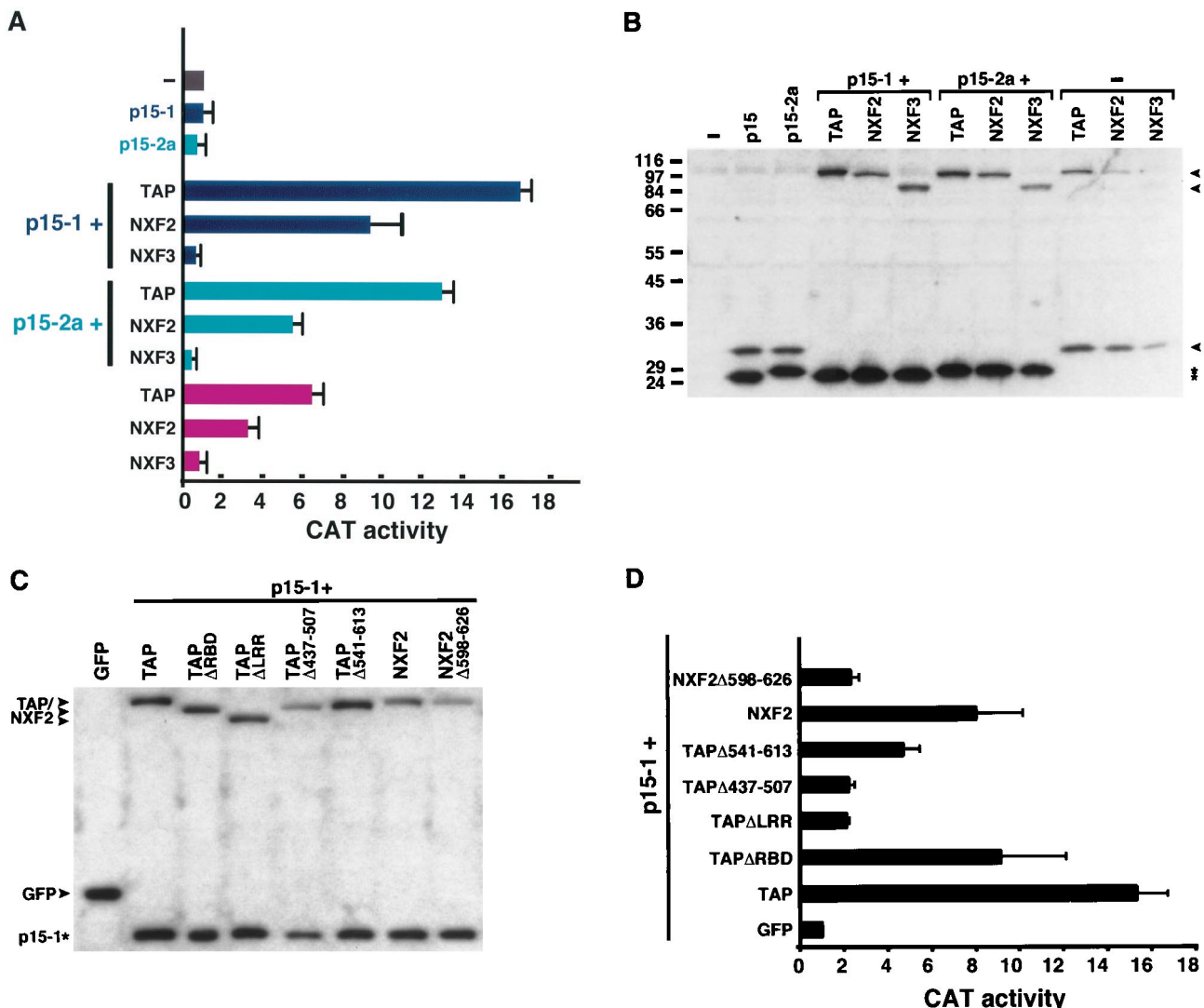


FIG. 7. NXF2 exhibits general RNA nuclear export activity. (A to D) Human 293 cells were transfected with a mixture of plasmids encoding β -Gal, CAT, and either GFP alone (-) or fused to the N termini of TAP, NXF2, NXF3, and various TAP and NXF2 mutants as indicated on the left. pEGFP-N3 derivatives encoding zz-tagged versions of p15-1 and p15-2a were cotransfected as indicated. The cells were collected 40 h after transfection, and β -Gal and CAT activities were determined. Data from three separate experiments were expressed relative to the activities measured when GFP alone was coexpressed with pDM138. The data are means \pm standard deviations. (B and C) Protein expression levels were analyzed by Western blotting with anti-GFP antibodies. (B) Arrowheads indicate the positions of NXF proteins fused to GFP or of GFP itself, while the asterisks show the positions of p15 proteins.

To analyze nucleoporin binding *in vivo*, the subcellular localization of NXF2 and NXF3 fused to GFP was investigated in transfected HeLa cells and compared to that of GFP-tagged TAP. GFP-tagged NXF2 and NXF3 were evenly detected in the nucleoplasm and were excluded from the nucleolus. Moreover, a fraction of NXF3 could be detected in the cytoplasm (Fig. 6D, -Tx). To visualize a potential nuclear envelope association, transfected cells were extracted with Triton X-100 prior to fixation (Fig. 6D, +Tx). As previously observed for TAP, a fraction of NXF2 was resistant to detergent extraction and remained associated with the nuclear envelope while NXF3 was not detected at the nuclear rim following Triton extraction. Furthermore, NXF2 and TAP mutants that do not interact with nucleoporins *in vitro* were not detected at the nuclear envelope upon Triton extraction (Fig. 6E).

NXF2, but not NXF3, can stimulate RNA export. We have developed an assay that tests mRNA export stimulation of TAP and its homologues. In this assay, TAP and TAP-like

proteins are cotransfected with the reporter plasmid pDM138 (14) in human 293 cells. As mentioned above, transfection with this plasmid yields only trace levels of CAT enzyme activity (13, 14). However, cotransfection with vectors expressing TAP and p15 nuclear retention to be bypassed and export of the unspliced transcripts to be promoted, increasing CAT activity (Fig. 7A). To test the effect of TAP-like proteins on *cat* gene expression, human 293 cells were cotransfected with a constant amount of pDM138 reporter plasmid, plasmids encoding TAP, NXF2, or NXF3 together with plasmids encoding p15-1 or p15-2a (Fig. 7A and D). Protein expression levels were analyzed by Western blotting (Fig. 7B and C). Overexpression of the TAP protein together with p15-1 increased *cat* expression by 15- to 17-fold compared to the expression levels obtained when only pDM138 vector was transfected, whereas coexpression of TAP with p15-2a resulted in 13-fold activation of *cat* expression (Fig. 7A). Coexpression of NXF2 with p15-1 or p15-2a activated *cat* expression up to 10- or 6-fold, respectively.

This level of induction may reflect the lower expression levels of NXF2 compared to TAP (Fig. 7B and C). In contrast, when coexpressed with p15-1 or p15-2a, NXF3 had no effect on *cat* activity, even though its expression levels in the presence of p15-1 were similar to that of TAP (Fig. 7A and B). Overexpression of p15-1 or p15-2a, in the absence of exogenous TAP or in the presence of a deletion mutant of TAP (TAP Δ 437–507) that no longer interacts with p15, had no effect on CAT activity (Fig. 7A and D). In contrast, overexpression of TAP or NXF2 in the absence of exogenous p15 resulted in a significant but modest increase in CAT activity (Fig. 7A); however, the levels of expression of TAP and NXF2 in the absence of p15 were also reduced (Fig. 7B). Therefore, p15-1 and p15-2a appear to increase the stability of TAP-like proteins. In summary, TAP and NXF2, when coexpressed with p15-1 or p15-2a, stimulate the export of the unspliced pre-mRNA, while NXF3 did not stimulate CAT gene expression. The ability of TAP and NXF2 to export pDM138 pre-mRNA is likely to reflect the genuine export activity of these proteins, as this activity could be abolished with various mutations in the TAP sequence, implying the need for a functional protein (Fig. 7D). In particular, this activity requires the LRRs and the NTF2-like domain. In contrast, the RBD and the NPC binding domain of TAP were not strictly required (Fig. 7D) (see Discussion). Thus, the lack of RNA export activity of NXF3 may not be due to the truncation of the UBA domain but to the deletion of part of the LRRs.

DISCUSSION

In this study, we present a combined evolutionary and functional characterization of the family of TAP-like proteins in higher eukaryotes. Members of this protein family were called NXF. We have further characterized two of four putative human NXF proteins, namely, NXF2 and NXF3, and have shown that NXF2 exhibits RNA export activity.

NXF proteins heterodimerize with p15. Previously, we have shown that TAP heterodimerizes with p15-1 via its NTF2-like domain (40). In this study, we show that the human genome encodes at least two p15 homologues and that both interact with TAP, NXF2, and NXF3 and participate in RNA nuclear export. However, the precise role of p15 in TAP-mediated export is not well defined. p15 binding is not strictly required for TAP-mediated export of CTE-bearing substrates (4, 8, 16) but appears to play a role in the general export activity of the NXF proteins (Fig. 7A and D). Whether these effects are due to a direct role of p15 in export or to an increased stability of NXF proteins when coexpressed with p15 is unclear.

The interaction between the NTF2-like domains of TAP and p15-1 is mediated by multiple rather than a few critical residues (40). Indeed, mutation of residues located at the heterodimer interface reduced but did not completely abolish heterodimerization in vitro (40). This provides an explanation for the TAP, NXF2, and NXF3 interactions with p15-1 and p15-2a studied here, as these interactions occur even though not all interface residues are conserved. The NTF2-like domain also occurs in Mex67p, the *S. pombe* and *S. cerevisiae*, NXF homologue (40). In *S. cerevisiae*, this domain is implicated in interaction with a protein known as Mtr2p (35, 38). Mtr2p does not exhibit obvious sequence similarities with p15, but secondary-structure predictions suggest that it could be a p15 analogue (40).

Functional conservation of the UBA-like domain. The nucleoporin binding domain of TAP includes a UBA domain (40). The known structure of UBA domains suggests a conserved loop (NWD at positions 593 to 595 in human TAP) is

involved in the interaction with nucleoporins. Replacement of these three residues by alanines was previously shown to block the ability of TAP to promote CTE-dependent export of a precursor mRNA in quail cells (15). Moreover, single-amino-acid changes in this loop are sufficient to impair binding of TAP and *C. elegans* NXF1 to nucleoporins in vitro and in vivo (40, 41) (Fig. 6). The mutational analysis of the UBA-like domain of NXF2 presented here further supports the prediction that the conserved loop residues of the UBA-like domain have a critical role in the interaction of NXF proteins with nucleoporins. Conversely, based on these observations, it was possible to predict that NXF proteins having a truncated UBA domain are unlikely to directly interact with nucleoporins. This prediction was confirmed for NXF3.

Surprisingly, in spite of its conservation, the UBA domain of Mex67p is not sufficient for nucleoporin binding, and Mex67p lacking the UBA domain can bind to nucleoporins in the presence of Mtr2p (38). The possibility that vertebrate NXF proteins lacking the NPC binding domain can still interact with nucleoporins in the presence of p15 requires further investigation; however, NXF3 did not associate with nucleoporins either in vivo or in vitro when coexpressed with p15 (data not shown).

TAP binds Nup98 in vitro, but this interaction is not required for its localization at the nuclear rim, as in *Nup98*^{-/-} cells, TAP remains at the nuclear envelope (43). The observation that NXF2 localizes at the nuclear rim and can promote export of the pDM138 pre-mRNA in the absence of Nup98 binding is consistent with the observation that *Nup98*^{-/-} cells do not display an overt export inhibition phenotype (43). Thus, although TAP and NXF2 interact with multiple nucleoporins in vitro, the nucleoporins that are responsible for their localization at the nuclear rim remain to be identified. Moreover, the mechanism by which NXF proteins regulate their binding to nucleoporins is unknown.

Role of NXF proteins in RNA nuclear export. In yeast, Mex67p is involved in the export of bulk polyadenylated RNAs (36). Evidence for an essential role in mRNP export has been recently obtained for the *C. elegans* protein NXF1 (41). Moreover, TAP is directly implicated in the export of simian type D retroviral RNAs bearing the CTE (8, 12). Although we cannot exclude the possibility that some TAP homologues may have a function other than export, the conservation of their structural organization and the observation that at least three members of the NXF family are implicated in RNA export suggest that these proteins are likely to participate, directly or indirectly, in the export of cellular mRNAs to the cytoplasm. The diversification of NXF proteins in higher eukaryotes compared to yeast may reflect a greater substrate complexity or tissue-specific requirements. Consistent with this possibility is the observation that human NXF5 is expressed in brain (Lin et al., submitted).

NXF proteins may associate with cellular mRNPs directly, by binding to the mRNA, or indirectly, through interaction with hnRNP-like proteins. Recently, several TAP partners that could facilitate its interaction with cellular mRNPs have been identified. These include E1B-AP5, RAE1, and members of an evolutionarily conserved family of hnRNP-like proteins, the Yra1p/REF proteins (4, 37, 39). Aside from these, other RNA binding proteins may also facilitate TAP binding to the mRNPs, as Y14, an hnRNP-like protein that preferentially associates with spliced mRNAs, has recently been shown to be present in a complex containing TAP (18). In vitro, Y14 interacts with TAP and NXF2 (data not shown); therefore, it is possible that Y14, directly or indirectly, recruits NXF proteins to mRNPs in a post-splicing-dependent manner (18). Besides Y14, several other proteins form splicing-dependent inter-

actions with mRNA. These include the splicing coactivator SRm160, the acute myeloid leukemia-associated protein DEK, and several unidentified proteins (23, 25). These proteins may also link NXFs with mRNAs. NXF proteins may then be more efficiently loaded on mRNAs that have been produced by splicing. Therefore, it is possible that the pDM138 precursor mRNA cannot efficiently compete with other mRNAs for binding to NXFs, i.e., NXFs may be limiting for this substrate; hence, its export can be stimulated by overexpression of NXF-p15 heterodimers. Consistent with this is the observation that overexpression of TAP-p15 heterodimers does not stimulate export of reporter mRNAs that are efficiently expressed (I. C. Braun and E. Izaurralde, unpublished data).

TAP-mediated export of pDM138 pre-mRNA requires the LRRs and the NTF2-like domain, while deletion of the RBD or of the NPC binding domain impaired but did not abolish export (Fig. 7D). This is in sharp contrast to the situation observed when TAP-mediated export of pDM138-CTE is monitored in quail cells. In this case, both the RBD and the NPC binding domain are absolutely required (Fig. 4F). The RBD of TAP is required in *cis* to the LRRs for specific binding to the CTE RNA (24). Hence, this domain is essential for TAP-mediated export of CTE-containing substrates, whereas binding of TAP to pDM138 pre-mRNA may be mediated by protein-protein interactions. We have previously reported that the requirements for the NTF2-like and UBA domains of TAP are substrate dependent (4, 8). Indeed, in *Xenopus* oocytes, TAP-mediated export of CTE-bearing intron lariats is independent of these domains (8), while export of U6-CTE requires the UBA domain but not the NTF2-like domain (4). In quail cells, TAP-mediated export of pDM138-CTE pre-mRNA is abolished by mutations or deletions of the UBA domain (15) (Fig. 4) but is only reduced by mutations preventing p15 binding (16). Finally, the C-terminal domain of Mex67p is important but not essential for mRNA export (38). Thus, the functionality of NXF protein domains may be influenced by the specific set of proteins associated with the RNP export substrate. Discovery of the precise roles of NXF protein domains and the mechanism by which these proteins mediate directional transport of RNP substrates across the NPC remains an important goal for the future.

ACKNOWLEDGMENTS

The technical support of Michaela Rode is gratefully acknowledged. We thank Tom Hope and Matthias Dobbstein for the kind gift of plasmids pDM138 and pDM138-CTE. We thank Birthe Fahrenkrog, Maarten Fornerod, Iain W. Mattaj, and Christel Schmitt for critical reading of the manuscript. We are grateful to Barbara Felber, Guy Froyen, and Peter Marynen for communicating their results prior to publication.

This study was supported by the German Ministry of Research and Technology (BMBF), the Swiss National Science Foundation, the European Molecular Biology Organization (EMBO), and the Human Frontier Science Program Organization (HFSPO).

A.H. and M.S. contributed equally to this work.

REFERENCES

- Adams, M. D., S. E. Celniker, R. A. Holt, C. A. Evans, J. D. Gocayne, P. G. Amanatides, S. E. Scherer, P. W. Li, R. A. Hoskins, et al. 2000. The genome sequence of *Drosophila melanogaster*. *Science* **287**:2185–2195.
- Almeida, F., R. Saffrich, W. Ansorge, and M. Carmo-Fonseca. 1998. Microinjection of anti-coilin antibodies affects the structure of coiled bodies. *J. Cell Biol.* **142**:899–912.
- Altschul, S. F., T. L. Madden, A. A. Schaffer, J. Zhang, Z. Zhang, W. Miller, and D. J. Lipman. 1997. Gapped BLAST and PSI-BLAST: a new generation of protein database search programs. *Nucleic Acids Res.* **25**:3389–3402.
- Bachi, A., I. C. Braun, J. P. Rodrigues, N. Panté, K. Ribbeck, C. von Kobbe, U. Kutay, M. Wilm, D. Görlich, M. Carmo-Fonseca, and E. Izaurralde. 2000. The C-terminal domain of TAP interacts with the nuclear pore complex and promotes export of specific CTE-bearing RNA substrates. *RNA* **6**:136–158.
- Bear, J., W. Tan, A. S. Zolotukhin, C. Taberero, E. A. Hudson, and B. K. Felber. 1999. Identification of novel import and export signals of human TAP, the protein that binds to the CTE element of the type D retrovirus mRNAs. *Mol. Cell. Biol.* **19**:6306–6317.
- Bharathi, A., A. Ghosh, W. A. Whalen, J. H. Yoon, R. Pu, M. Dasso, and R. Dhar. 1997. The human RAE1 gene is a functional homologue of *Schizosaccharomyces pombe* rae1 gene involved in nuclear export of Poly(A)+ RNA. *Gene* **198**:251–258.
- Black, B. E., L. Lévesque, J. M. Holaska, T. C. Wood, and B. Paschal. 1999. Identification of an NTF2-related factor that binds RanGTP and regulates nuclear protein export. *Mol. Cell. Biol.* **19**:8616–8624.
- Braun, I. C., E. Rohrbach, C. Schmitt, and E. Izaurralde. 1999. TAP binds to the constitutive transport element (CTE) through a novel RNA-binding motif that is sufficient to promote CTE-dependent RNA export from the nucleus. *EMBO J.* **18**:1953–1965.
- Brown, J. A., A. Bharathi, A. Ghosh, W. Whalen, E. Fitzgerald, and R. Dhar. 1995. A mutation in the *Schizosaccharomyces pombe* rae1 gene causes defects in poly(A)+ RNA export and in the cytoskeleton. *J. Biol. Chem.* **270**:7411–7419.
- The *C. elegans* Sequencing Consortium. 1998. Genome sequence of the nematode *C. elegans*: a platform for investigating biology. *Science* **282**:2012–2018.
- Galtier, N., M. Gouy, and C. Gautier. 1996. SEAVIEW and PHYLO_WIN: two graphic tools for sequence alignment and molecular phylogeny. *Comput. Appl. Biosci.* **12**:543–548.
- Grüter, P., C. Taberero, C. von Kobbe, C. Schmitt, C. Saavedra, A. Bachi, M. Wilm, B. K. Felber, and E. Izaurralde. 1998. TAP, the human homologue of Mex67p, mediates CTE-dependent RNA export from the nucleus. *Mol. Cell* **1**:649–659.
- Hope, T. J., X. Huang, D. McDonald, and T. G. Parslow. 1990. Steroid-receptor fusion of the human immunodeficiency virus type 1 Rev transactivator: mapping cryptic functions of the arginine-rich motif. *Proc. Natl. Acad. Sci. USA* **87**:7787–7791.
- Huang, X., T. J. Hope, B. L. Bond, D. McDonald, K. Grahl, and T. G. Parslow. 1991. Minimal Rev-response element for type 1 human immunodeficiency virus. *J. Virol.* **65**:2131–2134.
- Kang, Y., and B. R. Cullen. 1999. The human TAP protein is a nuclear mRNA export factor that contains novel RNA-binding and nucleocytoplasmic transport sequences. *Genes Dev.* **13**:1126–1139.
- Kang, Y., H. P. Bogerd, and B. R. Cullen. 2000. Analysis of cellular factors that mediate nuclear export of RNAs bearing the Mason-Pfizer monkey virus constitutive transport element. *J. Virol.* **74**:5863–5871.
- Katahira, J., K. Sträßer, A. Podtelejnikov, M. Mann, J. U. Jung, and E. Hurt. 1999. The Mex67p-mediated nuclear mRNA export pathway is conserved from yeast to human. *EMBO J.* **18**:2593–2609.
- Kataoka, N., J. Yong, V. N. Kim, F. Velazquez, R. A. Perkinson, F. Wang, and G. Dreyfuss. 2000. Pre-mRNA splicing imprints mRNA in the nucleus with a novel RNA-binding protein that persists in the cytoplasm. *Mol. Cell* **6**:673–682.
- Klebe, C., F. R. Bischoff, H. Pönstingl, and A. Wittinghofer. 1995. Interaction of the nuclear GTP-binding protein Ran with its regulatory proteins RCC1 and RanGAP1. *Biochemistry* **34**:639–647.
- Kraemer, D., and G. Blobel. 1997. mRNA binding protein mrnp 41 localizes to both nucleus and cytoplasm. *Proc. Natl. Acad. Sci. USA* **94**:9119–9124.
- Kutay, U., E. Izaurralde, F. R. Bischoff, I. W. Mattaj, and D. Görlich. 1997. Dominant-negative mutants of importin- β block multiple pathways of import and export through the nuclear pore complex. *EMBO J.* **16**:1153–1163.
- Mattaj, I. W., and L. Englmeier. 1998. Nucleocytoplasmic transport: the soluble phase. *Annu. Rev. Biochem.* **67**:256–306.
- Le Hir, H., E. L. Maquat, and J. M. Moore. 2000. Pre-mRNA splicing alters mRNP composition: evidence for stable association of proteins at exon-exon junctions. *Genes Dev.* **14**:1098–1108.
- Liker, E., E. Fernandez, E. Izaurralde, and E. Conti. The structure of the mRNA nuclear export factor TAP reveals a *cis* arrangement of a non-canonical RNP domain and a leucine-rich-repeat domain. *EMBO J.*, in press.
- McGarvey, T., E. Rosonina, S. McCracken, Q. Li, R. Arnaout, E. Mientjes, A. J. Nickerson, D. Awrey, J. Greenblatt, G. Grosveld, and B. J. Blencowe. 2000. The acute myeloid leukemia-associated protein DEK forms a splicing-dependent interaction with exon-product complexes. *J. Cell Biol.* **150**:309–320.
- Morency, C. A., J. R. Neumann, and K. O. Russian. 1987. A novel rapid assay for Chloramphenicol-acetyl transferase gene expression. *BioTechniques* **5**:444–448.
- Murphy, R., J. L. Watkins, and S. R. Wente. 1996. GLE2, a *Saccharomyces cerevisiae* homologue of the *Schizosaccharomyces pombe* export factor RAE1, is required for nuclear pore complex structure and function. *Mol. Biol. Cell* **7**:1921–1937.
- Nakielnny, S., and G. Dreyfuss. 1999. Transport of proteins and RNAs in and out of the nucleus. *Cell* **99**:677–690.
- Parks, T. D., K. K. Leather, E. D. Howard, S. A. Johnston, and W. G.

- Dougherty. 1994. Release of proteins and peptides from fusion proteins with a recombinant plant virus proteinase. *Anal. Biochem.* **216**:413–417.
30. Pasquinelli, A. E., R. K. Ernst, E. Lund, C. Grimm, M. L. Zapp, D. Rekosh, M.-L. Hammarskjöld, and J. E. Dahlberg. 1997. The constitutive transport element (CTE) of Mason-Pfizer Monkey Virus (MPMV) accesses an RNA export pathway utilized by cellular messenger RNAs. *EMBO J.* **16**:7500–7510.
 31. Pritchard, C. E. J., M. Fornerod, L. H. Kasper, and J. M. A. van Deursen. 1999. RAE1 is a shuttling mRNA export factor that binds to a GLEBS-like NUP98 motif at the nuclear pore complex through multiple domains. *J. Cell Biol.* **145**:237–253.
 32. Ryan, K., and S. R. Wente. 2000. The nuclear pore complex: a protein machine bridging the nucleus and cytoplasm. *Curr. Opin. Cell Biol.* **12**:361–371.
 33. Saavedra, C. A., B. K. Felber, and E. Izaurralde. 1997. The simian retrovirus-1 constitutive transport element CTE, unlike HIV-1 RRE, utilises factors required for cellular RNA export. *Curr. Biol.* **7**:619–628.
 34. Saitou, N., and M. Nei. 1987. The neighbor-joining method: a new method for reconstructing phylogenetic trees. *Mol. Biol. Evol.* **4**:406–425.
 35. Santos-Rosa, H., H. Moreno, G. Simos, A. Segref, B. Fahrenkrog, N. Panté, and E. Hurt. 1998. Nuclear mRNA export requires complex formation between Mex67p and Mtr2p at the nuclear pores. *Mol. Cell Biol.* **18**:6826–6838.
 36. Segref, A., K. Sharma, V. Doye, A. Hellwig, J. Huber, R. Lührmann, and E. Hurt. 1997. Mex67p, a novel factor for nuclear mRNA export, binds to both poly(A)⁺ RNA and nuclear pores. *EMBO J.* **16**:3256–3271.
 37. Sträßer, K., and E. Hurt. 2000. Yra1p, a conserved nuclear RNA-binding protein, interacts directly with Mex67p and is required for mRNA export. *EMBO J.* **19**:410–420.
 38. Sträßer, K., J. Baßler, and E. Hurt. 2000. Binding of the Mex67p/Mtr2p heterodimer to FXFG, GLFG, and FG repeat nucleoporins is essential for nuclear mRNA export. *J. Cell Biol.* **150**:695–706.
 39. Stutz, F., A. Bachi, T. Doerks, I. C. Braun, B. Séraphin, M. Wilm, P. Bork, and E. Izaurralde. 2000. REF, an evolutionarily conserved family of hnRNP-like proteins, interacts with TAP/Mex67p and participates in mRNA nuclear export. *RNA* **6**:638–650.
 40. Suyama, M., T. Doerks, I. C. Braun, M. Sattler, I. Izaurralde, and P. Bork. 2000. Prediction of structural domains of TAP reveals details of its interaction with p15 and nucleoporins. *EMBO Rep.* **1**:53–58.
 41. Tan, W., A. S. Zolotukhin, J. Bear, D. J. Patenaude, and B. K. Felber. The mRNA export in *C. elegans* is mediated by Ce-TAP1, an orthologue of human TAP and *S. cerevisiae* Mex67p. *RNA*, in press.
 42. Thompson, J. D., D. G. Higgins, and T. J. Gibson. 1994. CLUSTAL W: improving the sensitivity of progressive multiple sequence alignment through sequence weighting, position-specific gap penalties and weight matrix choice. *Nucleic Acids Res.* **22**:4673–4680.
 43. Wu, X., L. H. Kasper, T. Ralitsa, R. T. Mantcheva, B. M. A. Fontoura, G. T. Mantchev, G. Blobel, and J. M. A. van Deursen. NUP98 is required for gastrulation, proper nuclear pore complex assembly and efficient protein import. *J. Cell Biol.*, in press.

2.1.2 Paper 2:

NXF5, a novel member of the nuclear RNA export factor family, is lost in a male patient with a syndromic form of mental retardation

Jun, L., Frints, S., Duhamel, H., Herold, A., Abad-Rodrigues, J., Dotti, C., Izaurrealde, E., Marynen, P., Froyen, G. (2001) *Curr Biol* **11**, 1381-1391.

Context

The work presented in this manuscript was initiated and mainly carried out in a laboratory at the University of Leuven concerned with the molecular mechanisms causing X-linked mental retardation. The analysis of the molecular basis causing mental retardation in a male patient pointed to a gene (*nxf5*) belonging to the NXF family. As members of this family are implicated in nuclear mRNA export, a possible role of NXF5 in this process was suggested.

Summary of results and conclusions

The analysis of the genetic defects of the patient identified an X-chromosomal inversion [*inv(X) (p21.1;q22)*]. The Xq22 breakpoint was found to be positioned in the *nxf5* gene, which lies in a cluster of *nxf* genes including *nxf2-5*. RT-PCR analysis showed that no *nxf5* mRNA can be detected in the patient while the levels of mRNAs encoded by neighboring (e.g. *nxf2*, *nxf3* mRNAs) or housekeeping genes is not affected. The *nxf5* gene products were further characterized and five different isoforms (generated by alternative splicing) were isolated. Compared to TAP, the *nxf5* isoform encoding the longest ORF (*nxf5a*) encodes a protein that is N- and C-terminally truncated but comprises the RBD-, the LRR and the NTF-like domains, although an internal stretch of 35 amino acids is missing in the NTF2-like domain. As NXF proteins have been implicated in nuclear RNA export, the ability of NXF5a to bind RNA was investigated. The recombinantly expressed RBD of NXF5a was found to bind RNA in a gel mobility assay, similar to the RBDs of human TAP or NXF2.

Since NXF proteins function in mRNA export only when forming heterodimers with p15, the ability of NXF5a to interact with p15 was analyzed. NXF5a was shown to interact with p15-1 and p15-2 in GST-pull down assays. The localization of GFP-tagged NXF5a was analyzed in different cell lines. NXF5a was found to be mainly cytoplasmic in a human and a monkey cell line of non-neuronal origin. In fully mature hippocampal neurons NXF5a was detected in the entire cell body and in small aggregates in some neurites.

Moreover, two murine NXF family members (*nxf-a* and *nxf-b*) were identified and (partially) cloned. Both map to the mouse X chromosome. The expression patterns of both mouse *nxf* members was analyzed by real-time PCR and shown to be very high in early

stages of embryogenesis, but very low in later embryonic stages. In the adult mouse, highest levels were detected in the brain.

Altogether, the investigation of the Xq breakpoint found in a male patient with a syndromic form of mental retardation resulted in the identification of the *nx* gene cluster in which *nx5* is split by the breakpoint, resulting in its functional nullisomy. As NXF5 has some of the features critical for an mRNA export factor (RNA binding, heterodimerization with p15) and the closest mouse orthologues of NXF5 are mainly expressed in the neural system, NXF5 was suggested to play a role in nuclear mRNA export in neurons.

Contribution

As part of a collaboration with the Marynen laboratory I designed and performed the experiments shown in Figures 4 A and 4B. Overall, I contributed about 10% of the data presented in this paper.

***NXF5*, a novel member of the nuclear RNA export factor family, is lost in a male patient with a syndromic form of mental retardation**

Lin Jun*, Suzanna Frints*, Hein Duhamel*, Andrea Herold†, Jose Abad-Rodrigues‡, Carlos Dotti‡, Elisa Izaurralde†, Peter Marynen* and Guy Froyen*

Background: Although X-linked mental retardation (XLMR) affects 2%–3% of the human population, little is known about the underlying molecular mechanisms. Recent interest in this topic led to the identification of several genes for which mutations result in the disturbance of cognitive development.

Results: We identified a novel gene that is interrupted by an inv(X)(p21.1;q22) in a male patient with a syndromic form of mental retardation. Molecular analysis of both breakpoint regions did not reveal an interrupted gene on Xp, but identified a novel nuclear RNA export factor (*NXF*) gene cluster, Xcen-*NXF5-NXF2-NXF4-NXF3-Xqter*, in which *NXF5* is split by the breakpoint, leading to its functional nullisomy. The predicted *NXF5* protein shows high similarity with the central part of the presumed mRNA nuclear export factor TAP/*NXF1*. Functional analysis of *NXF5* demonstrates binding to RNA as well as to the RNA nuclear export-associated protein p15/*NXT*. In contrast to TAP/*NXF1*, overexpression studies localized *NXF5* in the form of granules in the cell body and neurites of mature hippocampal neurons, suggesting a role in mRNA transport. The two newly identified mouse *nxf* homologs, *nxf-a* and *nxf-b*, which also map on X, show highest mRNA levels in the brain.

Conclusions: A novel member of the nuclear RNA export factor family is absent in a male patient with a syndromic form of mental retardation. Although we did not find direct evidence for the involvement of *NXF5* in MR, the gene could be involved in development, possibly through a process in mRNA metabolism in neurons.

Background

X-linked mental retardation (XLMR) is clinically variable and genetically heterogeneous. Mental retardation (MR) is considered to be a developmental brain disorder. The impact of genetic factors on this development is estimated at 35% in severe MR (IQ < 50) and 15% in mild MR (50 < IQ < 70). Recent advances in molecular genetics and positional cloning led to the identification of genes that might be instrumental for cognitive development [1–3]. The identification of such genes should help to improve our knowledge of the molecular and cellular mechanisms underlying the physiological and pathophysiological development of cognitive functions.

The generation of eukaryotic mRNAs involves a number of processes (transcription, splicing, capping, polyadenylation, nuclear export, transport, translation, and decay) that are tightly regulated by a broad range of interacting molecules. The identification of all these molecules as well as

the precise mechanism of interplay has yet to be discovered. Nuclear export of mRNA to the cytoplasm is a signal-mediated, energy-dependent, and highly selective process of which many steps are still unclear [4]. The human protein TAP/*NXF1* has been proposed to function as a nuclear export receptor for mRNA [5]. TAP/*NXF1* binds RNA and other RNA binding proteins and shuttles between the nucleus and the cytoplasm [5–7]. The TAP/*NXF1* protein contains three main functional domains: the N-terminal part (residues 1–372), which binds RNA; the middle part (residues 371–551), which binds p15/*NXT*; and the C-terminal ubiquitin-associated (UBA)-like domain (residues 508–619), which binds proteins of the nuclear pore complex (NPC) [5, 8]. Evidence for the involvement of TAP/*NXF1* in nuclear export of mRNA has been obtained from studies in yeast and in *Caenorhabditis elegans* in which the TAP orthologs, Mex67p and Ce*NXF1*, respectively, have been demonstrated to be essential for this process [9, 10]. Also, indirect evidence

Addresses: *Human Genome Laboratory, Flanders Interuniversity Institute for Biotechnology, University of Leuven, B-3000 Leuven, Belgium. †European Molecular Biology Laboratory (EMBL), D-69117 Heidelberg, Germany. ‡Cavalieri Ottolenghi Scientific Institute, Università degli Studi di Torino, 10043 Orbassano (TO), Italy.

Correspondence: Guy Froyen
E-mail: guy.froyen@med.kuleuven.ac.be

Received: 1 June 2001
Revised: 26 July 2001
Accepted: 7 August 2001

Published: 18 September 2001

Current Biology 2001, 11:1381–1391

0960-9822/01/\$ – see front matter
© 2001 Elsevier Science Ltd. All rights reserved.

for TAP/NXF1-mediated export of cellular mRNAs has been published [11–13]. Recently, it was suggested that the interaction of TAP/NXF1 with p15/NXT is required for efficient mRNA export [14].

In this study, we report on the identification of a novel gene, *NXF5*, that might be associated with a syndromic form of XLMR through investigation of an inv(X) (p21.1;q22) in a male patient. The novel gene at Xq is split by the breakpoint, leading to its functional nullisomy. The gene shows high similarity to the mRNA nuclear export factor *TAP/NXF1*, and it is part of a cluster of homologous genes, since three additional genes were identified within a region of 1 Mb on Xq22. Functional analysis of *NXF5* demonstrated general affinity for RNA as well as for the TAP/NXF1-associated protein p15/NXT. In contrast to TAP/NXF1, which localizes to the nucleus, *NXF5* is also localized in the cytoplasm of cultured cells and more importantly in the form of aggregates in the cell body as well as in some of the neurites of mature hippocampal neurons. Screening of mouse BAC clone filters and database searches identified two novel mouse *nxf* homologs, *nxf-a* and *nxf-b*. Although the general mRNA expression levels are low, the highest expression of both genes was found in the brain of adult mice. For *nxf-a*, even higher levels were found at E7.5 dpc whole embryos. Taken together, our results indicate that the interruption of the human *NXF5* gene affects the normal development, including the cognitive network, possibly via its function in mRNA metabolism. However, no disease-associated mutations have been identified so far.

Results

Cloning the breakpoints of inv(X)(p21.1;q22)

Details on the cloning of the breakpoints will be described elsewhere (S. Frints et al., unpublished data). Briefly, the breakpoints were defined by FISH analysis using a cluster of YACs at Xp11.4–22. First, the YAC clone 790d6 and later the PAC clone dJ1051h1 were shown to span the Xp breakpoint. Restriction map analysis, Southern blot hybridization, and vectorette-based cloning approaches performed according to standard procedures revealed the sequences at both breakpoints in patient A059. The Xq breakpoint could be located in a sequenced cosmid (cV434E11) from Xq22.

The potential disease gene is not at the Xp breakpoint

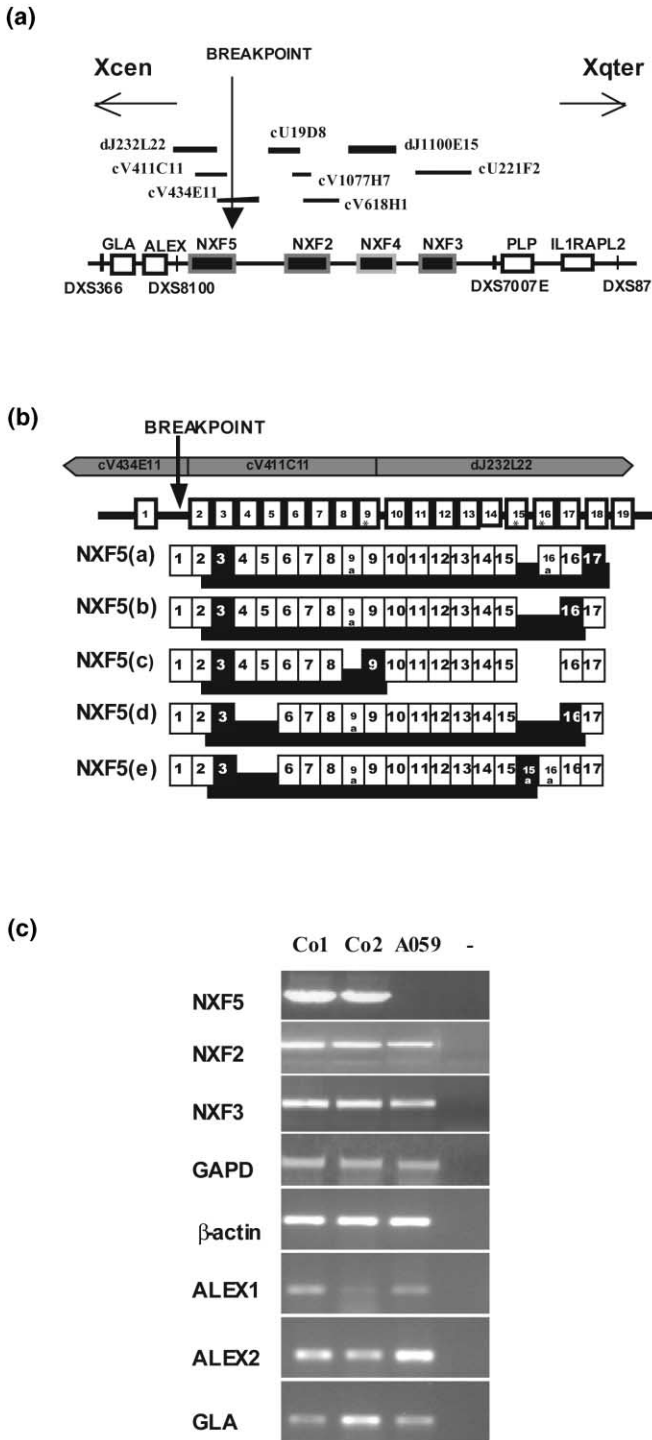
Since two chromosome X regions are affected by the inversion, we had to define which locus (Xp or Xq) contains a potential MR-associated gene. A map of the Xp breakpoint was generated, and analysis of an ~40-kb random sequence with different gene prediction programs only detected the *SRPX* gene. A literature search [15, 16] identified a gene contig at the Xp breakpoint “*CYBB-TCTEIL-breakpoint-SRPX-RPGR-OTC*”. The shortest distance between the breakpoint and a gene (*SRPX*) was

estimated at 50 kb. In addition, a particularly interesting case of a boy (SB) with a microdeletion on Xp21 extending from *CYBB* to *RPGR* was described [16, 17]. SB was reported to have chronic granulomatous disease, retinitis pigmentosa, and McLeod phenotype. This patient was not mentally handicapped (de Saint Basile, personal communication). The extent of the Xp deletion in SB was confirmed in our lab by PCR-based STS mapping (data not shown). From these results, we conclude that the potential MR gene is not at the Xp breakpoint.

The Xq breakpoint is present in an *NXF* gene cluster and leads to functional nullisomy of *NXF5*

We analyzed the Xq22 region using the genomic sequences of clones cV434E11, cV411C11, and dJ232L22 (Figure 1a). Several predicted exon sequences showed similarity to the mRNA nuclear export factor TAP/NXF1. Primers derived from the potential exons were used for RT-PCR and RACE-PCR experiments as described in the Materials and methods. Using human fetal brain polyA(+) RNA as well as total RNA derived from EBV-transformed cell lines, we cloned the complete *NXF5* gene. Detection of exon-intron boundaries by the comparison of genomic and cDNA sequences revealed the existence of 19 exons. *NXF5* potentially codes for at least five different protein isoforms (*NXF5a–e*; GenBank accession numbers AJ277654–AJ277658, respectively) derived from alternative splicing of the transcript affecting the presence of exons 4 and 5, the choice of acceptor sites in exons 9 and 16, and the choice of donor site in exon 15 (Figure 1b). In all isoforms, the putative translation initiation codon, which is in agreement with the Kozak consensus sequence, is present in exon 3. The largest isoform (*NXF5a*) reveals a single ORF of 1191 nt that encodes a protein of 397 amino acids. The Xq breakpoint is positioned in intron 1 of *NXF5* and therefore does not interrupt the presumed coding sequence. In order to define whether the breakpoint interferes with the *NXF5* mRNA expression, RT-PCR was performed, starting with total RNA from EBV-transformed cell lines of A059 and of controls. After heminested PCR analysis, specific amplification of the coding region of *NXF5* was obtained for the controls but not for the A059-derived sample (Figure 1c). Amplification of *GAPD* and β -*actin* were taken as controls. Position effects of the Xq breakpoint on genes in the direct neighborhood of *NXF5* were examined by RT-PCR. At the Xqter side of *NXF5*, expression of *NXF2* and *NXF3* was investigated by heminested PCR. Centromeric to the *NXF* gene cluster, transcripts of two genes of the recently mapped *ALEX* gene cluster (*ALEX1* and *ALEX2*) [18] as well as the *GLA* gene were quantified. No significant expression changes were observed between the patient and controls for any of the genes investigated. Each quantitation was done in triplicate, of which Figure 1c shows a representative result. Since the region selected for amplification of *NXF5* is present in all isoforms, divergence

Figure 1



The breakpoint at Xq interrupts the novel gene *NXF5* within the *NXF* gene cluster. **(a)** A schematic representation of the genomic region containing the breakpoint at Xq. The breakpoint is located in clone cV434E11 and maps at Xq22. The positions of neighboring clones in this region are shown by horizontal bars. Sequence analysis revealed the presence of a gene cluster consisting of four highly homologous sequences oriented as Xcen-*NXF5*-*NXF2*-*NXF4*-*NXF3*-Xqter and pinpoints the breakpoint in the first intron of the *NXF5* gene. The *NXF4* pseudogene is represented by the light box. The positions of

of isoform usage can be excluded. These results show that *NXF5* mRNA expression is completely shut off by the inversion, and, hence, no protein is produced.

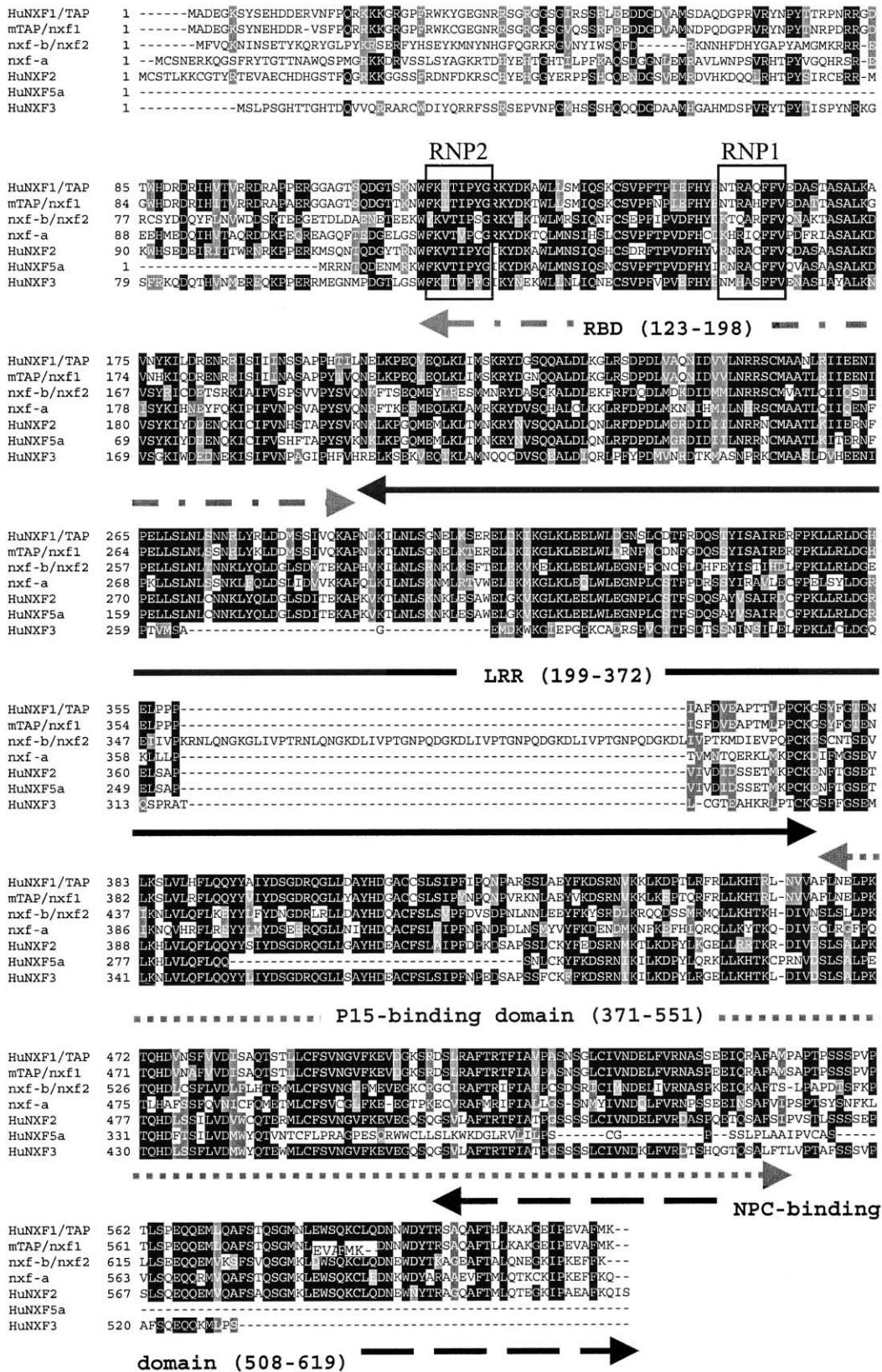
Three additional genomic clones on Xq22 (cV618H1, cU221F2, and dJ1100E15) were identified by BLAST to contain sequences highly similar to *NXF5*. In addition, ESTs derived from or partially derived from these genomic clones reveal homology to *NXF5* and *TAP/NXF1*. Using RT-PCR and RACE approaches, we obtained the full-length cDNA sequence of *NXF2* (GenBank accession number AJ277659), derived from cV618H1, and a partial cDNA sequence of *NXF3* (GenBank accession number AJ277660), derived from cU221F2. A potential *NXF* gene present in dJ1100E15 (*NXF4*) most probably is a pseudogene, since it contains stop codons in all reading frames shortly after the presumed start codon. The *NXF* gene cluster is located within a region of approximately 1 Mb between the *GLA* and *PLP* genes. The genomic organization is “Xcen-*GLA*-*ALEX*-*NXF5*-*NXF2*-*NXF4*-*NXF3*-*PLP*-Xqter” (Figure 1a). The complete cDNA sequences of *NXF2* and *NXF3* have recently been described [13].

Mutation screening did not reveal a disease-associated mutation

Detailed information on this screen will be described elsewhere (S. Frints *et al.*, unpublished data). Briefly, we combined SSCP with sequencing of PCR products that showed aberrant SSCP patterns to detect potential point mutations in the exons and their flanking intron sequences for the *NXF2* and *NXF5* genes. A total of 115 probands from XLMR and supposed XLMR families, either syndromic or nonspecific, were selected for SSCP analysis. For 17 of these families, the disease locus was mapped to Xq22. A different SSCP pattern amongst the probands was observed in four positions of *NXF5* and in two positions of *NXF2*. Four of these changes showed a high frequency (>10%) in the screened population. The

STSs are indicated as DXS numbers. Note that the figure is not drawn to scale. **(b)** A scheme of the genomic organization of *NXF5* and its different isoforms. The position of the clones covering the gene is indicated at the top. Exons are shown as numbered boxes. Exons with alternative splice sites are marked with an asterisk. The exon usage of the five isoforms (a-e) was determined by RT-PCR, with the predicted start codon located in the third exon of each isoform (gray boxes). The coding regions are shown as black bars, and the exons containing the stop codon are indicated in black. **(c)** The expression of *NXF5* is abolished in the patient. Heminested RT-PCR was performed for the detection of *NXF5* mRNA expression on cDNAs derived from EBV-transformed cell lines of the patient (A059) and two control individuals (Co1 and Co2). Negative PCR controls are indicated by a hyphen. Expression of genes in the direct neighborhood of *NXF5* was checked by RT-PCR. These genes are *NXF2* and *NXF3* at the telomeric side and *ALEX1*, *ALEX2*, and *GLA* at the centromeric side of the Xq breakpoint. The housekeeping genes *GAPD* and β -*actin* were also included. PCR products were analyzed on a 1.5% agarose gel.

Figure 2



two changes with a frequency < 5% were checked in a control population and found to be single-nucleotide polymorphisms.

The predicted structure of the novel NXF proteins reveal homology with TAP/NXF1

BLAST analysis showed that all members of the *NXF* gene cluster encode proteins that reveal significant similarity to human, mouse, and rat *TAP/NXF1*. Alignment of the human and mouse NXF proteins is illustrated in Figure 2. TAP/NXF1 consists of three functional domains: an N-terminal domain (residues 1–372), which binds RNA and several RNA binding proteins, a p15/NXT-heterodimerization domain (middle part), and a C-terminal nuclear pore complex (NPC) binding region [4, 13]. The N-terminal domain of TAP/NXF1 includes a noncanonical RNP-type RNA binding domain (RBD), four leucine-rich repeats (LRRs), and a region of more divergent sequences N-terminal to the RBD [19]. The NXF2 and NXF3 proteins show 74% and 72% similarity, respectively, to TAP/NXF1, with conservation of the structural domains [13]. If TAP/NXF1 is taken as a reference, the NXF5 protein starts at position 107 and comprises the conserved RBD and the LRRs but lacks the most divergent sequences N-terminal to the RBD. The p15/NXT binding domain is also highly conserved but lacks a stretch of 35 amino acids (394–429 in TAP/NXF1). The C-terminal domain of NXF5 is much shorter, with a conserved N-terminal part but a completely different C terminus.

Identification of two novel *nxf* homologs in the mouse

To define the mouse orthologs of the novel *NXF* genes, we screened mouse BAC filters and searched the mouse EST database at NCBI with the cDNA sequences of *NXF5* and *NXF2*. Database searches revealed, in addition to murine *TAP/nxf1*, three potential *nxf* homologs, which we called *nxf-a* (GenBank accession numbers AA474219 and AW543149), *nxf-b* (GenBank accession number AW555775), and *nxf-c* (GenBank accession number AW543152). RACE experiments were performed, and sequences of the full-length *nxf-a* and partial *nxf-b* genes were submitted to GenBank (accession numbers AJ305318 and AJ305319, respectively). Meanwhile, the cDNA sequence of *nxf-b* (also called *nxf2*) was obtained by two independent groups (GenBank accession numbers NM_031259 and AY017476). The similarity of full-length *nxf-a* and *nxf-b* with the mouse TAP/NXF1 protein is 63% and 70%, respectively. For the available C-terminal sequence of the presumed *nxf-c* protein, the similarity is

54%. However, all attempts to amplify this presumed gene on a genomic as well as on a cDNA level failed. Therefore, we cannot yet define this single EST as an *nxf* homolog. In order to screen for additional *nxf* homologs as well as to isolate mouse *nxf* genomic sequences, we used different fragments of the *nxf-a* and *nxf-b* genes, covering the entire coding regions, to screen a mouse genomic BAC library. The positive BAC clones 417D19 and 420L6 contain genomic sequences of the *nxf-a* gene, while the *nxf-b* genomic sequences were identified in BAC 277M12 and 452M12, as determined by PCR and partial sequence analysis. In this screen, we were unable to identify BAC clones containing other *nxf* genes, including the *nxf-c* gene. The almost complete genomic sequence of *nxf-b* is now available from contig AC024363. FISH experiments mapped both *nxf* genes to mouse chromosome X. Moreover, both signals are present at the same location, indicating that a similar *nxf* gene cluster is present on the mouse X chromosome. Alignment of the predicted proteins with their human counterparts is shown in Figure 2. Note that *nxf-b* contains an additional 70-amino acid domain that consists of a repeat of 13–15 amino acids (RNLQNGK[L]GLIVPT). This repeat domain does not show any homology with other protein regions. It is yet not possible to define the exact orthology of the human and mouse *NXF* genes, except for *TAP/NXF1*. The identity of the *nxf-a* protein with human NXF2, NXF3, and NXF5 is 73%, 69%, and 71%, respectively. For *nxf-b*, the identity is 71%, 67%, and 72%, respectively. The identity between human and mouse TAP/NXF1 is 82%.

***NXF* genes are low-abundance genes with predominant expression in the brain of mice**

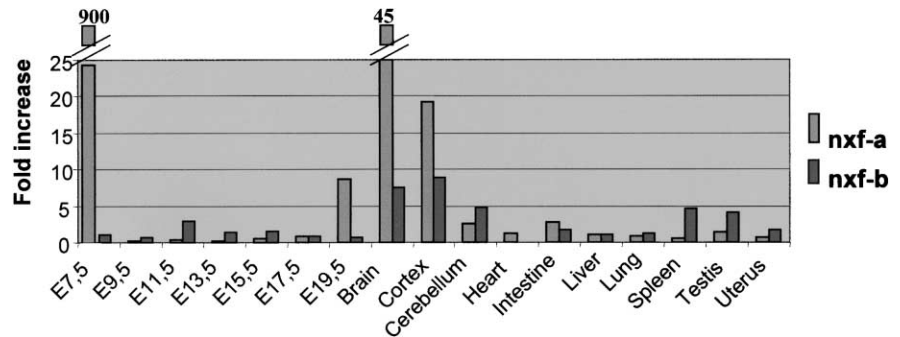
A human multiple tissue Northern blot hybridization did not reveal any signals for *NXF2* or *NXF5*, indicating that both represent low-abundance transcripts. Our previous results obtained from RT-PCR and RACE experiments on fetal brain-derived and EBV-transformed cell line-derived cDNAs point in the same direction, since two rounds of PCR were always required in order to detect the amplicons. Moreover, not a single *NXF5*-derived EST was found in human databases. Temporal and spatial expression patterns of mouse *nxf-a* and *nxf-b* were investigated by real-time quantitation. RNA samples derived from mouse embryos at different stages and from different tissues of adult mice were analyzed. Each *nxf* primer/probe combination was first validated to check the amplification efficiency with that of the endogenous control, β -*actin*. This allows for a comparison between the two *nxf*

Multiple sequence alignment of the NXF family of proteins of human and mouse. CLUSTALW alignment of human NXF1/TAP, NXF2, NXF3, and NXF5a and mouse mTAP/nxf1, nxf-a, and nxf-b/nxf2. The domain structures indicated below the alignment (RBD, LRR, p15 binding domain, and NPC binding domain) are based on the human

TAP/NXF1 protein. The ribonucleoprotein (RNP) consensus motif regions, RNP1 and RNP2, are boxed. HuNXF5a lacks the most N- and C-terminal sequences. The unique repeat motif of *nxf-b/nxf2* is present within the LRR.

Figure 3

Relative mRNA expression levels of the mouse *nxf-a* and *nxf-b* genes. The expression was quantified by the Taqman procedure on the ABI-PRISM7700 from total RNA samples extracted from mouse embryos at different stages (E7.5–E19.5) and from tissues of adult mice. Expression levels of *nxf-a* (light bars) and *nxf-b* (dark bars) were first normalized toward the housekeeping gene β -actin (comparative C_T method) and then mutually compared based on the similar *nxf-a* and *nxf-b* mRNA levels in the liver sample. Consequently, the fold differences of both genes can be relatively compared. The fold-increase values obtained for *nxf-a* in the E7.5 and brain samples are given above the bar.



genes based on β -actin mRNA levels. Equal normalized amounts for *nxf-a* and *nxf-b* mRNAs were demonstrated in the liver sample, so this was used as the calibrator to which each sample was compared. As is the case for *NXF2* and *NXF5*, both mouse *nxf* genes are also low-abundance genes. Starting from as much as 50 ng reverse-transcribed RNA, 35 cycles were not sufficient for most of the samples to generate a fluorescence signal that reached the threshold value. As can be seen in Figure 3, expression of *nxf-a* at the early stage of the embryo was very high (E7.5 dpc), then dropped significantly at E9.5 dpc and stayed low until E19.5 dpc. In the adult mouse, the highest expression was found in the brain ($C_t = 28$), with substantial expression in the cerebral cortex. In all other tissues tested, including the cerebellum, the mRNA levels are more than 20-times below those obtained in the brain. Subsequently, RNA in situ hybridization was performed on E19.5 dpc embryos and adult brain sections with different *nxf-a* probes, but we could not detect any signals in either of the samples (data not shown). Levels of *nxf-b* mRNA were also highest in the brain of adult mice, but when compared to *nxf-a*, the expression here was about 5-times lower (Figure 3). The cerebral cortex seems to contribute most to these levels, although expression in the cerebellum was also noticed. Compared to the liver calibrator sample, the *nxf-b* mRNA levels were also elevated in the spleen and testes, while those in all other samples tested stayed very low.

NXF5 binds RNA and p15/NXT and localizes as granules in the cytoplasm of hippocampal cells

The RNA binding affinity of NXF5 was tested with the predicted RNA binding domain (RBD; amino acids 1–92) of NXF5a fused to GST. The purified GST-RBD fusion product was incubated with an RNA probe, and the resulting complexes were analyzed in a gel mobility retardation assay (Figure 4a). The RBD of NXF2 was taken as a positive control, while the same region of NXF3 was used as a negative control [13]. The RBD of NXF5 bound

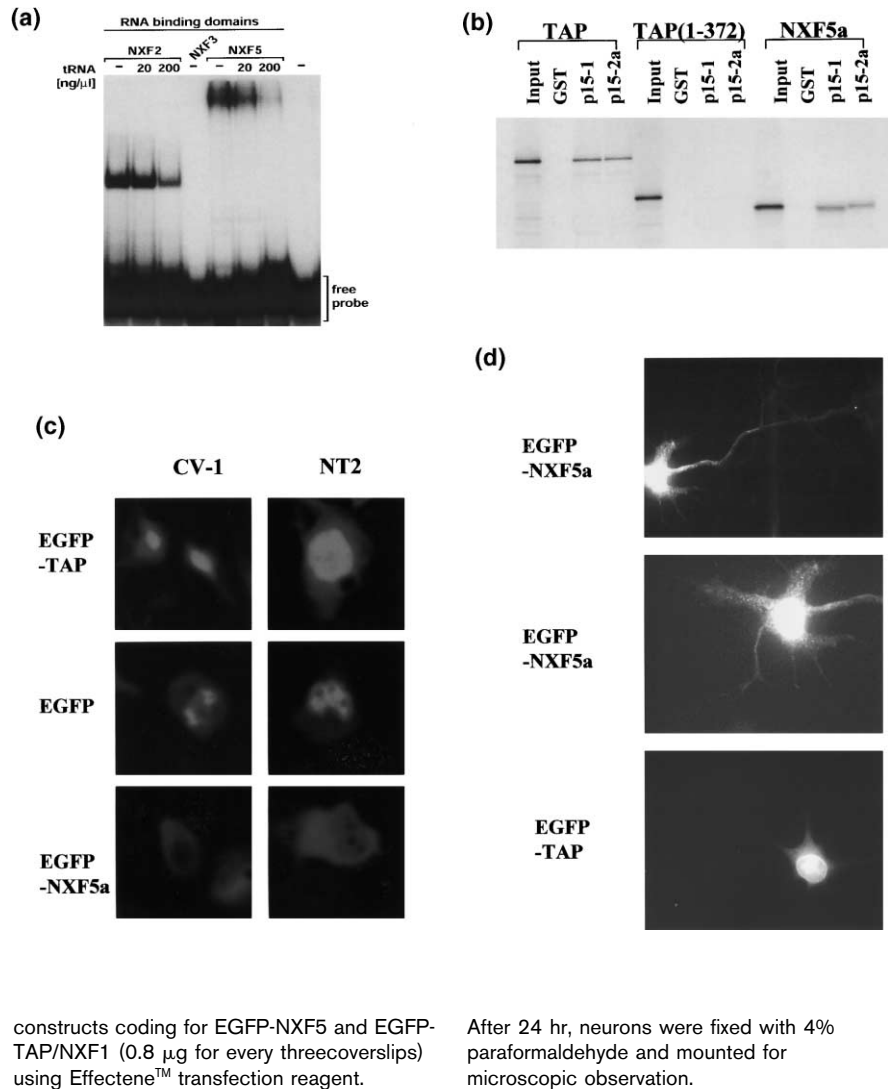
to the RNA probe; however, the NXF5a-RNA complexes migrate slower than the NXF2-RNA complexes, suggesting that the former complexes may contain multiple NXF5 molecules. This binding is nonspecific, since it was competed for by tRNA. Binding of in vitro-translated NXF5a to p15-1 and p15-2a fused to GST was analyzed in a GST pull-down assay. As demonstrated in Figure 4b, both p15/NXT proteins bind to NXF5a as well as to the positive control, TAP/NXF1. This means that the TAP/NXF1 region 394–429, which is absent in NXF5, is not essential for p15/NXT binding. The N-terminal domain of TAP/NXF1 (1–372) did not bind to the fusion proteins, while GST alone did not associate with either of the NXF proteins. GST pull-down experiments did not reveal any binding of NXF5 to the nucleoporin fusion product, GST-CAN (data not shown). The construct used for localization of NXF5a (EGFP-NXF5a) in the monkey CV-1 and human NT2 cell lines demonstrated that NXF5a is mainly present in the cytoplasm of the cells, although nuclear staining, with the exclusion of the nucleoli, was also noticeable (Figure 4c). The reverse fusion construct NXF5a-EGFP demonstrated a similar staining pattern (data not shown). The control EGFP-TAP fusion protein was exclusively localized in the nucleus. In contrast to TAP/NXF1, NXF5 did not localize to the nuclear rim (data not shown). Intracellular distribution of overexpressed GFP-NXF5 and GFP-TAP/NXF1 in fully mature hippocampal neurons in culture (11 days) demonstrated intense GFP-NXF5 fluorescence in the entire cell body and in the form of small aggregates in some of the neurites, most likely the cell's dendrites (Figure 4d). GFP-TAP/NXF1 is largely, if not exclusively, concentrated in the cell nucleus, with a clear enrichment in the nuclear membrane.

Discussion

We have identified and characterized an *NXF* gene cluster through investigation of the Xq breakpoint of an inv(X)(p21.1;q22) in a male patient (A059) with a syndromic form of mental retardation. The gene cluster on

Figure 4

Binding and localization studies of NXF5a. **(a)** A gel mobility shift assay was performed with [³²P]UTP random RNA probe (10,000 dpm/reaction), produced by in vitro transcription of the polylinker of pBluescript-SK with the Ampliscribe T7 transcription kit and 1 μg purified RNA binding domains of GST-NXF2, GST-NXF3, and GST-NXF5a. Unlabeled competitor tRNA was added as indicated above the lanes. Mixtures were incubated for 30 min at 30°C and run on a 5% native PAA gel in 0.5 × TBE at 210 V for 2 hr. Dried gels were exposed overnight to X-Omat film at -70°C. The free RNA probe is indicated at the right. **(b)** GST pull-down assay with p15 proteins. Binding assays were performed with in vitro-translated [³⁵S]methionine TAP, TAP(1-372), or NXF5a and immobilized GST, GST-p15-1, or GST-p15-2a on glutathione agarose beads. One tenth of the input and one quarter of the bound fraction for each protein was analyzed on 12% PAA SDS-PAGE. Dried gels were exposed to BioMax film at -70°C. **(c)** Intracellular distribution in monkey CV-1 and human NT2 cells of the EGFP-TAP and EGFP-NXF5a constructs (0.5 μg plasmid/2.10⁴ cells/well). EGFP alone was used as a negative control. After transfection of the DNA constructs with the FuGENE6 transfection reagent, cells were incubated for 20 hr and fixed with 4% formaldehyde for 15 min. Signals were visualized with a MRC 1024 confocal microscope. **(d)** Intracellular distribution in mature hippocampal neurons of E18 rats. Primary hippocampal neurons were seeded at 10⁵ cells/well on poly-L-lysine-coated coverslips and kept in 5% CO₂ at 36.5°C. After 7 hr, the coverslips were transferred to a 6-cm dish containing astrocytes in minimal essential medium (MEM) and N2 supplements. Ten-day-old hippocampal neurons were transfected with cDNA



Xq22 consists of four genes organized as Xcen-*NXF5*-*NXF2*-*NXF4*-*NXF3*-Xpter. *NXF5* is disrupted in its 5' UTR by the inversion, leading to its functional nullisomy. Mutation analysis detected four polymorphisms, but did not reveal any disease-related nucleotide changes. *NXF5* shows high sequence similarity with the nuclear export factor TAP/NXF1 and was shown to bind to RNA as well as to the p15/NXT proteins. However, in contradiction to TAP/NXF1, it is predominantly localized in the cytoplasm of cells and more particularly in the cell body and neurites of hippocampal neurons. The *NXF5* gene, of which at least five isoforms exist, seems to be expressed at low abundance. In the adult mouse, the expression of the presumed orthologs *nxf-a* and *nxf-b* is highest in the brain when compared to other tissues, pointing to a brain-specific role. Interestingly, compared to those found in the brain, 20-fold higher levels of *nxf-a* mRNA are detected at E7.5 dpc, the time point at which neurulation starts. From

these results, it is likely that the protein is involved in posttranscriptional regulation of mRNA, and, therefore, the question arises whether the loss of *NXF5* results in altered mRNA metabolism in the MR patient.

The breakpoint in the gene is situated in the 5' UTR between exons 1 and 2. Consequently, no expression is detectable in the EBV-transformed cell line derived from A059, whereas cell lines from controls yield an amplification product after heminested RT-PCR. Whether the *NXF5* promoter induces the transcription of a gene at Xp21.1 remains to be further investigated, although extensive database analyses did not reveal the presence of a gene in the neighborhood of the Xp breakpoint. Deletion of a region extending the Xp breakpoint, as was described in one boy [17], did not result in MR, indicating that no MR gene is present in this deleted region and, hence, position effects of the Xp breakpoint can also be

excluded. However, we cannot exclude a gain-of-function resulting from the overexpression of a gene on Xp. Screening for a potential position effect of the Xq breakpoint on the most neighboring genes (within a 0.4-Mb interval at each side) did not reveal an altered expression pattern for any of these genes in the patient compared to controls providing strong evidence for the involvement of NXF5.

The structural organization of the NXF2 protein is highly similar to that of TAP/NXF1. It consists of an N-terminal domain containing the RBD and the leucine-rich repeats, a middle NTF2-like domain that binds p15/NXT, and an NPC binding domain at the C-terminal end of the protein [5, 13, 19]. Recently, NXF2 has been shown to bind to RNA, p15/NXT, and nucleoporins [13]. The same study demonstrated NXF3 binding to p15/NXT, but no affinity for RNA or nucleoporins was observed. Preliminary functional analysis of NXF5 was performed using the isoform with the longest ORF (NXF5a). NXF5a contains a truncated N-terminal domain and NPC binding domain but an almost complete p15/NXT-heterodimerization domain. Our studies demonstrate that NXF5a is able to bind to RNA as well as to the p15/NXT proteins, p15-1 and p15-2a, suggesting that it may contribute to mRNA nuclear export. p15/NXT has recently been shown to act as a cofactor in the TAP/NXF1-dependent export of RNA [14, 20]. However, the NXF5a protein does not bind nucleoporins *in vitro* nor localizes at the nuclear rim *in vivo*, consistent with the absence of a C-terminal NPC binding domain. In this context, it is possible that the shorter NXF forms (NXF3 and NXF5), which do not bind to nucleoporins, act as regulatory proteins for the export factors TAP/NXF1 and NXF2. The existence of several isoforms might create an even more complex regulatory system. Alternatively, NXF proteins lacking the NPC binding domain may have a different function from nuclear export. Indeed, in contrast to TAP/NXF1, which is mainly localized within the nucleus, both NXF5 and NXF3 are also detected in the cytoplasm, suggesting a cytoplasmic function. In this respect, the granular somatodendritic localization of NXF5 in hippocampal neurons, reminiscent of the labeling seen for both the endogenous and overexpressed *staufen* in the same cells [21, 22], suggests a role in polarized cytoplasmic transport and localization of mRNAs in neurons. It is speculated that such proteins play a role in synaptic plasticity [23]. The published suggested amino acid sequence of NXF5 [13] was derived from the genomic sequence and contains two stop codons (depicted as x in Figure 3 of this reference). Our RACE experiments revealed the correct cDNA and amino acid sequences of five NXF5 isoforms. The highly divergent amino acid sequence at the C-terminal part of NXF5, compared to TAP/NXF1 and NXF2, is due to an alternative splice acceptor site used in exon 15 of NXF5 (exon 22 in NXF2). This causes a frame shift (position 349 of NXF5) and, subsequently, a premature stop codon

(position 397). The existence of additional isoforms cannot be excluded.

It is not clear yet whether the *NXF* gene cluster in man is evolutionary conserved in mice. Beside mouse *TAP/nxf1*, we identified three potential *nxf* genes in database searches (*nxf-a*, *-b*, and *-c*). All attempts to amplify different regions of the presumed *nxf-c* gene at the cDNA or genomic DNA level failed. This suggests that the published sequence of this EST could be artifactual. Based on the complete *nxf-a* and *nxf-b* cDNA sequences, we were not able to determine which mouse homolog is the ortholog of human *NXF5*. Both genes contain the complete NPC binding domain, which is absent in NXF5. Interestingly, the BACs containing *nxf-a* and *-b* genes both map at the same position of the mouse X chromosome, indicating the presence of a similar *nxf* gene cluster in the mouse genome. Mapping of the *nxf-b* (*nxf2*) gene to mouse chromosome X was also recently described [24]. In the same study, the *nxf-b* (*nxf2*) mRNA was predominantly found in mouse testes and was identified as a spermatogonia-specific gene.

The involvement of RNA binding proteins in cognitive development has already been implicated by studying the fragile-X-associated protein, FMRP, responsible for the most common form of inherited mental retardation [25]. Indeed, FMRP has been demonstrated to bind RNA *in vitro* [26, 27] and to contain sequence motifs that are commonly found in RNA binding proteins. FMRP is also endowed with a nuclear localization signal (NLS) and a nuclear export signal (NES), suggesting that it shuttles between the nucleus and the cytoplasm. In addition, FMRP is associated with ribosomes in an RNA-dependent manner [28, 29]. *In situ* hybridization experiments in mouse brain demonstrated that FMRP is expressed at elevated levels in neurons of the cortex and hippocampus. Besides the involvement in RNA binding, the existence of different *NXF5* isoforms resembles the situation of *FMR1* as well as its homologs *FXR1* and *FXR2*. Localization studies of some of these isoforms report a specific spatial expression pattern [30–32]. This suggests a specific function for each of the different isoforms, but this remains to be further investigated. Differential interaction with other proteins, like NUFIP, might represent another way to create specificity [33]. A similar mechanism has been proposed for NXF proteins through their interaction with different partners [13]. Recently, FMRP has been proposed as a negative regulator of translation through inhibition of the assembly of 80S ribosomes on the target mRNA [34].

NXF5 as well as *NXF2* mRNA expression levels are low, since successful amplification always needed two rounds of PCR and their mRNAs could not be detected on a multiple tissue Northern blot. In the mouse system, we

studied the temporal and spatial expression of *nxf-a* and *nxf-b* mRNAs by real-time quantitation. Interestingly, the highest expression of both genes was obtained in the brain of adult mice. The levels of *nxf-a* in the cerebral cortex can account for the major part of the relatively high levels in the brain. The elevated levels in the brain of adult mice can already be noticed at the embryonic stage E19.5 dpc. The relative extremely high expression levels at E7.5 dpc might be indicative of an important role for this gene product in embryonic development. At this time point, substantial cell proliferation occurs with subsequent organization of the major systems of the embryo followed by neurulation. Expression of other genes involved in cognitive development, like *IL1RAPL* and *TM4SF2*, are predominantly found in the hippocampus and cortex of the brain [35, 36]. We did not yet include hippocampus in this study. In situ hybridization of *nxf-a* on E19.5 dpc and brain sections did not reveal any signals, most probably due to current restrictions in sensitivity. Compared to *nxf-a*, the *nxf-b* mRNA levels are about 5-fold lower in the brain. Again, cerebral cortex levels were highest, but expression was also noticed in the cerebellum, spleen, and testes. It is not yet clear why Page et al. could not identify *nxf-b* (*nxf2*) in the brain [24]. The use of different primer sets that amplify different isoforms might be a potential explanation. The available ESTs from these genes were almost all derived from E7.5 dpc libraries (except one obtained from an ovary-derived library).

An extensive SSCP mutation analysis study, followed by sequence analysis of aberrant bands, was performed for the *NXF5* and *NXF2* genomic sequences (S. Frints et al., unpublished). Two silent mutations and one intronic polymorphism in the *NXF5* gene and one silent mutation and one intronic polymorphism in *NXF2* were identified in our MR patient-derived samples. A number of MR loci have been linked to Xq22, although these usually fail to exclude more distal regions. No deletion syndromes are reported in this region, and only a few studies report a cytogenetically recognizable Xq duplication, including Xq22, which is also associated with mental retardation and short stature [37]. So, if mutations exist in this gene, they will be very rare, as is the case for many disease-associated genes.

Conclusions

We identified a novel member of the nuclear RNA export factor family through investigation of a centromeric inversion of the X chromosome in a male patient with a syndromic form of mental retardation. Binding of *NXF5* to RNA and p15/*NXT* supports a role in nuclear RNA export, although localization studies suggest a function in RNA transport. Expression profiling of two potential mouse orthologs point to a brain-specific function. In addition, a role in early development is suggested for one of these genes. Therefore, the nullisomy in the male MR

patient by the gene interruption might result in derangement of the export or transport of specific mRNAs, leading to this phenotype.

Our study suggests that interruption of this novel gene, *NXF5*, is associated with a disease phenotype including mental retardation and short stature. One of the major challenges will be to determine whether processes in the metabolism of a particular subset of mRNAs is affected in brain cells by knocking out the *NXF5* gene product.

Materials and methods

Patient description

Patient A059 is a 59-year-old male. He was clinically diagnosed with moderate to severe MR. He had a short stature, pectus excavatum, general muscle wasting, and facial dysmorphism including hypertelorism, large protruding ears, long nose, big mouth, and small chin. His karyotype revealed a pericentric inversion of the X chromosome: 46,Y,inv(X)(p21.1;q22). This patient will be described elsewhere in more detail (S. Frints et al., unpublished data).

Genomic clone resources and structure analysis

YACs at Xp11.4–22 are from the Genome Research database of the Whitehead Institute/MIT Center (WCX.6; http://carbon.wi.mit.edu:8000/cgi-bin/contig/phys_map). The PAC clone dj1051h1 that mapped at the Xp breakpoint was obtained from Roswell Park Cancer Institute (<http://www.roswellpark.org/>). An integrated STS/YAC physical, genetic and transcript map of Xq21.3–q23/24 is available [38, 39]. A particular region of Xq22, from DXS366 to DXS87, where the Xq breakpoint mapped, was sequenced in the Sanger Center (CHR_Xctg18; <http://www.sanger.ac.uk/HGP/ChrX/>). We determined exon-intron boundaries through sequence comparison between cloned cDNA and genomic DNA available from the Sanger Center (<http://www.sanger.ac.uk/HGP/ChrX/>).

RACE and SSCP analysis

Total RNA from EBV-transformed human PBLs or from mouse tissue was extracted with the Trizol reagent (Life Technologies). RACE experiments were performed on total RNA or directly on human fetal brain Marathon-Ready cDNA (Clontech) with oligo(dT)14–18 or random hexamers according to standard procedures [40]. For mouse transcripts, total RNA from the brain was used as the source. RACE products were cloned into pGEM-T-easy vectors (Promega) for subsequent sequence analysis. Screening for mutations in exons and their flanking intron sequences of the *NXF5* and *NXF2* genes was performed with standard SSCP methods [40], except that the analysis was done on multiplexed amplicons of varying lengths. The analysis was performed on probands from XLMR families, which map at Xq22, and on single-case male MR patients (S. Frints et al., unpublished data).

NXF expression in patient A059

The expression levels of the *NXF2*, *NXF3*, *NXF5*, *ALEX1*, *ALEX2*, *GLA*, β -actin, and *GAPD* genes in patient A059 and controls were determined from EBV-transformed PBLs by RT-PCR according to standard procedures [40]. Heminested PCR was performed for *NXF2*, *NXF3*, and *NXF5*. The other genes were amplified in single PCR runs of 32 cycles for β -actin and *GAPD*, 38 cycles for *ALEX1*, and 35 cycles for *ALEX2* and *GLA*. Primer sequences can be obtained from the Supplementary material available with this article online.

Identification and expression of mouse orthologs

To identify mouse orthologs of the human *NXF* genes, the mouse EST database at NCBI (<http://www3.ncbi.nlm.nih.gov/>) was searched with *NXF* cDNA sequences. The mouse BAC ES (II) filter (IncyteGenomics) containing 36,864 individual clones with a genomic coverage of 3 \times was first hybridized with an *NXF5*-derived probe for which the sequence is 98% identical to *NXF2*. The mouse *TAP/nxf1* cDNA probe covering

the same region was used as a control. Later, the same filters were hybridized with different regions of the mouse *nxf-a* and *nxf-b* ORFs according to standard procedures [40]. Determination of similarity percentages was done by WU-blast analysis (<http://www.proweb.org/proweb/Tools/WU-blast.html>). Gene-specific PCR products were quantified in real-time on an ABI PRISM 7700 Sequence Detection System (Applied BioSystems). Total RNA was extracted from mouse embryos (E) at different stages as well as from various tissues of adult Swiss mice (total brain, cerebral cortex, cerebellum, heart, intestine, liver, lung, spleen, testes, and uterus). For the embryo-derived samples, whole embryos were taken for E7.5 and E9.5, total head was used for E11.5 and E13.5, and fetal brain was dissected from E15.5, E17.5, and E19.5 embryos. RNA was extracted with Trizol. After DNase I treatment, 1 μ g was reverse transcribed with random primers (LifeTechnologies) and subjected to amplification as described earlier [41]. The expression of each *nxf* gene was normalized toward the expression of the β -actin endogenous control, which was also used for comparison of expression levels between the different *nxf* genes. Primers (for and rev) and probes for *nxf-a*, *nxf-b*, *nxf-c*, and β -actin were designed with the Primer3 software (Applied BioSystems) and can be obtained from the Supplementary material of this article. Quantitation was performed from two independent experiments.

Construction of expression vectors

All expression constructs were made with the longest isoform of the *NXF5* gene (*NXF5a*). Restriction sites were introduced via the primers in a PCR with Pfu Turbo DNA polymerase (Stratagene), and all constructs were sequence verified on an ABI-PRISM310 (Applied BioSystems). For in vitro translation, BamHI and Apal sites were introduced into the 5'- and 3'-ends, respectively, of the full-length cDNA of *NXF5a* and subsequently cloned into pcDNA3.1/myc-His (Invitrogen). GST fusion constructs of the full-length, N-terminal (1–92 and 1–266) and C-terminal (266–397) cDNA fragments were cloned as BamHI-Sall fragments into the vector pGEX-5X-1 (Amersham Pharmacia Biotech). For localization studies in mammalian cells, the full-length *NXF5a* cDNA was cloned as C- and N-terminal fusions to GFP via EglII-Sall cloning in pEGFP-C1 and Sall-BamHI cloning in pGFP-N3 (both from Clontech), respectively. Additional plasmids for the localization of TAP/NXF1, for the production of labeled RNA, as well as for the expression of TAP/NXF1, TAP(1-372), p15-1, and p15-2a are described elsewhere [8, 14].

NXF5 binding and localization studies

The [³²P]UTP random RNA probe was produced by in vitro transcription of the polylinker of pBluescript-SK (Stratagene) with the Ampliscribe T7 transcription kit (EpiCentre Technologies) and purified on PAA gel. [³⁵S]methionine in vitro-translated protein was produced with the TnT kit (Promega) and analyzed by SDS-PAGE. Expression and purification of GST fusion proteins in BL21(DE3) was done as described by Grüter [12]. GST pull-down and in vitro binding assays were performed as described by Herold [14]. GFP fusion constructs were transfected in the monkey CV-1 (ATCC CCL-70) and human NT2 (ATCC CRL-1973) cell lines with the FuGENE6 transfection reagent (Roche, Mannheim). Cells were fixed after 20 hr with 4% formaldehyde for 15 min. Coverslips were mounted in VectaShield medium (Vector Laboratories). Fluorescent signals were analyzed with a MRC 1024 confocal microscope (Nikon). In vivo localization studies at the nuclear rim were done as described by Bachi [5]. Primary hippocampal neurons derived from rat embryos were cultured according to de Hoop [42]. In brief, the hippocampi of E18 rats were dissected, trypsinized, and physically dissociated. The cells were then washed in HBSS, and 100,000 cells were plated onto poly-L-lysine-treated glass coverslips in tissue culture dishes containing minimal essential medium and 10% heat-inactivated horse serum. The cells were kept in 5% CO₂ at 36.5°C. After 7 hr, the coverslips were transferred to a 6-cm dish containing astrocytes in minimal essential medium (MEM) and N2 supplements. Cell were fed weekly and transfected after 11 days in vitro. Ten-day-old hippocampal neurons grown on Poly-L-Lysine-coated coverslips were transfected with cDNA constructs coding for GFP-NXF5 and GFP-TAP/NXF1 (0.8 μ g DNA every three coverslips) using Effectene transfection reagent (Qiagen) according to

manufacturer instructions. Cells were incubated overnight with the transfection mixture and transferred afterwards to glia-conditioned N2 medium. After 24 hr, neurons were fixed with 4% paraformaldehyde and mounted for microscopic observation.

Supplementary material

Supplementary material including descriptions of primers and probes that were used in this study for the amplification of genes is available at <http://images.cellpress.com/supmat/supmatin.htm>. Table 1 gives the primers used in RT-PCR and RACE experiments, and Table 2 gives those for real-time quantitation.

Acknowledgements

The authors are grateful to the clinical Genetics Department of Leuven, Dr. Stefan Claes and Dr. Koen Devriendt for clinical diagnosis of the patient, and Lut Van den Berghe for the collection of patient's materials and the processing of clinical data. We thank Ben Hamel (University Hospital Nijmegen, The Netherlands) Claude Moraine (Centre Hospitalier de Tours, France), Hans H. Ropers (Max-Plank-Institute for Molecular Genetics, Berlin-Dahlem, Germany), Jamel Chelly (INSERM Unité 129-ICGM, Paris, France), and Jean-Pierre Fryns (Clinical Genetics University, Leuven, Belgium) from the European XLMR Consortium. We are grateful to Barbara Felber for obtaining the *nxf-b/nxf2* sequence prior to publication and to Nicole Mentens for expert technical assistance. We would also like to thank the medical staff of the institute for mentally handicapped people in Geel (Belgium) for their helpful collaboration. This work was supported by a Research Grant (G-0299.01) of the Fund for Scientific Research – Flanders (Belgium) (F.W.O.–Vlaanderen).

References

1. Toniolo D: **In search of the MRX genes.** *Am J Med Genet* 2000, **97**:221-227.
2. Chelly J: **MRX review.** *Am J Med Genet* 2000, **94**:364-366.
3. Géczy J, Mulley J: **Genes for cognitive function: developments on the X.** *Genome Res* 2000, **10**:157-163.
4. Nakielnny S, Dreyfuss G: **Transport of proteins and RNAs in and out of the nucleus.** *Cell* 1999, **99**:677-690.
5. Bachi A, Braun IC, Rodrigues JP, Pante N, Ribbeck K, von Kobbe C, et al.: **The C-terminal domain of TAP interacts with the nuclear pore complex and promotes export of specific CTE-bearing RNA substrates.** *RNA* 2000, **6**:136-158.
6. Kang Y, Bogerd HP, Yang J, Cullen BR: **Analysis of the RNA binding specificity of the human tap protein, a constitutive transport element-specific nuclear RNA export factor.** *Virology* 1999, **262**:200-209.
7. Braun IC, Rohrbach E, Schmitt C, Izaurralde E: **TAP binds to the constitutive transport element (CTE) through a novel RNA-binding motif that is sufficient to promote CTE-dependent RNA export from the nucleus.** *EMBO J* 1999, **18**:1953-1965.
8. Katahira J, Strasser K, Podtelejnikov A, Mann M, Jung JU, Hurt E: **The Mex67p-mediated nuclear mRNA export pathway is conserved from yeast to human.** *EMBO J* 1999, **18**:2593-2609.
9. Segref A, Sharma K, Doye V, Hellwig A, Huber J, Lührmann R, et al.: **Mex67p, a novel factor for nuclear mRNA export, binds to both poly(A)⁺ RNA and nuclear pores.** *EMBO J* 1997, **16**:3256-3271.
10. Tan W, Zolotukhin AS, Bear J, Patenaude DJ, Felber BK: **The mRNA export in *Caenorhabditis elegans* is mediated by Ce-NXF-1, an ortholog of human TAP/NXF and *Saccharomyces cerevisiae* Mex67p.** *RNA* 2000, **6**:1762-1772.
11. Grüter P, Taberner C, von Kobbe C, Schmitt C, Saavedra C, Bachi A, et al.: **TAP, the human homolog of Mex67p, mediates CTE-dependent RNA export from the nucleus.** *Mol Cell* 1998, **1**:649-659.
12. Kang Y, Cullen BR: **The human Tap protein is a nuclear mRNA export factor that contains novel RNA-binding and nucleocytoplasmic transport sequences.** *Genes Dev* 1999, **13**:1126-1139.
13. Herold A, Suyama M, Rodrigues JP, Braun IC, Kutay U, Carmo-Fonseca M, et al.: **TAP (NXF1) belongs to a multigene family of putative RNA export factors with a conserved modular architecture.** *Mol Cell Biol* 2000, **20**:8996-9008.
14. Braun IC, Herold A, Rode M, Conti E, Izaurralde E: **Overexpression of TAP/p15 heterodimers bypasses nuclear retention and stimulates nuclear mRNA export.** *J Biol Chem* 2001, **276**:20536-20543.

15. Meindl A, Carvalho MR, Herrmann K, Lorenz B, Achatz H, Lorenz B, *et al.*: **A gene (*SRPX*) encoding a sushi-repeat-containing protein is deleted in patients with X-linked retinitis pigmentosa.** *Hum Mol Genet* 1995, **4**:2339-2346.
16. Meindl A, Dry K, Herrmann K, Manson F, Ciccodicola A, Edgar A, *et al.*: **A gene (*RPGR*) with homology to the *RCC1* guanine nucleotide exchange factor is mutated in X-linked retinitis pigmentosa (*RP3*).** *Nat Genet* 1996, **13**:35-42.
17. de Saint-Basile G, Bohler MC, Fischer A, Cartron J, Dufier JL, Griscelli C, *et al.*: **Xp21 DNA microdeletion in a patient with chronic granulomatous disease, retinitis pigmentosa, and McLeod phenotype.** *Hum Genet* 1988, **80**:85-89.
18. Kurochkin IV, Yonemitsu N, Funahashi SI, Nomura H: **ALEX1, a novel human armadillo repeat protein that is expressed differentially in normal tissues and carcinomas.** *Biochem Biophys Res Commun* 2001, **280**:340-347.
19. Liker E, Fernandez E, Izaurrealde E, Conti E: **The structure of the mRNA export factor TAP reveals a cis arrangement of a non-canonical RNP domain and an LRR domain.** *EMBO J* 2000, **19**:5587-5598.
20. Guzik BW, Levesque L, Prasad S, Bor YC, Black BE, Paschal BM, *et al.*: **NXT1 (p15) is a crucial cellular cofactor in TAP-dependent export of intron-containing RNA in mammalian cells.** *Mol Cell Biol* 2001, **21**:2545-2554.
21. Kiebler MA, Hemraj I, Verkade P, Köhrmann M, Fortes P, Marion RM, *et al.*: **The mammalian staufen protein localizes to the somatodendritic domain of cultured hippocampal neurons: implications for its involvement in mRNA transport.** *J Neurosci* 1999, **19**:288-297.
22. Köhrmann M, Luo M, Kaether C, DesGroseillers L, Dotti CG, Kiebler MA: **Microtubule-dependent recruitment of Staufen-green fluorescent protein into large RNA-containing granules and subsequent dendritic transport in living hippocampal neurons.** *Mol Biol Cell* 1999, **10**:2945-2953.
23. Martin KC, Barad M, Kandel ER: **Local protein synthesis and its role in synapse-specific plasticity.** *Curr Opin Neurobiol* 2000, **10**:587-592.
24. Wang PJ, McCarrey JR, Yang F, Page DC: **An abundance of X-linked genes expressed in spermatogonia.** *Nat Genet* 2001, **27**:422-426.
25. Khandjian EW, Bardoni B, Corbin F, Sittler A, Giroux S, Heitz D, *et al.*: **Novel isoforms of the fragile X related protein FXR1P are expressed during myogenesis.** *Hum Mol Genet* 1998, **7**:2121-2128.
26. Siomi H, Choi M, Siomi MC, Nussbaum RL, Dreyfuss G: **Essential role for KH domains in RNA binding: impaired RNA binding by a mutation in the KH domain of FMR1 that causes fragile X syndrome.** *Cell* 1994, **77**:33-39.
27. Ashley CT Jr, Wilkinson KD, Reines D, Warren ST: **FMR1 protein: conserved RNP family domains and selective RNA binding.** *Science* 1993, **262**:563-566.
28. Tamanini F, Meijer N, Verheij C, Willems PJ, Galjaard H, Oostra BA, *et al.*: **FMRP is associated to the ribosomes via RNA.** *Hum Mol Genet* 1996, **5**:809-813.
29. Corbin F, Bouillon M, Fortin A, Morin S, Rousseau F, Khandjian EW: **The fragile X mental retardation protein is associated with poly(A)⁺ mRNA in actively translating polyribosomes.** *Hum Mol Genet* 1997, **6**:1465-1472.
30. Sittler A, Devys D, Weber C, Mandel JL: **Alternative splicing of exon 14 determines nuclear or cytoplasmic localisation of fmr1 protein isoforms.** *Hum Mol Genet* 1996, **5**:95-102.
31. Khandjian EW: **Biology of the fragile X mental retardation protein, an RNA-binding protein.** *Biochem Cell Biol* 1999, **77**:331-342.
32. Kirkpatrick LL, McIlwain KA, Nelson DL: **Alternative splicing in the murine and human FXR1 genes.** *Genomics* 1999, **59**:193-202.
33. Bardoni B, Schenck A, Mandel JL: **A novel RNA-binding nuclear protein that interacts with the fragile X mental retardation (*FMR1*) protein.** *Hum Mol Genet* 1999, **8**:2557-2566.
34. Laggerbauer B, Ostareck D, Keidel E, Ostareck-Lederer A, Fischer U: **Evidence that fragile X mental retardation protein is a negative regulator of translation.** *Hum Mol Genet* 2001, **10**:329-338.
35. Carrié A, Jun L, Bienvenu T, Vinet MC, McDonnell N, Couvert P, *et al.*: **A new member of the IL-1 receptor family highly expressed in hippocampus and involved in X-linked mental retardation.** *Nat Genet* 1999, **23**:25-31.
36. Zemni R, Bienvenu T, Vinet MC, Sefiani A, Carrié A, Billuart P, *et al.*: **A new gene involved in X-linked mental retardation identified by analysis of an X;2 balanced translocation.** *Nat Genet* 2000, **24**:167-170.
37. Shapira M, Dar H, Bar-El H, Bar-Nitzan N, Even L, Borochowitz Z: **Inherited inverted duplication of X chromosome in a male: report of a patient and review of the literature.** *Am J Med Genet* 1997, **72**:409-414.
38. Kendall E, Evans W, Jin H, Holland J, Vetrie D: **A complete YAC contig and cosmid interval map covering the entirety of human Xq21.33 to Xq22.3 from DXS3 to DXS287.** *Genomics* 1997, **43**:171-182.
39. Srivastava AK, McMillan S, Jermak C, Shomaker M, Copeland-Yates SA, Sossey-Alaoui K, *et al.*: **Integrated STS/YAC physical, genetic, and transcript map of human Xq21.3 to q23/q24 (*DXS1203-DXS1059*).** *Genomics* 1999, **58**:188-201.
40. Sambrook J, Fritsch EF, Maniatis T: *Molecular Cloning: A Laboratory Manual*, 2nd edn. New York: Cold Spring Harbor Laboratory Press; 1989.
41. De Backer MD, de Hoogt RA, Froyen G, Odds FC, Simons F, Contreras R, *et al.*: **Single allele knock-out of *Candida albicans* CGT1 leads to unexpected resistance to hygromycin B and elevated temperature.** *Microbiology* 2000, **146**:353-365.
42. de Hoop MJ, Meyn L, Dotti CG: **Culturing hippocampal neurons and astrocytes from fetal rodent brain.** In *Cell Biology: A Laboratory Handbook*, 2nd edn. Edited by Celis JE. San Diego, CA: Academic Press; 1998: 154-163.

2.2 Role of *Drosophila* NXFs, p15 and UAP56 in nuclear mRNA export

2.2.1 Paper 3:

NXF1/p15 heterodimers are essential for mRNA nuclear export in *Drosophila*

Herold, A., Klymenko, T., Izaurralde, E. (2001) *RNA* 7, 1768-1780.

Context

The genomes of higher eukaryotes encode multiple NXF proteins. Apart from TAP, several human NXF proteins display features required to act as mRNA export receptors (Braun *et al.*, 2001; Herold *et al.*, 2000; Yang *et al.*, 2001). The analysis of the precise function of individual human TAP homologues *in vivo* remained difficult, as easy and efficient knockout or knockdown techniques for human model systems were not available at the time this study was initiated. Thus it was still unclear whether metazoan NXFs are functionally redundant or whether their multiplication reflects an adaptation to a greater substrate complexity or to tissue-specific requirements. To address these questions we decided to switch to another eukaryotic model system in which the role of the individual NXF proteins in mRNA export could be studied more easily. We made use of a *Drosophila* tissue-culture system in which the expression of endogenous proteins can be specifically and efficiently silenced by RNAi.

Summary of results and conclusions

The *Drosophila* genome encodes four putative NXF proteins (NXF1-4) and one p15 homologue. We isolated full-length cDNAs encoding NXF1, NXF2, NXF3 and p15 and a partial cDNA encoding NXF4. For that, the predictions presented in Herold *et al.*, (2000) were refined and completed using RACE. We demonstrated that *p15* and *nxf1-3* are expressed in embryos and various *Drosophila* cell lines including the Schneider cell line 2 (S2) while *nxf4* mRNA was not detectable. All four NXF proteins contain at least some domains typical of the NXF family: the LRR and the NTF2-like domains are present in NXF1-3. The UBA-like domain is present in NXF1 and NXF2, but has diverged in NXF3. NXF4 lacks the NTF2-like and UBA-like domains. The RBD and N-terminal regions are less conserved in the *Drosophila* NXF proteins when compared to TAP (see Introduction, Figure 5).

When NXF1-3 were tested for their ability to bind p15 *in vitro*, all three NXF members were able to interact with p15, albeit NXF2 only with low affinity. Tagged versions of NXF1 and p15 were transiently expressed in S2 cells and their localization was determined. Both were found mainly in the nucleus, a fraction of the proteins associating

with the nuclear envelope. NXF2 was detected in the nucleus and the cytoplasm, but could not be clearly visualized at the nuclear envelope.

We next investigated the function of the individual NXF proteins and p15 by depleting their endogenous pools from S2 cells using RNAi and investigating the resulting effects on nuclear mRNA export. Western and Northern blot analyses showed that the depletion of NXF1-3 and p15 from S2 cells was efficient and specific. Since the depletion of NXF1 or p15 resulted in a strong inhibition of cell growth, we concluded that these two proteins have an essential function. The depletion of NXF2-4 had no effect on cell growth. To monitor the effects of the knockdowns on nuclear mRNA export we determined the distribution of poly(A)⁺ RNA in cells depleted of either NXF1-4 or p15 by FISH with an oligo(dT) probe. Poly(A)⁺ RNA was mainly localized to the cytoplasm of control cells and in cells depleted of NXF2-4. In contrast, cells depleted of NXF1 or p15 showed a strong accumulation of poly(A)⁺ RNA inside the nucleus, indicating a general block of nuclear mRNA export. Consistently, the synthesis of new proteins was strongly reduced in these cells, as demonstrated by metabolic labeling. The mRNA export block was further confirmed by fluorescent in situ hybridization (FISH) with a probe directed against the *rp49* mRNA. This mRNA was mainly localized to the nucleus in cells depleted of NXF1 or p15, while it was cytoplasmic in control cells or cells depleted of NXF2. To test if NXF1 and p15 are also essential for the nuclear export of heat shock mRNAs, we followed the induction of heat shock protein synthesis by metabolic labeling at elevated temperatures. In NXF1 and p15 knockdowns, the expression of heat shock proteins was strongly inhibited. Following experiments demonstrate that this failure to produce heat shock proteins was caused by the inhibition of export of the corresponding heat shock mRNAs to the cytoplasm: Northern blot analysis demonstrated that the mRNAs had been transcriptionally induced and correctly spliced, indicating that neither transcription nor splicing were substantially inhibited. FISH directed against *hsp70* or *hsp83* mRNAs showed that these mRNAs were blocked in the nuclear compartment in most cells depleted of NXF1 or p15, while they were almost exclusively cytoplasmic in control cells or cells depleted of NXF2. Thus the nuclear export of heat shock (e.g. *hsp83*, *hsp70*) and non-heat shock mRNAs (e.g. *rp49*), including intron-containing (*rp49*, *hsp83*) and intronless (*hsp70*) mRNAs is inhibited in cells depleted of NXF1 or p15.

Altogether these data indicate that only NXF1:p15 heterodimers (but not NXF2-4) are general mRNA export factors in S2 cells, while the other members of the NXF family play more specialized or different roles.

In this manuscript we also analyzed the expression patterns of human *tap*, *nxf2*, *nxf3* and the two human *p15* homologues using multiple tissue Northern blots. We demonstrated that *tap*, *p15-1* and *p15-2* mRNAs are ubiquitously expressed. In contrast, human *nxf2* and *nxf3* transcripts showed a tissue-specific pattern of expression and were

mainly found in testis. Thus, if human NXF2 or NXF3 acted as mRNA export factors they could do so only in certain cell types. In contrast, *Drosophila nxf1-3* did not display a tissue-specific pattern of expression in *Drosophila* embryos, suggesting that they might fulfill housekeeping functions, although a tissue-specific pattern of expression in later stages of development cannot be ruled out.

Contribution

I designed and performed all experiments besides the *in vitro* binding assay presented in Fig 2B; Furthermore, I established all techniques concerning *Drosophila* cell culture in the lab including the culturing, transfection, RNAi, FISH and metabolic labeling. Tetyana Klymenko was involved in the initial cloning of some cDNAs and in the production of antibodies. I also assembled all figures and wrote a draft of the manuscript. Overall, I contributed 95% of the published material.

NXF1/p15 heterodimers are essential for mRNA nuclear export in *Drosophila*

ANDREA HEROLD, TETYANA KLYMENKO, and ELISA IZAURRALDE

European Molecular Biology Laboratory, 69117 Heidelberg, Germany

ABSTRACT

The conserved family of NXF proteins has been implicated in the export of messenger RNAs from the nucleus. In metazoans, NXFs heterodimerize with p15. The yeast genome encodes a single NXF protein (Mex67p), but there are multiple *nxf* genes in metazoans. Whether metazoan NXFs are functionally redundant, or their multiplication reflects an adaptation to a greater substrate complexity or to tissue-specific requirements has not been established. The *Drosophila* genome encodes one p15 homolog and four putative NXF proteins (NXF1 to NXF4). Here we show that depletion of the endogenous pools of NXF1 or p15 from *Drosophila* cells inhibits growth and results in a rapid and robust accumulation of polyadenylated RNAs within the nucleus. Fluorescence in situ hybridizations show that export of both heat-shock and non-heat-shock mRNAs, as well as intron-containing and intronless mRNAs is inhibited. Depleting endogenous NXF2 or NXF3 has no apparent phenotype. Moreover, NXF4 is not expressed at detectable levels in cultured *Drosophila* cells. We conclude that Dm NXF1/p15 heterodimers only (but not NXF2-NXF4) mediate the export of the majority of mRNAs in *Drosophila* cells and that the other members of the NXF family play more specialized or different roles.

Keywords: mRNA export; nuclear export; NXF; NXT; p15; *small bristles*; TAP

INTRODUCTION

Messenger RNAs are exported from the nucleus as large ribonucleoprotein (mRNP) complexes composed of an RNA molecule and several distinct proteins. Their export occurs through nuclear pore complexes (NPCs) and is a receptor-mediated process (reviewed by Mattaj & Englmeier, 1998; Nakielnny & Dreyfuss, 1999). Studies in yeast and in vertebrate cells aimed at identifying export receptors for mRNPs have converged on an evolutionarily conserved family of proteins known as the nuclear export factor (NXF) family (reviewed by Conti & Izaurralde, 2001). The yeast genome encodes a single NXF protein, Mex67p, but there are two *nxf* genes in *Caenorhabditis elegans* (Ce), four in *Drosophila melanogaster* (Dm) and five putative genes in *Homo sapiens* (Hs; Herold et al., 2000; Tan et al., 2000; Jun et al., 2001; Yang et al., 2001). Hs NXF1 is also known as TAP and will be referred to as TAP.

Proteins of the NXF family have several conserved structural domains. From the N- to the C-terminus these are: an RNP-type RNA-binding domain, a leucine-rich

repeat (LRR) domain, a middle region showing sequence and structural similarities to the nuclear transport factor 2 (the NTF2-like domain) and a C-terminal region related to ubiquitin associated (UBA) domains (the UBA-like domain; Fig. 2A; Herold et al., 2000; Liker et al., 2000; Suyama et al., 2000; Fribourg et al., 2001).

The NTF2-like domains of TAP, Hs NXF2, and Hs NXF3 heterodimerize with the small protein p15, which is also related to NTF2 (Katahira et al., 1999; Herold et al., 2000; Fribourg et al., 2001), but the NTF2-like domain of *Saccharomyces cerevisiae* (Sc) Mex67p binds to Mtr2p (Santos Rosa et al., 1998; Strässer et al., 2000). Mtr2p is not related in sequence to p15 but might be its functional analog (Katahira et al., 1999; Fribourg et al., 2001). The NTF2-like domain of TAP bound to p15 and the UBA-like domain mediate binding to nucleoporins, the components of the NPC (Fribourg et al., 2001). The role of the NTF2- and UBA-like domains in nucleoporin binding is conserved in Hs NXF2, Ce NXF1, and Sc Mex67p (Bear et al., 1999; Herold et al., 2000; Kang et al., 2000; Strässer et al., 2000; Tan et al., 2000; Yang et al., 2001).

NXF proteins not only share a similar structural domain organization, but at least five members of the NXF family exhibit RNA export activity or have been shown to participate directly in the export of mRNA to

Reprint requests to: Elisa Izaurralde, European Molecular Biology Laboratory, Meyerhofstrasse 1, 69117 Heidelberg, Germany; e-mail: izaurralde@embl-heidelberg.de.

the cytoplasm. This suggests that NXFs represent a family of RNA export factors. However, a different function cannot be excluded. Indeed, whereas Sc Mex67p and Ce NXF1 are essential for the export of bulk polyadenylated RNAs [poly(A)⁺ RNA] (Segref et al., 1997; Tan et al., 2000), the function of Ce NXF2 is unknown, and its knockdown has no apparent phenotype (Tan et al., 2000).

TAP has been identified as the cellular protein recruited by the constitutive transport element (CTE) of simian type D retroviruses to promote the nuclear export of viral transcripts (Grüter et al., 1998). In *Xenopus laevis* oocytes, titration of TAP with an excess of CTE RNA blocks the export of cellular mRNAs (Pasquinelli et al., 1997; Saavedra et al., 1997). This, and the observation that coexpression of TAP and p15 in *S. cerevisiae* partially restores growth of the otherwise lethal *mex67/mtr2* double knockout (Katahira et al., 1999), strongly suggests a role for TAP in mRNA export. Consistently, overexpression of TAP/p15 heterodimers in human cultured cells, or microinjection of the recombinant proteins in *Xenopus laevis* oocytes, stimulates export of RNAs that are otherwise exported inefficiently (Braun et al., 2001). In addition, TAP/p15 heterodimers elicit nuclear export when either of them is tethered directly to a precursor mRNA that is normally retained within the nucleus (Braun et al., 2001; Guzik et al., 2001; Yang et al., 2001).

Despite the wealth of accumulated information, however, the identification of cellular mRNAs exported by TAP has remained elusive. The multiplication of *nxf* genes in metazoans has raised the question as to whether these proteins are functionally redundant or are specialized to export specific mRNA classes. Hs NXF2 is 58% identical to TAP and its coexpression with p15 in cultured cells also promotes the nuclear exit of inefficiently exported RNAs (Herold et al., 2000). Also, in the presence of p15, Hs NXF2, and NXF3 both promote export when tethered directly to an inefficiently spliced precursor mRNA (Yang et al., 2001; A. Herold & E. Izaurralde, unpubl. results). Thus, at least three out of five Hs NXFs exhibit RNA export activity. In *Drosophila*, at least two out of four NXF proteins (NXF1 and NXF2) have all the structural domains characteristic of the NXF family (Herold et al., 2000) and are expected a priori to be implicated in mRNP export.

In addition to the roles of the different NXFs in metazoans, the role of p15 is an open question in the mRNA export pathway. Based on the homology of p15 with NTF2, it has been reported that p15 binds RanGTP and is implicated in the export of tRNA and of substrates exported by CRM1 (Black et al., 1999, 2001; Ossareh-Nazari et al., 2001). Binding of p15 to Ran has not been reproduced in other laboratories (Katahira et al., 1999; Herold et al., 2000) and is incompatible with the known structure of the protein (Fribourg et al., 2001). The observation that p15 is required for

the export of RNA mediated by TAP, NXF2, and NXF3, together with structural studies (Herold et al., 2000; Braun et al., 2001; Fribourg et al., 2001; Guzik et al., 2001), suggest that p15 forms a single structural and functional unit with the NTF2-like domains of the NXF proteins with which it heterodimerizes.

The emergence of double-stranded RNA interference (dsRNAi) technique, which has been applied successfully to deplete endogenous proteins from cultured *Drosophila* cells (Clemens et al., 2000), provides the opportunity to investigate the role of p15 and NXF proteins in vivo. Using this approach, we show that depletion of either NXF1 or p15 inhibits cell growth and results in a severe nuclear accumulation of poly(A)⁺ RNA. In contrast, depletion of NXF2 or NXF3 has no apparent phenotype. We conclude that NXF1/p15 heterodimers are essential for the export of bulk mRNA in *Drosophila* cells. The other NXF homologs are likely to play more specialized roles, perhaps reflecting the greater substrate diversity of metazoa.

RESULTS

***Drosophila* NXF1–3 are expressed in different cell lines and throughout embryogenesis**

The multiplication of the *nxf* genes in metazoans compared to yeast may reflect a redundancy in the mRNA export pathway or an adaptation to tissue- or substrate-specific requirements. To distinguish between these possibilities, we have analyzed the expression patterns of Hs and Dm NXFs. To this end, we have isolated full-length cDNAs encoding Dm NXF1, NXF2, NXF3, and p15 and a partial cDNA encoding Dm NXF4. Isolation and characterization of Hs NXFs and p15 was reported previously (Herold et al., 2000; Jun et al., 2001). Multiple tissue northern blot analysis shows that only TAP and the two Hs p15 homologs are ubiquitously expressed (Fig. 1A and data not shown). NXF2 is mainly expressed in testis (Fig. 1A). NXF3 is detected at a high level in testis and at low level in kidney (Fig. 1A). NXF5 is not detectable by northern blot but it could be amplified by PCR on cDNA derived from human fetal brain (Jun et al., 2001). Similar expression patterns were previously reported for TAP (Yoon et al., 1997) and recently for Hs NXFs (Jun et al., 2001; Yang et al., 2001). These expression patterns suggest that Hs NXF2–5 have tissue-specific functions and are unlikely to act as general export receptors of bulk mRNA.

The expression pattern of Dm NXFs was investigated by RT-PCR in different cell lines and in *Drosophila* embryos at different stages of development (Fig. 1B). NXF1–3 cDNAs could be amplified from all samples tested (Fig. 1B, lanes 1–5). The amplification was specific, as no product was obtained when the reverse transcriptase was omitted (Fig. 1B, lanes 6–10). More-

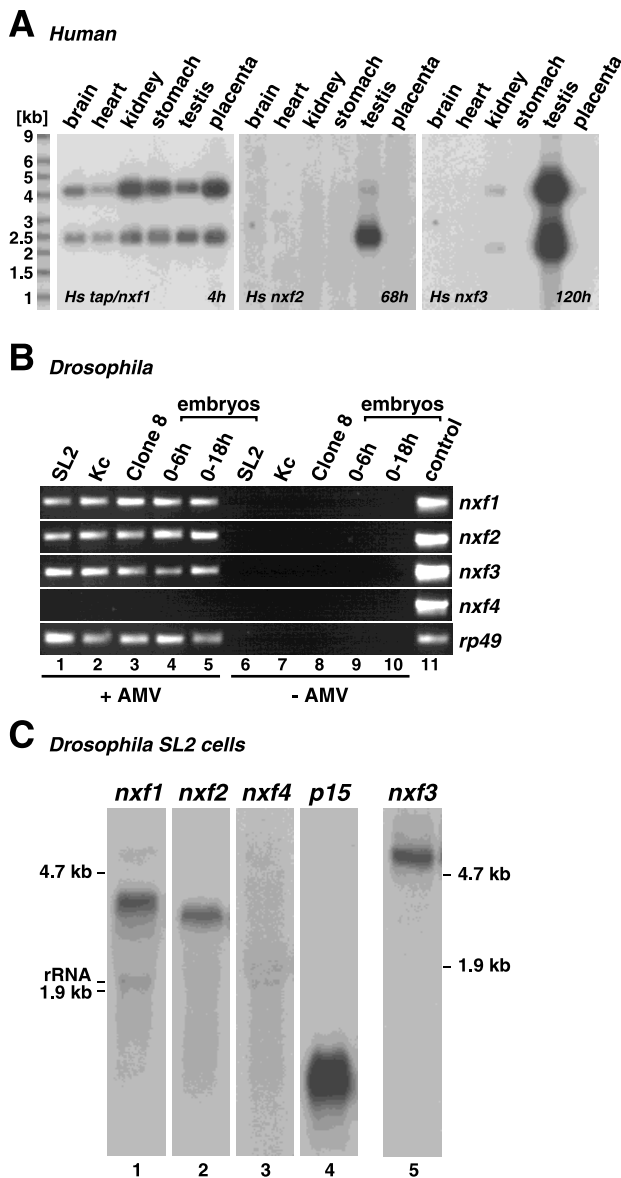


FIGURE 1. Comparison of Hs and Dm NXFs expression patterns. **A:** Tissue-specific expression pattern of TAP, Hs NXF2, and Hs NXF3. A human multiple tissue northern blot was consecutively hybridized with specific probes, as indicated. The exposure times are indicated on the right of each panel. **B:** The expression of Dm NXFs was investigated by semiquantitative RT-PCR on total RNA isolated from the embryonic cell lines SL2 and Kc, the Imaginal Disc cell line (clone 8), and embryos at different stages of development. **C:** Detection of Dm *nxf*s and *p15* mRNAs by northern blot analysis. Twenty micrograms of total RNA from SL2 cells were loaded in lanes 1–4 and 30 μ g in lane 5. For *nxf4*, no signal was detected even after prolonged exposures.

over, the amplicons had the mobility of the product obtained when plasmids containing the corresponding cDNAs were used as templates (Fig. 1B, lane 11). No *nxf4* product was obtained using two different primer sets after 25 cycles of amplification. This indicates that *nxf4* mRNA represents a low-abundance transcript. The results obtained by RT-PCR were confirmed for *Drosophila* Schneider cells (SL2 cells) by northern blot

analysis (Fig. 1C). Moreover, in situ analysis indicates that Dm NXF1–3 are expressed ubiquitously throughout embryonic development, whereas no signal above background levels is detected for *nxf4* (Korey et al., 2001; Wilkie et al., 2001; data not shown; C. Korey and D. van Vactor, pers. comm.).

Domain organization of *Drosophila melanogaster* NXF homologs

Comparison of the deduced amino acid sequence of Dm NXFs with TAP reveals that Dm NXF1 is more closely related to TAP than to the other Dm NXF homologs. Indeed, Dm NXF1 displays 35% sequence identity with TAP and about 20% identity with Dm NXF2–4. In addition, whereas Hs NXFs are at least 50% identical to each other (Herold et al., 2000), Dm NXFs are less well conserved and display about 20% sequence identity with any other Dm NXF.

Despite the divergence in the amino acid sequences, the overall domain organization of Dm NXFs is similar to that of TAP and other members of the NXF family. The LRR and the NTF2-like domains are present in NXF1, NXF2, and NXF3 (Fig. 2A). The C-terminal UBA-like domain is also present in NXF1 and NXF2 but has diverged in NXF3. In particular, a conserved tryptophane residue (W594 in TAP; Herold et al., 2000; Suyama et al., 2000) is not present in Dm NXF3. NXF4 lacks the NTF2-like and the UBA-like domains mediating the direct association with the NPC (Fribourg et al., 2001). The noncanonical RNP-type RNA-binding domain (RBD) and the N-terminal sequences upstream of the RBD are less well conserved. In NXF2, these sequences are predicted to contain additional LRRs.

The NTF2-like domain of Hs NXF proteins binds to p15 and is required for NXF function (Braun et al., 2001; Fribourg et al., 2001). We therefore investigated whether Dm NXF proteins interact with Dm p15. [³⁵S]methionine-labeled NXF1, NXF2, and NXF3 were synthesized in vitro in rabbit reticulocyte lysates and assayed for binding to glutathione agarose beads coated with Dm or Hs p15 fused to glutathione S-transferase (GST). NXF1 and NXF3 were selected on beads coated with either of the p15 proteins (Fig. 2B, lanes 3 and 4) but not on control beads coated with GST (Fig. 2B, lane 2). Dm NXF2 exhibits low affinity for p15. TAP displays a species-specific interaction profile, as it binds preferentially to Hs p15. As expected, the C-terminal domain of TAP (fragment 371–619), but not its N-terminal half (fragment 1–372), bound to Hs p15.

The subcellular localization of Dm NXF1, NXF2, and p15 fused to an HA-tag was investigated in transfected SL2 cells and compared to the localization of the endogenous nuclear protein Dm REF1 (Stutz et al., 2000). HA-tagged NXF1 and p15 were evenly spread throughout the nucleoplasm and were excluded from the nucleolus (Fig. 2C). Depending on the expression level,

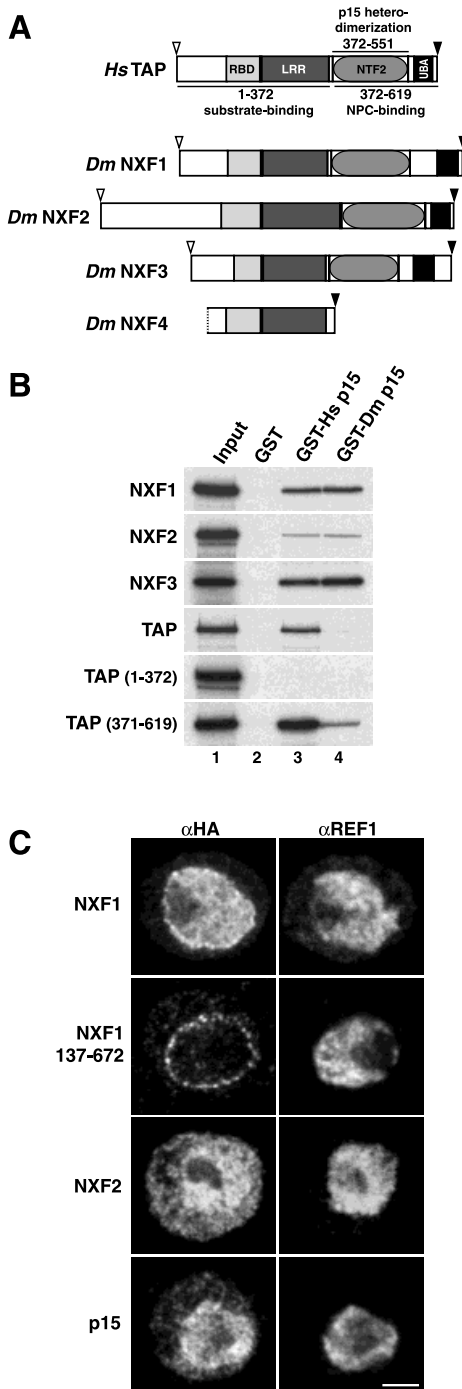


FIGURE 2. Domain organization and subcellular localization of Dm NXFs. **A:** RBD: noncanonical RNP-type RNA binding domain; LRR: leucine-rich repeat domain; NTF2: NTF2-like domain; UBA: UBA-like domain; open triangles: initiation codon; black triangles: stop codon. NXF4 sequence lacks the 5' end. **B:** Dm NXF1 and Dm NXF3 interact with Dm p15 in vitro. GST-pull-down assays were performed with in vitro synthesized, [³⁵S]methionine-labeled proteins indicated on the left of the panels, and recombinant GST or GST fused to Hs or Dm p15 as indicated above the lanes. One-tenth of the input (lane 1) and one-quarter of the bound fractions (lanes 2–4) was analyzed by SDS-PAGE and fluorography. Analysis of the supernatants ensured that proteins were not degraded during the experiment (not shown). **C:** SL2 cells were transfected with plasmids expressing HA fusions of NXF1, NXF2, p15, and a N-terminal truncation of NXF1 (137–672), as indicated on the left. HA-tagged proteins were visualized by indirect immunofluorescence. Cells were double-labeled with anti-REF1 antibodies. Scale bar = 2.5 μ m.

p15 could also be detected in the cytoplasm (Fig. 2C). As reported for TAP and Hs p15, a fraction of Dm NXF1 and Dm p15 associated with the nuclear envelope. Nuclear envelope association mediated by the C-terminal domain of TAP can be clearly visualized by deleting the N-terminal nuclear localization signal. This reduces the nuclear uptake of the protein and the nucleoplasmic signal (Bachi et al., 2000). The nuclear envelope association of Dm NXF1 was confirmed by deleting the N-terminal sequences upstream of the RBD (NXF1 137–672). The truncated protein was localized predominantly at the nuclear rim in a punctuate pattern (Fig. 2C), suggesting that Dm NXF1 binds to nucleoporins in vivo. Dm NXF2 was detected in both the nucleoplasm and the cytoplasm (Fig. 2C). Thus, despite the fact that NXF2 contains all structural domains characteristic of NXF proteins, it has low affinity for p15 and does not clearly localize at the nuclear rim.

Depletion of NXF1 and p15 proteins by dsRNAi inhibits cell growth

To deplete endogenous Dm p15 and NXF1–4, SL2 cells were transfected with dsRNAs corresponding to N-terminal fragments of the proteins. As a control, a dsRNA corresponding to an N-terminal fragment of green fluorescent protein (GFP) was transfected. Strikingly, depletion of NXF1 and p15 results in a dramatic inhibition of cell growth as early as 2 days after transfection (Fig. 3A), indicating that these proteins are essential. Depletion of NXF2–4 has no effect on cell growth compared to untreated cells or cells transfected with GFP dsRNA (Fig. 3A).

To determine the efficiency and specificity of the depletion, we transfected dsRNAs corresponding to NXF1, NXF2, and p15 into SL2 cells and performed a time-course western blot analysis with antibodies raised against the recombinant proteins. Only 2 days after transfection, the steady-state expression levels of NXF1 and NXF2 were already reduced to about 10 to 20% of the levels detected in untreated cells (Fig. 3B, day 2 versus day 0), whereas p15 levels were reduced down to 20–30%. No recovery of the protein expression levels was observed even 8 days after transfection (Fig. 3B). The depletion is specific for the following reasons. First, the expression level of an unrelated protein, the translation initiation factor eIF4G, was not affected by NXF1, p15, or NXF2 dsRNAs (Fig. 3B). Second, transfection of the unrelated GFP dsRNA had no effect on the expression of any of the proteins tested (Fig. 3C, lanes 1 and 2). More importantly, NXF1 protein levels are not affected in cells transfected with NXF2 dsRNA. Similarly, NXF2 expression levels are unaffected in cells transfected with NXF1 or control (GFP) dsRNA (Fig. 3C). In the absence of specific antibodies directed to NXF3, the efficiency of NXF3 depletion was determined by northern blot (Fig. 3D). The

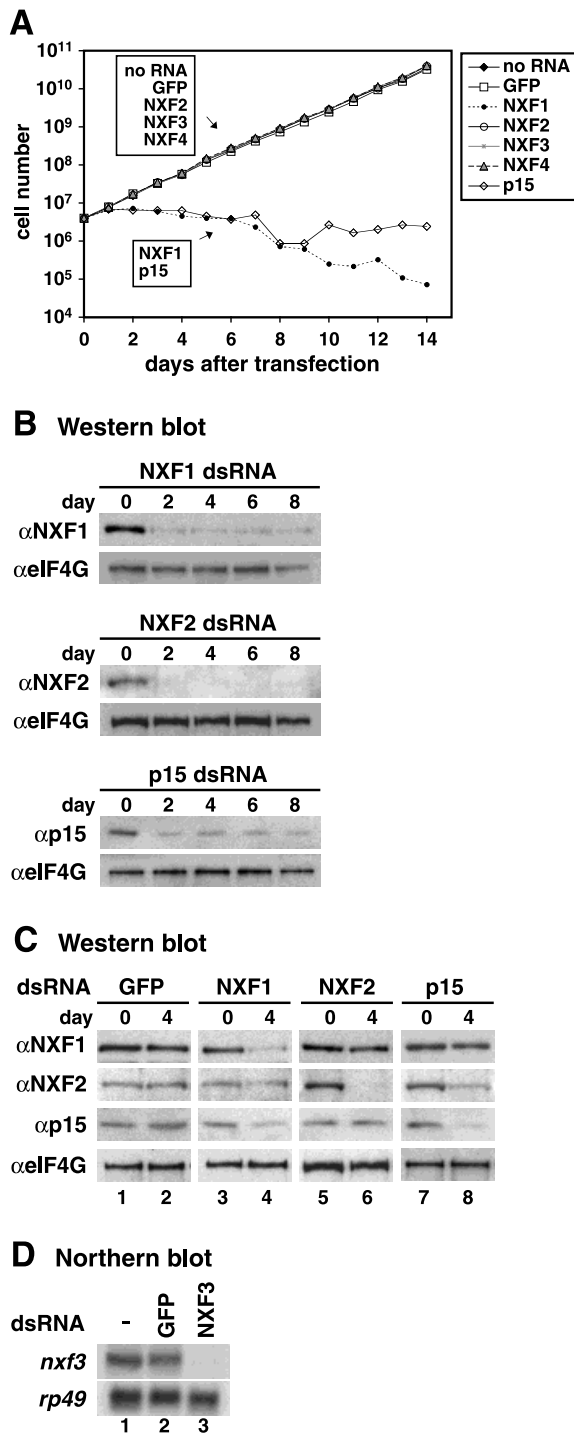


FIGURE 3. Depletion of NXF1 and p15 inhibits cell growth. **A:** SL2 cells growing in suspension were transfected with dsRNA specific for NXF1–4, p15, or GFP. Cell numbers were determined every day. On days 4 and 8, cells were retransfected with NXF2–4 and GFP dsRNAs. **B:** Two to 8 days after transfecting the indicated dsRNAs, SL2 cells were analyzed by western blotting with antibodies raised against recombinant NXF1, NXF2, p15, and the unrelated protein eIF4G as a control. **C:** The depletion of NXF1 and NXF2 is specific. SL2 cells were transfected with GFP, NXF1, NXF2, or p15 dsRNA as indicated above the lanes. Four days after transfection NXF1, NXF2, p15, and eIF4G protein levels were analyzed by western blotting of total cell lysates. **D:** Six days posttransfection, total RNA isolated from SL2 cells from the same experiment as in **A** was analyzed for the presence of *nxf3* mRNA by northern blot. The same filter was probed for the presence *rp49* mRNA.

nxf3 mRNA was degraded in cells transfected with the corresponding dsRNA (Fig. 3D, lane 3). Transfection of GFP dsRNA does not affect *nxf3* mRNA levels (Fig. 3D, lane 2). The effect of NXF3 dsRNA is specific, as the mRNA coding for the ribosomal protein rp49 was not degraded (Fig. 3D, lower panel).

In transiently transfected human 293 cells, the steady-state expression level of TAP is increased when Hs p15 is cotransfected (Herold et al., 2000; Braun et al., 2001). Therefore we tested if the marked growth defect observed in cells depleted of p15 was indirect and caused by NXF1 destabilization or mislocalization. As shown in Figure 3C, NXF1 protein is not destabilized in cells that have been depleted of p15 (lanes 7–8). Even 1 week after transfection of p15 dsRNA, the steady-state expression level of NXF1 was not reduced (not shown). NXF2, in contrast, was partially destabilized in cells depleted of p15 (Fig. 3C, lanes 7–8) suggesting that despite a weak binding in vitro (Fig. 3C), these proteins may form heterodimers in vivo. Unexpectedly, expression of p15 was slightly but reproducibly reduced in cells depleted of NXF1 (Fig. 3C, lanes 3–4).

The subcellular localization of HA-tagged Dm NXF1 and NXF2 did not change when transiently expressed in cells depleted of p15. HA-tagged p15 also remained predominantly nuclear in cells depleted of NXF1 (data not shown). Because NXF1 is neither destabilized nor mislocalized in cells depleted of p15, we conclude that in the absence of p15, NXF1 cannot perform its essential function.

Polyadenylated RNAs accumulate in the nucleus of cells depleted of NXF1 or p15

The intracellular distribution of bulk poly(A)⁺ RNA in control cells and in cells depleted of NXF1–4 or p15 was investigated by in situ hybridization with a Cy3-labeled oligo(dT) probe. The nuclear envelope was stained with the monoclonal antibody mAb414, which recognizes several nucleoporins, or with fluorescently labeled wheat germ agglutinin (WGA).

At steady state, a large fraction of poly(A)⁺ RNA is cytoplasmic in untreated SL2 cells or cells transfected with control GFP dsRNA (Fig. 4A, panel a; Fig. 4B, panels a and e). In contrast, NXF1 depletion results in a robust nuclear accumulation of poly(A)⁺ RNAs (Fig. 4A, panel e; Fig. 4B, panel b). The poly(A)⁺ signal is widespread within the nucleoplasm and is excluded from the large nucleolus characteristic of this cell line (Fig. 4A, panel e). This change in the distribution of poly(A)⁺ RNA is also observed in cells depleted of endogenous p15 (Fig. 4A, panel m; Fig. 4B, panel c). The nuclear accumulation of poly(A)⁺ RNA correlates with the depletion of the targeted proteins, as it is detected in about half or one-third of the cell population as early as 40 h after transfecting NXF1 or p15 dsRNAs,

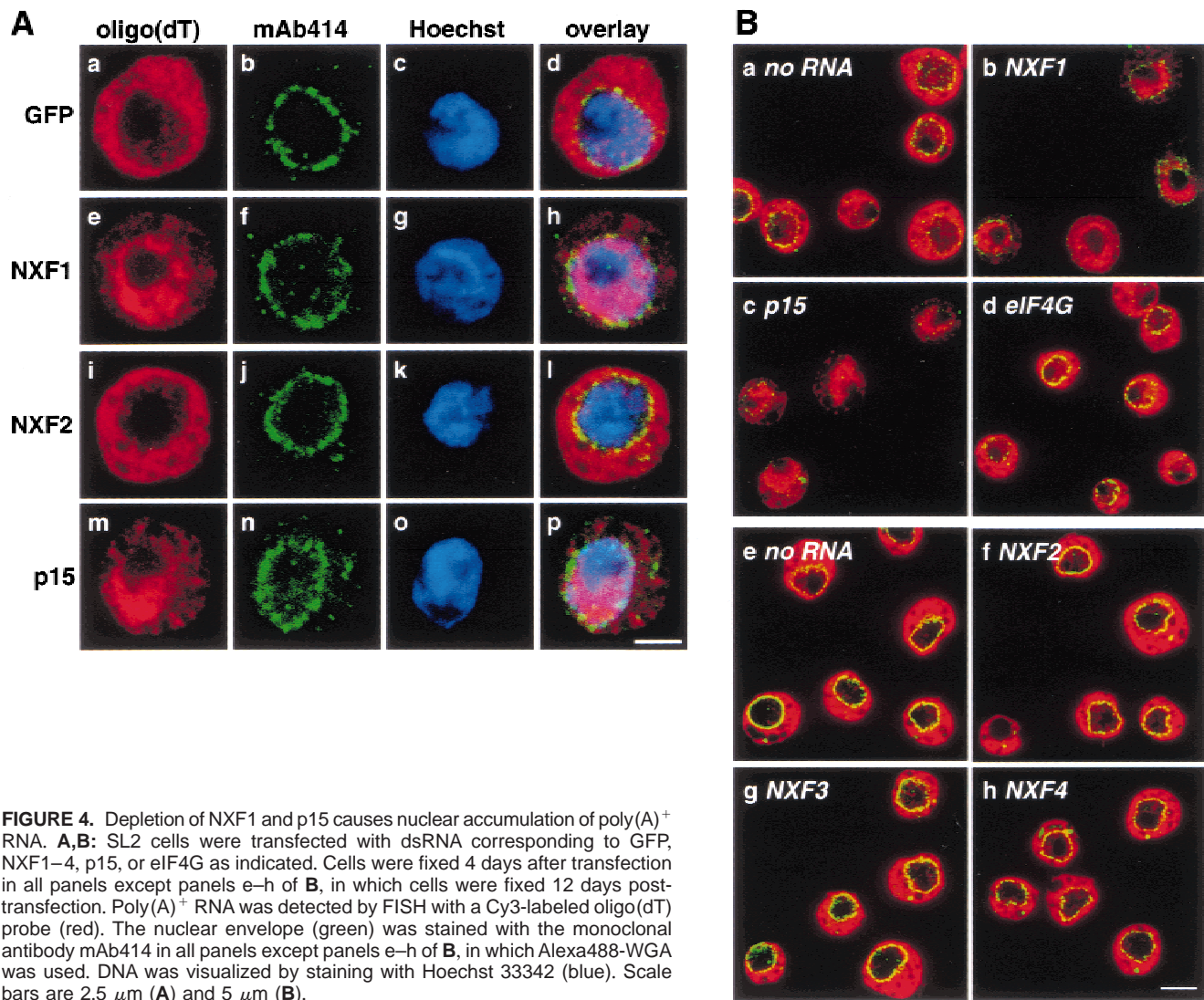


FIGURE 4. Depletion of NXF1 and p15 causes nuclear accumulation of poly(A)⁺ RNA. **A,B:** SL2 cells were transfected with dsRNA corresponding to GFP, NXF1–4, p15, or eIF4G as indicated. Cells were fixed 4 days after transfection in all panels except panels e–h of **B**, in which cells were fixed 12 days post-transfection. Poly(A)⁺ RNA was detected by FISH with a Cy3-labeled oligo(dT) probe (red). The nuclear envelope (green) was stained with the monoclonal antibody mAb414 in all panels except panels e–h of **B**, in which Alexa488-WGA was used. DNA was visualized by staining with Hoechst 33342 (blue). Scale bars are 2.5 μ m (**A**) and 5 μ m (**B**).

respectively (data not shown). The accumulation can be observed in almost all cells 65 h after transfection.

In cells depleted of NXF2–4, poly(A)⁺ RNAs localize mainly to the cytoplasm, as in control cells (Fig. 4A, panel i; Fig. 4B, panels f–h). Thus, in the presence of NXF1, depletion of NXF2–4 does not affect the export of bulk poly(A)⁺ RNA. Moreover, the fact that NXF2 protein is present in cells depleted of NXF1 (Fig. 3C, lanes 3 and 4), but does not restore cell growth or poly(A)⁺ mRNA export, suggests that these proteins are not functionally redundant. Alternatively, the expression levels of NXF2 or of NXF3 in SL2 cells might not be sufficient to compensate for the depletion of NXF1. Quantitative western blots indicate that NXF2 is indeed, about four times less abundant than NXF1 in SL2 cells. However, overexpression of NXF2, with or without p15, does not rescue the NXF1-knockdown phenotype (data not shown).

The nuclear accumulation of poly(A)⁺ RNA observed in cells depleted of NXF1 and p15 is not a direct con-

sequence of the inhibition of cell growth, as depletion of eIF4G also results in a strong growth defect, which is not accompanied by a nuclear accumulation of poly(A)⁺ RNA (Fig. 4B, panel d). Together, our data suggest that the growth arrest observed in cells depleted of NXF1 or p15 is a consequence of a general block to mRNA export.

Depletion of NXF1 or p15 results in a general block of protein synthesis

The general inhibition of mRNA export in SL2 cells depleted of NXF1 or p15 was confirmed by metabolic labeling (Fig. 5A). Cells depleted of NXF1, NXF2, or p15 were pulse labeled with [³⁵S]methionine 4 days after transfecting the corresponding dsRNAs. Total lysates from equivalent numbers of cells were analyzed by SDS-PAGE and fluorography. The incorporation of [³⁵S]methionine into newly synthesized proteins was reduced in cells depleted of NXF1 or p15 in compar-

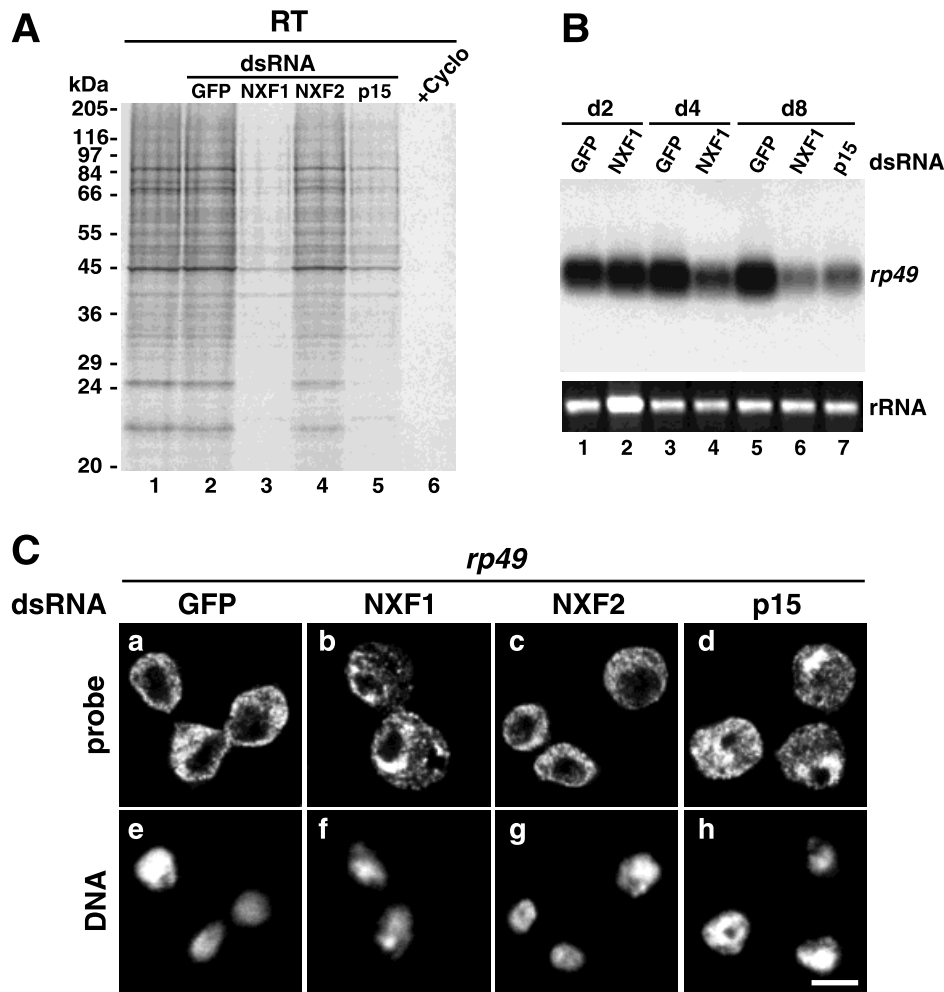


FIGURE 5. Depletion of NXF1 and p15 results in a general block of protein synthesis and leads to nuclear accumulation of *rp49* mRNA. **A:** SL2 cells were transfected with GFP, NXF1, NXF2, and p15 dsRNA. Four days after transfection, cells were pulse labeled with [³⁵S]methionine for 1 h. Total-cell extracts were analyzed by SDS-PAGE followed by fluorography. [³⁵S]methionine incorporation is dramatically reduced in cells depleted of NXF1 or p15 (lanes 3 and 5), or when cyclohexamide (20 μg/mL) was included during the labeling reaction (lane 6). **B:** Northern blot analysis using a *rp49*-specific probe. SL2 cells were transfected with the indicated dsRNAs and total RNA was isolated 2 (lanes 1 and 2), 4 (lanes 3 and 4), or 8 (lanes 5–7) days after transfection. Five micrograms of total RNA were loaded per lane. The lower panel shows the corresponding rRNA stained with ethidium bromide. **C:** SL2 cells were transfected with indicated dsRNAs. Four days after transfection cells were fixed, and *rp49* mRNA was detected by FISH using a digoxigenin-labeled probe. **a–d:** *rp49* signal; **e–h:** DNA staining. Scale bar = 5 μm.

son to control cells (Fig. 5A, lanes 3 and 5 versus 1 and 2). This inhibition of protein synthesis affects most proteins to a similar extent, suggesting that NXF1 and p15 are involved in the nuclear export of most mRNAs. No decline in protein labeling was observed in cells depleted of NXF2 (Fig. 5A, lane 4).

To investigate whether the inhibition of protein synthesis is caused by a block to mRNA export and not to transcription, we analyzed the expression level and the localization of *rp49* mRNA, which is an abundant mRNA in SL2 cells. Northern blot analysis showed that 4 days after transfection of NXF1 dsRNA, the expression levels of this message were reduced in comparison to the levels detected in control cells (Fig. 5B, lanes 3 and 4). Notably, 8 days after transfection, the steady-state ex-

pression levels of the *rp49* mRNA were strongly reduced in cells depleted of NXF1 or p15 in comparison to control cells (Fig. 5B, lanes 5–7). Whether this strong reduction in *rp49* mRNA level is caused by a change in the turnover of this mRNA or by a reduced transcriptional activity in cells in which mRNA export has been inhibited for 8 days has not been investigated.

The subcellular localization of the endogenous *rp49* mRNA was analyzed 4 days after transfection by FISH. The *rp49* mRNA was detected predominantly in the nucleus of 50–65% of cells depleted of NXF1 or p15 (Fig. 5C, panels b and d). In control cells and cells depleted of NXF2, the *rp49* message was found in the cytoplasm (Fig. 5C, panels a and c). Fluorescently labeled sense probe did not yield a signal over back-

ground when employed in the RNA-FISH procedure (not shown). These results indicate that the inhibition of protein synthesis is in part due to an mRNA export block in cells where NXF1 and p15 have been knocked down. A reduced transcriptional activity or an increased turnover of mRNAs that cannot exit the nucleus also contributes to the observed phenotype.

Inhibition of heat-shock response by depletion of NXF1 or p15

To investigate whether heat-shock mRNAs are also exported via the NXF1/p15 pathway, we followed the production of heat-shock proteins in cells depleted of NXF1 or p15 shifted to 33–37 °C. Incubation of cultured *Drosophila* cells at these elevated temperatures induces the massive transcription and translation of a set of well-characterized heat-shock genes, whereas production of non-heat-shock proteins is inhibited (reviewed by Echalié, 1997). This was observed in untreated cells and control cells transfected with GFP or NXF2 dsRNAs (Fig. 6A, lanes 1, 2, and 4). In cells depleted of NXF1 or p15, expression of heat-shock proteins was inhibited (Fig. 6A, lanes 3 and 5). Northern blot analyses showed that both in depleted and control cells *hsp70* mRNA was strongly induced after shifting the cells for 1 h to 37 °C (Fig. 6B, lanes 2, 4, and 6). This indicates that the inhibition of HSP70 protein synthesis in NXF1 or p15 depleted cells is not caused by a failure to transcribe the *hsp70* mRNA.

The levels of *hsp83* mRNA before and after heat shock at 33 °C or 37 °C were also analyzed. *hsp83* differs from all other heat-shock mRNAs in that it is normally expressed to relatively high levels even without exposure to heat stress, and in being the only heat-shock gene containing an intron (Echalié, 1997). When cells were shifted to 33 °C or 37 °C, *hsp83* mRNA synthesis was induced to comparable levels in control cells and cells depleted of NXF1 or p15 (Fig. 6C, lanes 2, 5, 8 and 3, 6, 9). As splicing is inhibited at 37 °C (Yost & Lindquist, 1986), the unspliced *hsp83* pre-mRNA was also detected after shifting the cells to this temperature (Fig. 6C, lanes 3, 6, and 9, asterisk). This accumulation of unspliced *hsp83* pre-mRNA occurs in depleted cells as well as in control cells at 37 °C, but was not observed in cells depleted of NXF1 or p15 at temperatures below 37 °C. Thus, the inability to express heat-shock proteins in cells depleted of NXF1 or p15 is not due to an inhibition of transcription or splicing of the corresponding mRNAs.

Nuclear export of *hsp70* and *hsp83* mRNAs is inhibited in cells depleted of NXF1 or p15

The intracellular distribution of *hsp70* and *hsp83* mRNAs was determined in cells depleted of NXF1 or p15 by FISH. In control cells, the *hsp70* mRNA is detected

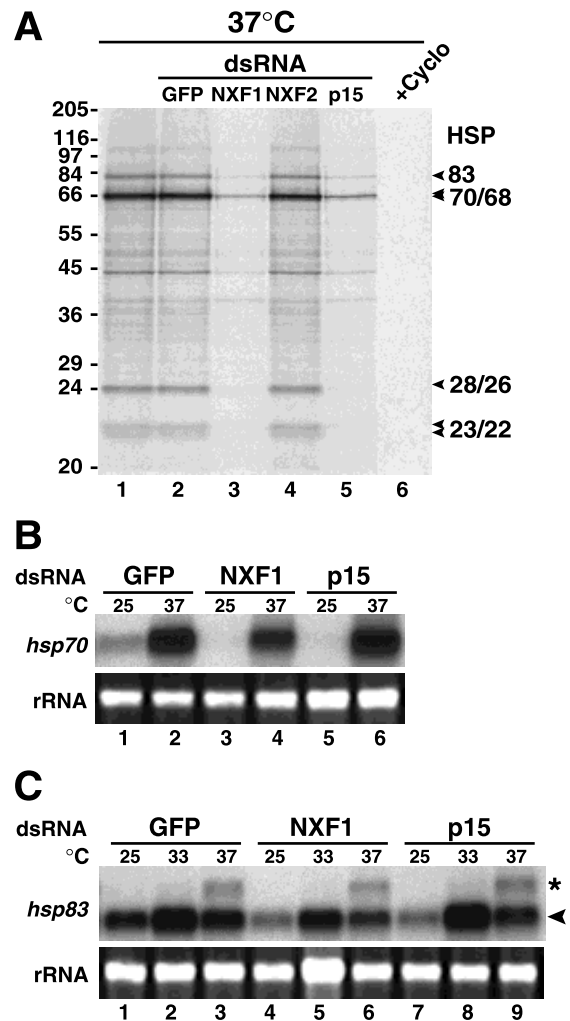


FIGURE 6. Cells depleted of NXF1 or p15 cannot produce heat-shock proteins. **A:** Four days after transfection with the indicated dsRNAs, SL2 cells were shifted to 37 °C and subjected to a metabolic pulse labeling as in Figure 5A. Total-cell extracts were analyzed by SDS-PAGE followed by fluorography. The heat-shock response is inhibited in cells depleted of NXF1 or p15 (lanes 3 and 5) or when cycloheximide is present during the labeling reaction. **B,C:** SL2 cells were transfected with the indicated dsRNAs. Eight days after transfection, cells were either kept at 25 °C (lanes 1, 3, 5 in **B**; lanes 1, 4, 7 in **C**) or subjected to a 1-h heat shock at the indicated temperatures (lanes 2, 4, and 6 in **B**; lanes 2, 3, 5, 6, 8, and 9 in **C**). Five micrograms of total RNA was analyzed by northern blot using probes specific for *hsp70* or *hsp83* mRNAs. The lower panel shows the ethidium bromide stained ribosomal RNA. The asterisk indicates the position of the unspliced *hsp83* precursor mRNA that accumulates at 37 °C, and the fully spliced mRNA is indicated by an arrowhead.

mainly in the cytoplasm and the intensity of the signal increases when cells are shifted to 37 °C prior to fixation (Fig. 7A, panels a and e). In contrast, a clear nuclear accumulation of *hsp70* mRNA is observed in cells depleted of NXF1 or p15 (Fig. 7A, panels b and d). This accumulation was detected in more than 70% (NXF1) or 50% (p15) of the cells, respectively. The localization of *hsp70* mRNA in cells depleted of NXF2 is indistinguishable from that of control cells (Fig. 7A, panel c).

When *hsp83* mRNA FISH analysis was performed, the signals detected before and after heat shock did

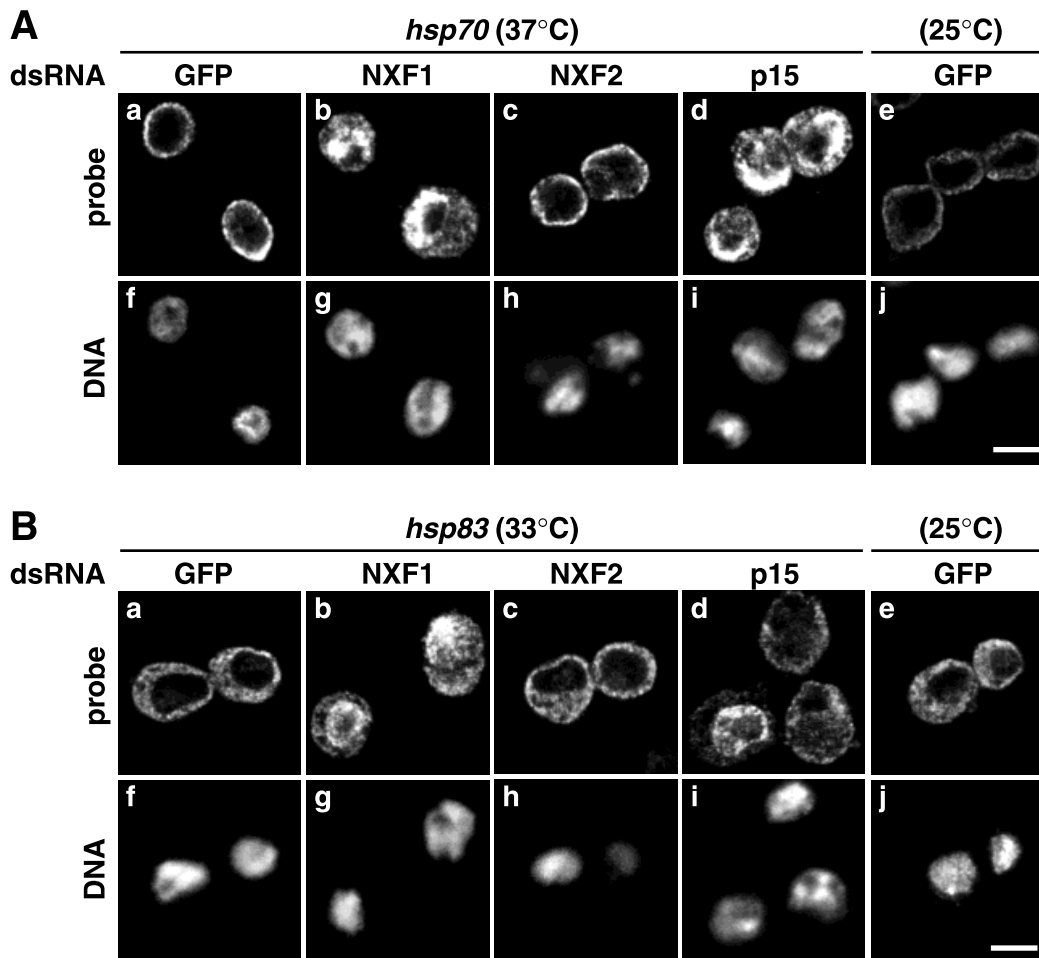


FIGURE 7. *hsp70* and *hsp83* mRNA accumulate in the nucleus of cells depleted of NXF1 or p15. **A:** SL2 cells were shifted to 37°C for 1 h 4 days after transfecting the indicated dsRNAs. *hsp70* mRNA was detected by FISH using a digoxigenin-labeled RNA probe. **a–e:** *hsp70* signal; **f–j:** DNA staining. Scale bar = 5 μ m. **B:** In situ hybridizations were performed with a probe specific for *hsp83* mRNA after shifting the cells 1 h to 33°C. **a–e:** *hsp83* signal; **f–j:** DNA staining. *hsp83* mRNA is detected in cells before transcriptional induction at 33°C (**e**).

not differ significantly in intensity (Fig. 7B, panels a and e), because this mRNA is already expressed at room temperature (Fig. 6C). The localization of *hsp83* mRNA was analyzed in cells depleted of NXF1 or p15 after transcriptional induction at 33°C. Incubation at 37°C was avoided, because at this temperature, in addition to the cytoplasmic signal, a nuclear signal was observed even in control cells, most likely due to the inhibition of splicing (data not shown). After shifting the cells for 1 h to 33°C, the *hsp83* mRNA localized to the cytoplasm of control cells (Fig. 7B, panel a). In cells depleted of p15 or NXF1, the distribution of *hsp83* mRNA changed significantly either to a predominantly nuclear localization (about 40% of the cells) or an even distribution between cytoplasm and nucleus (approximately 45% of the cells; Fig. 7B, panels b and d). Cells depleted of NXF2 show the same distribution as control cells (Fig. 7B, panel c). No signal over background was detected when sense probes were employed (not shown). Hence, we conclude that the lack of heat-

shock protein synthesis in cells depleted of NXF1 or p15 is caused by the inability of heat-shock mRNAs to leave the nucleus.

DISCUSSION

In this study, we have investigated the role of *Drosophila* NXFs and p15 in mRNA nuclear export by specifically depleting these proteins by dsRNAi. We show that although NXF2–4 knockdowns have no apparent phenotype, depletion of either NXF1 or p15 inhibits cell growth and results in a robust nuclear accumulation of bulk poly(A)⁺ RNA. Because the steady-state expression level of NXF1 is not affected in cells depleted of p15, we conclude that both NXF1 and p15 are essential for mRNA nuclear export. This together with previous biochemical, structural, and functional studies (Katahira et al., 1999; Suyama et al., 2000; Braun et al., 2001; Fribourg et al., 2001; Guzik et al., 2001), indicates that the two proteins act as heterodimers. We

also show that, contrary to expectation, the majority of mRNAs are exported by NXF1/p15 heterodimers and the multiplication of *nxf* genes in higher eukaryotes does not reflect a redundancy in the export pathway of bulk mRNA.

mRNA export in *Drosophila* is mediated by NXF/p15 heterodimers

The nuclear accumulation of poly(A)⁺ RNA in cells depleted of NXF1 or p15 correlates well with the reduction of the endogenous protein levels and the cell growth arrest (Figs. 3 and 4) and is similar to the phenotype described in *S. cerevisiae* haploid strains carrying conditional mutations in *mex67* or *mtr2* (Kadowaki et al., 1994; Segref et al., 1997; Santos Rosa et al., 1998). A block to mRNA export in *S. cerevisiae* leads to hyperadenylation of the transcripts accumulating in the nucleus (Hilleren & Parker, 2001; Jensen et al., 2001). This implies that the nuclear signals detected by oligo(dT) in situ hybridizations following export inhibition may not necessarily correlate with the efficiency of the export block. However, in yeast cells carrying mutations in *mex67*, the results obtained by FISH with oligo(dT) were confirmed for individual mRNAs using specific probes. In particular, *ASH1* mRNA, *PGK1* mRNA, and heat-shock mRNAs have been shown to accumulate in the nucleus in *mex67* conditional mutants at the restrictive temperature (Hurt et al., 2000; Vainberg et al., 2000; Jensen et al., 2001). Inhibition of heat-shock mRNA export was also confirmed by the absence of heat-shock protein synthesis in these cells following heat stress (Hurt et al., 2000; Vainberg et al., 2000; Jensen et al., 2001).

We have not investigated whether hyperadenylation occurs in *Drosophila* cells following mRNA export inhibition. Nevertheless, we can exclude the possibility that the nuclear signal detected in cells depleted of NXF1 or p15 using an oligo(dT) probe is due only to hyperadenylation of nascent transcripts, because FISH analysis using probes to detect specific mRNAs show that these mRNAs were indeed mislocalized in these cells. Moreover, the inhibition of protein labeling in cells depleted of NXF1 or p15 suggests that export of most mRNAs is affected. In addition, heat-shock protein synthesis is eliminated in cells depleted of NXF1 or p15. Our data indicate that Dm NXF1/p15 heterodimers are essential for the export of heat-shock and non-heat-shock mRNAs. The fact that export of an intronless mRNA (*hsp70*) and of intron-containing mRNAs (i.e., *hsp83* and *rp49*) is inhibited, indicates that Dm NXF1/p15 heterodimers mediate export of both spliced and intronless mRNAs as previously suggested for TAP/p15 (Braun et al., 2001; Rodrigues et al., 2001). Consistently, in the accompanying manuscript by Wilkie et al. (2001), it is shown that Dm NXF1 is the ubiquitous

mRNA export receptor required in all tissues and stages of development.

Dm NXF1 is encoded by the *Drosophila* gene *small bristles* (*sbr*), for which multiple alleles have been described. Mutations in this gene affect several tissues during *Drosophila* development including the morphogenesis of embryonic neurons and muscles. Moreover, adult flies have smaller and thinner sensory bristles and are defective in the development of the female germ line and/or in spermatogenesis. These tissue-specific effects of *sbr* alleles are likely to reflect an increased sensitivity to a reduction in mRNA export and therefore in protein synthesis in these tissues (Korey et al., 2001; Wilkie et al., 2001, and references therein).

NXF1/p15 form a single functional unit

Crystallographic studies on the NTF2-like domain of TAP bound to p15 indicate that these proteins form a single structural unit (Fribourg et al., 2001). Our data indicate that Dm NXF1/p15 form a single functional unit and cannot promote export in the absence of the other subunit of the heterodimer. However, although the NTF2-like domain of NXFs is conserved, p15 is not. In *S. cerevisiae*, Mex67p heterodimerizes with Mtr2p (Santos Rosa et al., 1998; Strässer et al., 2000). The lack of sequence conservation between Mtr2p and p15 is compatible with a structural role for these proteins, such as allowing the proper folding of the NTF2-like domains of NXFs, which in turn mediates binding to the NPC (Fribourg et al., 2001). Whether p15 or Mtr2p contribute not only to NPC association but also to cargo binding is an open question. It is interesting to note that the fact that NXFs are functional only as heterodimers with p15 or Mtr2p could provide a mechanism for regulating their activity.

Role of *nxf* genes in metazoans: Tissue-specific or housekeeping functions?

In this study, we show that Dm NXF2–4 cannot sustain growth or export of bulk mRNA in cells depleted of NXF1. A possible explanation for this observation is that the physiological expression levels of NXF2–4 may be insufficient to restore export. This is indeed the case for NXF4, which is either not expressed or expressed at very low levels in SL2 cells and in *Drosophila* embryos. The expression level of Dm NXF2 is approximately fourfold lower than that of NXF1, and thus similar to the levels of NXF1 protein after depletion. However, overexpression of Dm NXF2 does not rescue NXF1-knockdown (data not shown). These results together with the divergence of NXF2–4 sequences point to a nonredundant function.

Dm NXF1 is expressed in all tissues and in all developmental stages (Korey et al., 2001; Wilkie et al.,

2001). Similar to *nxf1*, *nxf2*, and *nxf3* mRNAs are expressed in different *Drosophila* cell lines and are evenly detected in *Drosophila* embryos throughout development (Fig. 1B; C. Korey & D. Van Vactor, pers. comm.). This suggests that Dm NXF2–3 may have a house-keeping role, although a tissue-specific pattern of expression in adult flies cannot currently be ruled out. In contrast, Hs NXF2, NXF3, and NXF5 exhibit a tissue-specific expression pattern. Whether Hs or Dm NXFs promote export of specific transcripts in cells where they are expressed needs to be established, but it is also possible that some of these proteins may have a different function. The divergence of Dm NXF2–4 relative to Hs NXF2–5 and their different expression patterns indicates that the role of these proteins in vivo can only be accessed in the homologous systems.

MATERIALS AND METHODS

Cloning of *nxf*s and p15 cDNAs

The prediction of genes encoding Dm NXF and p15 homologs has been reported previously (Herold et al., 2000). The corresponding cDNAs were amplified by PCR using a *Drosophila* embryonic cDNA library or *Drosophila melanogaster* quick-clone cDNA (Clontech). All PCR reactions were performed with the Expand™ high-fidelity PCR system (Roche). The amplified cDNAs were cloned into a derivative of pBS-SK (pBS-SKHA) and sequenced. These cDNAs were used for all further subcloning steps. NXF1 is the product of the gene known as *small bristles* (Korey et al., 2001; Wilkie et al., 2001; accession numbers AJ251947 and AJ318090). The NXF2 sequence data has been submitted to the European Molecular Biology Laboratory (EMBL) database under accession number AJ312282 and is identical to the prediction in the Flybase (gene CG4118). Full-length p15 cDNA was amplified by PCR and is identical to the sequence of Dm NXT1 (accession number AF156959).

The NXF3 cDNA is represented in the genomic sequence AE003536 and in the EST clone AT29009. The NXF3 clone used in Figure 2B corresponds to nt 218264–219265 of the genomic sequence AE003536. An *nxf4* gene prediction can be found in the Flybase (gene CG14604) and partially overlaps with the EST (AT07692). Sequencing the entire insert present in this EST clone, however, showed that it corresponds to nt 261141 to 262142 of the genomic sequence AE003672.2 and that the 5' end of the predicted *nxf4* gene needs to be redefined. In our studies, the insert present in the EST clone (AT07692) was used directly for further studies.

Plasmids, recombinant protein expression, and in vitro binding assays

Plasmids allowing the expression of HA-tagged NXF1, NXF1 fragment 137–672, NXF2, or p15 in SL2 cells, were generated by inserting the corresponding cDNAs into a pBS-based vector containing the *Drosophila* actin promoter and the BgH1 terminator (pBSact). Plasmids allowing the expression of glu-

tathione S-transferase (GST) fusions of NXF1, NXF2, or p15 in *Escherichia coli* were generated by inserting the corresponding cDNAs between the *EcoRI* and *NotI* sites of pGEX5X-3 (NXF1137–672), the *NcoI* and the *EcoRI* sites of pGEXCS (NXF2), or the *NcoI* and *BamHI* sites present in pGEXCS (p15). A plasmid encoding a GST fusion of NXF2 amino acids 1–326 was made by digesting plasmid pGEXCS-NXF2 with *SphI* and *EcoRI* followed by recircularization. Plasmids encoding Hs p15 or TAP and its derivatives have been described previously (Braun et al., 2001; Bachi et al., 2000). Recombinant proteins were expressed in *E. coli* BL21 (DE3) LysS and purified as previously described (Grüter et al., 1998). For the generation of [³⁵S]labeled proteins, the combined in vitro transcription-translation (TnT) kit from Promega was used. GST pull-down experiments were performed as described (Bachi et al., 2000).

RNA isolation, RT-PCR, and northern blots

To determine the expression pattern of human NXFs, a multiple tissue northern blot (Origene) was consecutively hybridized using probes comprising the first 0.3 kb of the corresponding coding regions. Slot blot analysis confirmed that these probes do not cross-hybridize.

Total RNA was isolated from cultured cells or Dm embryos using TRIzol Reagent (Life Technologies). Reverse transcription was performed with AMV reverse transcriptase (Promega) on 2 μg of total RNA and was primed with oligo(dT)₁₅. One-tenth of these reactions served as template in the subsequent PCR reactions performed using specific primers.

For northern blotting, total RNA was separated in denaturing formaldehyde agarose gels and blotted onto a positively charged nylon membrane (GeneScreen Plus, NEN Life Science). [³²P]labeled probes were generated by random priming using standard methods or by linear PCR using the Strip-EZ PCR kit (Ambion). Hybridizations were carried out in ULTRAhyb solution (Ambion). Slot blot assays confirmed that the probes used do not cross-hybridize and that all probes exhibit a detection limit of less than 2 pg.

A plasmid containing the complete coding region of rp49 in pOT2 was provided by Heinrich Jasper (EMBL, Germany). Plasmids comprising the first 1,200 bp of HSP70 and the last 1,300 bp of HSP83 cDNAs were kindly provided by Carl Wu (Bethesda, USA).

Cell culture and RNA interference

SL2 cells were propagated at 25 °C in Schneider's *Drosophila* medium supplemented with 10% foetal bovine serum, 100 U/mL penicillin and 100 μg/mL streptomycin. dsRNAi was performed essentially as described by Clemens et al. (2000). NXF1 and NXF3 dsRNAs correspond to a fragment comprising amino acids 137–354 and 166–382, respectively. NXF2, eIF4G, and GFP (enhanced GFP from vector pEGFP-C1) dsRNA correspond each to the first 650 bp of the coding regions. p15 dsRNA corresponds to the first 350 nt of p15 coding region. Fifteen micrograms of dsRNA were used per 6-well dish containing ~10⁶ cells. NXF4 dsRNA correspond to nt 261148–261798 of the genomic sequence AE003672.2.

Preparation of total cell extracts and western blotting

Total-cell extracts were prepared by washing the cells with PBS and resuspending them directly in SDS-sample buffer at a concentration of $\sim 30,000$ cells/ μL . Extracts were sonicated to shear genomic DNA. Typically 5–15 μL of this extract was used for western blot analysis. Rabbit polyclonal antibodies raised to recombinant GST-NXF1 (fragment 137–672) and GST-NXF2 (residues 1–326) were diluted 1:500. A rat polyclonal antibody was raised to Dm p15 expressed in *E. coli* as a hexa-histidine fusion protein. This antiserum was diluted 1:750. Anti-eIF4G antibodies were diluted 1:5,000. Bound primary antibody was detected with alkaline-phosphatase coupled anti-rabbit or anti-rat antibodies (Western-Star kit from Tropix).

In vivo protein labeling

SL2 cells transfected with dsRNA ($\sim 2 \times 10^6$) were transferred to 15-mL Falcon tubes, washed once with serum-free M3 *Drosophila* medium lacking methionine (Sigma), and incubated in 200 μL of this medium for 20 min at 25°C. After this preincubation period, 200 μL of methionine-free medium supplemented with 125 $\mu\text{Ci}/\text{mL}$ of [^{35}S]methionine (Pro-mix in vitro cell labeling mix; Amersham) were added. Cells were either kept at 25°C or immediately shifted to 37°C by immersing the tubes in a water bath. After 1 h, cells were washed twice with ice-cold PBS and directly resuspended in 100 μL SDS sample buffer. Aliquots of 25 μL were analyzed by SDS-PAGE and fluorography.

Fluorescence in situ hybridization (FISH) and immunofluorescence

SL2 cells were allowed to adhere to poly-D-Lysine-coated coverslips for 2 min, washed once in PBS, and fixed with 3.7% paraformaldehyde in PBS for 10 min. After fixation, cells were washed in PBS, permeabilized for 10 min with PBS containing 0.5% Triton X-100 and washed again with PBS.

To detect poly(A)⁺ RNA, cells were incubated for 15 min at 37°C in prehybridization buffer (2 \times SSC, 20% formamide, 0.2% BSA, 1 mg/mL of total yeast tRNA). For hybridization, the coverslips were transferred to a humidified chamber and covered with 20 μL of hybridization buffer (prehybridization buffer plus 10% dextran sulfate) supplemented with 0.1 pmol/ μL oligo(dT)₅₀ fluorescently end labeled with Cy3 molecules. The cells were hybridized for 2–3 h at 37°C and washed successively two times for 5 min with 2 \times SSC/20% formamide (at 42°C), 2 \times SSC (at 42°C), 1 \times SSC, and PBS. Subsequent indirect immunofluorescence with mAb414 (BaBco) antibodies diluted 1:1,000 was performed as described (Almeida et al., 1998). Alexa488-coupled goat secondary antibody (Molecular probes) was used in a dilution of 1:750. Alternatively, nuclear envelopes were stained with Alexa Fluor488-WGA conjugates (dilution 1:1,500). DNA was stained with Hoechst 33342 (Molecular probes). Cells were mounted using Fluoromount-G (Southern Biotechnology Associates, Inc.).

For FISH analysis of *hsp70*, *hsp83*, and *rp49* mRNA digoxigenin-labeled antisense RNA probes were synthesized

using the DIG RNA labeling mix and T3/T7/SP6 RNA polymerases (Roche). Probes were diluted 1:100 from stocks at 0.05–0.1 $\mu\text{g}/\mu\text{L}$. Hybridizations were performed as described above with the following modifications. After permeabilization, cells were washed for 5 min with 2 \times SSC/50% formamide and then incubated for 15 min in prehybridization buffer (2 \times SSC, 50% formamide, 50 mM sodium phosphate, pH 7.3, 300 $\mu\text{g}/\text{mL}$ sonicated single-stranded DNA) at 58°C. Hybridization was done overnight at 58°C with 25 μL hybridization buffer per coverslip (prehybridization buffer plus 10% dextran sulphate and 10 mM ribonucleoside vanadyl complex) containing the digoxigenin-labeled RNA probe. Cells were washed three times for 10 min with 2 \times SSC/50% formamide, twice for 15 min with 2 \times SSC, and twice for 10 min with 1 \times SSC at 58°C. To detect the digoxigenin-labeled probes, cells were washed with PBS and incubated with a polyclonal sheep anti-digoxigenin antibody (1:100 in PBT; Roche). After several washes with PBT, cells were incubated with a Cy3-conjugated rabbit anti-sheep antibody (1:250 in PBT; Jackson ImmunoResearch), washed with PBS, and fixed and mounted as above. Images were taken with a confocal laser scanning microscope (LSM 510 from Carl Zeiss).

To investigate the subcellular localization of NXF1, NXF2, and p15, SL2 cells ($\sim 2 \times 10^6$) were transfected using the calcium-phosphate method with 2 μg of plasmid DNA encoding HA-tagged versions of the proteins. Sixty hours after transfection, indirect immunofluorescence was performed as for the FISH experiments. Cells were double labeled with an anti-HA antibody (bAbco) and an affinity purified polyclonal antibody (KJ58; Rodrigues et al., 2001) that detects Dm REF1.

ACKNOWLEDGMENTS

We are grateful to Ilan Davis, Christopher A. Korey, David Van Vactor, and Gavin Wilkie for communicating results prior to publication. The technical assistance of Michaela Rode is gratefully acknowledged. We thank José Manuel Sierra for the kind gift of anti-eIF4G antibodies, Rolando Rivera-Pomar for a plasmid encoding eIF4G, Carl Wu for providing various heat-shock cDNA clones, Stephen Cohen for Clone 8 cells, Harald Saumweber for Kc cells, and Mikita Suyama for gene prediction and sequence analysis. This study was supported by the European Molecular Biology Organization (EMBO).

Received August 17, 2001; returned for revision
September 17, 2001; revised manuscript received
September 27, 2001

REFERENCES

- Almeida F, Saffrich R, Ansoorge W, Carmo-Fonseca M. 1998. Micro-injection of anti-coilin antibodies affects the structure of coiled bodies. *J Cell Biol* 142:899–912.
- Bachi A, Braun IC, Rodrigues JP, Pante N, Ribbeck K, von Kobbe C, Kutay U, Wilm M, Görlich D, Carmo-Fonseca M, Izaurralde E. 2000. The C-terminal domain of TAP interacts with the nuclear pore complex and promotes export of specific CTE-bearing RNA substrates. *RNA* 6:136–158.
- Bear J, Tan W, Zolotukhin AS, Tabernero C, Hudson EA, Felber BK. 1999. Identification of novel import and export signals of human TAP, the protein that binds to the CTE element of the type D retrovirus mRNAs. *Mol Cell Biol* 19:6306–6317.

- Black BE, Holaska JM, Lévesque L, Ossareh-Nazari B, Gwizdek C, Dargemont C, Paschal BM. 2001. NXT1 is necessary for the terminal step of Crm1-mediated nuclear export. *J Cell Biol* 152:141–156.
- Black BE, Levesque L, Holaska JM, Wood TC, Paschal BM. 1999. Identification of an NTF2-related factor that binds Ran-GTP and regulates nuclear protein export. *Mol Cell Biol* 19:8616–8624.
- Braun IC, Herold A, Rode M, Conti E, Izaurralde E. 2001. Overexpression of TAP/p15 heterodimers bypasses nuclear retention and stimulates nuclear mRNA export. *J Biol Chem* 276:20536–20543.
- Clemens JC, Worby CA, Simonson-Leff N, Muda M, Maehama T, Hemmings BA, Dixon JE. 2000. Use of double-stranded RNA interference in *Drosophila* cell lines to dissect signal transduction pathways. *Proc Natl Acad Sci USA* 97:6499–6503.
- Conti E, Izaurralde E. 2001. Nucleocytoplasmic transport enters the atomic age. *Curr Opin Cell Biol* 3:310–319.
- Echalier G. 1997. *Drosophila cells in culture*. San Diego, California: Academic Press.
- Fribourg S, Braun IC, Izaurralde E, Conti E. 2001. Structural basis for the recognition of a nucleoporin FG repeat by the NTF2-like domain of the TAP/p15 mRNA nuclear export factor. *Mol Cell* 8:645–656.
- Grüter P, Taberero C, von Kobbe C, Schmitt C, Saavedra C, Bachi A, Wilm M, Felber BK, Izaurralde E. 1998. TAP, the human homolog of Mex67p, mediates CTE-dependent RNA export from the nucleus. *Mol Cell* 1:649–659.
- Guzik BW, Levesque L, Prasad S, Bor YC, Black BE, Paschal BM, Rekosh D, Hammarskjöld ML. 2001. NXT1 (p15) is a crucial cellular cofactor in TAP-dependent export of intron-containing RNA in mammalian cells. *Mol Cell Biol* 21:2545–2554.
- Herold A, Suyama M, Rodrigues JP, Braun IC, Kutay U, Carmo-Fonseca M, Bork P, Izaurralde E. 2000. TAP/NXF1 belongs to a multigene family of putative RNA export factors with a conserved modular architecture. *Mol Cell Biol* 20:8996–9008.
- Hilleren P, Parker R. 2001. Defects in the mRNA export factors Rat7p, Gle1p, Mex67p, and Rat8p cause hyperadenylation during 3'-end formation of nascent transcripts. *RNA* 7:753–764.
- Hurt E, Strässer K, Segref A, Bailer S, Schlaich N, Presutti C, Tollervey D, Jansen R. 2000. Mex67p mediates nuclear export of a variety of RNA polymerase II transcripts. *J Biol Chem* 275:8361–8365.
- Jensen TH, Patricio K, McCarthy T, Rosbash M. 2001. A block to mRNA nuclear export in *S. cerevisiae* leads to hyperadenylation of transcripts that accumulate at the site of transcription. *Mol Cell* 7:887–898.
- Jun L, Frints S, Duhamel H, Herold A, Abad-Rodriguez J, Dotti C, Izaurralde E, Marynen P, Froyen G. 2001. NXF5, a novel member of the nuclear RNA export factor family, is lost in a male patient with a syndromic form of mental retardation. *Curr Biol* 11:1381–1391.
- Kadowaki T, Hitomi M, Chen S, Tartakoff AM. 1994. Nuclear mRNA accumulation causes nucleolar fragmentation in yeast mtr2 mutant. *Mol Biol Cell* 11:1253–1263.
- Kang Y, Bogerd HP, Cullen BR. 2000. Analysis of cellular factors that mediate nuclear export of RNAs bearing the Mason-Pfizer monkey virus constitutive transport element. *J Virol* 74:5863–5871.
- Katahira J, Strässer K, Podtelejnikov A, Mann M, Jung JU, Hurt E. 1999. The Mex67p-mediated nuclear mRNA export pathway is conserved from yeast to human. *EMBO J* 18:2593–2609.
- Korey CA, Wilkie G, Davis I, Van Vactor D. 2001. *small bristles*, DmNXF1, is required for the morphogenesis of multiple tissues during *Drosophila* development. *Genetics*. In press.
- Liker E, Fernandez E, Izaurralde E, Conti E. 2000. The structure of the mRNA nuclear export factor TAP reveals a *cis* arrangement of a non-canonical RNP domain and a leucine-rich-repeat domain. *EMBO J* 19:5587–5598.
- Mattaj JW, Englmeier L. 1998. Nucleocytoplasmic transport: The soluble phase. *Annu Rev Biochem* 67:265–306.
- Nakielnny S, Dreyfuss G. 1999. Transport of proteins and RNAs in and out of the nucleus. *Cell* 99:677–690.
- Ossareh-Nazari B, Maison C, Black BE, Levesque L, Paschal BM, Dargemont C. 2001. RanGTP-Binding Protein NXT1 facilitates nuclear export of different classes of RNA in vitro. *Mol Cell Biol* 21:4562–4571.
- Pasquinelli AE, Ernst RK, Lund E, Grimm C, Zapp ML, Rekosh D, Hammarskjöld M-L, Dahlberg JE. 1997. The constitutive transport element (CTE) of Mason-Pfizer Monkey Virus (MPMV) accesses an RNA export pathway utilized by cellular messenger RNAs. *EMBO J* 16:7500–7510.
- Rodrigues JP, Rode M, Gatfield D, Blencowe BJ, Carmo-Fonseca M, Izaurralde E. 2001. REF proteins mediate the export of spliced and unspliced mRNAs from the nucleus. *Proc Natl Acad Sci USA* 98:1030–1035.
- Saavedra CA, Felber BK, Izaurralde E. 1997. The simian retrovirus-1 constitutive transport element CTE, unlike HIV-1 RRE, utilizes factors required for cellular RNA export. *Curr Biol* 7:619–628.
- Santos-Rosa H, Moreno H, Simos G, Segref A, Fahrenkrog B, Panté N, Hurt E. 1998. Nuclear mRNA export requires complex formation between Mex67p and Mtr2p at the nuclear pores. *Mol Cell Biol* 18:6826–6838.
- Segref A, Sharma K, Doye V, Hellwig A, Huber J, Lüthmann R, Hurt E. 1997. Mex67p, a novel factor for nuclear mRNA export binds to both poly(A)⁺ RNA and nuclear pores. *EMBO J* 16:3256–3271.
- Strässer K, Bassler J, Hurt E. 2000. Binding of the Mex67p/Mtr2p heterodimer to FXFG, GLFG, and FG repeat nucleoporins is essential for nuclear mRNA export. *J Cell Biol* 150:695–706.
- Stutz F, Bachi A, Doerks T, Braun IC, Séraphin B, Wilm M, Bork P, Izaurralde E. 2000. REF, an evolutionary conserved family of hnRNP-like proteins, interacts with TAP/Mex67p and participates in mRNA nuclear export. *RNA* 6:638–650.
- Suyama M, Doerks T, Braun IC, Sattler M, Izaurralde E, Bork P. 2000. Prediction of structural domains of TAP reveals details of its interaction with p15 and nucleoporins. *EMBO Rep* 1:53–58.
- Tan W, Zolotukhin AS, Bear J, Patenaude DJ, Felber BK. 2000. The mRNA export in *C. elegans* is mediated by Ce NXF1, an orthologue of human TAP/NXF1 and *S. cerevisiae* Mex67p. *RNA* 6:1762–1772.
- Vainberg IE, Dower K, Rosbash M. 2000. Nuclear export of heat shock and non-heat-shock mRNA occurs via similar pathways. *Mol Cell Biol* 20:3996–4005.
- Wilkie GS, Zimyanin V, Kirby R, Korey CA, Francis-Lang H, Sullivan W, Van Vactor D, Davis I. 2001. *Small bristles*, the *Drosophila* ortholog of human TAP/NXF1 and yeast Mex67p, is essential for mRNA nuclear export in all tissues throughout development. *RNA* 7:1781–1792.
- Yang J, Bogerd HP, Wang PJ, Page DC, Cullen BR. 2001. Two closely related human nuclear export factors utilize entirely distinct export pathways. *Mol Cell* 8:397–406.
- Yoon DW, Lee H, Seol W, DeMaria M, Rosezweig M, Jung JU. 1997. Tap: A novel cellular protein that interacts with tip of herpes virus saimiri and induces lymphocyte aggregation. *Immunity* 6:571–582.
- Yost HJ, Lindquist S. 1986. RNA splicing is interrupted by heat shock and is rescued by heat shock protein synthesis. *Cell* 45:185–193.

2.2.2 Paper 4:

Genome-wide analysis of mRNA nuclear export pathways in *Drosophila*

Herold, A., Teixeira L., and Izaurralde, E. (2003) *Submitted*.

Context

Although it was known that NXF1:p15 heterodimers and the RNA-helicase UAP56 are essential for the export of bulk poly(A)⁺ RNA in *Drosophila* (Gatfield *et al.*, 2001; Herold *et al.*, 2001), it was still unclear whether all mRNAs are exported *via* the same pathway or whether there are mRNAs that reach the cytoplasm by alternative routes. We had shown previously that the depletion of NXF2 or NXF3 does not result in any obvious effect on bulk mRNA export (Herold *et al.*, 2001). So we were particularly interested in the question of whether NXF2 and/or NXF3 might be responsible for the nuclear export of only a small subset of mRNAs. We also wanted to analyze effects caused by the inhibition of Crm1, since Crm1 had been suggested to mediate export of specific mRNAs by serving as an alternative export receptor. Furthermore, it was not known whether there are classes of mRNAs which require UAP56 function but not NXF1:p15 for export or *vice versa*. To address these questions, we combined RNAi in *Drosophila* cells with microarray analysis.

Summary of results and conclusions

We silenced the expression of individual *nxf* genes (*nxf1*, 2 and 3), *p15* or *uap56* by RNAi in *Drosophila* cells and monitored the effects on cytoplasmic and total mRNA levels using microarrays. To study the role of Crm1 in mRNA export, we also selectively inactivated Crm1 with the drug leptomycin B (LMB). As a prerequisite for this study, a protocol to isolate cytoplasmic RNA which is virtually free of nuclear contaminants was established. For each export factor, a pool of cytoplasmic and total RNAs from independent knockdowns/treatments was prepared, and the relative levels of about 6000 different mRNAs were determined in at least two microarray experiments using two independent biological samples. Depletion of NXF2 or NXF3 (5 days after transfection) did not result in any detectable mRNA export defect as the only mRNAs that were consistently different from the reference sample were the *nxf2* and *nxf3* mRNAs themselves. The inhibition of Crm1 by LMB (12h treatment) affected the expression levels of less than 2% of detectable mRNAs. In contrast, when Schneider cells were depleted of NXF1, p15 or UAP56 (4 days after transfection), most mRNAs (about 75%) were underrepresented in the cytoplasm compared to control cells as expected after export inhibition. Surprisingly, most of these mRNAs were also underrepresented in samples of total RNA. We investigated if these overall lower levels were a consequence of a higher turnover rate of mRNAs after inhibition of export by determining the half-lives of several mRNAs that were underrepresented in total and cytoplasmic preparations. None of these

mRNAs had a higher turnover rate in NXF1-depleted cells, suggesting that the overall decrease in mRNA levels was not caused by posttranscriptional decay.

Comparing the profiles obtained with cells depleted of NXF1, p15 or UAP56, we observed that the overall expression patterns of these three knockdowns were extremely similar, with least differences between the NXF1 and p15 knockdowns. The wide effect on mRNA levels and the striking similarities of expression profiles in cells depleted of NXF1, p15 and UAP56 indicate that these proteins define a single and major mRNA export pathway.

Although most mRNAs showed decreased levels in NXF1-, p15- or UAP56-depleted cells, the cytoplasmic levels of a small subset of mRNAs were unchanged after depletion of any of these factors. As the half-lives of at least some of these mRNAs were in the range of hours, the unchanged cytoplasmic levels could not solely be attributed to high stability of these transcripts. Rather, these transcripts could reach the cytoplasm despite the general export block. We also analyzed if these mRNAs were exported by Crm1, but none of the candidates was significantly affected in the LMB experiment. Thus these mRNAs either exit the nucleus through a yet unidentified transport receptor, or are able to recruit the "normal" mRNA export machinery more efficiently than bulk mRNA.

We also identified a set of mRNAs affected differently in the UAP56 knockdown from the NXF1 or p15 knockdown. Among these were some mRNAs which were underrepresented in NXF1- and p15-depleted cells, but not in UAP56-depleted cells, indicating that these transcripts require NXF1:p15 function for export, but not UAP56.

Finally, we analyzed mRNAs which were upregulated after a block of mRNA export. Surprisingly, we observed that amongst these were mRNAs encoding known nuclear mRNA export factors, such as NXF1, p15, UAP56 or REF1. This suggested the presence of a feedback loop by which the block of nuclear export leads to increased levels of mRNAs encoding transport factors. We showed that transcriptional upregulation as well as stabilization of the respective mRNAs contributed to the increased steady-state levels. Prompted by these observations, we investigated whether the depletion of NXF1, p15 or UAP56 resulted in the upregulation of unknown components of the nuclear export pathway. We selected four candidate mRNAs from the group of mRNAs, which were upregulated after export inhibition and analyzed their possible role in mRNA export by silencing their expression by RNAi. Importantly, the depletion of one of the candidate proteins, Ssrp, resulted in a highly abnormal distribution of poly(A)⁺ RNA which accumulated in nuclear foci. This suggested a role for Ssrp in the nuclear export of poly(A)⁺ RNA.

Altogether, we present in this study the first analysis of mRNA export on a global scale in higher eukaryotes. We demonstrated that NXF1, p15 and UAP56 define the major mRNA export pathway in *Drosophila*. Furthermore, we were able to identify a set of

mRNAs which are exported despite the depletion of NXF1, p15 and UAP56, and some requiring NXF1:p15 but not UAP56. In addition, our analysis revealed a feedback loop by which a block to mRNA export triggers the upregulation of genes implicated in this process.

Contribution

I designed, performed and analyzed all experiments; L. Teixeira provided the microarrays. I also wrote the manuscript with the help of Dr Elisa Izaurralde. I established the protocol to prepare cytoplasmic RNA and introduced all techniques concerning microarray experiments in our lab (including all the analysis). My contribution to this paper is 95%.

Genome-wide analysis of mRNA nuclear export pathways in *Drosophila*

Manuscript submitted

Andrea Herold, Luis Teixeira and Elisa Izaurralde*
EMBL, Meyerhofstrasse 1, 69117 Heidelberg, Germany

*Correspondence should be addressed to:

Elisa Izaurralde
EMBL
Meyerhofstrasse 1
69117 Heidelberg, Germany
Tel: +49 6221 387 389
Fax: +49 6221 387 518
e-mail: izaurralde@embl-heidelberg.de

Running title: Genome-wide analysis of mRNA nuclear export

Abstract

NXF1, p15 and UAP56 are essential nuclear mRNA export factors. The fraction of mRNAs exported by these proteins or *via* alternative pathways is unknown. We have analyzed the relative abundance of nearly half of the *Drosophila* transcriptome in the cytoplasm of cells treated with leptomycin-B (LMB) or depleted of export factors by RNAi. While the vast majority of mRNAs were unaffected by LMB, the levels of most mRNAs changed significantly in cells depleted of NXF1, p15 or UAP56. This wide effect on mRNA levels and the striking similarities of mRNA expression profiles in NXF1, p15 and UAP56 knockdowns indicate that these proteins define the major mRNA export pathway in higher eukaryotes. Our analysis also revealed a feedback loop by which a block to mRNA export triggers the upregulation of genes involved in this process.

Keywords: nuclear export / mRNA export / CRM1 / NXF1 / UAP56 /

Introduction

Fully processed mRNAs are exported from the nucleus to the cytoplasm where they direct protein synthesis. Within the past few years, factors implicated in this process have been identified through genetic and biochemical experiments in yeast, fruit fly, frog oocytes and human cells. Among these are several RNA binding proteins, the DEAH-box helicase UAP56 and the heterodimeric nuclear export receptor NXF1:p15 (reviewed by Izaurralde, 2002; Reed and Hurt, 2002). Metazoan NXF1 (also known as TAP in humans) belongs to the conserved family of NXF proteins, which includes yeast Mex67p. p15 is conserved in metazoa but not in *S. cerevisiae*, instead, the protein Mtr2p is predicted to be functionally analogous to p15 in this organism. NXF1:p15 dimers promote the translocation of mRNA cargos across the nuclear pore complex (NPC) by interacting directly with nucleoporins. Their interaction with mRNAs is thought to be mediated by adaptor proteins (reviewed by Izaurralde, 2002).

The putative RNA helicase UAP56 (also known as Sub2p in yeast) was first implicated in splicing (reviewed by Linder and Stutz, 2001). Recent studies, however, provided evidence for an essential role of this protein in early steps of the mRNA export process by binding cotranscriptionally to nascent mRNAs and facilitating the recruitment of adaptor proteins (Gatfield *et al.*, 2001; Jensen *et al.*, 2001; Kiesler *et al.*, 2002; Libri *et al.*, 2002; Luo *et al.*, 2001; Strasser and Hurt, 2001; Strasser *et al.*, 2002; Zenklusen *et al.*, 2002). These adaptors include members of the evolutionarily conserved family of REF proteins (Stutz *et al.*, 2000). Yra1p (one of the *S. cerevisiae* members of this family) is essential for mRNA export (Strasser and Hurt, 2000; Stutz *et al.*, 2000; Zenklusen *et al.*, 2001), whereas *Drosophila* REF1 is not, indicating that other adaptors can recruit NXF1:p15 dimers to mRNAs in higher eukaryotes (Gatfield and Izaurralde, 2002).

The essential role of NXF1:p15 dimers and of UAP56 in mRNA export is well-established in *S. cerevisiae* and *Drosophila*. In these organisms, inactivation or depletion of these proteins results in a strong accumulation of bulk polyadenylated RNA [poly(A)⁺ RNA] within the nucleoplasm, suggesting that export of a large proportion of mRNAs is affected (Gatfield *et al.*, 2001; Herold *et al.*, 2001; Jensen *et al.*, 2001; Segref *et al.*, 1997; Strasser and Hurt, 2001; Wiegand *et al.*, 2002; Wilkie *et al.*, 2001). Fluorescent *in situ* hybridizations using probes to detect specific mRNAs have led to the identification of a few mRNAs that depend on these three proteins for export, including mRNAs encoding heat shock proteins (Herold *et al.*, 2001; Hurt *et al.*, 2000; Jensen *et al.*, 2001; Strasser and Hurt, 2001; Vainberg *et al.*, 2000; Wilkie *et al.*, 2001).

Although mRNA export is becoming increasingly well understood in yeast, the mRNA export pathway in higher eukaryotes remains ill-defined. In particular, it is unclear whether NXF1, p15 and UAP56 are components of the same pathway or whether there are classes of mRNAs that require NXF1:p15, but not UAP56 and *vice versa*. On a genomic scale, the fraction of mRNAs whose export is mediated by NXF1:p15 dimers and UAP56 is unknown.

Another issue that remains unsolved is whether there are classes of mRNAs that reach the cytoplasm through alternative routes, *e.g.* by recruiting other export receptors. Recent studies have indicated that CRM1, a nuclear export receptor belonging to the importin- β (karyopherin) family, might mediate export of a larger than previously anticipated fraction of mRNAs (Gallouzi and Steitz, 2001). Moreover, the observation that there are two NXF proteins in *C. elegans* and four in *Drosophila* and humans (reviewed by Izaurralde, 2002) has raised the possibility that different classes of mRNAs may reach the cytoplasm by recruiting different members of the NXF family.

A role for human NXF2 and NXF3 in mRNA export is suggested by the observation that both can promote export of reporter mRNAs in cultured cells (Herold *et al.*, 2000; Yang *et al.*, 2001). The observation that these proteins are expressed mainly in testis indicates that they may act as tissue-specific export factors (Herold *et al.*, 2001; Yang *et al.*, 2001). In contrast, in *Drosophila* embryos NXF2 and NXF3 are expressed ubiquitously (Herold *et al.*, 2001). However, *Drosophila* cells depleted of NXF2 or NXF3 do not exhibit a detectable growth or export phenotype, suggesting that their cargos can only be non-essential mRNAs in cultured cells (Herold *et al.*, 2001).

In order to shed light on nuclear mRNA export pathways on a genome-wide scale in higher eukaryotes, we have analyzed the relative abundance of nearly one-half of the *Drosophila* transcriptome in the cytoplasm of *Drosophila* Schneider (S2) cells in which export factors have been depleted by RNAi (RNA interference). We show that the vast majority of transcripts are underrepresented in the cytoplasm of cells depleted of NXF1, p15 or UAP56 as compared to control cells. Only a small number of mRNAs are apparently not affected by the depletions and a subset of mRNAs appear to be exported by NXF1:p15 dimers independently of UAP56. In contrast, no significant changes in mRNA expression profiles are observed in cells depleted of NXF2 or NXF3. Furthermore, inhibition of the CRM1-mediated export pathway by leptomycin-B (LMB) affects the expression levels of less than 2% of detectable mRNAs. These observations, together with the wide effect on mRNA levels in cells depleted of NXF1, p15 or UAP56, indicate that these proteins define the major mRNA export pathway in higher eukaryotes.

Results

Depletion of NXF1, p15 or UAP56 causes widespread changes in the expression of the *Drosophila* transcriptome

To analyze nuclear mRNA export pathways at the genomic level, cDNA microarrays representing a total of about 6000 different genes (Supplemental Experimental Procedures), were used to screen mRNA levels in total and cytoplasmic samples isolated from S2 cells depleted of UAP56, p15 or the individual NXF proteins (NXF1, 2 and 3) by RNAi. The efficiency of all depletions was confirmed by RT-PCR and, except for NXF3, by Western blot (data not shown). NXF1, p15 and UAP56 knockdowns were confirmed further by the inhibition of cell proliferation and the concomitant strong nuclear accumulation of poly(A)⁺ RNA (Supplemental Fig. 1; Gatfield *et al.*, 2001; Herold *et al.*, 2001).

The relative abundance of each transcript was analyzed four days (NXF1, p15 and UAP56) or five days (NXF2 and NXF3) after transfection with dsRNA in two-color microarray hybridization experiments. As reference samples, total and cytoplasmic RNAs isolated from cells transfected in parallel with GFP dsRNA were used. To reduce potentially insignificant variations in the preparation of the RNA, three cytoplasmic and two total RNA preparations were isolated from a single knockdown experiment. These preparations were pooled with the equivalent preparations isolated from an independent knockdown, to minimize differences in knockdown efficiencies. These pools of 6 cytoplasmic or 4 total RNA preparations from 2 independent knockdowns are referred as to 'cytoplasmic or total samples'. We confirmed that all cytoplasmic RNA preparations were free of nuclear contamination by

testing for the absence of rp49 and hsp83 precursor mRNAs, as described in Supplemental Figure 2.

A representative measurement with one cytoplasmic sample for each export factor is shown in Figure 1A. When NXF2 or NXF3 were targeted by RNAi, the only mRNAs consistently different from the reference sample (*i.e.* at least 1.5-fold different in three independent measurements) were the *nxf2* and *nxf3* mRNAs themselves (red circles, Fig. 1A). In contrast, when NXF1, p15 or UAP56 were depleted, the levels of most mRNAs changed significantly (Fig. 1A). Since most mRNAs were underrepresented in NXF1, p15 and UAP56 knockdowns, external spike-in RNAs were used for normalization (Supplemental Experimental Procedures).

To compare further the effects of the NXF1, p15 and UAP56 depletions, we sorted all detectable mRNAs into 3 classes according to their relative expression levels (Fig. 1B). These include mRNAs that were at least 1.5-fold underrepresented compared to the reference sample (in blue), not significantly changed (less than 1.5-fold different from the reference, in yellow), or at least 1.5-fold overrepresented (in red). Within these classes, the dashed areas represent subgroups of mRNAs for which more stringent cutoff values were used (at least 2-fold over- or underrepresented; less than 1.2-fold regulated).

An mRNA was only considered for further analysis if it could be assigned to the same subclass in measurements performed with two independent cytoplasmic or total samples for each export factor. About three-quarters (76–77%) of detectable mRNAs were underrepresented (at least 1.5-fold down) in the cytoplasm of cells depleted of NXF1, p15 or UAP56; 22% were less than 1.5-fold different from the control and only 1% were overrepresented (at least 1.5-fold up) (Fig. 1B). When total RNA samples isolated on day 4 from NXF1-, p15- or UAP56-depleted cells were analyzed, about one-half (51–58%) of detectable mRNAs were underrepresented compared to the reference sample, 38–45% were not significantly changed, and 1–4% were overrepresented (Fig. 1B).

As the accumulation of mRNAs in the nucleus should result in their cytoplasmic depletion, a widespread reduction of cytoplasmic mRNA levels upon depletion of NXF1, p15 or UAP56 was expected. In contrast, the overall reduction in total mRNA levels was *a priori* counterintuitive. However, a similar reduction in total mRNA levels has been observed in yeast cells in which mRNA export is inhibited (see Discussion). Experiments described below indicate that this overall decrease in mRNA levels is a consequence of the mRNA export block.

The overall reduction of mRNA levels is a specific effect of the nuclear export block

To validate the microarray data, we selected representative mRNAs of each class and determined their relative levels by Northern blot (Fig. 2A and Table I). The changes observed in the microarray experiment always showed the same positive or negative trend as the changes measured by Northern blot (Table I), both in total and cytoplasmic samples. mRNAs that were not significantly different from control samples in the array experiment were only slightly different from control samples when measured by Northern blot. We also confirmed the positive or negative trend of several other mRNAs by RT-PCR (data not shown).

To ensure that the global changes of mRNA expression levels observed in NXF1-, p15- or UAP56-depleted cells is caused by the inhibition of mRNA export, rather than being a non-specific response to the depletion of essential proteins, we analyzed total RNA samples isolated 6 days after depletion of the essential translation factor eIF4G. We have shown before that depletion of eIF4G from S2 cells strongly impairs cell proliferation, but does not lead to the nuclear accumulation of poly(A)⁺ RNA (Herold *et al.*, 2001).

To highlight differences in mRNA expression patterns between cells depleted of NXF1, p15, UAP56, or eIF4G, we selected mRNAs which were highly regulated (at least 2-fold up or at least 5-fold down) in the NXF1 knockdown and investigated their expression levels in the other three knockdowns (Fig. 2B). While these mRNAs exhibited strikingly similar expression profiles in p15 and UAP56 samples, in most cases their levels remained unchanged in cells depleted of eIF4G (79% less than 1.5-fold regulated). Northern blot analysis confirmed that mRNAs showing higher or lower levels in NXF1, p15 and UAP56 knockdowns

were usually not strongly affected by depletion of eIF4G (Figs 2A and 5B). We conclude that mRNAs over- or underrepresented after depletion of NXF1, p15 and UAP56 do not represent mRNAs that are generally regulated in response to the inhibition of translation or cell proliferation.

Similarly, genes that are highly regulated in eIF4G-depleted cells (in this case, at least 2-fold up or down) showed incoherent levels of expression in NXF1, p15 and UAP56 knockdowns (Fig. 2C). These results indicate that the mRNA expression profiles displayed by NXF1-, p15- or UAP56-depleted cells represent a specific signature of these knockdowns.

A block of mRNA nuclear export causes an overall reduction of total mRNA levels

To obtain support for the hypothesis that the decreased mRNA levels in the total samples are an effect of the mRNA export block, we analyzed RNA samples isolated 2 days after transfection of cells with NXF1 dsRNA. At this time point, about 60% of all detectable mRNAs were underrepresented in the cytoplasm, but less than 25% were in the total samples (Fig. 1B, day 2 and Fig. 4E). Thus, the cytoplasmic depletion of mRNAs precedes the overall reduction of total mRNA levels, suggesting that the latter may be a secondary consequence of the mRNA export inhibition.

In cells in which mRNA export is inhibited, we would have expected the reduction of mRNA levels to be more obvious in the cytoplasmic rather than in the total samples. To test whether this was the case, we selected mRNAs which were at least 2-fold underrepresented in the cytoplasmic samples of NXF1-, p15- or UAP56-depleted cells, and analyzed their relative levels in total RNA samples. In the three knockdowns the average relative mRNA levels were lower in the cytoplasmic samples (Fig. 3A, blue numbers at the bottom of each graph). Moreover, the difference between total and cytoplasmic average expression levels was greater on day 2 than on day 4. Finally, when the average relative levels of mRNAs at least 2-fold overrepresented in the cytoplasmic samples of NXF1-, p15- or UAP56-depleted cells were analyzed, we observed higher average levels in the total samples, providing additional evidence for an export block.

The reduction of cytoplasmic and total mRNA levels is not a direct consequence of higher mRNA turnover rates

The experiments described above suggest that the overall decrease in abundance of most mRNAs observed in cells depleted of NXF1, p15 or UAP56 is caused by the export inhibition. However, these experiments do not reveal the mechanism by which this decreased expression is achieved. One possibility is that mRNAs accumulating within the nucleus have a higher turnover rate. To test this, we measured the half-lives of 4 representative mRNAs selected from those that were underrepresented in total and cytoplasmic samples in cells depleted of NXF1 (Fig. 3B and data not shown). None of these mRNAs had a higher turnover rate in NXF1 knockdowns as compared to control cells, regardless of whether samples were collected 2 or 4 days after transfecting NXF1 dsRNA (Fig. 3B, solid vs. dashed lines). On the contrary, some of the selected mRNAs had an increased stability. For instance, the half-life of *dom* mRNA is *ca.* 2 h in wild-type cells and longer than 6 h in NXF1-depleted cells (Fig. 3B).

We also measured the half-lives of seven mRNAs selected from those whose expression in cytoplasmic samples of NXF1-depleted cells was unchanged (2 mRNAs, Fig. 3C) or was increased (5 mRNAs, Fig. 6C and data not shown). Again, the half-lives of these mRNAs remained unchanged or increased in depleted cells (Figs 3C and 6C). Although we cannot rule out that some mRNA species might have a reduced stability in NXF1 knockdowns, together these results favor a model in which the overall decrease in mRNA levels is not caused by posttranscriptional mRNA decay.

Depletion of NXF1, p15 or UAP56 leads to strikingly similar mRNA expression profiles

As shown in Figure 2B, mRNAs that are highly over- or underrepresented in total samples isolated from NXF1-depleted cells are coherently regulated in p15 or UAP56 knockdowns. This is also observed when all detectable mRNAs in the cytoplasmic samples of cells depleted of NXF1, p15 or UAP56 are compared (Fig. 4A). The mRNA expression pattern caused by the depletion of NXF1 is more similar to that of p15 depletion than to that of the UAP56 knockdown (Fig. 4A). Indeed, the only mRNAs that were significantly different in NXF1 and p15 knockdowns were those targeted by RNAi themselves (Fig. 5A and Supplemental Table III).

To investigate further the uniformity of the cellular response to the depletion of NXF1, p15 or UAP56, we selected mRNAs belonging to specific classes in cytoplasmic samples of the NXF1 knockdown (at least 2-fold overrepresented, at least 2-fold underrepresented or less than 1.2-fold changed; red, blue and yellow dashed areas respectively) and analyzed their levels in p15 or UAP56 knockdowns (Fig. 4B). Of the mRNAs that were at least 2-fold underrepresented in the NXF1 knockdown, 99% or 90% were at least 1.5-fold underrepresented in p15 or UAP56 knockdowns, respectively (Fig. 4B). Overall, mRNAs that were not changed, over- or underrepresented in one experiment usually showed the same trend in the other two experiments, with smaller deviations between the NXF1 and p15 data than between NXF1 and UAP56 or p15 and UAP56 knockdown experiments. This also holds true when total RNA samples are compared (data not shown). The striking similarity of the patterns of mRNA expression in NXF1 (or p15) and UAP56 knockdowns strongly suggest that these proteins act in the same pathway.

Export of a subset of transcripts is apparently unaffected by NXF1, p15 or UAP56 depletion

Although most mRNAs show decreased expression levels in NXF1-, p15- or UAP56-depleted cells, the cytoplasmic levels of 23 mRNAs were unchanged after depletion of any one of these three export factors (less than 1.2 fold regulated in all measurements). For 20 of these mRNAs the total levels were also not significantly affected (Supplemental Table I). These mRNAs were not depleted from the cytoplasmic fraction despite the general nuclear export block, suggesting that they could have been exported independently of NXF1, p15 and UAP56 or could recruit these proteins very efficiently, so that the residual levels of these proteins in depleted cells were not limiting for their export. Alternatively, these mRNAs could have extremely low turnover rates.

To distinguish between these possibilities, the stability of two mRNAs belonging to this class was determined. The stability of cg1239 mRNA was only slightly changed, while the stability of cg7840 mRNA was increased in cells depleted of NXF1 (Fig. 3C). Nonetheless, the half-lives of both mRNA species were not long enough (*e.g.* cg1239 half-life <2h) to account for unchanged cytoplasmic levels in cells in which mRNA export has been efficiently blocked for at least 2 days (as judged by oligo(dT) *in situ* hybridization; Supplemental Fig. 1). We therefore conclude that neither transcription nor export of these mRNAs is significantly inhibited. These mRNAs thus represent transcripts that can either recruit NXF1, p15 and UAP56 more efficiently than bulk mRNA or exit the nucleus *via* an alternative export pathway. Because a role for NXF2 or NXF3 in this putative alternative pathway could be ruled out, it was of interest to investigate whether these mRNAs were exported by CRM1.

CRM1 is not a major mRNA export receptor in Drosophila

The CRM1-export pathway was inhibited by LMB, which prevents CRM1 binding to RanGTP and the export cargo (reviewed by Görlich and Kutay, 1999). The efficiency of the LMB treatment was confirmed by analyzing the subcellular localization of two endogenous proteins, PYM and Extradenticle, which are both exported by CRM1 (Supplemental Fig. 3). Because CRM1 has been implicated in multiple export processes (*i.e.* export of various proteins, spliceosomal U snRNAs and ribosomal subunits), prolonged exposure to LMB leads to pleiotropic effects including the accumulation of poly(A)⁺ RNA within the nucleus of yeast

and human cells (reviewed by Görlich and Kutay, 1999). To avoid these indirect effects, we isolated total and cytoplasmic RNA samples from cells treated with LMB for 12h. This time was chosen from the observation that the half-life of *ca.* 70% of *Drosophila* mRNAs is between 1–7h (our unpublished observations; Lengyel *et al.*, 1977). Thus, we reasoned that a 12h LMB-treatment should be long enough to detect changes in expression levels of at least 70% of transcripts, but short enough to avoid indirect effects. Consistently, no nuclear accumulation of poly(A)⁺ RNA was observed in S2 cells treated with LMB for 12h (Supplemental Fig. 3).

Next, we randomly selected 10 mRNAs among the 20 transcripts whose levels remained unchanged in cells depleted of NXF1, p15 or UAP56 and analyzed their expression levels by semi-quantitative RT-PCR in total and cytoplasmic samples of cells treated with LMB (Fig. 4C and data not shown). A rough estimation of the half-life of these transcripts was obtained by analyzing their levels in total RNA samples isolated from cells treated with actinomycin D for 2h and 8h (Fig. 4C). In agreement with our prediction, 7 out of 10 transcripts were short-lived mRNAs (Fig. 4C and data not shown). Nonetheless, the levels of these mRNAs remained unchanged in total and cytoplasmic samples isolated from LMB-treated cells (Fig. 4C and Supplemental Table I). By RT-PCR we could detect a reduction in *dom* and *rp49* mRNA levels in cytoplasmic samples isolated from NXF1 depleted cells, as expected (Fig. 4C and Table I).

To confirm the RT-PCR data and monitor the expression levels of all mRNAs of this class we performed a microarray analysis with total and cytoplasmic samples isolated from two independent LMB treatments. None of the 20 transcripts whose levels remained unchanged in cells depleted of NXF1, p15 or UAP56 were affected by the LMB treatment (Fig. 4D group b, and Supplemental Table I). Although we cannot rule out that the long-lived mRNAs of this class (half-life >12h) reach the cytoplasm by recruiting CRM1, at least 7 out of 20 (and probably more) of these transcripts are not exported by CRM1.

The possibility that CRM1 mediates the export of a large proportion of transcripts could also be ruled out, as both in total and cytoplasmic RNA samples isolated from LMB-treated cells 98–99% of detectable mRNAs were unaffected (less than 1.5-fold different from the control sample), 1% were overrepresented (at least 1.5-fold up) and less than 0.5% were underrepresented (at least 1.5-fold down) (Fig. 4E). A list of mRNAs regulated in LMB-treated cells is provided in Supplemental Table II.

With the caveat that the kinetics and efficiency of the export inhibition by LMB and by depleting export factors by RNAi are not comparable, the RNA expression profiles observed in cytoplasmic or total RNA samples isolated from LMB-treated cells were in sharp contrast with the global changes observed in samples isolated from NXF1-depleted cells (day 2, Fig. 4E). Note that a 2 day-treatment with NXF1 dsRNA, corresponds to an export block of <20h as judged by oligo(dT) *in situ* hybridization (not shown).

Finally, the small subset of mRNAs that were underrepresented in the cytoplasm of LMB-treated cells, and thus potentially exported by CRM1, were also underrepresented in the cytoplasm of NXF1-depleted cells (day 2), suggesting that these mRNAs may not represent genuine CRM1 export cargoes (Fig. 4D group a, and Supplemental Table II). In summary, our observations argue against a role for CRM1 in the export of a large fraction of mRNAs.

A set of mRNAs is differently affected in NXF1, p15 or UAP56 knockdowns

Despite the similarities of the mRNA expression profiles in cells depleted of NXF1, p15 or UAP56, 32 mRNAs exhibiting differential expression in the three different knockdowns were detected (Fig. 5 and Supplemental Table III). Most mRNAs could be sorted into three classes: I, mRNAs targeted by RNAi (3/32); II, mRNAs underrepresented in the UAP56 knockdown, but not affected or overrepresented in the NXF1 and p15 knockdowns (15/32); III, mRNAs underrepresented in NXF1 and p15 knockdowns, but not affected or overrepresented in the UAP56 knockdown (12/32).

The microarray data were validated by RT-PCR for all mRNAs of class I, (Fig. 6B), and by Northern blot for four selected mRNAs belonging to classes II or III (Fig. 5B and data

not shown). One of the tested mRNAs of class III encodes the ribosomal protein S12. This and the additional class III mRNAs, which exhibit reduced expression levels in NXF1 and p15 knockdowns, but not in the UAP56 knockdown, are likely to be exported independently of UAP56 function. Despite the similarities in their expression pattern, however, the predicted function of the proteins encoded by class II or III transcripts is heterogeneous. The similar behavior of these mRNAs may be related to common sequence or structural elements present in the transcript.

A block of mRNA nuclear export causes the upregulation of genes involved in this process

Among the mRNAs differentially expressed in NXF1, p15 or UAP56 knockdowns were the mRNAs targeted by RNAi. Surprisingly, p15 mRNA was not only underrepresented in the corresponding p15 knockdown, but was overrepresented in NXF1 and UAP56 knockdowns (Fig. 5A and 6A). Similarly, *nxf1* mRNA was overrepresented in the p15 knockdown (Fig. 5A and 6A). UAP56 mRNA was overrepresented in samples isolated from NXF1-depleted cells on day 2. This upregulation was no longer observed on day 4 (Fig. 6A). Remarkably, the mRNA encoding REF1 was also overrepresented in cells depleted of NXF1, p15 or UAP56 (Fig. 6A and Supplemental Table IV). These data were verified by semi-quantitative RT-PCR (Fig. 6B). Notably, the increased levels of these mRNAs was detected in both total and cytoplasmic RNA samples, but did not usually result in a strong increase of the protein levels, because protein synthesis is impaired in these cells (Gatfield *et al.*, 2001; Herold *et al.*, 2001).

As the turnover rate of p15 mRNA was not significantly altered in NXF1 knockdowns (Fig. 6C), the increased steady-state levels of this mRNA is likely to be caused by a higher rate of transcription. In contrast, *ref1* mRNA was stabilized in cells depleted of NXF1 (Fig. 6C). We conclude that transcriptional upregulation and mRNA stabilization both contribute to the increased levels of transcripts encoding nuclear export factors. These results revealed the existence of a feedback loop by which a block to nuclear export leads to increased levels of mRNAs encoding transport factors.

Prompted by this observation, we investigated whether depletion of NXF1, p15 or UAP56 results in the upregulation of additional, unknown components of the nuclear mRNA export pathway. To identify potential candidates we generated a list of mRNAs that are at least 2-fold overrepresented in NXF1, p15 and UAP56 knockdowns (Supplemental Table IV). A closer inspection of these genes indicated that some encode proteins that are unlikely to be implicated in export (Supplemental Table IV), but in most cases the gene products were poorly characterized.

From this list we selected four candidate mRNAs encoding the following proteins: CG7163 (zinc-finger domain protein), CG15612 (protein belonging to the rhoGEF family), *Ssrp* (single-stranded RNA and DNA binding protein) and CG5205 (RNA helicase, component of U5 snRNP). Northern blot analysis confirmed that *ssrp* and *cg5205* transcripts were indeed overrepresented in NXF1, p15 and UAP56 knockdowns (Fig. 2A).

A possible role in export for these selected candidates was investigated by silencing their expression by RNAi and analyzing the distribution of bulk mRNA by oligo(dT) *in situ* hybridization. We monitored cell proliferation in parallel. In contrast to cells depleted of CG7163, CG15612 or CG5205, which showed no obvious growth or export phenotype (data not shown), cells depleted of *Ssrp* proliferated more slowly than control cells. This reduction of proliferation was significant, but was not as dramatic as that observed when NXF1 is depleted (data not shown). Moreover, approximately 6 days after transfection of *Ssrp* dsRNA, the size of cells increased compared to control cells (Fig. 6D).

Remarkably, starting from day 8, cells depleted of *Ssrp* displayed a highly abnormal distribution of poly(A)⁺ RNA (Fig. 6D). While in NXF1, p15 or UAP56 knockdowns poly(A)⁺ RNA accumulated evenly within the nuclear compartment (Fig. 6D and Supplemental Fig. 1), in *Ssrp*-depleted cells poly(A)⁺ RNAs accumulated in nuclear foci (Fig. 6D). These structures did not coincide with the nucleolus, and their staining was strongly reduced after RNase A

treatment, indicating that they consisted of RNA (data not shown). These results suggest a role for Ssrp in the nuclear export of polyadenylated RNAs.

Discussion

NXF1, p15 and UAP56 define a single mRNA export pathway in Drosophila

Although *Drosophila* NXF1, p15 and UAP56 have been shown to be essential for nuclear export of bulk mRNA (Gatfield *et al.*, 2001; Herold *et al.*, 2001; Wiegand *et al.*, 2002), prior to this study it was unclear whether the export of all mRNAs depends on these three proteins and whether mRNAs will be found that require NXF1 and p15 function, but not UAP56 function or *vice versa*. In this study we show that depletion of any one of these proteins results in strikingly similar changes in mRNA expression profiles, indicating that these three proteins define a single export pathway.

The virtually identical effects observed after depletion of NXF1 and p15 demonstrate that these proteins form a single functional unit, as reported previously (Fribourg *et al.*, 2001; Herold *et al.*, 2001; Wiegand *et al.*, 2002). Therefore we consider it unlikely that p15 may have a general export function independent of NXF proteins, as suggested by others (Ossareh-Nazari *et al.*, 2001). The similarities of the mRNA expression profiles in cells depleted of UAP56, NXF1 or p15 indicates that NXF1:p15 heterodimers can only be recruited to most mRNAs when UAP56 is present.

An exception to this rule is provided by a small group of mRNAs whose levels do not change in UAP56-depleted cells, but are decreased in the cytoplasm of cells depleted of NXF1 or p15 (Supplemental Table III, class III). These mRNAs may recruit NXF1:p15 heterodimers via a UAP56-independent mechanism. Further studies will be required to determine the specific features of this particular class of mRNAs.

Cotranscriptional mRNA decay may account for decreased mRNA levels after export inhibition

We show that the overall reduction in mRNA levels in total samples isolated from cells depleted of NXF1, p15 or UAP56 is a specific signature of the knockdowns, but the mechanism by which this decrease is achieved remains to be established. A block to mRNA export could lead to either a decreased stability of mRNAs accumulating within the nucleus, a reduction of the transcriptional activity in depleted cells, or a cotranscriptional degradation of newly synthesized mRNAs. Changes in transcription levels are very likely to contribute to the observed overall changes in gene expression. However, several lines of evidence indicate that transcription is not generally inhibited in depleted cells. First, in these cells the total levels of 10–15% of tested mRNAs remain unchanged (less than 1.2-fold), and 1–4% of mRNAs are upregulated (at least 1.5-fold) (Fig. 1B). Since mRNA export has been inhibited efficiently on day 2, unchanged or increased mRNA levels on day 4 cannot be attributed solely to a higher stability of the respective transcripts, but are also indicative of ongoing transcription. Second, heat shock mRNA synthesis can be induced in depleted cells to similar levels as in wild-type cells (Gatfield *et al.*, 2001; Herold *et al.*, 2001), indicating that the transcription machinery is functional in these cells.

Cotranscriptional mRNA degradation has been observed in yeast strains in which mRNA export has been inhibited as a consequence of mutations in genes encoding export factors, including *sub2* (Libri *et al.*, 2002; Zenklusen *et al.*, 2002). This reduction is overcome in a genetic background in which individual components of the exosome are inactivated (Libri *et al.*, 2002; Zenklusen *et al.*, 2002), suggesting that following an export block, nascent mRNAs are degraded by the exosome.

None of the underrepresented mRNAs tested in this study displayed a higher turnover rate in cells depleted of NXF1, suggesting that if degradation occurs it is not posttranscriptional. Thus it is possible that cotranscriptional decay contributes to the overall downregulation seen for most mRNAs. The basis of this decay is not known, but it has been

suggested that nascent mRNAs that cannot be assembled into a 'normal' mRNP are cotranscriptionally targeted for degradation (Libri *et al.*, 2002; Zenklusen *et al.*, 2002; Jensen and Rosbash, 2003). Assembly of aberrant mRNPs may occur when mRNA export is blocked by competition for nuclear RNA binding proteins by mRNAs accumulating within the nucleus. Consistent with a cotranscriptional mRNA decay mechanism, it has been recently reported that components of the exosome associate with elongating RNA polymerase II in *Drosophila* (Andrulis *et al.*, 2002).

Alternative export pathways

Prior to this study, the fraction of mRNAs that might be exported by alternative export pathways, *e.g.* by recruiting CRM1 or other members of the NXF family was unknown. Although we have identified 20 transcripts whose export was apparently not affected by the depletion of NXF1, p15 or UAP56, our data indicate that at least 7 (and probably more) of these mRNAs do not reach the cytoplasm by recruiting CRM1, and none of them is exported by NXF2 or NXF3. Notably, these mRNAs do not encode proteins with related biochemical functions, but may share common sequence or structural elements, enabling them either to recruit NXF1, p15 and UAP56 more efficiently or to have access to other unidentified export receptors.

Despite monitoring the relative cytoplasmic expression levels of about 6000 different mRNAs, we have not been able to identify any potential mRNA export substrate for NXF2 or NXF3. Moreover, less than 0.5% of detectable transcripts (those downregulated in LMB-treated cells), represent potential CRM1 cargoes. The possibilities that additional substrates were not represented on the array, or that some CRM1 substrates escape detection because they have long half-lives (>12h), cannot be ruled out. Also, it is possible that CRM1, NXF2 or NXF3 play a role in the export of specific transcripts expressed in different developmental stages or tissues, but not in S2 cells. Despite these caveats, our data suggest that only a small fraction of mRNAs is likely to reach the cytoplasm by an alternative route.

A feedback mechanism triggered by a block of nuclear export

This study led to the discovery of a feedback loop by which a block of nuclear export triggers the upregulation of genes encoding nuclear export factors. This upregulation is achieved both by transcriptional activation and stabilization of the respective mRNAs. The existence of this feedback mechanism prompted us to investigate whether some of the upregulated genes encode unknown transport factors. Remarkably, silencing the expression of one (Ssrp) out of four selected genes led to an accumulation of mRNAs in nuclear foci. The role of Ssrp *in vivo* is not well understood. The human homologue of Ssrp is a component of the FACT complex implicated in transcription elongation *in vitro* (Orphanides *et al.*, 1999). *Drosophila* Ssrp binds single-stranded DNA and RNA *in vitro* and has been shown to interact with CHD1, a chromatin remodeling ATPase recently implicated in transcriptional termination by RNA polymerase II (Alén *et al.*, 2002; Kelley *et al.*, 1999). Data presented in this study suggest that, in addition to a putative role in transcription, Ssrp is also implicated in export of poly(A)⁺ RNA to the cytoplasm, although the precise mechanism by which Ssrp plays a role in this process remains to be investigated.

Although, further studies are required to determine whether other upregulated mRNAs encode proteins involved in export, it is interesting to note that four of these mRNAs encode proteins of the ABC class of ATPases. A role in mRNA export for a non-membrane member of this protein family has been reported recently in *Schizosaccharomyces pombe* (Kozak *et al.*, 2002).

Materials and Method

Cell culture, RNA interference and fluorescent in situ hybridization

RNA interference and fluorescent *in situ* hybridizations were performed as described before (Herold *et al.*, 2001). Most dsRNAs used in this study have been described (Gatfield *et al.*, 2001; Herold *et al.*, 2001). Ssrp dsRNA corresponds to nucleotides 1 to 694 of Ssrp cDNA.

RNA isolation, RT-PCR and Northern blots

Cytoplasmic RNA was isolated by hypotonic lysis as described in Supplemental Experimental Procedures. Total RNA was isolated with TRIzol Reagent (Invitrogen). The concentration of all RNA samples was determined by measuring the optical density at 260 nm. The quality and the concentration of all RNA preparations was checked further by visualizing the rRNA in denaturing agarose gels and by RT-PCR as described in Supplemental Figure 2.

Northern blotting and RT-PCR were performed as described by Herold *et al.* (2001) except that random hexamers were used to prime the reverse transcription reaction. Probes recognizing ref1, y14, mago and p15 mRNAs correspond to the complete cDNA of the respective gene. Partial cDNA fragments corresponding to 18S rRNA, Ssrp, RpS12, SD06908, CG1239, CG7840, CG5205, Dom (CG4029, jumu) were amplified by PCR from a random-primed S2 cDNA library. The identity of the amplified product was confirmed by sequencing. These products served as templates to generate radiolabeled probes. All oligonucleotide sequences are available upon request.

Construction of Drosophila microarrays, microarray hybridizations, data acquisition and analysis

The precise array-layout is available in the ArrayExpress database at EBI. Construction of the microarrays, target-preparation, hybridization conditions, data acquisition and analysis are described in Supplemental Experimental Procedures.

Acknowledgements

We are grateful to G.K. Christophides, M. Muckenthaler, B. Minana, and C. Schwager for advice and reagents. We thank members of W. Ansorge and M. Hentze groups and the Gene Core Facility at EMBL for helpful discussions, and E. Furlong and D. Thomas for critical comments on the manuscript. L.T. was supported by the Programa Gulbenkian de Doutorado em Biologia e Medicina (Portugal) and a fellowship from the Fundação para a Ciência e Tecnologia (Portugal).

References

- Alen,C., Kent,N.A., Jones,H.S., O'Sullivan,J., Aranda,A., Proudfoot,N.J. (2002). A role for chromatin remodeling in transcriptional termination by RNA polymerase II. *Mol. Cell.*, **10**, 1441-52.
- Andrulis,E.D., Werner,J., Nazarian,A., Erdjument-Bromage,H., Tempst,P., Lis,J.T. (2002). The RNA processing exosome is linked to elongating RNA polymerase II in *Drosophila*. *Nature*, **420**, 837-841.
- Fribourg,S., Braun,I.C., Izaurralde,E., and Conti,E. (2001). Structural basis for the recognition of a nucleoporin FG repeat by the NTF2-like domain of the TAP/p15 mRNA nuclear export factor. *Mol. Cell.*, **8**, 645–656.
- Gallouzi,I.E., and Steitz,J.A. (2001). Delineation of mRNA export pathways by the use of cell-permeable peptides. *Science*, **294**, 1895–1901.
- Gatfield,D., Le Hir,H., Schmitt,C., Braun,I.C., Kocher,T., Wilm,M., and Izaurralde,E. (2001).

- The DExH/D box protein HEL/UAP56 is essential for mRNA nuclear export in *Drosophila*. *Curr. Biol.*, **11**, 1716–1721.
- Gatfield,D., and Izaurralde,E. (2002). REF1/Aly and the additional exon junction complex proteins are dispensable for nuclear export. *J. Cell Biol.* **159**, 579–588.
- Görlich,D., and Kutay,U. (1999). Transport between the cell nucleus and the cytoplasm. *Annu. Rev. Cell. Dev. Biol.*, **15**, 607–660.
- Herold,A., Suyama,M., Rodrigues,J.P., Braun,I.C., Kutay,U., Carmo-Fonseca,M., Bork,P., and Izaurralde,E. (2000). TAP (NXF1) belongs to a multigene family of putative RNA export factors with a conserved modular architecture. *Mol. Cell Biol.*, **20**, 8996-9008.
- Herold,A., Klymenko,T., and Izaurralde,E. (2001). NXF1/p15 heterodimers are essential for mRNA nuclear export in *Drosophila*. *RNA*, **7**, 1768-1780.
- Hurt,E., Strasser,K., Segref,A., Bailer,S., Schlaich,N., Presutti,C., Tollervey,D., and Jansen,R. (2000). Mex67p mediates nuclear export of a variety of RNA polymerase II transcripts. *J. Biol. Chem.*, **275**, 8361–8368.
- Izaurralde,E. A novel family of nuclear transport receptors mediates the export of messenger RNA to the cytoplasm. (2002). *Eur. J. Cell Biol.*, **81**, 577–584.
- Jensen,T.H., Boulay,J., Rosbash,M., and Libri,D. (2001). The DECD box putative ATPase Sub2p is an early mRNA export factor. *Curr. Biol.*, **11**, 1711–1715.
- Jensen,T.H., and Rosbash,M. (2003). Co-transcriptional monitoring of mRNP formation. *Nat. Struct. Biol.*, **10**, 10–12.
- Kelley,D.E., Stokes,D.G., and Perry,R. P. (1999). CHD1 interacts with SSRP1 and depends on both its chromodomain and its ATPase/helicase-like domain for proper association with chromatin. *Chromosoma*, **108**, 10–25.
- Kiesler,E., Miralles,F., and Visa,N. (2002). HEL/UAP56 binds cotranscriptionally to the Balbiani ring pre-mRNA in an intron-independent manner and accompanies the BR mRNP to the nuclear pore. *Curr. Biol.*, **12**, 859–862.
- Kozak,L., Gopal,G., Yoon,J.H., Sauna,Z.E., Ambudkar,S.V., Thakurta,A.G., Dhar,R. (2002). Elf1p, a member of the ABC class of ATPases, functions as a mRNA export factor in *Schizosaccharomyces pombe*. *J. Biol. Chem.*, **277**, 33580-33589.
- Lengyel,J.A., and Penman,S. (1977). Differential stability of cytoplasmic RNA in a *Drosophila* cell line. *Dev. Biol.*, **57**, 243–253.
- Libri,D., Dower,K., Boulay,J., Thomsen,R., Rosbash,M., and Jensen,T.H. (2002). Interactions between mRNA export commitment, 3'-end quality control and nuclear degradation. *Mol. Cell Biol.*, **22**, 8254–8266.
- Linder,P., and Stutz,F. (2001). mRNA export: travelling with DEAD box proteins. *Curr. Biol.*, **11**, R961–963.
- Luo,M.L., Zhou,Z., Magni,K., Christoforides,C., Rappsilber,J., Mann,M., and Reed,R. (2001). Pre-mRNA splicing and mRNA export linked by direct interactions between UAP56 and Aly. *Nature*, **413**, 644–647.
- Orphanides,G., Wu,W.H., Lane,W.S., Hampsey,M., and Reinberg,D. (1999). The chromatin-specific transcription elongation factor FACT comprises human SPT16 and SSRP1 proteins. *Nature*, **400**, 284–288.
- Ossareh-Nazari,B., Maison,C., Black,B.E., Levesque,L., Paschal,B.M. and Dargemont, C. (2001). RanGTP-Binding Protein NXT1 Facilitates Nuclear Export of Different Classes of RNA In Vitro. *Mol. Cell Biol.*, **20**, 4562–4571.
- Reed,R., and Hurt,E. (2002). A conserved mRNA export machinery coupled to pre-mRNA splicing. *Cell*, **108**, 523-31.
- Segref,A., Sharma,K., Doye,V., Hellwig,A., Huber,J., Luhrmann,R., and Hurt,E. (1997).

- Mex67p, a novel factor for nuclear mRNA export, binds to both poly(A)+ RNA and nuclear pores. *EMBO J.*, **16**, 3256–3271.
- Strasser,K., and Hurt,E. (2000). Yra1p, a conserved nuclear RNA-binding protein, interacts directly with Mex67p and is required for mRNA export. *EMBO J.*, **19**, 410–420.
- Strasser,K., and Hurt,E. (2001). Splicing factor Sub2p is required for nuclear mRNA export through its interaction with Yra1p. *Nature* **413**, 648–652.
- Strasser,K., Masuda,S., Mason,P., Pfannstiel,J., Oppizzi,M., Rodriguez-Navarro,S., Rondon,A.G., Aguilera,A., Struhl,K., Reed,R., and Hurt,E. (2002). TREX is a conserved complex coupling transcription with messenger RNA export. *Nature*, **417**, 304–308.
- Stutz,F., Bachi,A., Doerks,T., Braun,I.C., Seraphin,B., Wilm,M., Bork,P., and Izaurralde,E. (2000). REF, an evolutionary conserved family of hnRNP-like proteins, interacts with TAP/Mex67p and participates in mRNA nuclear export. *RNA*, **6**, 638–650.
- Vainberg,I.E., Dower,K., and Rosbash,M. (2000). Nuclear export of heat-shock and non-heat-shock mRNA occurs via similar pathways. *Mol. Cell. Biol.*, **20**, 3996–4005.
- Wiegand,H.L., Coburn,G.A., Zeng,Y., Kang,Y., Bogerd,H.P., and Cullen,B.R. (2002). Formation of Tap/NXT1 heterodimers activates Tap-dependent nuclear mRNA export by enhancing recruitment to nuclear pore complexes. *Mol. Cell. Biol.*, **22**, 245–256.
- Wilkie,G.S., Zimyanin,V., Kirby,R., Korey,C., Francis-Lang,H., Van Vactor, D., and Davis,I. (2001). Small bristles, the *Drosophila* ortholog of NXF-1, is essential for mRNA export throughout development. *RNA*, **7**, 1781–1792.
- Yang,J., Bogerd,H.P., Wang,P.J., Page,D.C., and Cullen,B.R. (2001). Two closely related human nuclear export factors utilize entirely distinct export pathways. *Mol. Cell*, **8**, 397–406.
- Zenklusen,D., Vinciguerra,P., Strahm,Y., and Stutz,F. (2001). The yeast hnRNP-Like proteins Yra1p and Yra2p participate in mRNA export through interaction with Mex67p. *Mol. Cell. Biol.*, **21**, 4219–4232.
- Zenklusen,D., Vinciguerra,P., Wyss,J.C., and Stutz,F. (2002). Stable mRNP Formation and Export Requires Cotranscriptional Recruitment of the mRNA Export Factors Yra1p and Sub2p by Hpr1p. *Mol. Cell. Biol.*, **22**, 8241–8253.

Legends to Figures

Figure 1. Depletion of NXF1, p15 or UAP56 results in global changes of mRNA levels.

(A) Scatter plot representation of individual measurements using cytoplasmic RNA samples isolated from different knockdowns. The normalized intensity values of the experimental samples are plotted against the normalized intensity values of the reference samples. In addition to the regression line (red line: same intensity in both samples), the 2-fold and the 5-fold lines (black dashed lines) are shown. Spots representing mRNAs targeted by RNAi are marked with a red circle. *nxf1* and *nxf2* were each represented by 2 spots.

(B) All detectable mRNAs were classified according to their relative expression levels. Only mRNAs that could be assigned to the same subclass in measurements performed with two independent samples for each export factor are shown. Blue: mRNAs at least 1.5-fold underrepresented. Yellow: mRNAs that were less than 1.5-fold different from the reference. Red: mRNAs at least 1.5-fold overrepresented. Within these classes, the dashed areas represent subgroups of mRNAs for which more stringent cutoff values were used (at least 2-fold over- or underrepresented; less than 1.2-fold regulated). The total number of genes considered for each pie chart (detectable mRNAs) is indicated in italics.

Figure 2. The general reduction of mRNA expression levels is a specific effect of the mRNA export inhibition.

(A) 10 μ g of total and cytoplasmic RNA samples were analyzed by Northern blot using probes to detect different selected mRNAs as indicated. Knockdown samples should be compared to the corresponding control samples isolated from cells treated in parallel with GFP dsRNA. RNA samples isolated from cells depleted of eIF4G were also analyzed. RNA samples were isolated 2, 4 or 6 days after transfection of dsRNAs, as indicated above the lanes. The lower panel shows the corresponding rRNA stained with ethidium bromide.

(B, C) The expression levels of mRNAs which were at least 2-fold up- or at least 5-fold down-regulated in total samples of NXF1-depleted cells were analyzed in p15, UAP56 and eIF4G knockdowns (B). The expression levels of mRNAs, which were at least 2-fold over- or underrepresented in total samples of eIF4G-depleted cells, were analyzed in NXF1, p15 and UAP56 knockdowns (C). RNA samples were isolated 4 or 6 days after transfection of dsRNAs, as indicated above the panels. Each mRNA is colored according to its relative expression level. The number of mRNAs displayed is indicated above the panels. The color bar indicates fold changes.

Figure 3. The general reduction in mRNA expression levels is not due to increased mRNA turnover rates.

(A) mRNAs that are at least 2-fold overrepresented (in red) or underrepresented (in blue) in the cytoplasmic samples of NXF1, p15 or UAP56 knockdowns. Each mRNA is represented as a line colored according to its relative expression level in the total RNA sample. The number of displayed mRNAs in the respective classes is indicated in brackets. The numbers in the top and bottom corners of each graph are the average relative expression levels of the respective classes.

(B) and (C) S2 cells were treated with NXF1 or GFP dsRNAs. Two or four days after transfection, treated or untreated cells were incubated with actinomycin D (5 μ g/ml) and total RNA was isolated 0.5, 1, 3 and 6 h after the addition of the drug. The levels of selected mRNAs were determined by Northern or slot blot analysis and normalized to rp49 mRNA (whose level does not change during the timescale of the experiment). Values are expressed as percentage of the levels at time 0 (set to 100%) and plotted as a function of time. The relative expression levels of the respective mRNAs in the NXF1 knockdowns (total samples) measured by microarray analysis are given in the top right corner of each graph.

Figure 4. Cells depleted of NXF1, p15 or UAP56 exhibit similar mRNA expression profiles.

(A) Comparison of the relative expression levels of all detectable mRNAs (4854) in cytoplasmic samples (day 4 for NXF1, p15 and UAP56; day 5 for NXF2 and NXF3). The mRNAs are colored according to their expression levels. For each mRNA the average levels from all measurements for each knockdown is shown. The experiment tree above was calculated using the distance option in the GeneSpring software (Euclidian distance).

(B) The cytoplasmic levels of mRNAs which were at least 2-fold overrepresented, at least 2-fold underrepresented, and less than 1.2-fold changed in cytoplasmic samples of NXF1-depleted cells were analyzed in cytoplasmic samples of p15 and UAP56 knockdowns (day 4). The number of mRNAs in each class is indicated. Red, blue and yellow dashed and undashed areas are as described in Figure 1B. The 'unclassified' mRNAs (gray) represent transcripts that were assigned to two different subclasses in two independent microarray measurements.

(C) Semi-quantitative RT-PCR was performed with cytoplasmic RNA samples isolated from S2 cells treated with LMB for 12h and cells depleted of NXF1 (day 4). The levels in the experimental sample should be compared to the corresponding control sample (without LMB treatment or GFP, respectively). The levels of the different mRNAs was analyzed in parallel in total RNA samples isolated from S2 cells treated with actinomycin D (5 μ g/ml) for 0, 2 or 8h.

(D) The expression levels of the 20 mRNAs that were unchanged in NXF1, p15 and UAP56 knockdowns (group b) and of the 9 mRNAs which were at least 1.5-fold underrepresented in the cytoplasmic samples of LMB-treated cells (group a) were analyzed in total and cytoplasmic samples of NXF1 knockdowns (day 2) and of LMB-treated cells. The 7 short-lived mRNAs shown in panel C are labeled with a green star.

(E) Comparison of the relative expression levels of all detectable mRNAs (4189) in cytoplasmic and total samples isolated from cells depleted of NXF1 (day 2) or treated with LMB (12h). In panels D and E, mRNAs are colored according to their average expression levels in measurements performed with 2 independent samples. The colorbar is shown in panel A.

Figure 5. A class of mRNAs that are differentially affected in NXF1, p15 and UAP56 knockdowns.

(A) List of differentially expressed mRNAs in the cytoplasm of cells depleted of NXF1, p15 and UAP56. The criteria applied to select these mRNAs can be found in Supplemental Table III. The four mRNAs tested by Northern blot analysis are marked with a green star. Each mRNA is colored according to its relative expression level. Note the different scale of the color bar in this figure. Spots representing the same mRNA are marked with brackets.

(B) Northern blot membranes shown in Figure 2A were probed for two candidate mRNAs present in the list. The signals obtained with SD06908 and RpS12 probes were quantified and compared to the values measured in the microarray experiment using the same pool of RNAs. Symbols are as in Figure 2A.

Figure 6. A block of nuclear mRNA export results in the upregulation of mRNAs encoding export factors.

(A) Average relative expression values for *nxf1*, *p15*, *uap56* and *ref1* mRNAs determined by microarray analysis of total RNA samples isolated from NXF1, p15 and UAP56 knockdowns. The values are fold changes averaged from two different measurements for each knockdown and also averaged if several spots represent one mRNA species.

(B) The values shown in Panel A (day 4) were confirmed by semi-quantitative RT-PCR with primers specific for 18S rRNA and *nxf1*, *p15*, *uap56* and *ref1* mRNAs.

(C) The stability of *p15* and *ref1* mRNAs in control cells and cells depleted of NXF1 (days 2 and 4) was determined as in Figure 3.

(D) S2 cells were transfected with dsRNA corresponding to GFP (control), *p15* or *Ssrp*. Cells were fixed 10 (GFP, *Ssrp*) or 5 (*p15*) days after transfection. Poly(A)⁺ RNA was detected by FISH with an oligo(dT) probe (red). The nuclear envelope was stained with Alexa488-WGA (green).

Table I. Comparison of relative expression levels measured by microarray analysis and Northern blotting. The signals from the Northern blot experiment shown in Figure 2 was quantified using a phosphoimager and compared to the value measured by the microarray analysis of the same RNA sample. Ribosomal RNA served as internal control for equal loading. Values are given as fold changes (positive values: overrepresented; negative values: underrepresented compared to the reference).

Table I. Herold et al.

| | | Total RNA | | | | | Cytoplasmic RNA | | | | |
|--------|----------|-----------|------|------|-------|-------|-----------------|------|------|-------|-------------|
| | | NXF1 | NXF1 | p15 | UAP56 | eIF4G | NXF1 | NXF1 | p15 | UAP56 | eIF4G |
| | | day2 | day4 | day4 | day4 | day4 | day2 | day4 | day4 | day4 | day4 |
| ref1 | Northern | 3.6 | 2.9 | 2.8 | 2.9 | -1.3 | 2.9 | 2.6 | 2.1 | 2.5 | -1.4 |
| | Array | 2.4 | 2.1 | 2.1 | 2.2 | -1.5 | 2.2 | 2.1 | 1.8 | 2.2 | <i>n.d.</i> |
| ssrp | Northern | 3.0 | 2.9 | 2.8 | 2.8 | 1.3 | 2.3 | 2.6 | 2.1 | 2.3 | 1.4 |
| | Array | 2.2 | 2.5 | 2.0 | 2.0 | 1.3 | 1.5 | 1.8 | 1.6 | 2.1 | <i>n.d.</i> |
| cg5205 | Northern | 3.7 | 4.3 | 3.8 | 2.4 | -1.1 | 2.5 | 3.8 | 2.8 | 1.6 | 1.3 |
| | Array | 4.2 | 4.7 | 3.7 | 2.7 | -1.2 | 2.1 | 3.4 | 2.9 | 1.7 | <i>n.d.</i> |
| cg1239 | Northern | 1.2 | 1.8 | 1.6 | 1.1 | -1.3 | 1.3 | 1.7 | 1.1 | 2.3 | 1.1 |
| | Array | 1.1 | 1.1 | -1.1 | -1.0 | 1.0 | -1.0 | -1.0 | 1.1 | 1.1 | <i>n.d.</i> |
| cg7840 | Northern | -1.7 | -1.4 | -1.5 | -1.8 | -1.8 | -1.4 | -1.4 | -1.7 | 1.1 | 1.3 |
| | Array | -1.2 | -1.1 | -1.1 | -1.2 | -1.9 | -1.2 | -1.1 | -1.0 | 1.1 | <i>n.d.</i> |
| dom | Northern | -1.9 | -2.0 | -1.8 | -2.2 | -1.2 | -2.7 | -3.0 | -3.1 | -3.3 | 1.4 |
| | Array | -5.0 | -3.9 | -4.4 | -7.2 | -1.6 | -5.1 | -5.3 | -5.2 | -7.0 | <i>n.d.</i> |
| y14 | Northern | -1.8 | -1.8 | -1.8 | -2.0 | -1.0 | -1.8 | -1.9 | -2.0 | -2.2 | -1.1 |
| | Array | -2.2 | -1.8 | -3.1 | -2.3 | -1.1 | -2.3 | -2.6 | -3.3 | -2.7 | <i>n.d.</i> |
| nup154 | Northern | -1.1 | -1.4 | -1.3 | -2.3 | 1.3 | -1.7 | -1.6 | -1.9 | -2.6 | 2.2 |
| | Array | -1.0 | -1.4 | -1.7 | -1.7 | 1.4 | -1.5 | -2.3 | -2.5 | -2.6 | <i>n.d.</i> |

Supplemental material

Experimental procedures

Isolation of cytoplasmic RNA

To isolate cytoplasmic RNA, 20–35 x 10⁶ S2 cells were pelleted for 5 min at 500g, washed once with serum-free medium, resuspended in 500 μ l ice-cold hypotonic buffer (10 mM HEPES, pH 7.9, 1.5 mM MgCl₂, 10 mM KCl, 0.5 mM DTT) and kept on ice for 15 min. This procedure permeabilizes S2 cells and extracts soluble cytoplasmic components. The cytoplasmic fraction was cleared from nuclear components by centrifugation at 700g for 8 min at 4°C. To remove residual nuclear contaminants, the cytoplasmic supernatant was recentrifuged twice (at 3300g for 5 min at 4°C and at 16000g for 1 min at room temperature). The supernatant was brought to 100 mM NaCl, 0.5% NP40, 10 mM EDTA, pH 8.0, 0.5% SDS and extracted twice with phenol:chloroform:isoamylalcohol (25:24:1) and once with chloroform:isoamylalcohol (24:1). RNA was ethanol-precipitated and resuspended in ddH₂O. The sample was brought to 40 mM Tris, pH 7.9, 6 mM MgCl₂, 10 mM NaCl, 2 mM spermidine, 10 mM DTT and treated with 2 units of RNase-free DNase I (Promega) for 30 min at 37°C. Following phenol:chloroform:isoamylalcohol and chloroform extractions, the RNA was ethanol-precipitated and resuspended in ddH₂O. RNA prepared with this method is virtually free of nuclear contaminants (Supplemental Figs 2A and B).

Construction of Drosophila microarrays

The microarray represents all the EST inserts from the *Drosophila* Gene Collection Release 1 (DGCr1.0, <http://www.fruitfly.org/DGC/index.html>) plus additional PCR products representing genes of special interest for this study, positive (spike-ins) and negative controls. The precise array-layout is available in the ArrayExpress database at EBI.

The PCR products serving as external positive and negative controls are described in Richter *et al.* (2002). Five different heterologous positive controls encoding three *A. thaliana* proteins, firefly luciferase and CAT were used. As negative controls two unclassified proteins from *A. thaliana*, Kanamycin resistance gene, Renilla Luciferase and mock spots (2xSSC) were used.

The PCR products were purified and spotted on aminosilane-coated glass slides essentially as described in Richter *et al.* (2002). Except for positive and negative control spots, each PCR product was spotted once per slide. External positive controls were spotted in 3 different dilutions. Each dilution was spotted 16 times per slide (*i.e.* 240 positive control spots per slide). Each negative control was spotted 16 times per slide. Spotting was performed so that each subgrid on the array contained several positive and negative control spots. After spotting, the slides were incubated at 60°C for 3–5h and at 100°C for 10 min.

Target-preparation and microarray hybridizations

For target-preparation, a modified Eberwine protocol was used (essentially as described in Dimopoulos *et al.*, 2002). As starting material for the generation of the ds cDNA we used 5 μ g of total or cytoplasmic RNA (essentially rRNA) supplemented with a mixture of five different external polyadenylated control RNAs (spike-ins, 50 pg each except for 6i18_52k of which only 15 pg were used). 5 μ g of amplified cRNA were subjected to a random primed first-strand reverse-transcription reaction in the presence of either Cy3-dUTP or Cy5-dUTP. Subsequent purification of the labeled target, prehybridization and hybridization was done as in Dimopoulos *et al.* (2002). The arrays were washed twice in 0.1 x SSC, 0.1% SDS (20 min), twice with 0.1x SSC (10 min), rinsed with ddH₂O, and dried.

Microarray data acquisition and analysis

All microarrays were scanned on a GenePix 4000B Microarray Scanner (Axon Instruments, Union City, CA, USA). The intensity values for each spot were calculated by subtracting the local background surrounding the spot (median F - median B). Spots were only considered for further analysis if the intensity values were higher than the average intensity plus twice the standard deviation of negative control spots in at least one of the two channels (= detectable mRNAs). After a region-dependent normalization, data were imported into GeneSpring 4.2. (Silicon Genetics). All experiments were normalized using an intensity-dependent normalization scheme (Lowess). In experiments with samples from NXF1, p15, UAP56 and eIF4G knockdowns or LMB-treated cells normalization to the positive controls was performed. Each measurement was repeated with an independent sample, in which the fluorescent dyes of experimental sample and reference were exchanged (dye swap). In experiments with NXF2 or NXF3 knockdowns, only cytoplasmic samples were used for microarray analysis. One of these was measured twice (including a dye-swap).

In a self-to-self control experiment the positive control spots (spike-ins) had an average ratio of 1.006 ± 0.162 after intensity-dependent normalization and were well distributed between low and high intensity spots. Since all genes had an average ratio of 1.004 ± 0.173 , we considered the positive controls to be representative of non-regulated genes, indicating that they can be used for normalization. As the average standard deviation of all positive control spots in all experiments was 0.211 ± 0.069 , we determined a fold change value of at least 1.5 being a significant cutoff. Spots starting with SC, AE or DB were not considered in the detailed analysis.

Legends to Supplemental Figures and Tables

Supplemental Figure 1: Depletion of NXF1, p15 or UAP56 causes nuclear accumulation of poly(A)⁺RNA.

S2 cells were transfected with dsRNAs corresponding to GFP (control), NXF1, p15 or UAP56 as indicated. Cells were fixed two or four days after transfection and poly(A)⁺ RNA was detected by FISH with a Cy3-labeled oligo(dT) probe. The nuclear envelope was stained with Alexa-488 wheat germ agglutinin. The same cells were used to prepare RNA for microarray analysis.

Supplemental Figure 2: Isolation of cytoplasmic mRNA from S2 cells.

(A) S2 cells were fractionated using different protocols. Total (T), cytoplasmic (C) and nuclear (N) fractions were collected and analyzed by Western blot as described before (Herold *et al.*, 2001). Extract from 10^5 cells was loaded per lane. The contamination of the cytoplasmic fractions with nuclear components was analyzed using antisera recognizing the nuclear proteins Ref1 and Fl(2)d. The extraction efficiency of cytoplasmic components was determined with an antiserum directed against tubulin. Mouse monoclonal anti-tubulin antiserum E7 was diluted 1:10000. Polyclonal rabbit antiserum against Fl(2)d (kindly provided by Juan Valcarcel; Penalva *et al.*, 2000) or against REF1 (Gatfield *et al.*, 2002), were diluted 1:1000 and 1:3000, respectively. A published protocol (Biessmann, 1980) using NP40 leads to leakage of nuclear components into the cytoplasmic fraction (see lane 2). In this study, cells were lysed in a hypotonic buffer (see Supplemental Experimental Procedures), which extracts the cytoplasmic components without further mechanical treatment, such as douncing (lanes 7–12). The cytoplasmic fraction obtained with this procedure is virtually free of nuclear proteins (lanes 8 and 11).

(B) The quality of 3 cytoplasmic RNA preparations isolated using hypotonic buffer was assessed by testing for the presence of rp49 and hsp83 precursor mRNAs. Both precursor mRNAs were found to be only barely detectable, while they could readily be detected in samples of total RNA (compare lanes 4–6 with lanes 1–3). Using real-time PCR, the levels of rp49 pre-mRNA in cytoplasmic samples were found to be less than 10% of the levels in total RNA preparations (data not shown).

Supplemental Figure 3: LMB blocks Crm1-dependent protein export.

(A, B) S2 cells were treated with Leptomycin B (dissolved in methanol) for 12h (final concentration 40ng/ml). Control cells were treated with equivalent amounts of methanol. The same cells were used to prepare RNA for microarray analysis.

(A) Cells were fixed and the localization of the endogenous proteins Extradenticle (EXD) and PYM was determined by indirect immunofluorescence. The nuclear envelope was stained with Alexa-488 wheat germ agglutinin. Alternatively, the nucleoplasm was stained with anti-REF1 antibodies. Indirect immunofluorescence was performed as described by Herold *et al.* (2001). PYM protein corresponds to the uncharacterized product of the *wigb* gene (Forler *et al.*, 2003). Antibodies recognizing PYM were raised in rats immunized with the recombinant protein expressed in *E. coli* as a GST fusion. A role for CRM1 in EXD nuclear export has been reported by Abu-Shaar *et al.*, (1999). Monoclonal anti-extradenticle antibodies (B11M) were kindly provided by Rob White and are described in Aspland and White (1997).

(B) Poly(A)⁺ RNA was detected by FISH with a Cy3-labeled oligo(dT) probe (red). The nuclear envelope was stained with Alexa-488 wheat germ agglutinin (green). Scale bar in all panels 5 μ m.

Supplemental Table I. mRNAs not affected by the knockdown of export factors. mRNAs that are less than 1.2-fold over- or underrepresented in all 8 measurements with cytoplasmic samples isolated from NXF1 (day 2 and 4), p15 and UAP56 (day 4) knockdowns and less than 1.5-fold changed in total samples. The expression levels of these mRNAs in total and cytoplasmic samples isolated from LMB treated cells (12h) are also indicated. Values are averages of 2 measurements performed with 2 independent samples for each export factor. The mRNAs tested by Northern blot (Fig. 2) are marked with a star. Short-lived mRNAs (as tested by RT-PCR, Fig. 4C) are marked in gray. The genes were annotated according to Flybase (<http://flybase.bio.indiana.edu>).

Supplemental Table II: mRNAs that are at least 1.5-fold over- or underrepresented in measurements performed with 2 independent total or cytoplasmic samples isolated from LMB-treated cells. The average expression levels of these mRNAs in samples isolated from NXF1 (day 2 and 4), p15 (day 4) and UAP56 (day 4) knockdowns are also indicated. The orange color indicates mRNAs that were at least 1.5-fold overrepresented in two independent total or cytoplasmic samples isolated from LMB-treated cells, respectively. The blue color indicates mRNAs that were at least 1.5-fold underrepresented. #DIV/0! indicates that in at least 1 of the 2 respective measurements, no data were obtained (bad spot).

Supplemental Table III: mRNAs that are differently affected in NXF1, p15 and UAP56 knockdowns. The values are averages of 2 measurements for each knockdown (cytoplasmic samples, day 4). The genes were annotated according to Flybase (<http://flybase.bio.indiana.edu>).

This list of mRNAs was generated applying the following selection criteria. First, all those mRNAs in p15 and UAP56 cytoplasmic samples were selected whose abundance was at least 2-fold different in the NXF1 knockdown. Only mRNAs with values differing not more than 1.5-fold between the two measurements for each export factor were considered. mRNAs belonging to the 'not changed' class (*i.e.* less than 1.2-fold up or down) in UAP56 and belonging to the 'down' class (*i.e.* at least 1.5-fold down) in NXF1 and p15 experiments were added to the list. Similarly, mRNAs belonging to the 'not changed' class in NXF1 and p15 knockdowns and to the 'down' class in UAP56 knockdown were selected. This list of 106 mRNAs was manually cleared of mRNAs that were not down in NXF1 and p15 experiments on day 4, but were in NXF1 on day 2. Furthermore, mRNAs which were 2-fold differently expressed in the knockdowns of two export factors, but had the same tendency (at least 1.5-fold over- or underrepresented) in both cases were removed.

Supplemental Table IV: mRNAs that are at least 2-fold overrepresented in 7 of 8 measurements performed with total samples isolated from NXF1 (day 2 and 4), p15 (day 4) and UAP56 (day 4) knockdowns.

The mRNAs that have been tested for a possible role in nuclear mRNA export are marked in gray. The annotation is according to Flybase (<http://flybase.bio.indiana.edu>).

References used in the Supplemental Material

- Abu-Shaar, M., Ryoo, H. D., and Mann, R. S. (1999). Control of the nuclear localization of Extradenticle by competing nuclear import and export signals. *Genes Dev* **13**, 935–945.
- Aspland, S. E., and White, R. A. (1997). Nucleocytoplasmic localisation of extradenticle protein is spatially regulated throughout development in *Drosophila*. *Development*, **124**, 741–747.
- Biessmann, H. (1980). Concentrations of individual RNA sequences in polyadenylated nuclear and cytoplasmic RNA populations of *Drosophila* cells. *Nucleic Acids Res.*, **8**, 6099–6111.
- Dimopoulos, G., Christophides, G. K., Meister, S., Schultz, J., White, K. P., Barillas-Mury, C., and Kafatos, F. C. (2002). Genome expression analysis of *Anopheles gambiae*: responses to injury, bacterial challenge, and malaria infection. *Proc. Natl. Acad. Sci. USA*, **99**, 8814–8819.
- Eberwine, J., Yeh, H., Miyashiro, K., Cao, Y., Nair, S., Finnell, R., Zettel, M., and Coleman, P. (1992). Analysis of gene expression in single live neurons. *Proc. Natl. Acad. Sci. USA*, **89**, 3010–3014.
- Forler, D., Köcher, T., Rode, M., Gentzel, M., Izaurralde, E., and Wilm, M. (2003). An efficient protein-complex purification method for functional proteomics in higher eukaryotes. *Nat. Biotechnol.*, **21**, 89–92.
- Gatfield, D., and Izaurralde, E. (2002). REF1/Aly and the additional exon junction complex proteins are dispensable for nuclear export. *J. Cell Biol.*, **159**, 579–588.
- Herold, A., Klymenko, T., and Izaurralde, E. (2001). NXF1/p15 heterodimers are essential for mRNA nuclear export in *Drosophila*. *Rna*, **7**, 1768–1780.
- Penalva, L. O., Ruiz, M. F., Ortega, A., Granadino, B., Vicente, L., Segarra, C., Valcarcel, J., and Sanchez, L. (2000). The *Drosophila* fl(2)d gene, required for female-specific splicing of Sxl and tra pre-mRNAs, encodes a novel nuclear protein with a HQ-rich domain. *Genetics*, **155**, 129–139.
- Richter, A., Schwager, C., Hentze, S., Ansorge, W., Hentze, M. W., and Muckenthaler, M. (2002). Comparison of fluorescent tag DNA labeling methods used for expression analysis by DNA microarrays. *Biotechniques*, **33**, 620–628, 630.

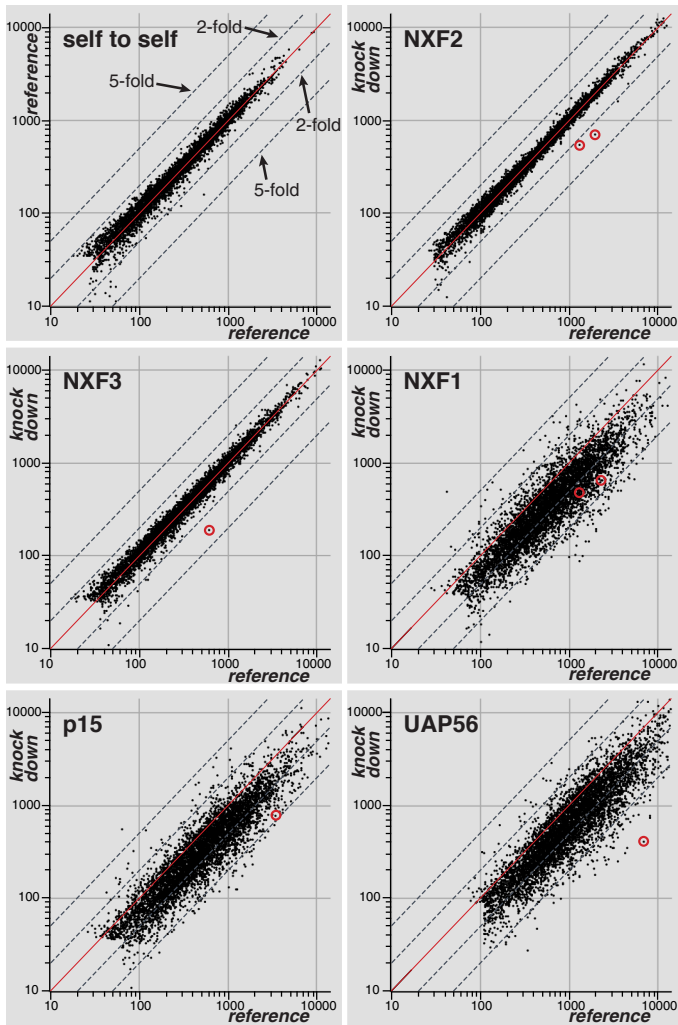
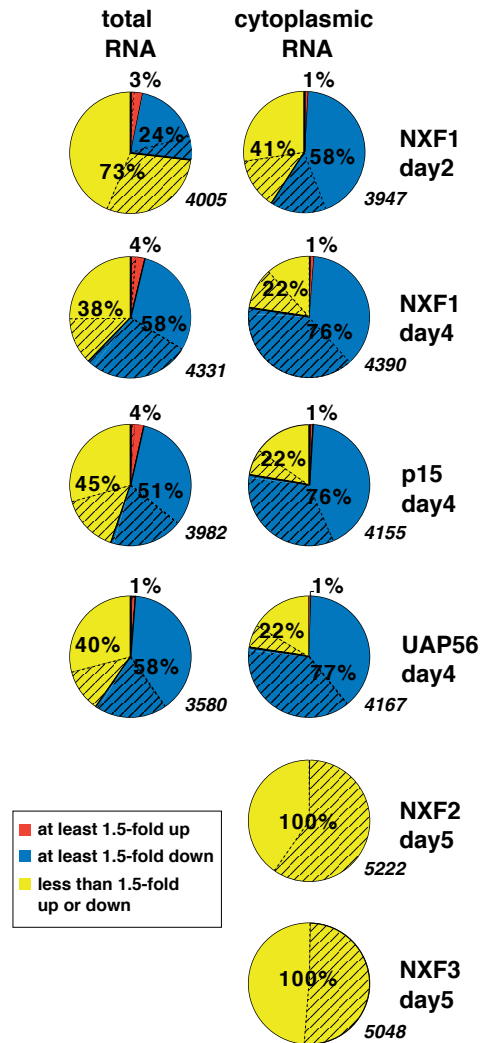
A**B**

Figure 1. Herold et al.

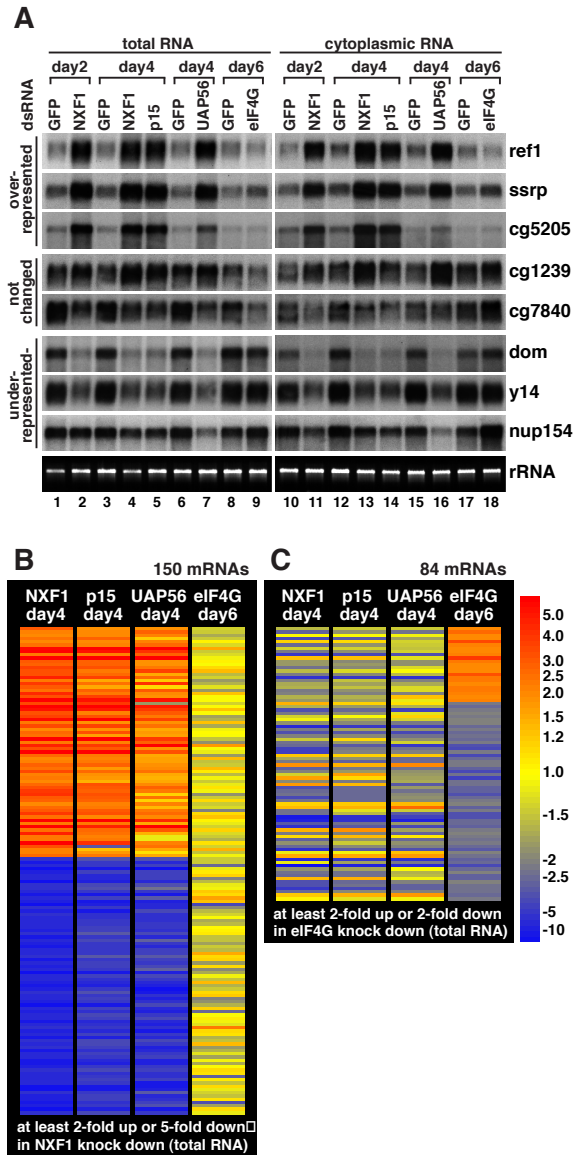
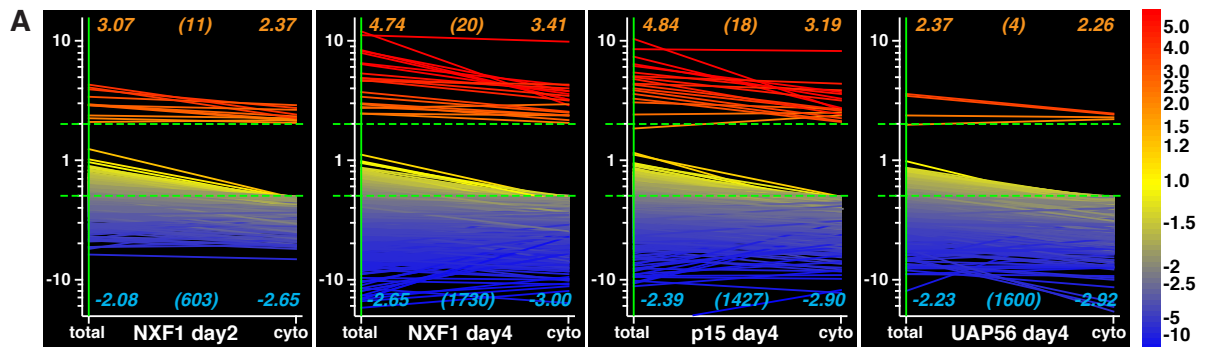
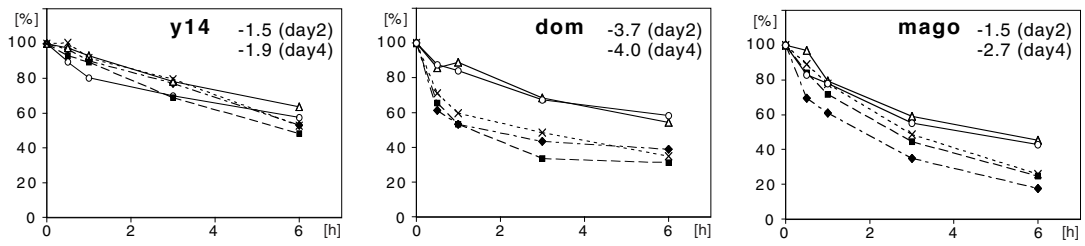


Figure 2. Herold et al.



B underrepresented mRNAs



C mRNAs with unchanged levels

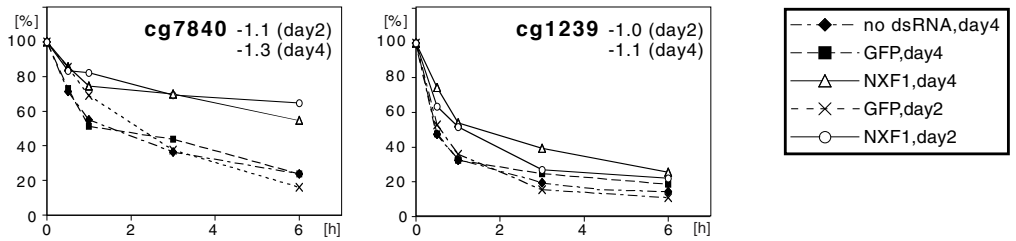
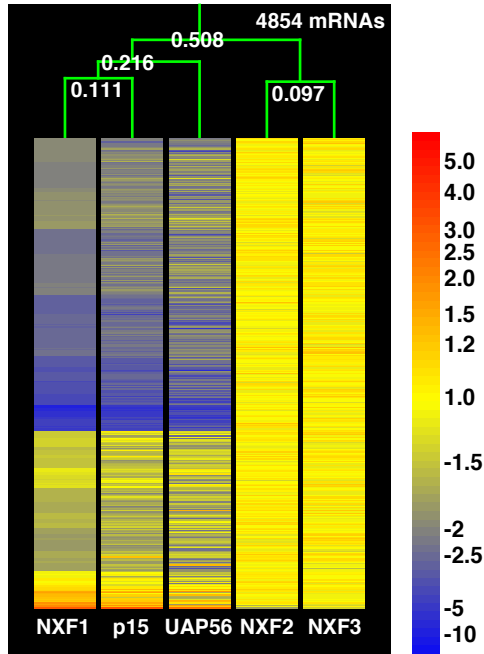
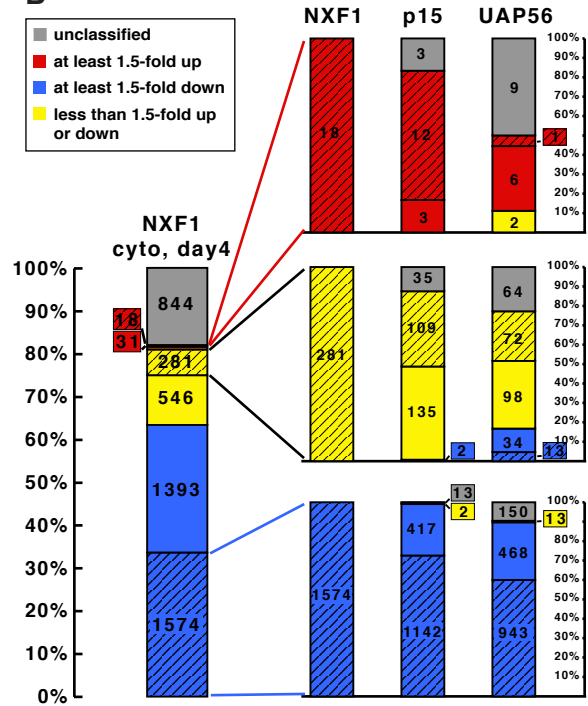


Figure 3. Herold et al.

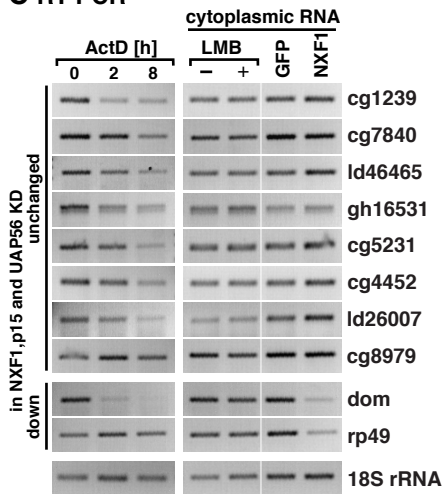
A



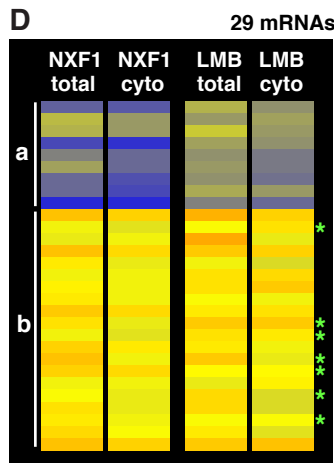
B



C RT-PCR



D



E

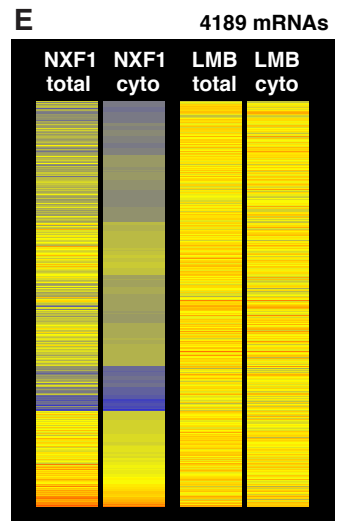
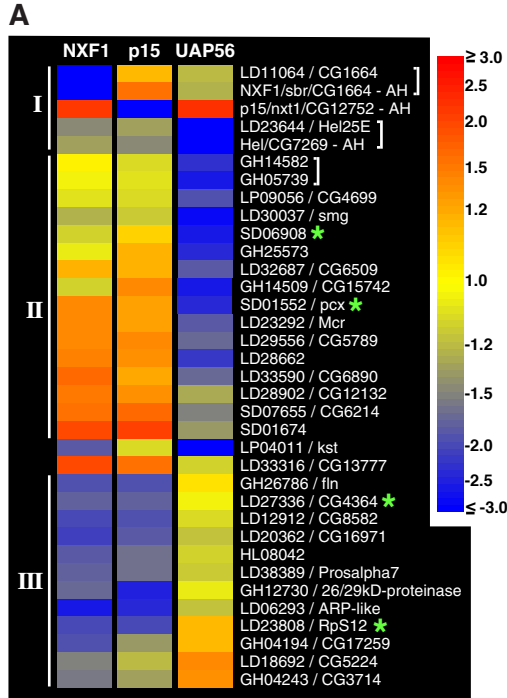


Figure 4. Herold et al.



B Northern blot

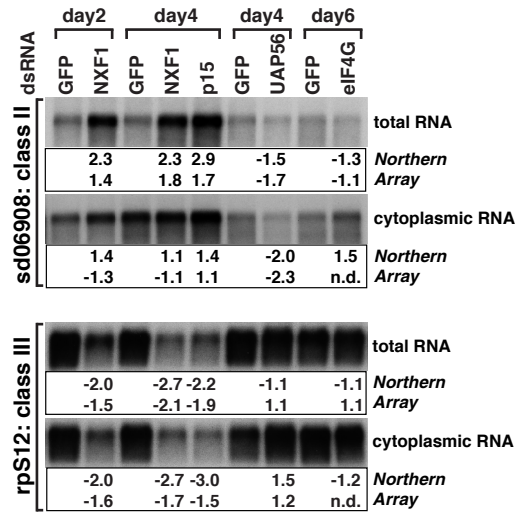
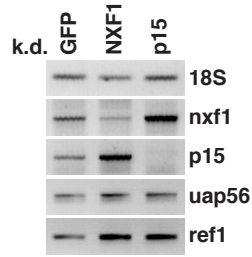


Figure 5. Herold et al.

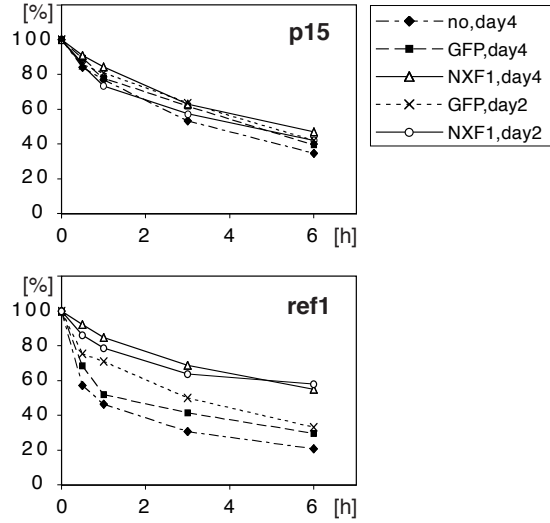
A Array

| k.d. | NXF1 | NXF1 | p15 | UAP56 |
|-------|------|------|------|-------|
| mRNA | day2 | day4 | day4 | day4 |
| nxf1 | -1.4 | -2.5 | 1.8 | 1.1 |
| p15 | 2.7 | 3.1 | -3.0 | 2.4 |
| uap56 | 1.9 | -1.2 | -1.2 | -6.1 |
| ref1 | 2.9 | 2.2 | 2.3 | 2.0 |

B RT-PCR



C mRNA stability



D In situ hybridization

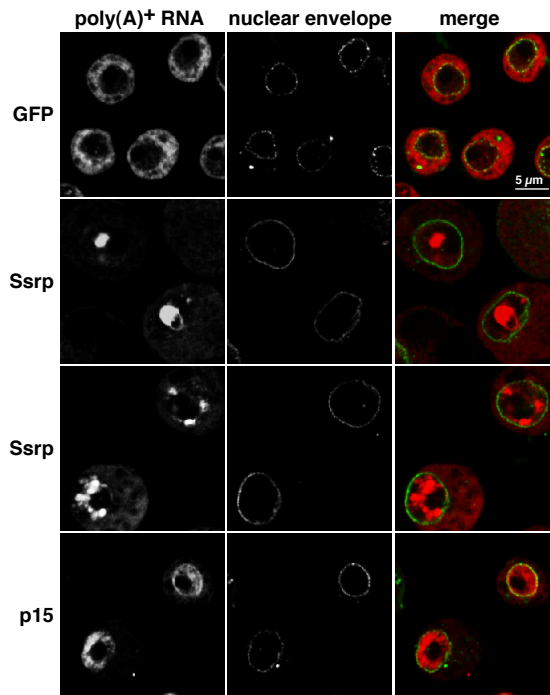
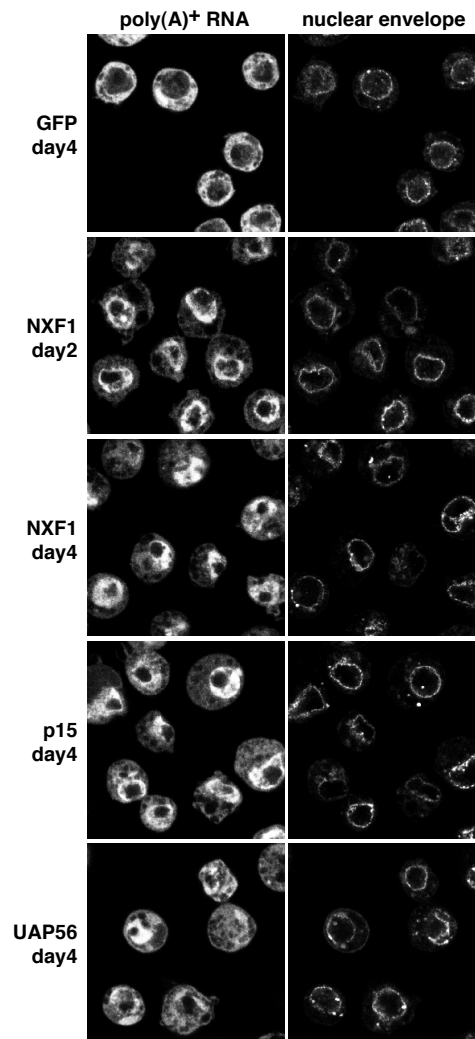
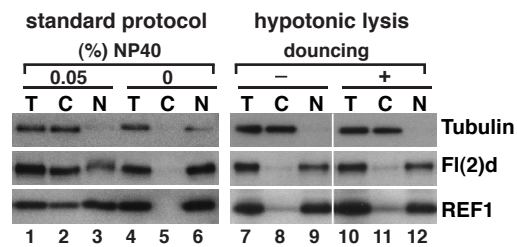


Figure 6. Herold et al.

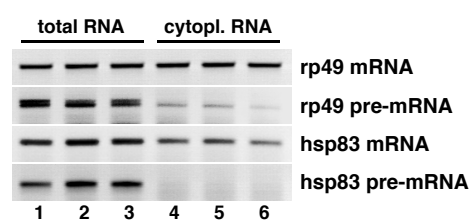


Supplemental Figure 1. Herold et al.

A Western blot

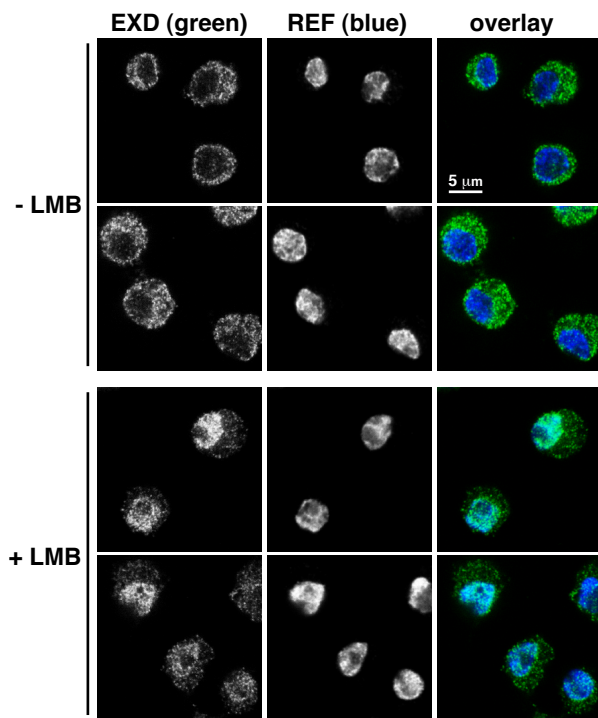


B RT-PCR

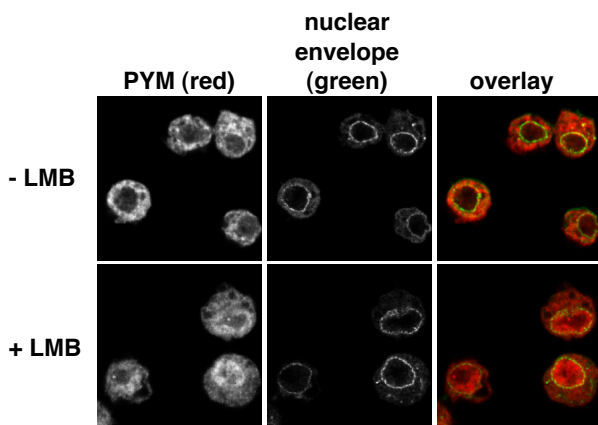
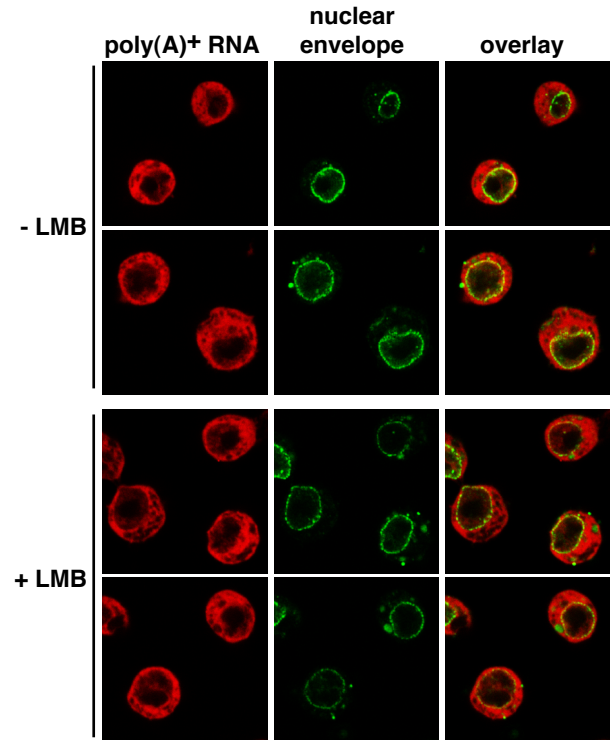


Supplemental Figure 2. Herold et al.

A Immunofluorescence



B *In situ* hybridization



Supplemental Figure 3.
Herold et al.

Supplemental Table I. mRNAs not affected by the knockdown of export factors.

mRNAs that are less than 1.2-fold over- or underrepresented in all 8 measurements with cytoplasmic samples isolated from NXF1 (day 2 and 4), p15 and UAP56 (day 4) knockdowns and less than 1.5-fold changed in total samples. The expression levels of these mRNAs in total and cytoplasmic samples isolated from LMB treated cells (12h) are also indicated. Values are averages of 2 measurements performed with 2 independent samples for each export factor. The mRNAs tested by Northern blot (Fig. 2) are marked with a star. Short-lived mRNAs (as tested by RT-PCR, Fig. 4C) are marked in gray. The genes were annotated according to Flybase (<http://flybase.bio.indiana.edu>).

| Gene Identifier | Gene name, Synonyms | Chromosome Arm | Cytogenetic map | Annotation | | | Microarray data (normalized fold changes, cytoplasmic samples) | | | | | Microarray data (normalized fold changes, total samples) | | | | | |
|------------------------|---|----------------|-----------------|--|--|-----------------------------|---|-----------|-----------|----------|------------|--|-----------|-----------|----------|------------|-------|
| | | | | Molecular function | Biological process | Cellular component | Protein domains | NXF1 day2 | NXF1 day4 | p15 day4 | UAP56 day4 | LMB | NXF1 day2 | NXF1 day4 | p15 day4 | UAP56 day4 | LMB |
| GH04473 / CG12955 | CG12955 | 2R | 51 E7 | | | | Kazal-type serine protease inhibitor family, Ovomuroid/PCI-1 like inhibitors | 1.15 | 1.01 | 1.02 | 1.10 | 1.15 | 1.32 | 1.09 | 1.08 | 1.26 | 1.50 |
| GH16531 | | | 95C2-D5 | | | | | -1.12 | -1.04 | -1.15 | -1.03 | 1.07 | -1.06 | -1.02 | -1.10 | -1.10 | -1.02 |
| GH07689 / CG4439 | CG4439 | 2R | 53C6 | leucyl aminopeptidase | | | Cytosol aminopeptidase, Leucine aminopeptidase, N-terminal domain, Zn-dependent exopeptidases | -1.05 | -1.21 | 1.01 | -1.10 | -1.27 | -1.09 | -1.34 | -1.26 | -1.23 | 1.46 |
| GH01278 / CG8979 | CG8979 | 2R | 48D5 | proteasome inhibitor | | | | 1.11 | -1.18 | -1.07 | -1.11 | 1.14 | 1.31 | -1.10 | 1.02 | -1.01 | 1.23 |
| GH13458 / Ela | Elastin-like, CG7021 | 3R | 96A22 | | | | | -1.10 | -1.03 | -1.02 | 1.02 | -1.17 | 1.03 | 1.01 | 1.11 | -1.03 | -1.07 |
| GH10531 / nAcRbeta-64B | nicotinic Acetylcholine Receptor beta 64B | 3L | 64B6 | nicotinic acetylcholine-activated cation-selective channel | Neurotransmitter-gated ion-channel, Nicotinic acetylcholine receptor details | | | -1.07 | 1.03 | -1.10 | -1.05 | 1.09 | -1.08 | -1.01 | -1.11 | -1.05 | 1.05 |
| GH28577 / igl | igloo, CG18285 | 2R | 51E3-5 | calmodulin binding | | | P-loop containing nucleotide triphosphate hydrolases | -1.07 | -1.14 | -1.04 | -1.08 | 1.24 | 1.00 | -1.14 | -1.02 | -1.06 | 1.05 |
| GH26186 / timp | tissue inhibitor of metalloproteases | 3R | 85F16 | metalloendopeptidase inhibitor | | extracellular | Tissue inhibitor of metalloproteinases, TIMP | -1.05 | -1.15 | 1.08 | 1.02 | -1.09 | 1.04 | 1.00 | -1.13 | -1.11 | -1.09 |
| LD24434 / CG10318 | dNC2, Drap1 | 2R | 57F7 | general transcriptional repressor | negative regulation of transcriptional pre-initiation complex | negative cofactor 2 complex | Histone-fold/TFIID-TAF/NF-Y domain | 1.10 | 1.01 | -1.05 | 1.09 | 1.08 | 1.24 | -1.03 | 1.01 | 1.04 | 1.03 |
| LD21662 / CG4452 | CG4452 | 3L | 67A | | | | Cysteine-rich domain | -1.08 | 1.01 | -1.06 | -1.16 | 1.24 | 1.08 | 1.12 | 1.13 | 1.11 | 1.19 |
| LD35060 / CG7840 (*) | CG7840 | 2L | 28F3 | 3-oxo-5-alpha-steroid 4-dehydrogenase | | | | -1.13 | -1.13 | -1.03 | 1.02 | 1.02 | -1.07 | -1.28 | -1.13 | 1.01 | 1.07 |
| LD26258 / CG9972 | CG9972 | 3L | 63A1 | | | | | 1.03 | -1.08 | -1.07 | 1.07 | -1.08 | 1.13 | -1.04 | -1.10 | -1.01 | -1.05 |
| LD26007 | meso18E | X | 18 E 3 | | | | Homeodomain-like | -1.06 | 1.12 | 1.04 | -1.02 | -1.09 | 1.25 | 1.26 | 1.35 | -1.01 | 1.22 |
| LD24887 / CG5231 | Lipoic acid synthase, Las | 3L | 77B6 | lipoic acid synthase | lipoic acid biosynthesis | mitochondrion | Lipoate synthase, Ribulose-phosphate binding barrel | 1.10 | 1.13 | -1.08 | -1.11 | -1.02 | 1.15 | 1.35 | 1.12 | -1.09 | -1.00 |
| LD48030 / CG12686 | CG12686 | X | 4C5 | | | | | -1.06 | -1.12 | -1.17 | -1.08 | 1.01 | -1.05 | -1.12 | 1.00 | -1.09 | -1.12 |
| LP01332 / CG1239 (*) | CG1239 | 3R | 83C1 | polynucleotide adenyltransferase | | | SAM (and some other nucleotide) binding motif, Generic methyl-transferase, S-adenosyl-L-methionine-dependent methyltransferases | -1.08 | -1.04 | -1.07 | -1.01 | -1.26 | -1.02 | -1.13 | -1.03 | -1.10 | 1.09 |
| LD46483 / CG9418 | BEST:LD07122 | 2R | 57C4 | DNA binding | DNA packaging | nucleus | HMG1/2 (high mobility group) box, HMG-box | -1.09 | 1.00 | -1.02 | -1.02 | -1.18 | 1.06 | 1.21 | 1.07 | 1.04 | 1.08 |
| LD46465 | | 2R | 59C3 | | | | Zinc finger, C2H2 type, Ribulose-phosphate binding barrel | -1.07 | 1.03 | -1.18 | -1.07 | -1.04 | 1.03 | -1.11 | -1.11 | -1.19 | -1.05 |
| LP05865 / CG5656 | CG5656 | 3L | 78C8 | alkaline phosphatase lysophosphatidate acyltransferase | | | Alkaline phosphatase family, Phosphatase/sulfatase | -1.01 | -1.12 | -1.11 | 1.03 | -1.21 | 1.10 | -1.16 | -1.15 | -1.04 | -1.02 |
| LD39624 / CG3209 | CG3209 | 2R | 60B8 | | | | Phospholipid and glycerol acyltransferase | 1.16 | -1.15 | 1.03 | -1.04 | 1.29 | 1.31 | -1.21 | -1.02 | 1.11 | 1.24 |

Supplemental Table II: mRNAs that are at least 1.5-fold over- or underrepresented in measurements performed with 2 independent total or cytoplasmic samples isolated from LMB-treated cells.

The average expression levels of these mRNAs in samples isolated from NXF1 (day 2 and 4), p15 (day 4) and UAP56 (day 4) knockdowns are also indicated.

The orange color indicates mRNAs that were at least 1.5-fold overrepresented in two independent total or cytoplasmic samples isolated from LMB-treated cells, respectively.

The blue color indicates mRNAs that were at least 1.5-fold underrepresented. #DIV/0! indicates that in at least 1 of the 2 respective measurements, no data were obtained (bad spot).

| Gene Identifier | LMB, total | LMB, cyto | NXF1, day2, total | NXF1, day2, cyto | NXF1, day4, total | NXF1, day4, cyto | p15, day4, total | p15, day4, cyto | UAP56, day4, total | UAP56, day4, cyto |
|-------------------------|------------|-----------|-------------------|------------------|-------------------|------------------|------------------|-----------------|--------------------|-------------------|
| GH28550 / CG11347 | 3.49 | 3.76 | 3.96 | 2.84 | 11.31 | 9.87 | 8.74 | 8.23 | 3.88 | 2.73 |
| LD08641 / CG2991 | 1.83 | 2.02 | -1.04 | -1.26 | 1.24 | -1.45 | 1.04 | -1.55 | -1.02 | -1.43 |
| LD09551 | 1.71 | 1.51 | -1.47 | -1.65 | -1.97 | -2.40 | -1.69 | -2.44 | -1.86 | -2.52 |
| LD15403 / nla | 1.83 | 1.03 | 1.19 | -1.27 | 1.10 | -1.12 | 1.23 | -1.10 | 1.03 | -1.23 |
| GH26789 / CG9674 | 2.24 | 2.20 | 1.08 | -1.62 | -1.81 | -2.43 | -2.05 | -2.67 | -2.50 | -3.27 |
| GH27226 | 1.68 | -1.30 | #DIV/0! | #DIV/0! | -1.16 | -1.55 | -1.29 | -1.01 | #DIV/0! | #DIV/0! |
| GH23529 / CG6942 | 4.54 | 3.27 | -1.34 | #DIV/0! | -1.28 | -1.27 | -1.40 | -1.46 | -1.26 | -1.43 |
| GH26763 | 1.70 | 1.67 | -2.44 | -3.29 | -2.64 | -2.79 | -2.13 | -2.50 | -1.53 | -1.99 |
| GM14009 / bgm | 3.56 | 3.28 | -1.44 | -1.80 | -2.75 | -4.24 | -3.07 | -4.65 | -1.61 | -2.08 |
| GM10015 / CG10359 | 1.72 | #DIV/0! | -1.17 | -1.33 | -1.29 | -1.69 | -1.01 | -1.52 | 1.08 | -1.72 |
| GM06507 / CG3074 | 1.75 | 1.27 | -1.01 | -1.40 | 1.62 | -1.74 | 1.66 | -1.43 | 1.49 | -1.29 |
| SD03066 / CG13868 | 1.73 | 2.40 | -1.17 | -1.71 | 1.88 | 1.03 | 1.65 | -1.32 | -1.04 | -1.52 |
| SD02860 | 1.62 | 1.16 | -4.13 | -2.22 | -14.93 | -4.26 | -10.75 | -3.97 | -5.00 | -3.05 |
| LD27718 / CG10120 | 1.74 | 1.69 | -1.46 | -1.90 | -2.25 | -2.76 | -2.00 | -2.79 | -2.32 | -3.53 |
| SD05726 / CG4427 | 1.91 | 2.11 | 1.41 | -1.14 | 1.84 | 1.38 | 1.65 | -1.12 | -1.14 | -1.21 |
| SD07613 / CG2064 | 2.18 | 1.42 | 2.57 | 1.59 | 2.75 | 1.57 | 2.77 | 1.49 | 2.83 | 2.06 |
| SD10012 / Mdr49 | 2.68 | 1.73 | 2.59 | -1.15 | 7.89 | 3.34 | 4.38 | 2.41 | 4.44 | 1.83 |
| SD09342 / CG7255 | 1.74 | 1.40 | -1.04 | -1.56 | 1.29 | 1.00 | 1.06 | -1.21 | -1.61 | -2.44 |
| SD09792 / CG13624 | 1.73 | 1.85 | 1.12 | -1.23 | 1.44 | -1.07 | 1.50 | 1.06 | -1.01 | -1.50 |
| SD01508 / CG8034 | 1.95 | 1.37 | -2.34 | -2.24 | -2.21 | -1.89 | -2.42 | -2.08 | -3.21 | -2.43 |
| LD36528 / CG3850 | 2.09 | 2.18 | 1.02 | -1.29 | -2.42 | -2.48 | -2.56 | -2.32 | -2.53 | -3.22 |
| LD37006 / CG18522 | 1.78 | 2.09 | 3.34 | 2.19 | 3.39 | 2.50 | 3.60 | 2.15 | 2.94 | 1.88 |
| LD35474 / CG5992 | 1.79 | 1.25 | -1.60 | -1.47 | -2.42 | -1.87 | -1.93 | -1.76 | -1.92 | -1.58 |
| LD35689 / CG10441 | 1.54 | 1.36 | 3.84 | 1.55 | 2.96 | 2.18 | 3.11 | 1.85 | 1.98 | -1.04 |
| GH18152 / Idgf1 | 2.29 | 2.42 | -2.49 | -2.08 | -2.98 | -1.54 | -2.21 | -1.70 | -1.58 | -1.42 |
| GH18014 / CG1600 | 2.08 | 2.13 | -1.78 | -1.99 | 1.24 | 1.02 | 1.22 | -1.20 | -1.56 | -1.84 |
| GH19047 / CG3829 | 1.65 | 1.46 | 2.73 | 1.31 | 2.54 | 1.62 | 3.30 | 1.98 | 1.50 | 1.27 |
| GH05668 / CG3364 | 1.71 | 1.21 | 1.03 | -1.22 | -1.01 | -1.32 | -1.19 | -1.18 | -1.12 | -1.35 |
| GH05949 / CG17294 | 1.66 | 1.66 | 1.24 | -1.09 | 1.11 | -1.23 | 1.11 | -1.34 | 1.55 | 1.22 |
| GH07466 / BcDNA:GH07466 | 1.77 | 1.32 | 3.12 | 1.77 | 5.31 | 3.79 | 5.43 | 3.60 | 4.99 | 2.66 |
| GH07066 / BcDNA:GH07066 | 1.89 | 1.25 | -1.25 | -1.43 | -1.67 | -1.98 | -1.58 | -2.04 | -1.61 | -2.08 |

| | | | | | | | | | | |
|-------------------------|-------|------|-------|-------|-------|-------|---------|-------|---------|---------|
| GH06306 | 1.86 | 1.49 | 2.60 | 1.65 | 2.95 | 2.25 | 2.65 | 1.97 | 2.46 | 1.89 |
| GH07269 / BcDNA:GH07269 | 1.67 | 2.14 | 1.11 | 1.04 | 1.04 | 1.38 | 1.07 | 1.16 | -1.10 | -1.08 |
| GH01635 / BcDNA:GH04929 | 2.02 | 2.31 | 1.43 | 1.07 | 1.45 | 1.16 | 1.38 | 1.05 | 1.66 | 1.29 |
| GH01208 / CG17292 | 1.67 | 1.76 | -2.64 | -3.25 | -3.09 | -3.68 | -2.82 | -3.85 | -3.76 | -4.78 |
| LP05177 / CG11880 | 1.60 | 1.64 | -1.39 | -1.39 | -1.92 | -1.43 | -1.62 | -1.48 | -1.59 | -1.57 |
| LP12257 | 1.91 | 1.70 | -3.19 | -2.36 | -2.86 | -2.24 | -3.07 | -2.55 | -4.15 | -3.09 |
| LD41905 / CG12505 | 1.82 | 2.34 | 1.89 | 1.06 | 8.53 | 3.20 | 6.43 | 3.31 | 3.69 | 2.47 |
| GH10517 / CG10433 | 1.68 | 1.61 | -1.65 | -1.82 | -1.44 | -1.39 | -1.34 | -1.54 | -1.42 | -1.31 |
| GH10582 / CG13848 | 1.67 | 1.55 | -1.59 | -2.07 | -2.10 | -2.65 | -1.62 | -2.34 | -1.86 | -2.38 |
| GH10708 / CG7314 | 2.61 | 2.21 | -1.15 | -1.46 | -1.55 | -1.94 | -1.43 | -2.00 | -1.70 | -1.95 |
| GH21160 / CG9026 | 1.61 | 1.60 | 2.02 | 1.12 | 1.46 | -1.17 | 1.79 | 1.28 | 2.07 | 1.43 |
| GH11824 / CG12162 | 1.76 | 1.02 | -1.25 | -1.33 | -1.71 | -1.22 | -1.58 | -1.71 | -1.51 | -1.44 |
| GH11385 / CG8913 | 1.54 | 1.69 | -2.29 | -1.94 | -3.62 | -2.60 | -2.88 | -2.59 | -2.43 | -2.35 |
| GH14433 / CG16987 | 2.28 | 1.71 | -1.14 | 1.12 | -2.19 | -1.20 | -2.40 | -1.55 | -3.98 | -2.20 |
| GH14412 | 1.61 | 1.70 | -1.03 | -1.12 | -1.12 | -1.25 | -1.12 | -1.22 | -1.19 | -1.57 |
| GH13883 / CG3168 | 2.22 | 1.81 | 1.01 | -1.34 | -1.39 | -1.23 | -1.21 | -1.35 | 1.06 | #DIV/0! |
| GM04645 / CG18578 | 1.78 | 1.65 | 2.10 | 1.48 | 2.86 | -1.19 | 2.34 | -1.17 | 2.31 | 1.72 |
| LD06393 / CG6084 | 1.57 | 1.62 | -1.85 | -2.49 | -3.42 | -4.46 | -2.99 | -4.22 | -2.24 | -4.61 |
| HL01062 / CG10960 | 1.47 | 1.74 | -1.51 | -1.47 | -2.94 | -2.32 | -1.72 | -1.75 | -1.95 | -1.82 |
| LD07143 / CG4294 | 1.46 | 1.81 | -1.38 | -1.93 | -1.55 | -2.65 | -1.52 | -2.28 | #DIV/0! | -2.25 |
| GH09258 / CG7069 | 1.36 | 1.61 | 1.19 | -1.07 | -1.38 | -1.52 | -1.24 | -1.31 | -1.54 | -1.78 |
| GH09112 / CG18066 | 1.20 | 1.56 | -1.18 | 1.02 | -1.08 | -1.23 | -1.23 | 1.01 | -1.00 | 1.03 |
| GM02347 / fu12 | 1.25 | 2.87 | -1.44 | -1.56 | -2.09 | -2.38 | -1.83 | -1.87 | -1.64 | -1.72 |
| GM01838 | -1.43 | 1.58 | -1.51 | -1.80 | -3.38 | -2.75 | -2.35 | -2.57 | -2.11 | -2.33 |
| LD01519 / CG11007 | -1.13 | 2.27 | -1.28 | -1.46 | -1.75 | -2.12 | -1.75 | -2.53 | -1.36 | -1.56 |
| SD02026 | 1.34 | 1.62 | 2.23 | 1.11 | 6.40 | 3.63 | 4.84 | 2.43 | 1.58 | -1.53 |
| SD07366 / CG6350 | 1.66 | 1.63 | 1.25 | -2.09 | -1.33 | -2.77 | -1.11 | -2.43 | -1.85 | -2.39 |
| SD06874 | 1.54 | 1.59 | 1.44 | 1.17 | -1.45 | -1.38 | -1.14 | -1.31 | -1.36 | -1.48 |
| LD22655 / CG2818 | 1.47 | 1.58 | -1.89 | -2.39 | -3.41 | -4.00 | -2.87 | -3.86 | -2.33 | -2.75 |
| LD22863 / rost | 1.40 | 1.73 | -2.30 | -2.03 | -5.00 | -4.44 | -3.65 | -3.77 | -2.62 | -2.92 |
| LD19437 | 1.31 | 1.81 | -1.41 | -1.67 | -1.87 | -1.87 | -1.49 | -1.72 | -1.40 | -2.03 |
| LD19266 / CG11804 | 1.42 | 1.65 | -2.86 | -3.04 | -2.15 | -2.21 | -1.63 | -2.04 | -2.56 | -4.07 |
| GH20337 / CG4233 | 1.46 | 1.71 | -2.40 | -2.87 | -4.67 | -5.03 | -3.44 | -4.42 | -2.93 | -3.42 |
| GH20987 / CtBP | 1.53 | 1.69 | 1.20 | -1.04 | 1.28 | 1.02 | 1.22 | -1.04 | 1.15 | -1.24 |
| GH02003 / CG10745 | 1.34 | 1.99 | -1.30 | -3.57 | -2.77 | -4.48 | -2.93 | -4.24 | -1.39 | -2.24 |
| LD40495 / CG5384 | 1.56 | 2.05 | 1.52 | -1.17 | 3.53 | 2.09 | 3.54 | 1.86 | 2.29 | 1.67 |
| LP03138 / Ald | 1.94 | 1.54 | -1.19 | -1.28 | -1.65 | -1.68 | #DIV/0! | -1.54 | -1.31 | -1.29 |
| LD44305 / BcDNA:GH04929 | 1.39 | 1.70 | 1.07 | -1.44 | 1.20 | -1.08 | 1.47 | -1.13 | 1.25 | -1.08 |
| GH13879 / CG9331 | 1.40 | 1.54 | 1.03 | -1.14 | -1.79 | -2.54 | -1.53 | -2.29 | -1.63 | -1.86 |
| GH12043 | 1.45 | 1.64 | 3.02 | 1.32 | 3.36 | 1.94 | 3.88 | 2.23 | 2.16 | 1.13 |

| | | | | | | | | | | |
|--------------------|-------|-------|---------|-------|---------|---------|---------|---------|---------|---------|
| LD46713 / CG7737 | 1.61 | 1.77 | #DIV/0! | -3.69 | -6.25 | -8.00 | -4.10 | -4.88 | -4.39 | -5.32 |
| GH13735 / CG3666 | 1.17 | 1.61 | -2.27 | -1.71 | -2.64 | -2.65 | -2.63 | -2.25 | -2.44 | -1.78 |
| GH18946 / Pxn | -1.69 | -1.57 | -2.40 | -3.09 | -13.70 | -10.75 | -9.01 | -7.14 | -8.55 | -10.53 |
| GM13306 / CG11143 | -1.70 | -1.61 | -1.39 | -1.73 | -3.91 | -3.76 | -2.36 | -2.75 | -2.51 | -2.70 |
| GH07967 / CG9338 | -1.52 | -1.70 | -2.38 | -3.57 | -6.37 | -6.85 | -4.35 | -6.41 | -3.24 | -4.29 |
| GH07925 / CG18168 | -2.09 | -2.43 | -6.17 | -7.04 | -12.05 | -15.87 | -10.53 | -13.33 | -8.47 | -11.63 |
| LD36052 / kls | -1.73 | -1.31 | -1.61 | -2.51 | -2.44 | -3.39 | -2.28 | -3.44 | -2.51 | -3.82 |
| SD08803 / Fs(2)Ket | -1.76 | -2.17 | -2.07 | -2.44 | -1.81 | -1.32 | -2.00 | -1.56 | -2.81 | -3.12 |
| SD09326 / CG11822 | -1.61 | -1.79 | -4.95 | -4.27 | -15.38 | -11.36 | -11.49 | -8.33 | -9.01 | -8.26 |
| GH06781 / CG15093 | -1.48 | -1.72 | -2.58 | -2.94 | #DIV/0! | #DIV/0! | #DIV/0! | -4.39 | #DIV/0! | #DIV/0! |
| LD13807 / CG3226 | -1.29 | -1.62 | -1.51 | -1.65 | -3.06 | -2.90 | -2.26 | #DIV/0! | -1.92 | -3.53 |
| LD43554 / CG5599 | -1.60 | -1.79 | -3.53 | -4.85 | -5.18 | -6.62 | -5.29 | -7.58 | -4.65 | -5.68 |
| LD21785 / CG5295 | -1.74 | -2.16 | -1.58 | -2.49 | -1.47 | -2.52 | -1.52 | -1.93 | -2.00 | -1.98 |
| GH11670 / CG4929 | -1.84 | -2.28 | -2.48 | -3.09 | -3.76 | -5.75 | -3.16 | -3.97 | -2.03 | -2.43 |

Supplemental Table III: mRNAs that are differently affected in NXF1, p15 and UAP56 knockdowns.

The values are averages of 2 measurements for each knockdown (cytoplasmic samples, day 4). The genes were annotated according to Flybase (<http://flybase.bio.indiana.edu>).

| Annotation | | | | | | | | Microarray data (normalized fold changes, cytoplasmic samples) | | |
|-----------------------|--|----------------|-----------------|--|---------------------------------------|---|--|--|-----------|-----------|
| Gene Identifier | Gene name, Synonyms | Chromosome Arm | Cytogenetic map | Molecular function | Biological process | Cellular component | Protein domains | NXF1, day4 | p15, day4 | Hel, day4 |
| Class I | | | | | | | | | | |
| LD11064 / CG1664 | sbr, nxfl | X | 9F7-8 | | poly(A)+ mRNA-nucleus export | nucleoplasm | RNI-like, NTF2-like | -3.03 | 1.13 | -1.22 |
| NXF1/sbr/CG1664 - AH | | | | | | | | -3.38 | 1.58 | -1.25 |
| p15/nxt1/CG12752 - AH | NTF2-related export protein 1 | 2R | 60A2 | | poly(A)+ mRNA-nucleus export | nucleus | Nuclear transport factor 2 (NTF2), NTF2-like | 2.23 | -4.78 | 2.31 |
| LD23644 / Hel25E | Helicase at 25E, Hel, CG7269 | 2L | 25 E2 | ATP dependent RNA helicase; RNA helicase | mRNA splicing | nucleus; spliceosome complex | DEAD/DEAH box helicase, Helicase C-terminal domain, P-loop containing nucleotide triphosphate hydrolases | -1.44 | -1.35 | -18.52 |
| Hel/CG7269 - AH | | | | | | | | -1.33 | -1.45 | -17.24 |
| Class II | | | | | | | | | | |
| GH14582 | Enhancer of Polycomb, CG7776 | 2R | 47F13-14 | | | | | 1.01 | -1.10 | -2.22 |
| GH05739 | | | | | | | | -1.03 | -1.10 | -2.60 |
| LP09056 / CG4699 | | 3R | 89A2 | | | | | -1.08 | -1.11 | -1.84 |
| LD30037 / smg | smaug, CG5263 | 3L | 66E4-5 | RNA binding; translation repressor | | | SAM/Pointed domain, SAM/Pointed domain | -1.27 | -1.21 | -2.77 |
| SD06908 | | | | | | | | -1.12 | 1.07 | -2.48 |
| GH25573 | | | | | | | | -1.07 | 1.19 | -2.25 |
| LD32687 / CG6509 | | 2L | 32F1 | | | | Guanylate kinase, PDZ domain (also known as DHR or GLGF), PDZ domain-like, PDZ domain-like | 1.18 | 1.17 | -1.75 |
| GH14509 / CG15742 | | X | 11 E9 | | | | | -1.13 | 1.41 | -2.56 |
| SD01552 / pcx | pecanex, CG3443 | X | 2E2-F1 | | | integral plasma membrane protein; plasma membrane | | 1.42 | 1.25 | -2.31 |
| LD23292 / Mcr | Macroglobulin complement-related, CG7586 | 2L | 28D3 | alpha-2 macroglobulin | | | Alpha-2-macroglobulin family, Alpha-2-macroglobulin family N-terminal region, Terpenoidcylases/Protein prenyltransferases, Alpha-macroglobulin receptor domain | 1.44 | 1.25 | -1.76 |
| LD29556 / CG5789 | | 3R | 96A2 | ATP-binding cassette (ABC) transporter; xenobiotic-transporting ATPase | | | ABC transporter transmembrane region, ABC transporter, AAA ATPase superfamily, P-loop containing nucleotide triphosphate hydrolases | 1.40 | 1.40 | -1.67 |
| LD28662 | poils aux pattes, pap, CG9936 | 3L | 78A1 | RNA polymerase II transcription mediator | transcription from Pol II promoter | mediator complex | | 1.46 | 1.40 | -2.11 |
| LD33590 / CG6890 | Tollo | 3L | 71B7 | transmembrane receptor | defense response; signal transduction | integral membrane protein; plasma membran | TIR domain, RNI-like, Toll/Interleukin receptor TIR domain | 1.70 | 1.22 | -1.66 |

| | | | | | | | | | | |
|-------------------|-------------------------|----|------|--------------------------------|--------------------------------------|-----------------|--|------|------|-------|
| LD28902 / CG12132 | e11.1 | | | | | | ARM repeat | 1.56 | 1.37 | -1.28 |
| SD07655 / CG6214 | | 2L | 33F2 | xenobiotic-transporting ATPase | | | ABC transporter transmembrane region, ABC transporter, AAA ATPase superfamily, P-loop containing nucleotide triphosphate hydrolases, P-loop containing nucleotide triphosphate hydrolases | 1.61 | 1.66 | -1.52 |
| SD01674 | kekkon-1, kek1, CG12283 | 2L | 33F4 | protein tyrosine phosphatase | protein amino acid dephosphorylation | plasma membrane | Immunoglobulin and major histocompatibility complex domain, Immunoglobulin C-2 type, Second domain of FERM, , Immunoglobulin, PDZ domain-like, PH domain-like, Outer arm dynein light chain 1, (Phosphotyrosine protein) phosphatases II, Ubiquitin-like | 2.03 | 2.08 | -1.38 |

| | | | | | | | | | | |
|-------------------|----------------|----|--------|--|---|--|--|-------|-------|-------|
| LP04011 / kst | karst, CG12008 | 3L | 63D2 | actin binding; microtubule binding; cytoskeletal protein binding | plasma membrane organization and biogenesis | apicolateral plasma membrane; spectrin | Spectrin repeat, Calponin-homology domain, CH-domain, SH3-domain, PH domain-like | -1.77 | -1.10 | -3.72 |
| LD33316 / CG13777 | milton | 2L | 27C6-7 | kinesin-associated mitochondrial adaptor | axon transport of mitochondrion | | | 2.03 | 1.62 | -1.12 |

Class III

| | | | | | | | | | | |
|------------------------------|-----------------------------------|----|--------|------------------------------------|----------------------------------|---|--|-------|-------|-------|
| GH26786 / fln | flightin, CG7445 | 3L | 76D4 | | | muscle fiber, striated muscle thick filament | | -1.90 | -1.91 | 1.00 |
| LD27336 / CG4364 | | 2L | 30C1 | | | | BRCT domain | -1.68 | -1.75 | -1.03 |
| LD12912 / CG8582 | Sh3 beta | 3L | 65F5 | | | | Copper/Zinc superoxide dismutase | -1.88 | -1.86 | -1.11 |
| LD20362 / CG16971 | | 3L | 61B2 | | | | | -1.96 | -1.74 | -1.20 |
| HL08042 | wings up A, wupA, CG7178 | X | 16F7 | tropomyosin binding; actin binding | muscle development; neurogenesis | | troponin complex | -1.78 | -1.59 | -1.12 |
| LD38389 / Prosalph7 | Proteasome alpha7 subunit, CG1519 | 2R | 46B7 | proteasome endopeptidase | | 20S core proteasome | Proteasome A-type subunit, Multispecific proteases of the proteasome | -1.69 | -1.62 | -1.16 |
| GH12730 / 26/29kD-proteinase | CG8947 | 3L | 70C | cathepsin K (thiol protease) | | | | -1.66 | -2.43 | -1.06 |
| LD06293 / ARP-like | CG7013 | 3R | 89B16 | | | extracellular | | -2.49 | -2.24 | -1.18 |
| LD23808 / RpS12 | CG11271 | 3L | 69F3 | structural constituent of ribosome | protein biosynthesis | cytosolic small ribosomal subunit (sensu Eukarya); ribosome | Ribosomal protein S12E, Ribosomal protein L7AE, L30e-like | -1.92 | -2.01 | 1.16 |
| GH04194 / CG17259 | | 2L | 23C2-3 | serine-tRNA ligase | seryl-tRNA aminoacylation | | Aminoacyl-transfer RNA synthetases class-II, tRNA synthetases, class-II (G, H, P and S), Seryl-tRNA synthetase, Seryl-tRNA synthetase N-terminal domain, A class II aminoacyl-tRNA synthetase N-domain, , Class II aaRS and biotin synthetases | -1.87 | -1.37 | 1.16 |
| LD18692 / CG5224 | | 2R | 55D1 | glutathione transferase | | | Glutathione S-transferases, C-terminal domain, Thioredoxin-like | -1.48 | -1.21 | 1.42 |
| GH04243 / CG3714 | | 2L | 24D6 | phosphoribosyltransferase | | | | -1.55 | -1.33 | 1.34 |

Supplemental Table IV: mRNAs that are at least 2-fold overrepresented in 7 of 8 measurements performed with total samples isolated from NXF1 (day 2 and 4), p15 (day 4) and UAP56 (day 4) knockdowns.

The mRNAs that have been tested for a possible role in nuclear mRNA export are marked in gray. The annotation is according to Flybase (<http://flybase.bio.indiana.edu>).

| Annotation | | | | | | | | Microarray data (normalized fold changes, average of 2 measurements, total samples) | | | |
|-------------------------|--|----------------|------------------|--|---|---|--|---|------------|-----------|-------------|
| Gene Identifier | Gene name, Synonyms | Chromosome Arm | Cytogenetic map | Molecular function | Biological process | Cellular component | Protein domains | NXF1, day2 | NXF1, day4 | p15, day4 | UAP56, day4 |
| GH18819 / CG1898 | HBS1 | 3L | 62B7 | translation release factor | translational termination | cytosol | GTP-binding elongation factor | 2.24 | 2.10 | 2.13 | 1.77 |
| GH06306 | ref(2)P, refractory to sigma, CG10360 | 2L | 37F1-37F1 (37D4) | | viral infectious cycle | nucleus | | 2.60 | 2.95 | 2.65 | 2.46 |
| SD09786 / CG15612 | CG15612 | 2R | 53F10-11 | | | | Dbl domain (dbl/cdc24 rhoGEF family), DBL homology domain, PLP-dependent transferases | 2.53 | 3.72 | 4.56 | 3.56 |
| GH18520 / CG5205 | CG5205 | 3R | 88F4 | helicase; RNA helicase | mRNA splicing | small nuclear ribonucleoprotein complex; snRNP U5 | DEAD/DEAH box helicase, Helicase C-terminal domain, P-loop containing nucleotide triphosphate hydrolases | 4.05 | 4.69 | 4.38 | 2.38 |
| GH08776 / CG7163 | CG7163 | 3L | 66C11 | | | | Zinc finger, C2H2 type, PAP/25A core domain, Nucleotidyltransferases | 4.40 | 6.51 | 6.16 | 3.27 |
| GH05885 / CG7163 | | | | | | | | 3.66 | 4.94 | 5.03 | 2.88 |
| LD41905 / CG12505 | CG12505 | 2R | 50F6 | | | | Zn-finger CCHC type | 1.89 | 8.53 | 6.43 | 3.69 |
| SD10157 / CG10076 | spire (spir) | 2L | 38C2 | actin binding | eggshell formation; pole plasm assembly | | FYVE/PHD zinc finger | 2.49 | 2.60 | 2.61 | 1.84 |
| SD06504 / Ssrp | Structure specific recognition protein | 2R | 60A2 | single-stranded DNA binding; single-stranded RNA binding; DNA secondary structure binding; | | nucleolus | HMG1/2 (high mobility group) box, Structure-specific recognition protein, HMG-box | 2.12 | 2.44 | 2.45 | 2.17 |
| DmAly/CG1101 - AH | Aly, REF1 | 3R | 84B4 | RNA binding; transcription co-activator | | | RNA-binding region RNP-1 (RNA recognition motif), RNA-binding domain, RBD | 2.94 | 2.23 | 2.28 | 2.00 |
| GH21463 / CG7388 | CG7388 | | 66A11 | | | | Kazal-type serine protease inhibitor family, ATP-dependent protease La (LON) domain, RING finger domain, C3HC4 | 2.83 | 2.40 | 2.38 | 2.26 |
| GH07816 / CG8678 | CG8678 | 2L | 39A1 | | | | Trp-Asp repeat (WD-repeat) | 3.42 | 5.09 | 4.48 | 3.45 |
| GH07466 / BcDNA:GH07466 | slamdance, sda | 3R | 97D3-4 | membrane alanyl aminopeptidase | | | Membrane alanyl dipeptidase, family M1 | 3.12 | 5.31 | 5.43 | 4.99 |
| GH24286 / CG9663 | CG9663 | 2L | | ATP-binding cassette (ABC) transporter | | | ABC transporter, AAA ATPase superfamily, P-loop containing nucleotide triphosphate hydrolases | 3.10 | 4.65 | 5.02 | 3.01 |

| | | | | | | | | | | | |
|--|-------------------------|----|--------|---|---------------|----------------------------------|--|------|-------|-------|------|
| LD17001 / CG11897 | CG11897 | 3R | 98F6 | multidrug transporter; xenobiotic-transporting ATPase | | | Nitrogenases component I a and b subunits, ABC transporter transmembrane region, ABC transporter, AAA ATPase superfamily, P-loop containing nucleotide triphosphate hydrolases | 3.68 | 8.55 | 7.44 | 2.98 |
| SD10012 / Mdr49 | Multidrug resistance 49 | 2R | 49E3-4 | multidrug transporter; xenobiotic-transporting ATPase | | integral plasma membrane protein | ABC transporter transmembrane region, ABC transporter, AAA ATPase superfamily, P-loop containing nucleotide triphosphate hydrolases | 2.59 | 7.89 | 4.38 | 4.44 |
| LD35689 / CG10441 | CG10441 | | 37B1 | xenobiotic-transporting ATPase | | | ABC transporter transmembrane region, ABC transporter, AAA ATPase superfamily, P-loop containing nucleotide triphosphate hydrolases | 3.84 | 2.96 | 3.11 | 1.98 |
| GH01205 / BcDNA:GH11322 GH11322 / BcDNA:GH11322 | BcDNA:GH11322 | 2L | 24 E1 | | cell adhesion | | Immunoglobulin and major histocompatibility complex domain, Immunoglobulin C-2 type, Immunoglobulin-like, Immunoglobulin, Fibronectin type III | 6.09 | 12.85 | 10.83 | 7.69 |
| | CG18522 | 3R | 88F5 | | | | 2Fe-2S Ferredoxin, Aldehyde oxidase and xanthine dehydrogenase, C terminus, Ferredoxin, [2Fe-2S] binding domain, CO dehydrogenase ISP C-domain like, 2Fe-2S ferredoxin-like, CO dehydrogenase molybdoprotein N-domain-like, CO dehydrogenase flavoprotein C-terminal domain-like, Molybdemum cofactor-binding domain, FAD-binding domain | 3.34 | 3.39 | 3.60 | 2.94 |
| SD07613 / CG2064 | CG2064 | 2R | 43 E10 | | | | Short-chain dehydrogenase/reductase (SDR) superfamily, Glucose/ribitol dehydrogenase, Insect alcohol dehydrogenase family, 2,3-dihydro-2,3-dihydroxybenzoate dehydrogenase (EntA), NAD(P)-binding Rossmann-fold domains | 2.57 | 2.75 | 2.77 | 2.83 |
| HL01076 / BcDNA:GH04929 | CG3132 | 3R | 87A3-4 | beta-galactosidase | | lysosome | Glycosyl hydrolases family 35, Galactose-binding domain-like, (Trans)glycosidases | 4.85 | 4.20 | 3.21 | 4.71 |
| GH22460 / Cyp28d1 | CG10833 | 2L | 25C8 | cytochrome P450 | | membrane; microsome | Cytochrome P450 enzyme, E-class P450 group I, E-class P450 group II, E-class P450 group IV, Cytochrome P450 | 2.91 | 2.37 | 2.50 | 2.51 |
| GH28550 / CG11347 | CG11347 | 3L | 64B6 | | | | | 3.96 | 11.31 | 8.74 | 3.88 |
| SD02026 | | | | | | | | 2.23 | 6.40 | 4.84 | 1.58 |
| GH12043 | CG30389 | 2R | 57C4-6 | | | | | 3.02 | 3.36 | 3.88 | 2.16 |
| GH14673 / CG10675 | CG10675 | 3R | 96C8 | | | | | 2.21 | 2.11 | 2.09 | 2.37 |

2.3 Functional analysis of TAP/NXF1 domains

2.3.1 Paper 5:

Overexpression of TAP/p15 heterodimers bypasses nuclear retention and stimulates nuclear mRNA export

Braun, I.C., Herold, A., Rode, M., Conti, E., and Izaurralde, E. (2001) *J Biol Chem* **276**, 20536-20543.

Context

The human TAP protein was first identified as the cellular factor exporting RNAs bearing the CTE of simian type D retroviruses, and is also implicated in the export of cellular mRNAs (Gruter *et al.*, 1998). The functional and structural domains of TAP as well as the partners interacting with TAP have been characterized in detail *in vitro* (Bachi *et al.*, 2000; Braun *et al.*, 1999; Katahira *et al.*, 1999). Previous *in vivo* studies have focused on the role of TAP domains in the export of CTE-containing RNAs (Bachi *et al.*, 2000; Braun *et al.*, 1999; Kang *et al.*, 2000; Kang and Cullen, 1999; Liker *et al.*, 2000). In this study, the role of the different TAP domains in the nuclear export of cellular mRNAs was investigated *in vivo*.

Summary of results and conclusions

In this manuscript, the reporter assay for mRNA export in cultured cells mentioned previously (Herold *et al.*, 2000) was used in two versions to analyze the importance of individual TAP domains *in vivo*. Both versions of the assay make use of a CAT reporter whose coding sequence is placed into an inefficiently spliced intron. Since the unspliced pre-mRNA is normally retained in the nucleus, only trace levels of CAT activity can be measured. As shown previously, overexpression of TAP:p15 heterodimers bypasses nuclear retention and promotes export of the reporter pre-mRNA leading to a significant increase in CAT activity (Herold *et al.*, 2000). The importance of individual TAP domains was analyzed by generating TAP variants lacking either the N-terminus (TAP derivative: 61-619), the RNA-binding domain (Δ RBD), the leucine-rich repeat domain (Δ LRR), the NTF2-like domain (Δ NTF2) or the UBA-like domain (Δ UBA). These molecules were then coexpressed with p15 and assayed for their ability to promote export of the reporter RNA. In the first version of the assay, the recognition and export of the reporter RNA by TAP depends on the intrinsic ability of TAP to recognize RNAs. The removal of the N-terminus or the UBA-like domain resulted in reduced export activity (*ca.* 15% of wild-type) while the deletion of the LRR or the NTF2-like domain abolished the export activity of TAP. We also generated TAP derivatives with point mutations in the LRR and UBA-like domains which caused phenotypes comparable to the ones seen when the entire domains were

deleted. Deletion of the RBD resulted in a moderate reduction of the export activity (to *ca.* 40%). In the second version of the export assay the TAP:p15 heterodimers were tethered directly to the reporter RNA *via* a Rev/RRE system making the stimulation of RNA export by the TAP mutants independent of their intrinsic ability to recognize the reporter RNA. In this assay the RBD becomes completely dispensable for export, while the LRR, the NTF2-like and the UBA-like domains still play a critical role. As the effects observed when deleting the N-terminus, the RBD or the LRR domain are less severe than in the first version of the assay, these domains seem to be crucial for cargo binding. Importantly, the export stimulation by wild-type TAP was similar independently of whether the tethering of the heterodimer was achieved through TAP or p15.

The role of the different TAP domains in mRNA export was further confirmed with an independent approach. *Xenopus* oocytes were coinjected with recombinant TAP derivatives and RNAs, and the amount of the different RNAs in cytoplasmic and nuclear fractions was determined. Similar to the transfection assay, the injection of TAP:p15 heterodimers stimulated the nuclear export of mRNAs which were otherwise inefficiently exported. When the different TAP mutants were tested, the results of the cell culture assays were essentially confirmed. Deletion of the RBD had only a moderate effect while the deletion of the N-terminus, the LRR, NTF2-like or UBA-like domain strongly reduced or abolished the export activity of TAP.

Altogether, the data presented in this study indicate that the formation of TAP:p15 heterodimers is required for TAP-mediated export: mutant TAP molecules (Δ NTF2) which cannot bind p15 do not exhibit export activity in any of the assays. Moreover, high levels of export activity can only be achieved if p15 is coexpressed with TAP. Finally, TAP can export RNAs efficiently when tethered to the RNA *via* its heterodimeric partner p15. Apart from the NTF2-like domain, the N-terminus, the UBA-like and LRR domain are also important for TAP function, the LRR domain being absolutely essential.

Contribution

I constructed most of the RevM10-fusions of TAP and TAP mutants for the tethering assay including design and construction the parental RevM10 vector (Figure 3). I also established and optimized the tethering assay in our lab. My contribution to this paper is about 15%.

Overexpression of TAP/p15 Heterodimers Bypasses Nuclear Retention and Stimulates Nuclear mRNA Export*

Received for publication, January 16, 2001, and in revised form, March 1, 2001
Published, JBC Papers in Press, March 19, 2001, DOI 10.1074/jbc.M100400200

Isabelle C. Braun, Andrea Herold, Michaela Rode, Elena Conti, and Elisa Izaurralde‡

From the European Molecular Biology Laboratory (EMBL), Meyerhofstrasse 1, D-69117 Heidelberg, Germany

Human TAP and its yeast orthologue Mex67p are members of the multigene family of NXF proteins. A conserved feature of NXFs is a leucine-rich repeat domain (LRR) followed by a region related to the nuclear transport factor 2 (the NTF2-like domain). The NTF2-like domain of metazoan NXFs heterodimerizes with a protein known as p15 or NXT. A C-terminal region related to ubiquitin-associated domains (the UBA-like domain) is present in most, but not all NXF proteins. *Saccharomyces cerevisiae* Mex67p and *Caenorhabditis elegans* NXF1 are essential for the export of messenger RNA from the nucleus. Human TAP mediates the export of simian type D retroviral RNAs bearing the constitutive transport element, but the precise role of TAP and p15 in mRNA nuclear export has not yet been established. Here we show that overexpression of TAP/p15 heterodimers bypasses nuclear retention and stimulates the export of mRNAs that are otherwise exported inefficiently. This stimulation of mRNA export is strongly reduced by removing the UBA-like domain of TAP and abolished by deleting the LRR domain or the NTF2-like domain. Similar results are obtained when TAP/p15 heterodimers are directly tethered to the RNA export cargo. Our data indicate that formation of TAP/p15 heterodimers is required for TAP-mediated export of mRNA and show that the LRR domain of TAP plays an essential role in this process.

Metazoan TAP and its yeast orthologue Mex67p are members of an evolutionarily conserved protein family, the NXF family, implicated in the export of messenger RNA from the nucleus (1). Mex67p, the *Saccharomyces cerevisiae* NXF homologue, and the *Caenorhabditis elegans* protein NXF1 are essential for the export of bulk polyadenylated RNAs to the cytoplasm (2, 3), whereas human TAP (also called Hs NXF1) has been directly implicated in the export of simian type D retroviral RNAs bearing the constitutive transport element (CTE)¹ (4). In *Xenopus laevis* oocytes, titration of TAP with an excess of CTE RNA prevents cellular mRNAs from exiting the nucleus

(4–6), strongly suggesting a role for TAP in mRNA nuclear export, but direct evidence has so far remained elusive.

Members of the NXF family of proteins have a conserved modular domain organization consisting of a non-canonical RNP-type RNA-binding domain (RBD), a leucine-rich repeat (LRR) domain, a middle region showing significant sequence similarity to nuclear transport factor 2 (the NTF2-like domain) and a C-terminal ubiquitin-associated (UBA)-like domain (Fig. 1 and Refs. 1, 7, and 8). The LRR and the NTF2-like domains are the most conserved features of NXF proteins, whereas the RBD and the C-terminal UBA-like domain are not always present in NXF proteins (1, 3).

The N-terminal half of TAP includes the LRR domain, the RBD, and a less conserved region upstream of the RBD (fragment 1–372, Fig. 1). This protein fragment exhibits general RNA binding affinity and mediates binding to several mRNA-associated proteins such as E1B-AP5 (9) and members of the Yra1p/REF protein family (10, 11). Furthermore, the RBD of TAP is required *in cis* to the LRR domain for specific binding to the CTE RNA (7). Hence, the RBD and the LRR domain are essential for TAP-mediated export of CTE-containing cargoes (1, 7, 12, 13). Mutations within the LRR domains of TAP and Mex67p have been reported to affect cellular mRNA export (11, 12), but these mutations involve residues that have important structural roles and their substitution probably results in nonspecific structural aberrations.

The NTF2-like domain of metazoan NXFs mediates binding to a protein known as p15 or NXT. p15 is also related to NTF2 (8, 15, 16) but unlike NTF2, which forms homodimers, p15 heterodimerizes with the NTF2-like domain of NXF proteins (1, 8). The human genome encodes at least two p15 homologues, p15-1 and p15-2, and both interact with TAP (1). The NTF2-like domain also occurs in *Schizosaccharomyces pombe* and *S. cerevisiae* Mex67p, although there is no obvious p15 homologue encoded by the yeast genome (8, 15, 16). In *S. cerevisiae* Mex67p, this domain is implicated in the interaction with a protein known as Mtr2p (14, 17). Prediction of Mtr2p secondary structure and the observation that co-expression of human TAP and p15 in *S. cerevisiae* partially restores growth of a strain carrying the otherwise lethal *mex67/mtr2* double knockout, suggest that Mtr2p may be a p15 functional analogue (8, 16).

A C-terminal fragment of TAP, the NPC-binding domain (Fig. 1, fragment 508–619), mediates direct interactions with nucleoporins and is necessary and sufficient for the localization of TAP to the nuclear rim (1, 9, 18). This fragment comprises the entire UBA-like domain and part of the NTF2-like domain, but p15 binding by TAP is not required for its interaction with nucleoporins (9). The UBA-like domain on its own (fragment 567–619) is not sufficient to localize TAP at the nuclear rim *in vivo*, but single amino acid changes in a conserved loop of this domain (NWD at positions 593–595 in human TAP) severely

* This work was supported by the European Molecular Biology Organization (EMBO) and the Human Frontier Science Program Organization (HFSPO). The costs of publication of this article were defrayed in part by the payment of page charges. This article must therefore be hereby marked "advertisement" in accordance with 18 U.S.C. Section 1734 solely to indicate this fact.

‡ To whom correspondence should be addressed: EMBL, Meyerhofstrasse 1, D-69117 Heidelberg, Germany. Tel.: 49-6221-387-389; Fax: 49-6221-387-518; E-mail: izaurralde@embl-heidelberg.de.

¹ The abbreviations used are: CTE, constitutive transport element; RBD, RNA-binding domain; LRR, leucine-rich repeat; NTF2, nuclear transport factor 2; UBA, ubiquitin associated-like domain; GFP, green fluorescent protein; HA, hemagglutinin; CAT, chloramphenicol acetyltransferase; snRNA, small nuclear RNA; CMV, cytomegalovirus; RRE, Rev response element; Ad-mRNA, adenovirus mRNA.

impair binding of TAP, Hs NXF2, and Ce NXF1 to nucleoporins *in vitro* and *in vivo* (1, 3, 8, 18). This suggests that high affinity binding to nucleoporins requires both the UBA-like domain and at least part of the NTF2-like domain. The UBA-like domain is conserved in yeast Mex67p, but only the *S. cerevisiae* protein has been shown to interact directly with nucleoporins (20). As with the metazoan proteins (1, 9), Mex67p lacking the UBA-like domain no longer localizes to the nuclear envelope (14), suggesting that the mode of interaction of yeast and metazoan NXF proteins with nucleoporins is conserved.

Previous studies have focused on the role of the individual domains of TAP in the export of CTE-bearing RNAs (1, 7, 9, 12, 13, 19). In this study we investigated the role of TAP domains in the export of cellular mRNAs. To this end, we developed assays to test mRNA export stimulation by TAP/p15 heterodimers in cultured cells and in *Xenopus* oocytes. These assays are based on the observation that overexpression of TAP with p15 bypasses nuclear retention and stimulates export of mRNAs that are normally not exported efficiently. Using these assays, we show that in the presence of p15, only full-length TAP efficiently stimulates export of a variety of mRNA export cargoes. The RBD is dispensable for the stimulation of mRNA export by TAP whereas the LRR and the NTF2-like domains are essential for this function. The first 60 amino acids of TAP and the UBA-like domain contribute substantially, but are not strictly required for TAP-mediated export of cellular mRNA. These results were confirmed by directly tethering TAP/p15 heterodimers to the RNA export cargo.

EXPERIMENTAL PROCEDURES

Plasmids—Most plasmids used in this study have been described before (1, 4, 7–9, 12). TAP Δ RBD corresponds to a deletion of residues 119–198 in the TAP protein sequence (7), TAP Δ LRR has residues 203–362 deleted (7), TAP Δ NTF2 and TAP Δ UBA correspond to the deletions TAP Δ 437–507 and TAP Δ 567–613 described before (9). TAP point mutants were generated using an oligonucleotide-directed *in vitro* mutagenesis system from Stratagene (Quick Change Site-directed Mutagenesis). For expression of TAP and TAP mutants as glutathione *S*-transferase fusions in *Escherichia coli*, the corresponding cDNAs were cloned between the *Nco*I and *Bam*HI sites of vector pGEXCS (21). TAP and TAP mutants were expressed in mammalian cells as fusions with green fluorescent protein (GFP). To this end, cDNA fragments encoding TAP or TAP mutants were excised from the corresponding pGEXCS constructs as *Nar*I-*Bam*HI fragments and cloned into the vector pEGFP-C1 (CLONTECH) between the *Acc*I and *Bam*HI restriction sites. p15-1 was expressed with an N-terminal tag consisting of two immunoglobulin-binding domains from protein A of *Staphylococcus aureus* (zz tag). For expression in *E. coli*, p15-1 cDNA was cloned into pQE70zz vector (1). Subsequently, the cDNA fragment encoding zzp15-1 was excised from pQE60zzp15-1 plasmid using the restriction sites *Hind*III-*Not*I and inserted into pEGFP-N3 vector (CLONTECH) cut with the same enzymes. This deletes the GFP coding sequence. For expression of TAP/p15 heterodimers in *E. coli*, a bicistronic plasmid was constructed by inserting a ribosome-binding site followed by the p15-2a cDNA downstream of the TAP coding sequence in plasmid pGEXCS-TAP.

Plasmid pCMV128 has been described (22, 23); plasmid pCH110 encoding β -galactosidase (β -gal) is from Amersham Pharmacia Biotech. cDNAs encoding HIV-1 Rev protein and the export-deficient mutant RevM10 were kindly provided by Françoise Stutz (University of Lausanne, Lausanne, Switzerland). These cDNAs were amplified by polymerase chain reaction and cloned between the *Age*I and *Bsr*GI sites of plasmid pEGFP-C1, thereby deleting the GFP coding sequence. The 5' polymerase chain reaction oligo introduced a HA-tag N-terminal so that Rev and RevM10 fusions can be detected by Western blot using anti-HA antibodies. The resulting plasmids, pCMV-Rev and pCMV-RevM10, were sequenced and used in subsequent cloning steps. Plasmids expressing RevM10 fusions of TAP mutants and p15-1 were generated by replacing the GFP coding sequence from the corresponding pEGFP-C1 plasmids by the HA-RevM10 coding sequence using the *Age*I and *Eco*RI restriction sites. TAP full-length and TAP Δ 567–613 were excised from the corresponding pGEXCS plasmids as *Nar*I-*Bam*HI fragments. The *Bam*HI site was blunted by T4 DNA polymerase. These cDNAs were cloned into the *Acc*I-*Sma*I sites of vector pCMV-RevM10.

Expression of Recombinant Proteins—Glutathione *S*-transferase protein fusions were expressed in *E. coli* BL21(DE3) strains. *E. coli* M15[pREP4] strain was used for expressing proteins cloned into the pQE60zz vector. Recombinant proteins were purified as previously described (4). For oocyte injections recombinant proteins were dialyzed against 1.5 \times phosphate-buffered saline supplemented with 10% glycerol.

DNA Transfections and CAT Assays—DNA transfections and CAT assays were performed essentially as described before (1), with the following modifications. Human 293 cells were transfected using Polyfect transfection reagent (Qiagen) according to the manufacturer's instructions. The transfected DNA mixture consisted of 0.25 μ g of the CAT reporter plasmid pCMV128, 0.5 μ g of pEGFP-C1 plasmid encoding TAP or TAP mutants, and/or 0.5 μ g of pEGFP-N3 plasmid encoding zzp15. Transfection efficiency was determined by including 0.5 μ g of pCH110 plasmid (Amersham Pharmacia Biotech), as β -galactosidase expression from this vector is not affected by TAP overexpression. The total amount of plasmid DNA transfected in each sample was held constant by adding the appropriate amount of the corresponding parental plasmids without insert, and was brought to a total of 2 μ g by adding pBSSKII plasmid when necessary. When Rev-M10 fusions were tested, the transfected DNA mixture consisted of 0.25 μ g of the CAT reporter plasmid pCMV128, 0.5 μ g of plasmids pCMV-RevM10-TAP or pCMV-RevM10-p15, and/or 0.5 μ g of plasmids pEGFP-C1-TAP or pEGFP-N3zzp15. Transfection efficiency was determined by including 0.5 μ g of pCH110 plasmid. Plasmids pCMV-Rev and pCMV-RevM10 were used as positive and negative controls, respectively. Cells were harvested 48 h after transfection and CAT activity was measured as described (24). Protein expression levels were analyzed by Western blot using anti-GFP or anti-HA antibodies.

Xenopus Oocyte Microinjections—All DNA templates for *in vitro* synthesis of labeled RNAs have been described. These were dihydrofolate reductase mRNA, U5 Δ Sm and U6 Δ ss snRNAs, U6-CTE, and human initiator methionyl tRNA (6, 9). AdHML81, Fushi tarazu (Ftz), and β -globin cDNAs have been described (25, 26). Ftz-218 and β -globin-247 cDNAs were kindly provided by Hervé Le Hir (Brandeis University). Oocyte injections and analysis of microinjected RNA by denaturing gel electrophoresis and autoradiography were performed as described (6). Quantitation was done by FluorImager (Fuji FLA-2000). The concentration of recombinant proteins in the injected samples is indicated in the figure legends.

RESULTS

Overexpression of TAP/p15 Heterodimers Promotes the Nuclear Exit of Inefficiently Spliced pre-mRNAs—Previously, we reported an assay that allows quantifying TAP-mediated stimulation of RNA nuclear export in cultured cells (1). In this assay, a TAP protein expression vector is co-transfected with the chloramphenicol acetyltransferase (CAT) gene encoded by the reporter plasmid pDM138 (22). This plasmid harbors the CAT coding sequence inserted into an intron, which is not efficiently spliced (22). Cells transfected with this plasmid retain the unspliced pre-mRNA in the nucleus, yielding only trace levels of CAT enzyme activity (22). Expression of TAP/p15 heterodimers bypass nuclear retention and promotes the export of the inefficiently spliced pre-mRNA, resulting in a 14–16-fold increase in CAT activity (1). In this study, we improved the sensitivity and expanded the dynamic range of the assay by using the reporter plasmid pCMV128 (Fig. 2A). This plasmid is related to pDM138 but has a CMV promoter instead of an SV40 promoter (23). Consequently, the basal level of CAT enzyme activity in cells transfected with pCMV128 is 10-fold higher than in cells transfected with pDM138 (not shown). Furthermore, co-expression of TAP/p15 heterodimers with the reporter pCMV128 caused a 44-fold increase in CAT activity (Fig. 2B). RNase protection analysis confirmed that TAP/p15 heterodimers enhanced *cat* gene expression by allowing the unspliced transcripts to enter the cytoplasm (not shown). As reported (1), overexpression of TAP in the absence of exogenous p15 results in a significant but modest increase of CAT activity, although, the levels of expression of TAP were also reduced (Fig. 2, B and C). Moreover, overexpression of p15 in the absence of exogenous TAP or in the presence of deletion mutants

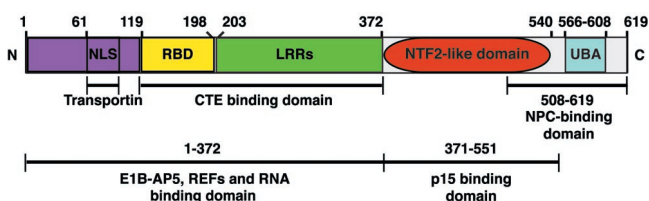


FIG. 1. Domain organization of human TAP protein. The N-terminal domain of TAP (residues 1–372) includes the minimal CTE-binding fragment (residues 102–372) and exhibits general RNA binding affinity. This domain also binds to several mRNA-associated proteins such as E1B-AP5 and REF/Aly, and carries an NLS recognized by transportin (1, 7, 9, 10). The N-terminal domain consists of an RNP-type RNA-binding domain (yellow), a leucine-rich repeat domain (green), and a less conserved region upstream of the RBD (purple). The domain boundaries of the RBD and the LRRs are as defined in the crystal structure of these domains (7). The C-terminal half of TAP consists of an NTF2-like domain (red) and a UBA domain (cyan). The minimal TAP fragments sufficient for p15 or nucleoporin binding (9) are indicated. Numbers indicate the position in the amino acid sequence.

of TAP that cannot bind p15 (TAP Δ NTF2 and TAP 1–372) had no significant effect on CAT expression (Fig. 2B). These results indicate that formation of TAP/p15 heterodimers is required for TAP-dependent stimulation of *cat* gene expression. These results also indicate that in cells overexpressing TAP, p15 becomes limiting, and vice versa, and thus no large pools of free TAP or p15 exist *in vivo*.

The LRR and NTF2-like Domains of TAP Are Essential for Its Export Activity—Using pCMV128 as a reporter we have investigated the role of TAP domains in RNA export. Tested TAP mutants include a deletion of the first 60 amino acids (TAP-(61–619)) and deletions of the RBD, the LRR, the NTF2-like and the UBA-like domains (TAP Δ RBD, TAP Δ LRR, TAP Δ NTF2, and TAP Δ UBA) (Fig. 1 and Table I). TAP fragments lacking the entire C-terminal half (TAP-(1–372)) or the N-terminal half (TAP-(371–619)) were included as negative controls. All tested TAP mutants localize within the nucleus when expressed in HeLa cells, with the exception of TAP fragment 371–619, which distributes between the nucleus and cytoplasm (Ref. 9 and data not shown).

In the absence of exogenous p15, none of the TAP mutants stimulated significantly *cat* gene expression (Fig. 2B, white bars), but their expression levels were also reduced in comparison with that of TAP (Fig. 2C). In the presence of p15, TAP mutants that bind p15 were expressed at a steady-state level comparable with that of wild-type TAP (Fig. 2C). Nevertheless, when assayed for the ability to induce CAT expression from pCMV128, TAP Δ LRR was completely defective, whereas TAP-(61–619) and TAP Δ UBA exhibited low, but significant residual activity. In contrast, TAP Δ RBD retained 38% of the activity of wild-type TAP (Fig. 2B, Table I). TAP mutant Δ NTF2, which does not bind p15 (8, 9), failed to stimulate CAT activity (Fig. 2B), but the expression of this mutant protein was reduced in comparison with that of the wild-type control (Fig. 2C, lane 13 versus 5). We therefore generated a second mutant in the NTF2-like domain of TAP by deleting residues 381–503. Despite that TAP-(Δ 381–503) does not bind p15, its expression at a steady-state level was comparable with that of TAP (not shown). However, this protein does not stimulate *cat* gene expression (Table I). These results provide strong support for the conclusion that formation of TAP/p15 heterodimers is required for TAP-mediated RNA export stimulation.

Since deletions of entire domains may affect multiple interactions or TAP folding, we tested the effect of introducing point mutations in the LRR (see below) and the UBA-like domains (Fig. 2B). The mutations targeted conserved residues exposed on the surface of the protein and were designed on the known three-dimensional structure of the LRR domain and the pre-

dicted structure of the UBA-like domain (7, 8). TAP mutants W594A and D595R have a single amino acid change in the conserved loop of the UBA-like domain and have impaired nucleoporin binding (1, 8). These mutants have an effect which is similar to removing the entire UBA-like domain (Fig. 2B), so we conclude that this domain is critical for TAP-dependent RNA nuclear export.

TAP/p15 Heterodimers Trigger Nuclear Export When Tethered to the RNA Export Cargo—Next, we tested the effect of tethering TAP/p15 heterodimers directly to the pCMV128 pre-mRNA. In this context, stimulation of RNA export by the various TAP mutants should be independent of their ability to bind RNA or RNA-associated proteins. TAP wild-type and mutants were fused to the C terminus of an HIV Rev protein defective in export (RevM10). RevM10 carries two point mutations in the nuclear export signal and, unlike wild-type Rev, cannot promote export of RNAs bearing the HIV Rev response element (RRE) (Ref. 27, reviewed in Ref. 28). However, RevM10 has an intact RRE-binding domain and can target the fusion protein to RRE-bearing RNAs (27–29). Vectors expressing RevM10 fusions were co-transfected into 293 cells with the CAT reporter plasmid pCMV128, which carries the RRE inserted in the intron (23). Expression of RevM10-TAP fusion moderately stimulated CAT activity, in contrast its co-expression with p15 increased CAT activity 250-fold (Fig. 3A). Similar results were recently reported by Guzik *et al.* (29). Conversely, tethering of p15 via the RevM10 protein had no significant effect on CAT activity, but its co-expression with TAP resulted in a 150-fold stimulation of *cat* gene expression (Fig. 3A). When neither TAP nor p15 were fused to RevM10 a 40-fold stimulation of CAT activity was measured, in agreement with data shown in Fig. 2A. Thus, the higher CAT activity measured when either subunit of the TAP/p15 heterodimer was fused to RevM10 is likely to be due to its direct binding to the RRE.

Using this assay we then tested the effect of deleting individual TAP domains. Western blot analysis indicate that in the presence of p15, the expression levels of TAP mutants fused to RevM10 were comparable to that of the wild type control (not shown). When TAP was tethered to the RNA, removing the first 60 amino acids reduced its export activity by 2.5–3-fold (Fig. 3B and Table I). Unexpectedly, we found that deletion of the RBD increased the ability of RevM10-TAP fusion to promote *cat* gene expression. A possible explanation for this observation is that removing the RBD reduces the nonspecific binding of TAP to other RNAs, thereby increasing the pool of protein able to bind to the RRE-containing RNA. The export activity of RevM10-TAP was reduced by removing the LRR domain and completely abolished by deleting the NTF2-like or the UBA-like domains (Fig. 3B and Table I). In summary, when TAP is directly tethered to its cargo the RBD becomes dispensable for its export activity while the LRR, the NTF2-like domain, and the UBA-like domain still play a critical role. However, a protein fragment comprising these domains (TAP-(200–619)) exhibited 14% of the activity of wild type TAP, suggesting that residues upstream of the RBD are important for TAP function. This result is consistent with the observation that the first 60 amino acids of TAP, although not strictly necessary, contribute to its export activity (Figs. 2B and 3B).

Mutations in the LRR Domain Impair TAP-mediated RNA Export—The mechanism by which deletion of the LRR domain abolishes TAP function is unclear because TAP Δ LRR exhibits general RNA binding affinity, binds to REFs, E1BAP5, p15, and nucleoporins *in vitro*, and localizes to the nuclear rim *in vivo* (not shown). LRR domains have a crescent shape with the convex surface formed by α -helices and the concave surface lined by β -strands (30). The concave β -sheet surface of LRR

TABLE I
Role of TAP domains in RNA export

The stimulation of Ad-mRNA export or of *cat* gene expression by TAP mutants in the presence of p15-1 is expressed as percentage of the activity of full-length TAP. Data are means from three independent experiments. In the first column, the domains in which the mutagenized residues are located are indicated in parentheses.

| TAP mutants + <i>zfp15</i> | Relative stimulation of Ad-mRNA export in oocytes | Relative stimulation of CAT expression in 293 cells | Relative stimulation of CAT expression by RevM10 fusions |
|----------------------------|---|---|--|
| TAP | 100% | 100% | 100% |
| TAP 61-619 | 19% | 15% | 39% |
| TAP ΔRBD | 75% | 38% | 240% |
| TAP ΔLRR | Inhibition | 3% | 27% |
| TAP D228K (LRR) | 91% | 122% | ND ^a |
| TAP E318R,E319R (LRR) | 30% | 3% | 4% |
| TAP D323K (LRR) | ND | 169% | ND |
| TAP ΔNTF2 | 6% | 0.7% | 0.4% |
| TAP Δ381-503 (NTF2) | 3% | 7% | ND |
| TAP ΔUBA | 9% | 13% | 3% |
| TAP W594A (UBA) | 6% | 13% | 5% |
| TAP D595R (UBA) | 9% | 3% | ND |

^a ND, not determined.

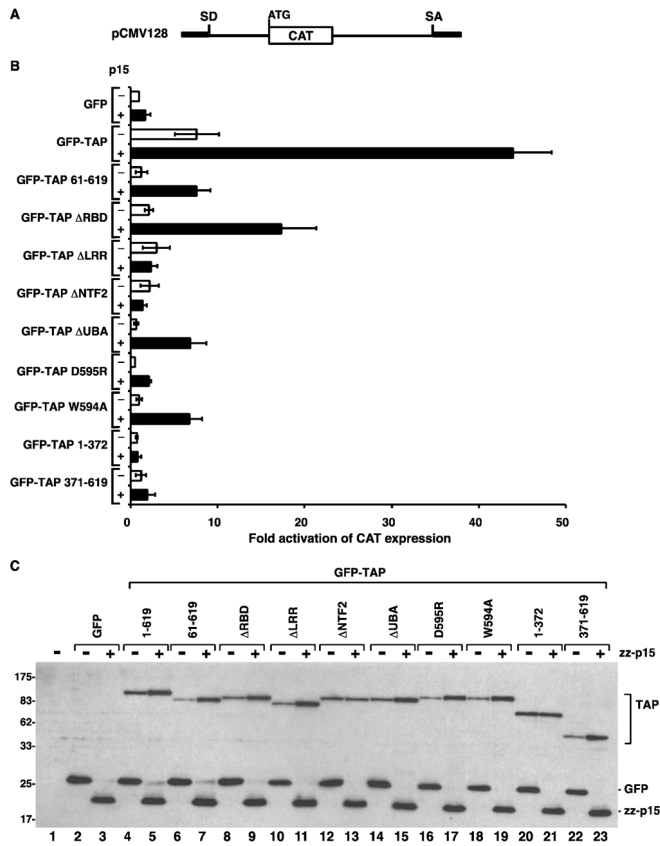


FIG. 2. The LRR and NTF2-like domains of TAP are essential for RNA export stimulation in 293 cells. *A*, schematic representation of the reporter gene encoded by the plasmid pCMV128 (23). *SD* and *SA* indicate the splice donor and acceptor sites of the intron. *B*, human 293 cells were transfected with a mixture of plasmids encoding β-Gal, CAT (pCMV128), and either GFP alone or fused N-terminal to TAP or various TAP mutants as indicated on the left. When indicated, a pEGFP-N3 derivative encoding *zfp15* was co-transfected (+p15, black bars). Cells were collected 48 h after transfection and β-Gal and CAT activity were determined. Data from three separate experiments are shown as fold activation of CAT activity relative to the activity measured when pCMV128 was co-transfected with parental plasmids without insert (-). The numbers are mean ± S.D. *C*, protein expression levels were analyzed by Western blot using anti-GFP antibodies. Lane 1 shows the untransfected control. The position of TAP mutants fused to GFP, of GFP itself, or of *zfp15* is shown on the right.

domains has been proposed to mediate protein-protein interactions (30). At the concave face of the LRR domain of TAP, there is a conserved electronegative area defined by residues Asp²²⁸,

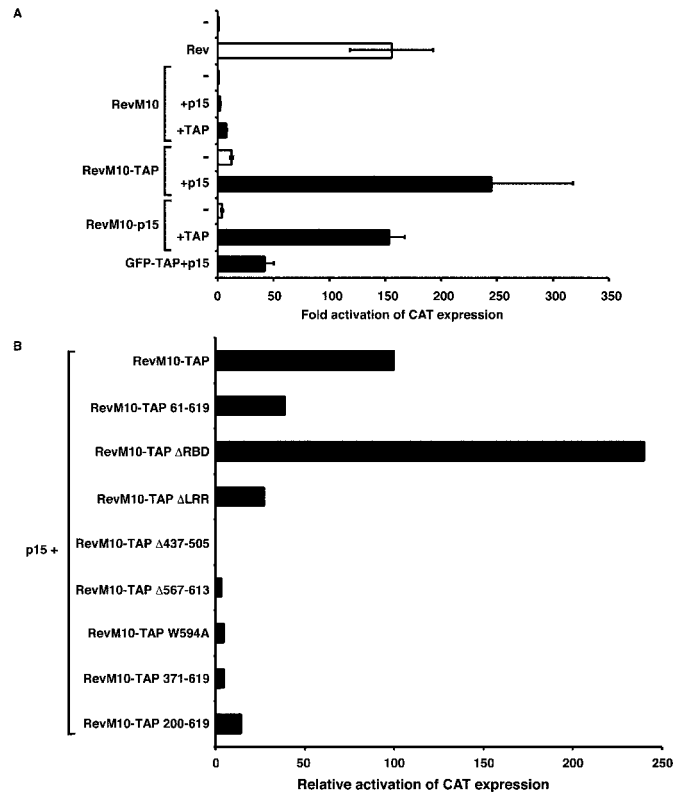


FIG. 3. TAP/p15 heterodimers promote export when tethered to RNA. *A*, human 293 cells were transfected with pCMV128, pCH110, and plasmids encoding RevM10 fusions of TAP or p15. When indicated, plasmids encoding GFP-TAP (+TAP) or *zfp15* (+p15) were co-transfected (black bars). As controls, the reporter plasmids were co-transfected with empty vectors (-) or vectors expressing Rev or RevM10. Data from three separate experiments are shown as fold activation of CAT activity relative to the activity measured when GFP was coexpressed with pCMV128. The numbers are mean ± S.D. *B*, 293 cells were transfected with pCMV128, pCH110, *zfp15*, and plasmids encoding TAP or TAP mutants fused to RevM10. The stimulation of *cat* gene expression by TAP mutants in the presence of p15-1 measured in three independent experiments is expressed as percentage of the activity of RevM10-TAP.

Glu³¹⁸, Glu³¹⁹, Asp³²³, and Asp³⁵² (7). Reverse-charge mutations of Asp²²⁸ (TAP D228K), which is conserved within the NXF family, and of Asp³²³, did not affect TAP-mediated expression of the *cat* gene (Table I). Asp³⁵² plays a structural role and was not mutated (7). In contrast, reverse-charge mutations of residues Glu³¹⁸ and Glu³¹⁹ (TAP E318R,E319R) dramatically reduced stimulation of *cat* gene expression by TAP in the two

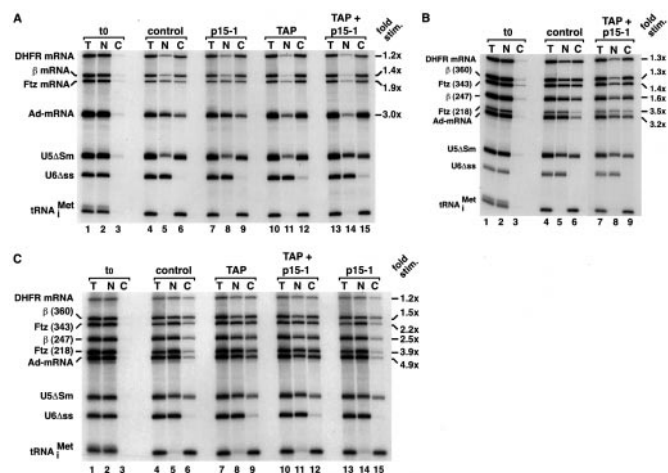


FIG. 4. TAP stimulates export of mRNAs that are normally inefficiently exported. *A-C*, *Xenopus* oocyte nuclei were injected with mixtures of ^{32}P -labeled RNAs and purified recombinant proteins as indicated. RNA samples from total oocytes (*T*), nuclear (*N*), and cytoplasmic (*C*) fractions were collected immediately after injection (t_0 ; lanes 1–3) or 90 min after injection in panels *A* and *B*. In lanes 4–15 of panel *C*, samples were collected 40 min after injection. RNA samples were analyzed on 8% acrylamide, 7 M urea denaturing gels. One oocyte equivalent of RNA, from a pool of 10 oocytes, was loaded per lane. The concentration of recombinant glutathione *S*-transferase-TAP in the injected samples was 0.8 mg/ml. The concentration of zpp15 in the injected samples was 2 mg/ml except for lanes 13–15 of panel *C*, in which p15 was injected at 10 mg/ml. On the left of panels *B* and *C*, the numbers in brackets indicate the size of the transcripts. The stimulation of export for each of the mRNAs tested was quantified and expressed as fractional stimulation relative to the export measured in control oocytes. The numbers on the right of the panels represent export stimulation by TAP/p15 heterodimers relative to control oocytes (fold stimulation of export).

assays described above (Table I). This mutant protein, however, stimulated export of an excised intron lariat bearing the CTE (7) and of an U6-CTE chimeric RNA (see below), indicating that it is properly folded. Thus, residues Glu³¹⁸ and Glu³¹⁹, which are located at the C-terminal edge of the concave surface of the LRR domain (opposite to Asp²²⁸), appear to be engaged in interactions that are critical for TAP-mediated export of cellular mRNA but not of CTE-bearing RNAs.

TAP Stimulates the Export of mRNAs That Are Otherwise Inefficiently Exported—To investigate whether TAP can directly stimulate export of cellular mRNA, *Xenopus* oocyte nuclei were coinjected with purified recombinant TAP and a mixture of labeled RNAs. This mixture consisted of U5ΔSm and U6Δss snRNAs, the human initiator methionyl tRNA (tRNA^{Met}), and various mRNAs that differ in their export efficiencies. These were dihydrofolate reductase, β-globin, and fushi tarazu (Ftz) mRNAs and a mRNA derived from the adenovirus major late region (Ad-mRNA). U6Δss RNA is not exported from the nucleus and serves as an internal control for nuclear injection (31). U5ΔSm RNA is exported via the CRM1 export pathway but, unlike wild type U5, is not subsequently reimported into the nucleus (32). Immediately after injection, all RNAs were nuclear (Fig. 4, lanes 1–3). After a 90-min incubation period, in control oocytes 67% of the dihydrofolate reductase and β-globin mRNA and 42% of the Ftz mRNA were cytoplasmic (Fig. 4A, lanes 4–6). As reported (33, 34), Ad-mRNA was less efficiently exported (28% export, Fig. 4A, lanes 4–6). Coinjection of recombinant TAP, however, resulted in a 2.6-fold stimulation of Ad-mRNA export, as 74.5% of this mRNA was detected in the cytoplasm (Fig. 4A, lanes 10–12). When recombinant p15 was coinjected with TAP, export of Ftz and Ad-mRNA was stimulated up to 1.9- and 3-fold, respectively (Fig. 4A, lanes 13–15). Nuclear exit of the efficiently

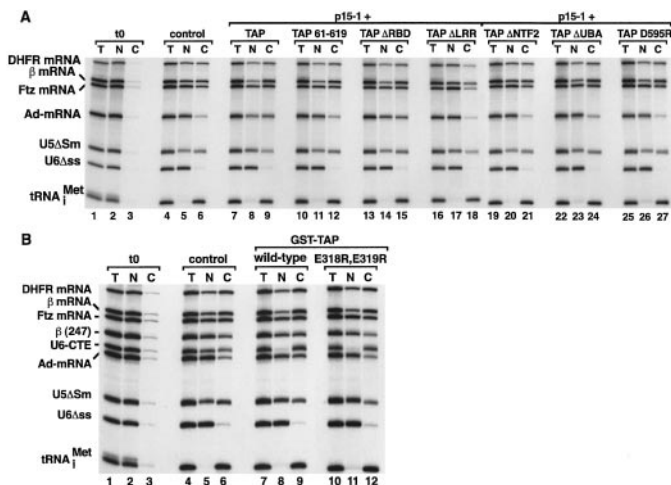


FIG. 5. Role of TAP domains in mRNA nuclear export stimulation. *A*, wild-type TAP and mutants were expressed in *E. coli* as glutathione *S*-transferase fusions. The recombinant proteins indicated above the lanes were injected into *Xenopus* oocyte nuclei together with recombinant zpp15 and a mixture of radiolabeled RNAs. This mixture consisted of dihydrofolate reductase, β-globin, Ftz, and Ad-mRNAs, U5ΔSm, and U6Δss snRNAs, and human initiator methionyl tRNA. The concentration of recombinant TAP and TAP mutants in the injected samples was 0.8 mg/ml and that of zpp15 was 2 mg/ml. *B*, purified recombinant TAP and TAP E318R,E319R were injected into *Xenopus* oocyte nuclei together with the mixture of radiolabeled RNAs described in panel *A* supplemented with U6-CTE RNA. zpp15 was not included as it interferes with the export of U6-CTE RNA. In both panels, RNA samples from total oocytes (*T*), nuclear (*N*), and cytoplasmic (*C*) fractions were collected immediately after injection (t_0 ; lanes 1–3, in both panels) or 90 min after injection, and analyzed on 8% acrylamide, 7 M urea denaturing gels. One oocyte equivalent of RNA, from a pool of 10 oocytes, was loaded per lane.

exported mRNAs (e.g. dihydrofolate reductase and β-globin) was only slightly or not further stimulated (Fig. 4A, lanes 13–15). Recombinant p15, in the absence of TAP, had no effect on the export of any of the RNA species tested (Fig. 4A, lanes 7–9). Stimulation of mRNA export by TAP was specific, since export of tRNA and U5ΔSm RNA was not affected (Figs. 4 and 5). Furthermore, the stimulatory effect of TAP could be obtained reproducibly using different preparations of recombinant protein and in several independent experiments (e.g. Figs. 4, A–C, and 5, A and B).

We also found that TAP directly stimulated export of other mRNAs. First, we decreased the export rate of β-globin and Ftz mRNAs by reducing the length of these transcripts from 360 and 343 nucleotides to 247 and 218 nucleotides, respectively (34). Fig. 4B shows that TAP stimulated the export of the shortened mRNAs (lanes 7–9). The effect of TAP was more dramatic on the export of Ad-mRNA and Ftz-218 mRNA, which are the least efficiently exported mRNAs. Second, we reduced the incubation time from 90 to 40 min so that less than 42% export was observed for all mRNAs tested (Fig. 4C, lanes 4–6). Under these conditions, p15 alone had no effect on export even though a 5-fold higher molar concentration was injected compared with Fig. 4A (Fig. 4C, lanes 13–15). Coinjection of TAP, with or without p15, stimulated the export of all mRNAs, except dihydrofolate reductase mRNA (Fig. 4C, lanes 7–12). Again, the stimulatory effect of TAP was more dramatic on the export of mRNAs that were less efficiently exported, suggesting that TAP is limiting for these cargoes. TAP/p15 heterodimers had no significant effect on the export of β-globin, Ftz and Ad-mRNA produced by *in vivo* splicing of the corresponding pre-mRNAs (not shown).

Role of TAP Domains in mRNA Export Stimulation in *Xenopus* Oocytes—Next, we investigated the role of individual TAP

domains in mRNA export stimulation in *Xenopus* oocytes. The TAP mutants described above were expressed in *E. coli* and injected into *Xenopus* oocyte nuclei together with p15 and the mixture of labeled RNAs described in Fig. 4A. After a 90-min incubation period, 34% of dihydrofolate reductase and Ftz mRNAs and 48% of β -globin mRNA moved to the cytoplasm, while only 13% of Ad-mRNA was exported (Fig. 5A, lanes 4–6). Coinjection of full-length TAP resulted in a 4.2-fold stimulation of Ad-mRNA export (Fig. 5A, lanes 7–9, and Table I). TAP Δ RBD stimulated Ad-mRNA export by 3.4-fold (Fig. 5A, lanes 13–15). In contrast, deletion of either the N-terminal 60 amino acids (TAP-(61–619)), the LRR, the NTF2-like domain, or the UBA-like domain strongly reduced or abolished the export activity of TAP (Fig. 5A, lanes 10–12 and 16–24, Table I).

The effect of introducing point mutations in the LRR domain and the UBA-like domain of TAP was also tested. In the LRR domain only the reverse-charge mutation of residues Glu³¹⁸ and Glu³¹⁹ to Arg impaired stimulation of Ad-mRNA export by TAP (TAP E318R,E319R; Fig. 5B, lanes 10–12). In contrast, this mutant protein stimulated export of an U6-CTE chimeric RNA (Fig. 5B, lanes 10–12). TAP mutant D595R had the same effect as deleting the entire UBA-like domain (Fig. 5A, lanes 25–27 versus 22–24).

Because all TAP mutants that were impaired in mRNA export stimulation exhibited general RNA binding affinity *in vitro* (not shown), their absence of export activity cannot be attributed to a failure to bind RNA, but is likely to reflect impaired binding to p15 (for TAP Δ NTF2 and TAP Δ 381–503) or to nucleoporins (for TAP Δ UBA and TAP D595R). It is currently unclear which interactions are affected by deleting the LRR domain or the first 60 amino acids of TAP. TAP-(61–619) has a reduced *in vitro* affinity for E1B-AP5 (9), but the significance of this interaction for TAP function *in vivo* has not yet been established.

DISCUSSION

This study provides direct evidence for a role of TAP/p15 heterodimers in nuclear mRNA export. TAP/p15 heterodimers directly stimulate the export of mRNAs that are otherwise exported inefficiently. TAP/p15 heterodimers have no significant effect on the export of mRNAs that are efficiently exported or are produced by *in vivo* splicing of the corresponding pre-mRNA, suggesting that TAP/p15 heterodimers are not limiting for these cargoes. The observation that in *Xenopus* oocytes titration of TAP by an excess of CTE RNA inhibits mRNA nuclear export irrespective of whether or not the mRNA has been generated by splicing (4–6), however, suggests that TAP/p15 heterodimers participate in the export of both spliced and intronless mRNAs.

The role of TAP domains in RNA export was analyzed in cultured cells and in *Xenopus* oocytes. Despite the differences between these cell types and the export cargoes analyzed, the results obtained in these two systems are in surprisingly good agreement (Table I). These results indicate that TAP-mediated export of mRNA strictly requires the LRR and NTF2-like domains, whereas deletion of the first 60 residues of TAP or of the UBA-like domain strongly impairs TAP function. The functional importance of the LRR and NTF2-like domains is underlined by the observation that these domains are the most conserved among NXF proteins (1). Only the RBD is dispensable for mRNA export stimulation by TAP. Similar results were obtained by tethering TAP to the RNA via the RevM10 protein, although in this case TAP mutants lacking the first 60 amino acids or the LRRs exhibited 39 and 27% of the activity of wild type TAP, respectively. This suggests that these domains are crucial for cargo binding by TAP but can be deleted when TAP is directly tethered to its cargo (Fig. 3).

Interaction of TAP with mRNP Export Cargoes—The association of TAP with cellular mRNA may be direct or mediated by protein/protein interactions. Recently, several TAP partners that might facilitate TAP binding to cellular mRNA have been identified. These include E1B-AP5 (9), RAE1/Gle2 (9), and REF proteins (also called Yra in yeast and Aly in mice) (10, 11, 34). Apart from these, other RNA-binding proteins may act as adaptors between TAP and cellular mRNPs. In particular, the splicing coactivator SRm160, the acute myeloid leukemia-associated protein DEK, RNPS1 and Y14, together with REFs, are components of a 335-kDa protein complex deposited by the spliceosome 20–24 nucleotides upstream of a splice junction (25, 26). These proteins, either individually or as a complex, bind mRNA in a splicing-dependent, but sequence-independent way or may facilitate the recruitment of TAP to mRNA following splicing (26, 34–37). Therefore, TAP may not be limiting for spliced mRNAs because splicing guarantees the recruitment of TAP partners, and hence of TAP, in a sequence-independent manner. In contrast, the pCMV128 pre-mRNA and some intronless mRNAs, depending on their primary sequence and/or their length, may not be able to recruit TAP partners or TAP efficiently. Thus, TAP may be limiting for these particular cargoes so their export can be stimulated by TAP overexpression. Consistent with this, nuclear exit of inefficiently exported, intronless mRNAs can also be stimulated by microinjection of recombinant REFs in *Xenopus* oocytes (34).

An Essential Role for the LRR Domain of TAP in mRNA Nuclear Export—In this article, we have presented evidence that the LRR domain is essential for TAP function. Furthermore, we show that residues located at the C-terminal edge of the concave face of the LRR domain are critical for TAP-mediated export of cellular mRNA but not of CTE-bearing RNAs. The concave β -sheet surface of LRR domains has been proposed to mediate protein-protein interactions (30). Deletion of the entire LRR domain of TAP does not affect binding to its known partners (E1BAP5, REFs, p15, and nucleoporins).² This suggests that the LRR domain of TAP binds one or more unidentified cellular ligands that are bypassed by the CTE, but is essential for export of cellular mRNA.

Formation of p15/TAP Heterodimers Is Required for TAP-mediated RNA Nuclear Export—The essential role of p15 in TAP-mediated RNA export was clearly demonstrated in cultured cells. Although co-expression of p15 increased the steady-state expression levels of TAP (Fig. 2C and Ref. 1), this effect was less dramatic than the stimulation of *cat* gene expression. For instance, the expression levels of GFP-TAP and RevM10-TAP were increased by a factor of 2–3-fold in the presence of p15, however, CAT activity was stimulated 40- and 250-fold, respectively, indicating that p15 not only stabilizes TAP but it is absolutely required for its export activity. The critical role of p15 in TAP-mediated export of intron-containing RNAs was also recently reported by Guzik *et al.* (29), although in this study a truncated form of TAP, (TAP-(61–619)) was used.

In *Xenopus* oocytes, injection of TAP-(Δ 381–503) and TAP-(Δ NTF2), which have no affinity for p15 (Refs. 8 and 9, this study), resulted in no export activity (Table I). Because in oocytes the recombinant proteins were stable (not shown), this suggests that TAP/p15 heterodimer formation is required for mRNA nuclear export. On the other hand, coinjection of p15 with TAP only slightly increased the mRNA export stimulation observed when TAP alone was injected, suggesting that p15 may not be limiting in the oocytes.

p15 has been implicated in export of tRNAs but also in

² I. C. Braun, A. Herold, M. Rode, E. Conti, and E. Izaurralde, unpublished results.

CRM1-mediated export of U snRNAs and leucine-rich NESs (38, 39). This export function of p15 was proposed to be dependent on its ability to interact with RanGTP. Binding of p15 to RanGTP is controversial, as this interaction could not be reproduced in other laboratories (1, 16). In *Xenopus* oocytes microinjection of p15 did not stimulate export of any of the RNA species tested (Figs. 4 and 5). Similarly, in cultured cells and in the absence of exogenous TAP, overexpression of p15 did not stimulate CAT expression even when it was tethered to the RRE-bearing pre-mRNA via RevM10 (Fig. 3). Moreover, co-expression of p15 with wild-type Rev did not significantly increase Rev-mediated export of RRE-containing pre-mRNAs (29).³ Together, these results suggest that p15 participates in mRNA export through its heterodimerization with TAP, or other members of the NXF family, and has no intrinsic export activity.

The UBA-like Domain of TAP Is Critical for Its Export Activity—The experiments described here indicate that the UBA-like domain contributes substantially to the export function of TAP, although a low but significant export activity was measured when this domain was deleted. Indeed, in the presence of p15, TAP Δ UBA and TAP W594A exhibited between 9 and 13% of the export activity of wild-type TAP (Table I). In *S. cerevisiae*, deletion of the UBA-like domain of Mex67p resulted in a thermosensitive growth phenotype and accumulation of polyadenylated RNAs within the nucleus, indicating that the UBA-like domain of Mex67p is required, but not essential for efficient mRNA nuclear export (14). In addition, Mex67p mutants lacking the UBA-like domain no longer localized to the nuclear rim (14). Overexpression of Mtr2p compensated for the lack of the UBA domain and restored growth, but not the nuclear envelope localization of the protein. Similarly, NXF proteins lacking the UBA-like domain do not localize at the nuclear rim when coexpressed with p15 (1). Thus, *in vivo* Mex67p and metazoan NXF proteins lacking the UBA-like domain have a residual export activity in the presence of Mtr2p or p15 and may still be able to interact transiently with nucleoporins, although at equilibrium they are no longer localized at the nuclear rim. The NTF2-like domain might, therefore, mediate transient binding to nucleoporins when the UBA domain is not present thereby sustaining a residual export activity. Consistent with this hypothesis, it has recently been shown that high affinity interactions between nucleoporins and transport receptors are dispensable for NPC passage (40). For instance, NTF2 homodimers localize to the nuclear rim and facilitate the nuclear import of RanGDP, however, a point mutation that abolishes nuclear rim localization (*i.e.* high affinity binding to the NPC) reduces but does not abolish the import function of NTF2 (40).

Distinct Requirements for TAP-mediated Export of Cellular and Viral mRNA—The results obtained in this study reveal different requirements for TAP-mediated export of cellular mRNA or of CTE-bearing RNAs. The RBD is dispensable for TAP-mediated export of mRNA but is essential for specific binding to the CTE RNA and therefore, for TAP-mediated export of CTE-containing cargoes (1, 7, 12, 13). Conversely, the first 60 amino acids of TAP have an important role in the stimulation of mRNA export, but are not required for TAP-mediated export of CTE-bearing RNAs (1, 9, 12, 13). Due to the lack of structural information, however, the role of these residues in mRNA nuclear export cannot currently be analyzed further. Interestingly, this domain is the least conserved among the NXF proteins (1). Our data suggest that the poor conservation of this domain does not reflect a non-essential function but may confer specific properties to the NXF proteins

(*i.e.* substrate specificity or binding to specific partners).

The requirement of the NTF2-like and the UBA-like domains for CTE export are cargo-dependent (9). In *Xenopus* oocytes TAP-mediated export of CTE-bearing intron lariats is independent of these domains (9, 12) while export of U6-CTE requires the UBA-like domain but not the NTF2-like domain (9). In quail cells, TAP-mediated export of an inefficiently spliced pre-mRNA carrying the CTE in the intron is abolished by mutations or deletions of the UBA-like domain (1, 19) but is only reduced by mutations preventing p15 binding (19).

Only the LRR domain is essential for export of both cellular mRNA and CTE-bearing RNAs, but its role in these processes is different. Indeed, reverse-charge mutations of Arg³¹⁸ and Arg³¹⁹ impaired mRNA export stimulation by TAP but supported CTE-dependent export (Ref. 7 and this study). Thus, it is likely that the mRNA export defect of this mutant is attributable to its inability to interact with some components of the nuclear export machinery that is required for mRNA nuclear export but bypassed by the CTE. This provides further support for the hypothesis that the mode of interaction of TAP with cellular mRNA is different from that with the CTE RNA and thus, that the CTE subverts TAP from its normal cellular function (7, 9, 12). Moreover, these results suggest that the assays described in this article are likely to reflect the genuine mRNA export activity of TAP.

Acknowledgments—We thank Tom Hope and Karen L. Beemon for the kind gift of plasmid pCMV128 and Françoise Stutz for the plasmids encoding HIV-1 Rev and Rev-M10 mutant. We are grateful to Brian Guzik and Marie-Louise Hammarskjöld for communicating results prior to publication and Kevin J. Chalmers and Scott Kuersten for critical reading of the manuscript.

REFERENCES

- Herold, A., Suyama, M., Rodrigues, J. P., Braun, I. C., Kutay, U., Carmo-Fonseca, M., Bork, P., and Izaurralde, E. (2000) *Mol. Cell Biol.* **20**, 8996–9008
- Segref, A., Sharma, K., Doye, V., Hellwig, A., Huber, J., Lüthmann, R., and Hurt, E. (1997) *EMBO J.* **16**, 3256–3271
- Tan, W., Zolotukhin, A. S., Bear, J., Patenaude, D. J., and Felber, B. K. (2000) *RNA* **6**, 1762–1772
- Grüter, P., Taberero, C., von Kobbe, C., Schmitt, C., Saavedra, C., Bachi, A., Wilm, M., Felber, B. K., and Izaurralde, E. (1998) *Mol. Cell* **1**, 649–659
- Pasquinelli, A. E., Ernst, R. K., Lund, E., Grimm, C., Zapp, M. L., Rekosh, D., Hammarskjöld, M.-L., and Dahlberg, J. E. (1997) *EMBO J.* **16**, 7500–7510
- Saavedra, C. A., Felber, B. K., and Izaurralde, E. (1997) *Curr. Biol.* **7**, 619–628
- Liker, E., Fernandez, E., Izaurralde, E., and Conti, E. (2000) *EMBO J.* **19**, 5587–5598
- Suyama, M., Doerks, T., Braun, I. C., Sattler, M., Izaurralde, I., and Bork, P. (2000) *EMBO Repts.* **1**, 53–58
- Bachi, A., Braun, I. C., Rodrigues, J. P., Panté, N., Ribbeck, K., von Kobbe, C., Kutay, U., Wilm, M., Görlich, D., Carmo-Fonseca, M., and Izaurralde, E. (2000) *RNA* **6**, 136–158
- Stutz, F., Bachi, A., Doerks, T., Braun, I. C., Séraphin, B., Wilm, M., Bork, P., and Izaurralde, E. (2000) *RNA* **6**, 638–650
- Sträßer, K., and Hurt, E. (2000) *EMBO J.* **19**, 410–420
- Braun, I. C., Rohrbach, E., Schmitt, C., and Izaurralde, E. (1999) *EMBO J.* **18**, 1953–1965
- Kang, Y., and Cullen, B. R. (1999) *Genes Dev.* **13**, 1126–1139
- Sträßer, K., Baßler, J., and Hurt, E. (2000) *J. Cell Biol.* **150**, 695–706
- Black, B. E., Lévesque, L., Holaska, J. M., Wood, T. C., and Paschal, B. (1999) *Mol. Cell Biol.* **19**, 8616–8624
- Katahira, J., Sträßer, K., Podtelejnikov, A., Mann, M., Jung, J. U., and Hurt, E. (1999) *EMBO J.* **18**, 2593–2609
- Santos-Rosa, H., Moreno, H., Simos, G., Segref, A., Fahrenkrog, B., Panté, N., and Hurt, E. (1998) *Mol. Cell Biol.* **18**, 6826–6838
- Bear, J., Tan, W., Zolotukhin, A. S., Taberero, C., Hudson, E. A., and Felber, B. K. (1999) *Mol. Cell Biol.* **19**, 6306–6317
- Kang, Y., Bogerd, H. P., and Cullen, B. R. (2000) *J. Virol.* **74**, 5863–5871
- Strawn, L. A., Shen, T., and Wente, S. R. (2000) *J. Biol. Chem.*
- Parks, T. D., Leuther, K. K., Howard, E. D., Johnston, S. A., and Dougherty, W. G. (1994) *Anal. Biochem.* **216**, 413–417
- Huang, X., Hope, T. J., Bond, B. L., McDonald, D., Grahl, K., and Parslow, T. G. (1991) *J. Virol.* **65**, 2131–2134
- McDonald, D., Hope, T. J., and Parslow, T. G. (1992) *J. Virol.* **66**, 7232–7236
- Morency, C. A., Neumann, J. R., and Russian, K. O. (1987) *Biotechnology* **5**, 444–448
- Le Hir, H., Moore, M. J., and Maquat, L. E. (2000) *Genes Dev.* **14**, 1098–1108
- Le Hir, H., Izaurralde, E., Maquat, L. E., and Moore, M. J. (2000) *EMBO J.* **19**, 6860–6869
- Mahim, M. H., Bohnlein, S., Hauber, J., and Cullen, B. R. (1989) *Cell* **58**, 205–214

³ I. C. Braun, A. Herold, and E. Izaurralde, unpublished data.

28. Cullen, B. R. (1998) *Virology* **249**, 203–210
29. Guzik, B. W., Levesque, L., Prasad, S., Bor, Y.-C., Balck, B. E., Paschal, B. M., Rekosh, D., and Hammarström, M.-L. (2001) *Mol. Cell. Biol.*, **7**, 2545–2554
30. Kobe, B., and Deisenhofer, J. (1994) *Trends Biol. Sci.* **19**, 415–421
31. Vankan, P., McGuigan, C., and Mattaj, I. W. (1992) *EMBO J.* **11**, 335–342
32. Fornerod, M., Ohno, M., Yoshida, M., and Mattaj, I. W. (1997) *Cell* **90**, 1051–1060
33. Luo, M.-J., and Reed, R. (1999) *Proc. Natl. Acad. Sci. U. S. A.* **96**, 14937–14942
34. Rodrigues, J. P., Rode, M., Gatfield, D., Blencowe, B. J., Carmo-Fonseca, M., and Izaurralde, E. (2000) *Proc. Natl. Acad. Sci. U. S. A.*, **98**, 1030–1035
35. Kataoka, N., Yong, J., Kim, V. N., Velazquez, F., Perkinson, R. A., Wang, F., and Dreyfuss, G. (2000) *Mol. Cell* **6**, 673–682
36. Zhou, Z., Luo, M.-J., Strasser, K., Katahira, J., Hurt, E., and Reed, R. (2000) *Nature* **407**, 401–405
37. McGarvey, T., Rosonina, E., McCracken, S., Li, Q., Arnaout, R., Mientjes, E., Nickerson, A. J., Awrey, D., Greenblatt, J., Grosveld, G., and Blencowe, B. J. (2000) *J. Cell Biol.* **150**, 309–320
38. Ossareh-Nazari, B., Maison, C., Black, B. E., Levesque, L., Paschal, B. M., and Dargemont, C. (2001) *Mol. Cell. Biol.* **20**, 4562–4571
39. Black, B. E., Holaska, J. M., Lévesque, L., Ossareh-Nazari, B., Carol Gwizdek, C., Dargemont, C., and Paschal, B. M. (2001) *J. Cell Biol.* **152**, 141–156
40. Ribbeck, K., and Görlich, D. (2001) *EMBO J.*, **20**, 1320–1330

2.3.2 Paper 6:

Nuclear export of mRNA by TAP/NXF1 requires two nucleoporin binding sites but not p15

Braun, I. C., Herold, A., Rode, M., and Izaurralde, E. (2002) *Mol Cell Biol* **22**, 5405-5418.

Context

TAP interacts with the NPC *via* two distinct structural domains: the UBA-like domain and the NTF2-like scaffold formed by the NTF2-like domains present in TAP and p15 (Fribourg *et al.*, 2001; Bachi *et al.*, 2000). Both domains contain a single nucleoporin-binding site and act synergistically to promote the association with the NPC. It was unclear whether the NTF2-like scaffold (and thereby p15) contributes only to NPC binding or whether it is also required for other functions. We therefore questioned whether TAP/NXF1 function requires these two *different* nucleoporin-binding domains or whether two copies of either domain in tandem are sufficient to promote nuclear export of mRNAs.

Summary of results and conclusions

We generated TAP derivatives having two UBA-like domains in tandem but no NTF2-like domain (TAP-2xUBA) or two NTF2-like domains in tandem but no UBA-like domain (TAP-2xNTF2). The RNA export activity of these proteins was tested in a CAT-reporter assay (see Braun *et al.*, 2001) and compared to the export activity of wild-type TAP or TAP derivatives lacking either the NTF2-like domain or the UBA-like domain. Constructs with only one nucleoporin-binding site displayed a strongly reduced export activity (5-12% compared to wild-type), while TAP-2xUBA and TAP-2xNTF2 retained about 60% activity. In the case of TAP-2xNTF2 this activity was dependent on coexpression of p15. TAP-2xUBA activity was independent of the presence of p15. When TAP-2xUBA was directly tethered to the reporter RNA (see Braun *et al.*, 2001) it also displayed about 50% of wild-type export activity. In this assay, the stimulation of export is independent of the intrinsic ability of the TAP derivative to recognize the cargo. As TAP-2xUBA displays similar export activity in both assays, the NTF2-like domain and hence p15 are unlikely to play a critical role in cargo binding.

TAP derivatives having three or four UBA-like domains in tandem exhibited export activities similar to that of TAP-2xUBA. These proteins had an increased affinity for nucleoporins as their predominant localization was at the nuclear envelope. When these constructs were transiently expressed at high levels, about 10-20% of transfected cells accumulated poly(A)⁺ RNA in the nucleus suggesting that their high concentration at the NPC interferes with normal mRNA export.

The results described above were confirmed in an independent system: recombinantly expressed TAP-2xUBA and TAP 3xUBA were injected into *Xenopus* oocytes, and their ability to stimulate mRNA export was determined. Similar to the observations described above, TAP-2xUBA and TAP 3xUBA were able to stimulate export of most mRNAs while TAP derivatives with only one nucleoporin binding site were not. When TAP-2xUBA or TAP 3xUBA was injected at high concentrations, a strong inhibition of mRNA, U5 snRNA and tRNA export was observed. Notably, some RNA export cargoes (e.g. specific RNAs carrying the CTE) required only one nucleoporin-binding site in TAP for efficient export suggesting that the requirements for NPC translocation are influenced by the nature of the transported cargo.

We next investigated if TAP-2xUBA could functionally replace wild-type TAP *in vivo* in *Drosophila* S2 cells. For that we generated a cell line stably expressing GFP-NXF1-2xUBA. The expression of endogenous *nxfl* or *p15* was silenced by RNAi which results in a strong nuclear accumulation of poly(A)⁺ RNA (Herold *et al.*, 2001). The expression of NXF1-2xUBA partially rescued mRNA export in *ca.* half of the cells depleted of either NXF1 or p15. Importantly, NXF1 did not accumulate within the cytoplasm in these cells. This suggests that the NTF2-like scaffold (and thereby p15) is not required for cargo release following export. We also investigated whether NXF1-2xUBA could restore growth of cells depleted of NXF1 or p15. While control cells died after prolonged periods of missing NXF1 or p15 function, a fraction of cells expressing NXF1-2xUBA survived this treatment. The fact that in the surviving population the fraction of cells expressing NXF1-2xUBA increased significantly indicates that these cells had a selective advantage, probably because they could partially overcome the nuclear export block.

Altogether our data demonstrate that two copies of either the NTF2-like scaffold or the UBA-like domain are sufficient to promote directional transport of mRNAs. The export activity of TAP/NXF1 is independent of p15 when two UBA-like domains provide the NPC-binding sites. Thus, as for the UBA-like domain, the main function of the NTF2-like scaffold is nucleoporin binding.

Contribution

I contributed to the experiments using the *Drosophila* cell culture system shown in Figure 6 and 7 and Table 2. My overall contribution to this manuscript is about 20%.

Nuclear Export of mRNA by TAP/NXF1 Requires Two Nucleoporin-Binding Sites but Not p15

Isabelle C. Braun, Andrea Herold, Michaela Rode, and Elisa Izaurralde*

European Molecular Biology Laboratory, D-69117 Heidelberg, Germany

Received 16 January 2002/Returned for modification 27 February 2002/Accepted 23 April 2002

Metazoan NXF1/p15 heterodimers promote export of bulk mRNA through nuclear pore complexes (NPC). NXF1 interacts with the NPC via two distinct structural domains, the UBA-like domain and the NTF2-like scaffold, which results from the heterodimerization of the NTF2-like domain of NXF1 with p15. Both domains feature a single nucleoporin-binding site, and they act synergistically to promote NPC translocation. Whether the NTF2-like scaffold (and thereby p15) contributes only to NXF1/NPC association or is also required for other functions, e.g., to impart directionality to the export process by regulating NXF1/NPC or NXF1/cargo interactions, remains unresolved. Here we show that a minimum of two nucleoporin-binding sites is required for NXF1-mediated export of cellular mRNA. These binding sites can be provided by an NTF2-like scaffold followed by a UBA-like domain (as in the wild-type protein) or by two NTF2-like scaffolds or two UBA-like domains in tandem. In the latter case, the export activity of NXF1 is independent of p15. Thus, as for the UBA-like domain, the function of the NTF2-like scaffold is confined to nucleoporin binding. More importantly, two copies of either of these domains are sufficient to promote directional transport of mRNA cargoes across the NPC.

Nucleocytoplasmic transport of macromolecules occurs through nuclear pore complexes (NPCs) and is mediated by saturable transport receptors. The receptors bind to nucleoporins, the components of the NPC, and to cargo molecules that need to be translocated across the pore. While the vast majority of transport receptors are members of a conserved family of proteins known as importins or exportins (or karyopherins), export of bulk mRNA is thought to be mediated by members of the conserved family of NXF proteins (reviewed in references 9, 26, and 27).

The yeast genome encodes a single NXF protein, Mex67p, but there are two NXFs in *Caenorhabditis elegans* and four in *Drosophila melanogaster* and *Homo sapiens* (14, 18, 33, 37, 41, 42). Of these, *Saccharomyces cerevisiae* Mex67p, *C. elegans* NXF1, and *D. melanogaster* NXF1 have been shown to be essential for the export of bulk polyadenylated RNA [poly(A)⁺ RNA] to the cytoplasm (15, 33, 37, 40). In *Schizosaccharomyces pombe*, Mex67p is implicated in but not essential for mRNA export (42).

Human NXF1 is also known as TAP and will be referred to as TAP. TAP is directly implicated in the nuclear export of simian type D retroviral RNAs bearing the constitutive transport element (CTE) (7, 12, 19). A role for TAP in the export of cellular mRNA is suggested by the observation that in *Xenopus laevis* oocytes, titration of TAP with an excess of CTE RNA leads to an mRNA export block (29, 32). Consistently, overexpression of TAP in human cultured cells or microinjection of the recombinant protein into *Xenopus* oocytes stimulates export of mRNAs that are otherwise exported inefficiently (8, 13, 14, 41).

TAP consists of two functional domains: an N-terminal cargo-binding domain and a C-terminal NPC-binding domain (Fig. 1). The cargo-binding domain comprises an N-terminal fragment for which no structural information is available, an RNP-type RNA-binding domain, and a leucine-rich repeat domain (24). The cargo-binding domain binds directly to the CTE RNA, exhibits a general affinity for RNA, and interacts with adaptor proteins that are thought to recruit TAP to cellular mRNA (7, 19, 21, 24; reviewed in reference 9).

The NPC-binding domain of TAP (residues 371 to 619) consists of two distinct structural domains connected by a flexible linker: the NTF2-like domain, which is related to nuclear transport factor 2 (NTF2), and a C-terminal region related to ubiquitin-associated (UBA) domains (the so-called UBA-like domain) (Fig. 1) (10, 11, 36). The NTF2-like domain of TAP interacts with p15 to form a compact heterodimer with an overall structure similar to that of the NTF2 homodimer (Fig. 1) (10, 21, 36).

With the exception of *D. melanogaster* NXF4, the NTF2-like domain is conserved in all members of the NXF family, including *S. cerevisiae* Mex67p, even though p15 is absent in budding yeast (14, 15, 21, 36). The NTF2-like domain of *S. cerevisiae* Mex67p heterodimerizes instead with Mtr2p, a putative p15 analogue (21, 35). The UBA-like domain, in contrast, is less well conserved among members of the NXF family and is absent in *D. melanogaster* NXF4, *C. elegans* NXF2, *H. sapiens* NXF3, and *H. sapiens* NXF5 (14, 15, 18, 37, 41).

Although no structural information is available on the binding of nucleoporins to the UBA-like domain, a hydrophobic surface patch that affects NPC association of this domain was identified by site-directed mutagenesis (11). Single point mutations in this domain and a deletion of the entire domain have a similar effect on nucleoporin binding, suggesting that this domain provides a single nucleoporin-binding site (10, 11). The recently solved structure of the NTF2-like domain of TAP

* Corresponding author. Mailing address: European Molecular Biology Laboratory, Meyerhofstrasse 1, D-69117 Heidelberg, Germany. Phone: 49 6221 387 389. Fax: 49 6221 387 518. E-mail: izaurralde@embl-heidelberg.de.

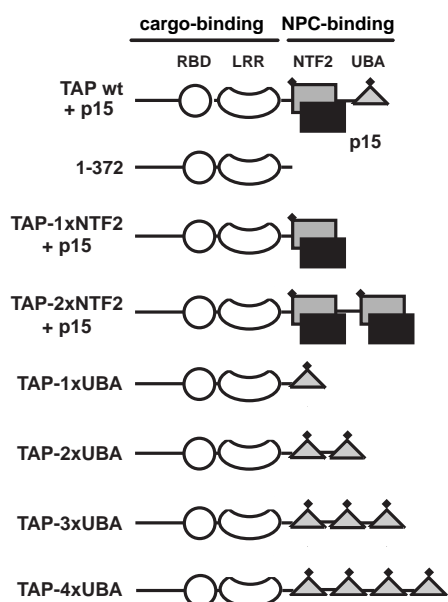


FIG. 1. Structural and functional domains of human TAP bound to p15. The cargo-binding domain of TAP (residues 1 to 372) consists of an RNP-type RNA-binding domain (RBD, residues 119 to 198), a leucine-rich repeat domain (LRR, residues 203 to 362), and a less well conserved region N-terminal to the RBD for which no structural information is available (residues 1 to 119). The NPC-binding domain of TAP consists of the NTF2-like domain (grey square, residues 371 to 551) bound to p15 (black square) and a UBA-like domain (triangle, residues 563 to 619). Each of these domains features a nucleoporin-binding site (solid diamond).

bound to p15 revealed that this heterodimeric NTF2-like scaffold also features a single nucleoporin-binding site located at the TAP side of the heterodimer (10). A clear implication of this structural study is that p15 contributes indirectly to nucleoporin binding by TAP by maintaining the proper folding of the NTF2-like domain (10).

Formation of TAP/p15 heterodimers is strictly required for TAP-mediated export of RNA cargoes that do not carry a CTE (8, 10, 13, 14, 39). CTE-bearing RNAs, in contrast, can be exported by TAP mutants that are impaired in p15 binding both in *Xenopus* oocytes and in cultured cells (1, 20). An essential role for metazoan p15 in the export of cellular mRNA was recently reported in *Drosophila* cells. In these cells, depletion of p15 by double-stranded RNA (dsRNA) interference inhibits growth and results in a strong nuclear accumulation of poly(A)⁺ RNA (15, 39). The growth arrest and the mRNA export block are observed in spite of the fact that *D. melanogaster* NXF1 is neither degraded nor mislocalized in cells depleted of p15 (15). Therefore, in the absence of p15, *D. melanogaster* NXF1 cannot perform its essential mRNA export function.

Despite the essential role of p15 and therefore of the NTF2-like domain of NXF1 in the export of cellular mRNA, it is still unclear whether this domain contributes only to the nucleoporin-binding activity of NXF1 or whether it would also have additional functions, such as being required for cargo binding and/or NXF1 recycling. Moreover, it has been proposed that p15 may impose a directionality on the export process by mod-

ulating the overall affinity of TAP/NXF1 for nucleoporins (22, 23, 39). In this study, we generated TAP derivatives that lack the NTF2-like domain but have two or more UBA-like domains. These proteins stimulate the export of a variety of RNA cargoes both in cultured cells and in *Xenopus* oocytes. This stimulation of export is independent of p15. A derivative of *D. melanogaster* NXF1 having two UBA-like domains but no NTF2-like domain partially restored mRNA export in *Drosophila* cells depleted of either endogenous p15 or NXF1. These results indicate that, as for the UBA-like domain, the role of the NTF2-like scaffold is confined to nucleoporin binding.

MATERIALS AND METHODS

Plasmids. Most of the plasmids used in this study have been described before (8). TAP-1xUBA carries a deletion of amino acid residues 372 to 551, encompassing the NTF2-like domain. TAP-1xNTF2 carries a deletion of residues 567 to 613, encompassing the UBA-like domain. In previous studies, the equivalent constructs were referred to as TAP Δ NTF2 and TAP Δ UBA, respectively (8, 10).

To generate TAP-2xNTF2, first a PCR-amplified DNA fragment encoding TAP-1xNTF2 (amino acid residues 1 to 551) was cloned between the *Nco*I and *Kpn*I sites of the pGEXCS vector. Second, a PCR-amplified DNA fragment encoding the NTF2-like domain of TAP (residues 372 to 551) was cloned at the 3' end of TAP-1xNTF2 between the *Kpn*I site and a *Bam*HI site of pGEXCS. To generate TAP-2xUBA, first a PCR-amplified DNA fragment encoding TAP-1xUBA was cloned between the *Nco*I and *Kpn*I sites of the pGEXCS vector. Second, a PCR-amplified DNA fragment encoding the UBA-like domain of TAP (residues 551 to 619) was cloned at the 3' end of TAP-1xUBA between the *Kpn*I site and a *Bam*HI site of pGEXCS. TAP-3xUBA was generated by in-frame insertion of a PCR-generated DNA encoding one UBA at the unique *Kpn*I site of pGEXCS-TAP-2xUBA. The 5' PCR primer used to amplify the UBA-like domain also introduced an in-frame *Not*I restriction site to enable us to determine the orientation of the cDNA fragment following insertion. TAP-4xUBA was generated by in-frame insertion of a PCR-generated DNA encoding one UBA at the unique *Not*I site of pGEXCS-TAP-3xUBA.

Expression of recombinant proteins. TAP and TAP mutants were expressed as glutathione *S*-transferase (GST) fusions in the *Escherichia coli* BL21-codonPlus strain (Stratagene) with the corresponding pGEXCS plasmids. TAP and TAP-1xNTF2 were coexpressed with untagged p15-1 protein. Recombinant proteins were purified as described previously (12). For oocyte injections, recombinant proteins were dialyzed against 1.5 \times phosphate-buffered saline (PBS) supplemented with 10% glycerol. TAP and TAP mutants were expressed in human cultured cells as fusions with enhanced green fluorescent protein (EGFP). To this end, cDNA fragments encoding these proteins were excised from the corresponding pGEXCS constructs as *Nar*I-*Bam*HI fragments and cloned into the vector pEGFP-C1 (Clontech) between the *Acc*I and *Bam*HI restriction sites. p15-1 was expressed with an N-terminal tag consisting of two immunoglobulin-binding domains from protein A of *Staphylococcus aureus* (zz tag) as described before (plasmid pEGFP-N3-zzp15-1) (8).

DNA transfections, CAT assays, and RNase protection. DNA transfections and chloramphenicol acetyltransferase (CAT) assays were performed as described before (8). Human 293 cells were transfected with Polyfect transfection reagent (Qiagen) according to the manufacturer's instructions. The transfected DNA mixture consisted of 0.25 μ g of the CAT reporter plasmid pCMV128 (16), 0.5 μ g of pEGFP-C1 plasmid encoding TAP or TAP mutants, and, when indicated, 0.5 μ g of pEGFP-N3 plasmid, encoding zzp15. Transfection efficiency was determined by including 0.5 μ g of pCH110 plasmid (Pharmacia) encoding β -galactosidase (β -Gal), as β -Gal expression from this vector is not affected by TAP overexpression (8). The total amount of plasmid DNA transfected in each sample was held constant by adding the appropriate amount of the corresponding parental plasmids without insert and was brought to a total of 2 μ g by adding pBSSKII plasmid.

When Rev-M10 fusions were tested, the pEGFP-C1 plasmids were replaced by plasmids encoding RevM10 fusions of TAP or TAP mutants (pCMV-HA-RevM10). Plasmid pCMV-HA-RevM10 was used as a negative control. Cells were harvested 48 h after transfection. CAT and β -Gal activities were measured as described previously (8). In all experiments, the induced CAT enzyme expression levels were normalized to the activity of the β -Gal internal control. Protein

expression levels were analyzed by Western blot with anti-GFP or antihemagglutinin (anti-HA) antibodies.

For RNase protection assays, total RNA was isolated from transfected cells with Trizol Reagent (Life Technologies). To isolate cytoplasmic RNA, cells were lysed for 30 s in 130 mM NaCl–5 mM KCl–25 mM Tris–0.2% NP-40–0.1% sodium deoxycholate–0.002% dextran sulfate. Following centrifugation for 1 min at $1,000 \times g$, the supernatant was extracted twice with phenol-chloroform, and the RNA was precipitated. Antisense riboprobes encompassing nucleotides 291 to 411 and 1 to 100 of the β -Gal and CAT open reading frames, respectively, were generated by *in vitro* transcription. Following DNase digestion, the probes were purified on denaturing 6% acrylamide–7 M urea gels, eluted, precipitated, and resuspended in 100% formamide at 300,000 cpm/ μ l.

The riboprobes (1 μ l each) were mixed with 10 μ g of cellular RNA and 40 μ g of yeast total RNA in a final volume of 50 μ l of hybridization buffer consisting of 40 mM PIPES [piperazine-*N,N'*-bis(2-ethanesulfonic acid), pH 6.4], 400 mM NaCl, 1 mM EDTA, and 80% formamide. The RNA mixtures were denatured by incubation at 85°C for 5 min. Hybridizations were carried out overnight at 50°C. The next day, 300 μ l of RNase digestion buffer [10 mM Tris (pH 8.0), 5 mM EDTA, 300 mM NaCl] was added to each sample. RNase digestions were carried out for 45 min at 37°C with 2 U of Rnase T₁ (Roche) and 12 μ g of RNase A per sample. Digestions were stopped by adding proteinase K (50 μ g per sample) and sodium dodecyl sulfate (SDS) to a final concentration of 0.5%. Samples were further incubated for 15 min at 37°C, extracted with phenol-chloroform, precipitated, resuspended in 80% formamide, and analyzed on a 6% acrylamide–7 M urea denaturing gel, followed by autoradiography.

To determine the subcellular localization of TAP derivatives, the corresponding pEGFP-C1 constructs were used. HeLa cells were transfected with FUGENE6 (Roche). Plasmid pEGFP-N3-zpp15-1 was cotransfected with wild-type TAP and TAP-2xNTF2. Approximately 20 h after transfection, cells were fixed in formaldehyde. Fluorescent *in situ* hybridization (FISH) was performed essentially as described before (15).

Xenopus oocyte microinjections. Oocyte injections and analysis of microinjected RNA by denaturing gel electrophoresis and autoradiography were performed as described previously (32). Quantitation was done by FluorImager (Fuji FLA-2000). The concentration of recombinant proteins in the injected samples is indicated in the figure legends. All DNA templates for *in vitro* synthesis of labeled RNAs have been described (1, 12, 17, 25, 32).

Drosophila cell culture and RNA interference. A plasmid allowing the expression of GFP-tagged *D. melanogaster* NXF1 in SL2 cells was generated by inserting the corresponding NXF1 cDNA into a pBS-based vector containing the *Drosophila* actin promoter upstream of the EGFP cDNA, followed by multiple cloning sites and the BgHI terminator (pBSactEGFP). *D. melanogaster* NXF1-1xUBA was derived from plasmid pBSactEGFP-DmNXF1 by deleting the NTF2-like domain (amino acid residues 360 to 547) by the QuikChange site-directed mutagenesis kit (Stratagene). The PCR primers were designed to introduce in-frame *Nsi*I and *Mfe*I sites at position 360. DmNXF1-2xUBA was generated by in-frame insertion of a PCR-generated DNA fragment encoding the UBA-like domain of *D. melanogaster* NXF1 (residues 611 to 672) within the *Nsi*I site of pBSactEGFP-NXF1-1xUBA. A *Bam*HI site was introduced at the 3' end of the UBA cDNA in order to determine the orientation of this fragment following insertion.

Stable *Drosophila* cell lines expressing GFP and GFP fusions of *D. melanogaster* NXF1, NXF1-1xUBA, and NXF1-2xUBA were established by cotransfecting the corresponding pBSactEGFP constructs with a plasmid encoding puromycin acetyltransferase at a ratio of 5:1. SL2 cells were transfected with Lipofectin (Invitrogen) according to the manufacturer's instructions and selected in medium containing 10 μ g of puromycin/ml. Cells expressing the GFP fusions were enriched by fluorescence-activated cell sorting.

dsRNA interference was performed essentially as described before (15). NXF1 dsRNA corresponds to a fragment comprising the NTF2-like domain (amino acids 360 to 546). p15 dsRNA corresponds to the first 350 nucleotides of the *D. melanogaster* p15 coding region. FISH with an oligo(dT) probe was performed as described previously (15).

RESULTS

A minimum of two nucleoporin-binding sites is required for TAP-mediated nuclear RNA export. Precise deletion of either of the nucleoporin-binding domains of TAP dramatically reduces its export activity (8, 10). To investigate whether the export activity of TAP mutants having only one nucleoporin-

binding domain could be rescued by duplication of the same domain, we generated TAP derivatives having two UBA-like domains in tandem but no NTF2-like domain (TAP-2xUBA) or two NTF2-like domains in tandem but no UBA-like domain (TAP-2xNTF2) (Fig. 1). The export activity of these proteins in cultured cells was measured with the CAT reporter assay as described previously (8). In this assay, TAP expression vectors are cotransfected with the CAT gene encoded by plasmid pCMV128 (Fig. 2A) (16). As an internal control, a plasmid encoding β -Gal was cotransfected (see Materials and Methods).

In pCMV128, the CAT coding sequence is inserted into an inefficiently spliced intron, so cells transfected with this plasmid retain the unspliced pre-mRNA in the nucleus, yielding only trace levels of CAT activity (16). Overexpression of TAP/p15 heterodimers bypasses nuclear retention and promotes export of the inefficiently spliced pre-mRNA, resulting in about a 40-fold increase in CAT activity (Fig. 2B) (8). In all experiments described below, the induced CAT enzyme activity was normalized to the activity of the β -Gal internal control.

Deletion of both the NTF2-like and the UBA-like domains (TAP 1 to 372) abolishes export, but a protein in which only the NTF2-like domain has been deleted (TAP-1xUBA) exhibits 5% of the export activity of wild-type TAP (Fig. 2B; Table 1) (8, 10). When a second UBA-like domain was inserted in TAP-1xUBA to generate TAP-2xUBA, export was rescued to about 55% of the activity observed with wild-type TAP (Fig. 2B). Similarly, deletion of the UBA-like domain of TAP (TAP-1xNTF2) resulted in 12% export activity, but a protein having two NTF2-like domains in tandem (TAP-2xNTF2) retained 61% of the export activity of wild-type TAP when coexpressed with p15 (Fig. 2B and Table 1).

Western blot assays indicated that the expression levels of TAP mutants were comparable to that of TAP (Fig. 2C) when the amount of cell lysates analyzed was normalized to the activity of the β -Gal internal control. Thus, TAP-2xNTF2 is as active as TAP-2xUBA, but its export activity depends on p15 coexpression, while TAP-2xUBA exhibits the same activity regardless of the presence of exogenous p15 (Table 1 and Fig. 2B, compare grey and black bars).

It has been demonstrated that TAP can mediate the nuclear export of an RNA if tethered to that RNA via the RNA-binding domain of either the MS2 coat protein or the export-defective human immunodeficiency virus (HIV) Rev protein RevM10 (8, 13, 41). In this context, stimulation of RNA export by TAP is independent of its ability to bind RNA or RNA-associated proteins. To investigate whether the reduced export activity of TAP-2xUBA resulted from an impaired ability to interact with the cargo, we determined its export activity by tethering the protein directly to the pCMV128 pre-mRNA. To this end, wild-type TAP, TAP-1xUBA, and TAP-2xUBA were fused to the C terminus of RevM10. Although RevM10 cannot promote export of RNAs bearing the HIV Rev response element (RRE), it can target the fusion protein to a pCMV128 pre-mRNA carrying the RRE inserted in the intron (8, 13, 16).

Vectors expressing RevM10 fusions were cotransfected into 293 cells with the CAT reporter plasmid pCMV128-RRE and a plasmid encoding β -Gal as an internal control. As reported (8), expression of the RevM10-TAP fusion moderately stimulated CAT activity. In contrast, its coexpression with p15 in-

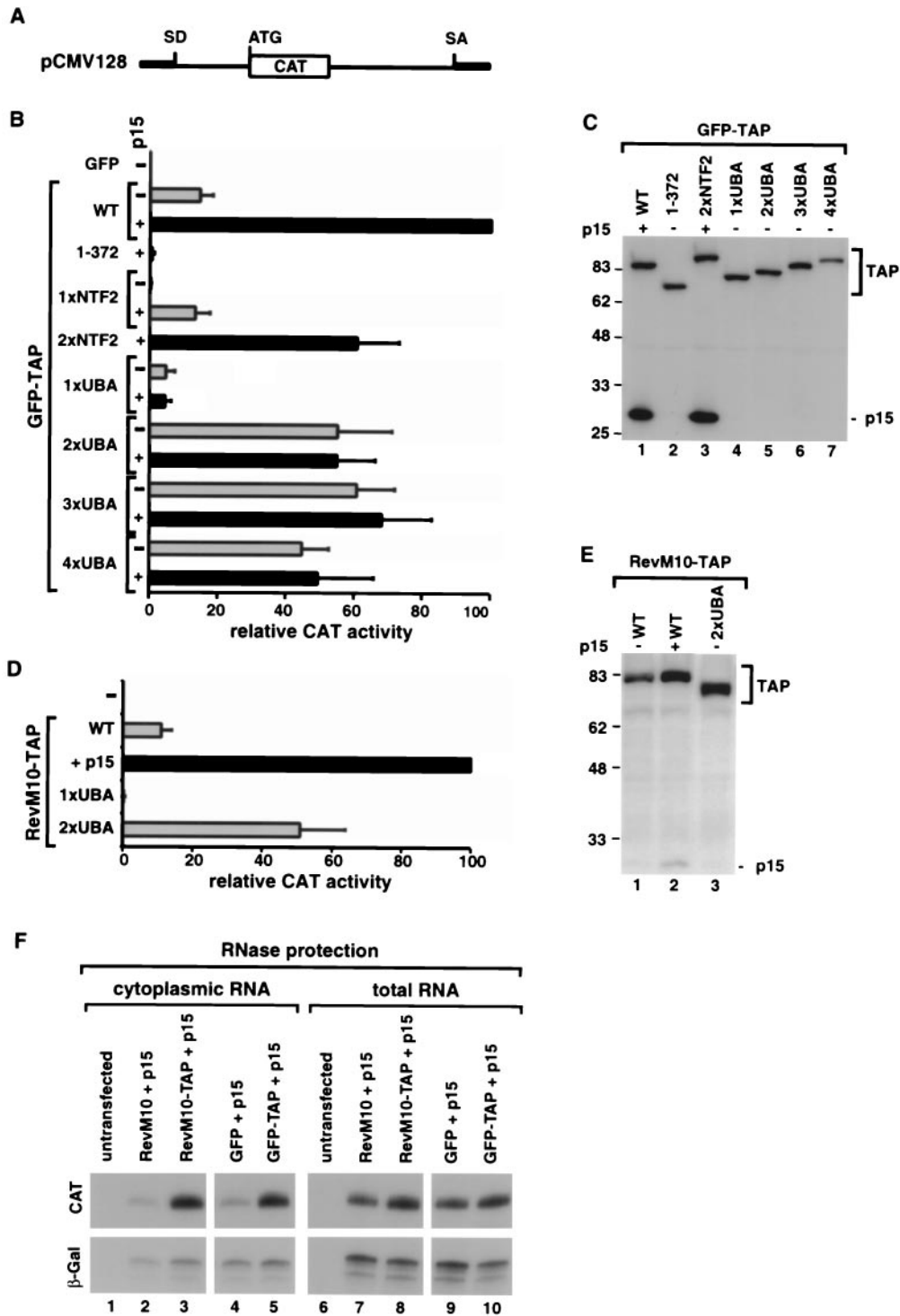


FIG. 2. Two nucleoporin-binding domains are required for TAP-mediated translocation of RNP cargoes across the NPC. (A) Schematic representation of the *cat* reporter gene encoded by plasmid pCMV128 (16). SD and SA indicate the splice donor and splice acceptor sites of the intron, respectively. (B) Human 293 cells were transfected with a mixture of plasmids encoding β -Gal (pCH110), CAT (pCMV128), and either GFP alone or GFP fused N-terminally to TAP or a TAP mutant, as indicated on the left. When indicated, a pGFP-N3 derivative encoding *zfp15* was cotransfected (+p15, black bars). Cells were collected 48 h after transfection, and β -Gal and CAT activities were determined. CAT activities were normalized to the activities of the β -Gal internal control. The stimulation of *cat* gene expression by TAP mutants measured in three independent experiments is expressed as a percentage of the activity of wild-type TAP. The values are means \pm standard deviations. (C) Protein expression levels were analyzed by Western blot with anti-GFP antibodies. The amount of cell extract loaded per lane was corrected for minor differences in transfection efficiencies, as revealed by the β -Gal internal control. The positions of TAP derivatives fused to GFP or of *zfp15* are shown on the right. (D) Human 293 cells were transfected with the reporter plasmids pCMV128-RRE and pCH110 and plasmids encoding RevM10 fusions of TAP, TAP-1xUBA, or TAP-2xUBA. When indicated, a plasmid encoding *zfp15* (+p15) was cotransfected (black bar). The

TABLE 1. Relative export activity of TAP derivatives^a

| TAP derivative | Mean stimulation (% of control) \pm SD | |
|------------------|--|-----------------|
| | <i>Xenopus</i> oocytes | Human 293 cells |
| TAP + p15 | 100 | 100 |
| TAP 1-372 | 0 | 0 |
| TAP-1xNTF2 + p15 | <10 | 12 \pm 4 |
| TAP-2xNTF2 + p15 | n.d. | 61 \pm 12 |
| TAP-1xUBA | <12 | 5 \pm 3 |
| TAP-1xUBA + p15 | n.d. | 4 \pm 2 |
| TAP-2xUBA | 61 \pm 10 | 53 \pm 20 |
| TAP-2xUBA + p15 | n.d. | 55 \pm 11 |
| TAP-3xUBA | 45 \pm 9 | 61 \pm 11 |
| TAP-3xUBA + p15 | n.d. | 68 \pm 14 |
| TAP-4xUBA | n.d. | 45 \pm 8 |
| TAP-4xUBA + p15 | n.d. | 49 \pm 18 |

^a The stimulation of Ad mRNA export in *Xenopus* oocytes or of *cat* gene expression in human 293 cells by TAP derivatives measured in three independent experiments is expressed as a percentage of the activity of full-length TAP. The concentration of the protein samples microinjected in *Xenopus* oocytes was 3 μ M. n.d., not determined.

creased CAT expression dramatically (by 200- to 250-fold) (Fig. 2D). TAP-1xUBA was used as a negative control because deletion of either the NTF2-like or the UBA-like domain abolished the export activity of RevM10-TAP (Fig. 2D) (8). In contrast, TAP-2xUBA fused to RevM10 retained 50% of the export activity of wild-type TAP. This export activity was observed in the absence of exogenous p15 (Fig. 2D). Western blot assays indicated that the expression level of TAP-2xUBA was comparable to that of TAP (Fig. 2E).

To confirm that the stimulation of CAT protein expression observed in the assays shown in Fig. 2B and 2D reflects an increased export of the unspliced *cat* mRNA encoded by pCMV128, we performed an RNase protection assay with cytoplasmic and total RNA fractions derived from transfected cells. Unspliced *cat* mRNA was detected at low levels in the cytoplasm of cells cotransfected with pCMV128 and the control vectors encoding p15 and either RevM10 or GFP alone (Fig. 2F, lanes 2 and 4). In contrast, the *cat* mRNA was exported to the cytoplasm of cells coexpressing p15 and TAP fused either to RevM10 or GFP (Fig. 2F, lanes 3 and 5). Therefore, TAP stimulates the nuclear export of the reporter RNA either by binding directly to that RNA via a heterologous RNA-binding domain (Fig. 2D) or by being recruited to that RNA, most probably via protein-protein interactions (Fig. 2B).

Altogether, these results indicate that a minimum of two nucleoporin-binding sites is required for TAP-mediated export of the pCMV128 reporter RNA. These binding sites can be provided by an NTF2-like domain followed by a UBA-like domain (as in the wild-type protein) or by two NTF2-like or two UBA-like domains in tandem. In the latter case, the export

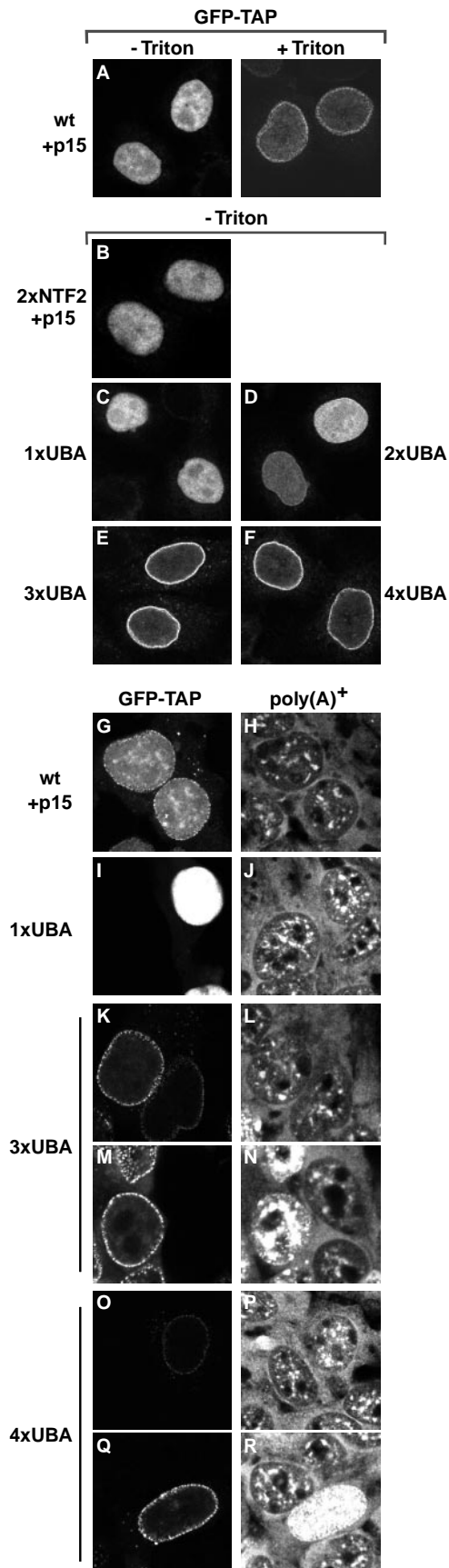
activity of TAP is independent of p15. Because a TAP derivative containing two UBA-like domains but no NTF2-like domain exhibited similar export activity regardless of whether this protein was tethered directly to the cargo, we conclude that the NTF2-like domain of TAP and hence p15 are unlikely to play a crucial role in cargo binding.

The export activity of TAP does not increase linearly with the number of nucleoporin-binding sites. The proteins having two UBA-like domains or two NTF2-like scaffolds in tandem exhibited about 50 to 60% of the export activity of wild-type TAP, suggesting that the two nucleoporin-binding sites in these constructs may not be accessible in the appropriate conformation for optimal binding to nucleoporins. We therefore investigated whether full restoration of export could be achieved by adding an increasing number of NPC-binding sites. TAP derivatives having three or four UBA-like domains in tandem had export activities similar to that with TAP-2xUBA (Fig. 2B and Table 1). Thus, once a minimum of two UBA-like domains is present, increasing the number of nucleoporin-binding sites does not have an additive effect on export efficiency.

To determine whether mislocalization of the proteins could account for these effects, the subcellular localization of TAP constructs fused to GFP was analyzed in transfected HeLa and 293 cells (Fig. 3). At equilibrium, TAP localizes mainly in the nucleoplasm (Fig. 3A) (1, 4, 21). The pool of TAP associated with the nuclear envelope could be visualized in cells extracted with Triton X-100 before fixation (Fig. 3A [+Triton]) (1). Under these conditions, most of the nucleoplasmic pool of the protein was solubilized, but the fraction of TAP localized at the nuclear periphery was resistant to detergent extraction. Strikingly, TAP-3xUBA and TAP-4xUBA were exclusively visualized at the nuclear envelope without Triton X-100 preextraction (Fig. 3E, F, K, M, O, and Q). In contrast, under these conditions, TAP-1xUBA, TAP-2xUBA, and TAP-2xNTF2 were predominantly nuclear, like wild-type TAP (Fig. 3B, C, and D).

The predominant localization of TAP-3xUBA and TAP-4xUBA at the nuclear rim suggests that these proteins have a higher affinity for nucleoporins and may interfere with the export process. We therefore analyzed the distribution of bulk poly(A)⁺ RNA in 293 cells expressing these TAP constructs by FISH with an oligo(dT) probe. Transfected cells expressing TAP-3xUBA and TAP-4xUBA at very high levels (as judged by the intensity of the GFP signal) accumulated poly(A)⁺ RNA within the nucleus (Fig. 3M, N, Q, and R). This inhibition of bulk mRNA export was observed in about 10 and 20% of cells expressing TAP-3xUBA and TAP-4xUBA, respectively, but not in cells in which TAP-1xUBA was expressed at similar or higher levels (Fig. 3I and J). Thus, it is possible that the reduced stimulation of CAT expression observed with TAP-

reporter plasmid pCMV128-RRE is identical to pCMV128 (panel A) but carries the HIV RRE inserted in the intron, downstream of the *cat* gene. The stimulation of *cat* gene expression by TAP mutants measured in three independent experiments is expressed as a percentage of the activity of RevM10-TAP coexpressed with p15. The values are means \pm standard deviations. (E) Protein expression levels were analyzed by Western blot with anti-HA antibodies. The amount of cell extract loaded per lane was normalized to the activity of the β -Gal internal control. The positions of TAP derivatives fused to RevM10 are shown on the right. (F) RNase protection analysis was performed with cytoplasmic or total RNA fractions isolated from 293 cells cotransfected with pCMV128 and plasmid pCH110 encoding β -Gal. In lanes 3, 5, 8, and 10, plasmids encoding p15 and RevM10 or GFP fusions of TAP were cotransfected. As controls, the reporter plasmids were cotransfected with empty vectors expressing RevM10 or GFP alone together with the plasmid expressing p15 (lanes 2, 4, 7, and 9).



4xUBA (45%) relative to TAP-3xUBA (61%) is in part due to an increased inhibitory effect of this protein.

Together, these observations agree with studies showing that high-affinity interactions between nucleoporins and transport receptors are dispensable for NPC passage (30). Indeed, a high rate of transport would be impossible if the individual interactions of the receptor with nucleoporins were of high affinity (30). Consistently, by increasing the number of UBA-like domains from two to four, the affinity for nucleoporins was increased (as judged by the localization of the constructs at the nuclear rim) without a corresponding increase in the export activity. Rather, these derivatives interfered with multiple export pathways (see also below), probably by saturating binding sites at the NPC.

TAP derivatives that lack the NTF2-like scaffold but have two or three UBA-like domains stimulate mRNA export in *Xenopus* oocytes. The ability of TAP-2xUBA and TAP-3xUBA to stimulate mRNA export directly was confirmed in *X. laevis* oocytes. Oocyte nuclei were injected with a mixture of labeled RNAs and purified TAP proteins expressed in *E. coli* as GST fusions (Fig. 4C). Wild-type TAP and TAP-1xNTF2 were co-expressed with p15 to ensure the proper folding of the NTF2-like domain. TAP-2xNTF2 could not be expressed at high levels in *E. coli*. The RNA mixture consisted of U5 Δ Sm and U6 Δ ss snRNAs, the human initiator methionyl tRNA, and two mRNAs differing in their export efficiencies (8, 25). These were fushi tarazu (Ftz) mRNA and an mRNA derived from the adenovirus major late region (Ad mRNA). U6 Δ ss RNA is not exported from the nucleus and serves as an internal control for nuclear injection (38). U5 snRNA and tRNAs are exported by CRM1 and exportin-t, respectively (reviewed in reference 26).

In preliminary experiments, the concentration of TAP-2xUBA and TAP-3xUBA required to stimulate mRNA export specifically was determined. A representative example of one of these experiments is shown in Fig. 4A. Oocyte nuclei were coinjected with increasing concentrations of TAP-2xUBA or TAP-3xUBA and the RNA mixture described above. The stim-

FIG. 3. TAP-3xUBA and TAP-4xUBA localize to the nuclear rim. (A) HeLa cells were transfected with a plasmid expressing GFP-TAP. When cells were directly fixed in formaldehyde, TAP was predominantly detected throughout the nucleoplasm, excluding nucleoli (-Triton). When cells were extracted with Triton X-100 prior to fixation, a punctate labeling pattern was visible at the nuclear periphery (+Triton). (B to F) HeLa cells were transfected with plasmids expressing GFP fusions of TAP derivatives as indicated. Approximately 20 h after transfection, cells were fixed in formaldehyde and directly observed with a confocal microscope. TAP-2xNTF2, TAP-1xUBA, and TAP-2xUBA were detected throughout the nucleoplasm (B, C, and D). An additional punctate labeling pattern was visible at the nuclear rim for TAP-2xUBA. TAP-3xUBA and TAP-4xUBA localized predominantly at the nuclear rim (E, F). (G to R) Human 293 cells were transfected with plasmids encoding GFP fusions of TAP derivatives as indicated. Approximately 20 h after transfection, bulk poly(A)⁺ RNA was detected by FISH with an indocarbocyanine-labeled oligo(dT) probe. All images were taken with the same settings so the GFP signals could be compared directly. In panels K, M, O, and Q, examples of cells expressing TAP-3xUBA or TAP-4xUBA at different levels are shown. In about 10 to 20% of transfected cells, TAP-3xUBA and TAP-4xUBA were expressed at higher levels (M and Q), resulting in a strong accumulation of the poly(A)⁺ signal within the nucleus (N and R). wt, wild type.

ulation of mRNA export in the presence of these proteins and in control oocytes was determined and compared to the stimulation obtained by injecting the optimal concentration of TAP/p15 heterodimers (Fig. 4A, right panel). The effect of the proteins on the export of U5 Δ Sm RNA was taken as an indication of the specificity. The nuclear localization of U6 Δ ss RNA and the export of tRNA were not affected in the range of concentrations tested. Quantitation of the effects on Ad mRNA of coinjection of TAP-2xUBA indicated that, as for TAP/p15, this protein stimulated mRNA export specifically when its concentration in the injected samples ranged between 1 and 3 μ M (Fig. 4A and data not shown). Stimulation of mRNA export was also observed at concentrations higher than 3 μ M, but at these concentrations an inhibitory effect on the export of U5 snRNA was observed (Fig. 4A). Similarly, for TAP-3xUBA, this inhibitory effect was detected when the concentration of the protein exceeded 2 μ M (not shown).

Next, we compared the effects of the recombinant proteins on the export of each of the RNA species by microinjecting them all at the same concentration. A representative example of these experiments is shown in Fig. 4B. In this example, following a 120-min incubation period, 32% of Ad mRNA was exported in control oocytes (Fig. 4B, lanes 4 to 6). In the presence of recombinant TAP/p15 heterodimers, about 80% of the injected Ad mRNA was exported (Fig. 4B, lanes 7 to 9). When recombinant TAP-2xUBA or TAP-3xUBA was coinjected, export of Ad mRNA was stimulated up to 58 and 55%, respectively (Fig. 4B, lanes 16 to 21). TAP derivatives having a single nucleoporin-binding domain (i.e., TAP-1xUBA and TAP-1xNTF2) had a minor or no effect on the export of Ad mRNA (Fig. 4B, lanes 10 to 15, and Table 1). Stimulation of Ad mRNA export by TAP and derivatives was specific, because export of tRNA and of U5 snRNA was not stimulated (Fig. 4B). On the contrary, as shown in Fig. 4A, these proteins partially inhibited U5 snRNA export at higher concentrations. Nuclear exit of the efficiently exported Ftz mRNA was only slightly stimulated (Fig. 4B, lanes 16 to 21 versus 4 to 6).

Quantitation of the effects on Ad mRNA export of the recombinant proteins obtained in three independent experiments is reported in Table 1. Interestingly, the ability of TAP derivatives to stimulate Ad mRNA export in *Xenopus* oocytes correlated well with their ability to increase *cat* gene expression in human 293 cells (Table 1) in spite of the differences between these cell types and the cargoes analyzed.

When TAP-2xUBA and TAP-3xUBA were injected at the highest achievable concentration (25 μ M), a strong inhibition of export of several mRNA species but also of U5 snRNA and tRNA export was observed (Fig. 4D, lanes 10 to 15 versus 4 to 6). At the same concentration, wild-type TAP interfered mainly with the export pathway of U5 snRNA (Fig. 4D, lanes 7 to 9). These results are consistent with those obtained in human cultured cells and indicate that, relative to wild-type TAP, TAP-2xUBA and TAP-3xUBA have an increased ability to compete for binding to the NPC with other transport receptors.

A single nucleoporin-binding domain of TAP is sufficient to promote NPC translocation of specific CTE cargoes. The results described above show that at least two nucleoporin-binding sites are required for TAP-mediated RNA export in transfected human cells and in *Xenopus* oocytes. In contrast, we

have previously reported that export of U6-CTE chimeric RNA, which is directly mediated by TAP, can be stimulated by a TAP mutant lacking the NTF2-like domain (TAP-1xUBA) but not by TAP-1xNTF2 (1). Since these experiments were conducted in the absence of exogenous p15, it is possible that the NTF2-like domain of TAP-1xNTF2 was not properly folded. We therefore reinvestigated the ability of TAP-1xNTF2 to export U6-CTE in the presence of p15.

Xenopus oocyte nuclei were coinjected with purified recombinant proteins and a mixture of labeled RNAs consisting of dihydrofolate reductase (DHFR) and Ad mRNAs, U5 Δ Sm and U6 Δ ss snRNAs, the human initiator methionyl tRNA, and U6-CTE RNA. Following a 90-min incubation period, U6-CTE RNA was inefficiently exported in control oocytes (Fig. 5A, lanes 4 to 6). Injection of TAP/p15 heterodimers resulted in a strong stimulation of U6-CTE RNA export (Fig. 5A, lanes 7 to 9). If U6-CTE was efficiently exported, it was stable during the 90-min incubation period, whereas if U6-CTE was not exported, it was partially degraded in the nuclear fraction (Fig. 5A, lanes 7 to 9 versus 4 to 6). In contrast to the results obtained with Ad mRNA, TAP-1xNTF2 in the presence of p15 stimulated export of U6-CTE RNA almost as efficiently as wild-type TAP (Fig. 5A, lanes 13 to 15). As expected, since one nucleoporin-binding domain was sufficient to export U6-CTE RNA (Fig. 5A, lanes 13 to 18) (1), both TAP-2xUBA and TAP-3xUBA strongly stimulated U6-CTE export (Fig. 5A, lanes 10 to 12, and data not shown).

We also investigated the effects of TAP derivatives on the export of an excised intron lariat bearing the CTE. In this study, we used a precursor mRNA derived from the adenovirus major late transcription unit (pBSAd1) carrying the simian retrovirus 1 CTE mutant M38 inserted in the intron (12, 32). The M38 mutant was chosen because it has only one binding site for TAP (loop A), while the wild-type CTE has two (12). Preliminary studies indicated that export stimulation by TAP of the intron lariat bearing M38 requires the presence of at least one nucleoporin-binding site on the protein. In contrast, as reported previously, export of the intron lariat carrying wild-type CTE can be stimulated by the N-terminal domain of TAP in *Xenopus* oocytes (7).

Based on the results obtained with the M38 mutant (Fig. 5B and data not shown) and taking into account the crucial role of the C-terminal half of TAP in mediating NPC binding (1, 10, 21, 39), we currently favor the idea that the N-terminal fragment of TAP stimulates export of the intron lariat bearing wild-type CTE indirectly, probably by binding to one loop of the CTE and facilitating the recruitment of endogenous *Xenopus* TAP to the second binding site. Why this facilitated binding appears to occur only in the context of the intron lariat but not when the CTE is inserted in a linear RNA such as U6-CTE is unclear.

The excised intron lariat carrying the CTE derivative M38 was reproducibly exported more efficiently by TAP constructs with one nucleoporin-binding site than by TAP-2xUBA (Fig. 5B, lanes 10 to 15 and 16 to 18). It is noteworthy that export of the spliced Ad mRNA was also stimulated by TAP-1xUBA. Together, these results indicate that either of the two nucleoporin-binding domains of TAP is sufficient to promote NPC translocation of at least some cargoes. Furthermore, a comparison of the different substrates analyzed in Fig. 4 and 5

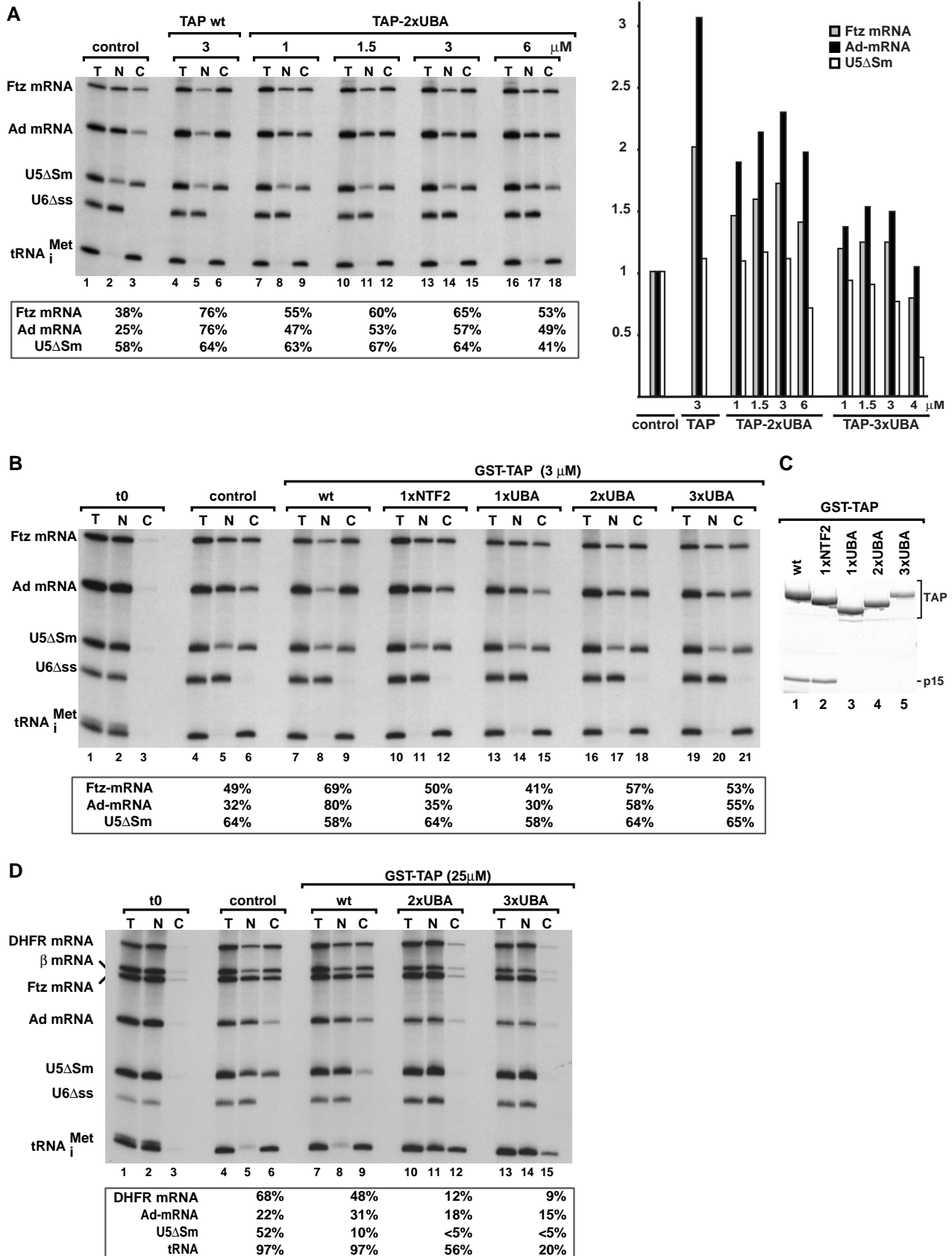


FIG. 4. TAP-2xUBA and TAP-3xUBA stimulate mRNA export in *Xenopus* oocytes. (A and B) *Xenopus* oocyte nuclei were injected with mixtures of ³²P-labeled RNAs and purified recombinant proteins as indicated. RNA samples from total oocytes (T) and nuclear (N) and

suggests that in addition to the differences in the export activity of the different forms of TAP, a second level of complexity is introduced by the requirements of different cargoes.

***Drosophila* NXF1 lacking the NTF2-like scaffold partially restores export of bulk mRNA in cells depleted of p15 or NXF1.** The possibility that the NTF2-like scaffold contributes to the interaction of TAP with cellular mRNAs or to TAP recycling after one round of export cannot be completely ruled out by the experiments described above, in which the export of specific RNAs was analyzed in the presence of excess TAP. We therefore set up an assay to test whether an NXF1 protein lacking the NTF2-like domain but carrying two UBA-like domains could equally support mRNA export in cells depleted of endogenous NXF1 or p15. This question was addressed in *Drosophila* Schneider cells (SL2 cells) because depletion of endogenous NXF1 or p15 by dsRNA interference in these cells is very efficient (15). Moreover, NXF1 or p15 depletion inhibits growth and results in a strong nuclear accumulation of poly(A)⁺ RNA, which can be monitored easily (15).

Polyclonal SL2 cell lines stably transfected with plasmids expressing GFP fusions of *D. melanogaster* NXF1, NXF1-1xUBA, or NXF1-2xUBA or GFP alone as a control were established. These cell lines are heterogeneous, and the GFP fusions are expressed at different levels in approximately 5 to 10% of the cell population. The subcellular localization of the recombinant proteins in these cell lines was investigated. All three NXF1 proteins localized predominantly within the nucleoplasm and were excluded from the nucleolus (Fig. 6A, C, and E). A clear rim staining was observed in most of the cells expressing wild-type NXF1 and NXF1-2xUBA (Fig. 6A and E). We also analyzed the distribution of poly(A)⁺ RNA by oligo(dT) in situ hybridization in the different cell lines. No nuclear accumulation of poly(A)⁺ RNA was observed (Fig. 6B, D, and F, and data not shown), suggesting that in these stably transfected cells, the recombinant proteins are expressed at levels that do not interfere with export.

Next, endogenous NXF1 or p15 was depleted from these cell lines by dsRNA interference. The efficiency of NXF1 or p15 depletion could be monitored by the dramatic inhibition of cell growth observed as early as 2 days after transfecting the corresponding dsRNAs. No recovery of cell growth was observed within 8 days after transfection (see also below) (15). The distribution of poly(A)⁺ RNA in cells expressing the GFP fusions was analyzed 5 days after addition of dsRNAs, and the percentage of cells accumulating poly(A)⁺ RNA within the

nucleus was determined in two independent experiments (Table 2).

In control cells expressing GFP, depletion of either NXF1 or p15 resulted in a severe nuclear accumulation of poly(A)⁺ RNA in about 90% of the cell population (Fig. 6H and Table 2). This was observed independently of whether GFP was expressed (Fig. 6G and H). As shown in Fig. 6H, the oligo(dT) signal was widespread in the nucleoplasm but was excluded from the large nucleolus, characteristic of SL2 cells. Expression of wild-type NXF1 partially restored export in less than 20% of cells depleted of p15 (Table 2). A similar partial restoration of export was observed in cells expressing NXF1-1xUBA, regardless of whether NXF1 or p15 had been depleted (Table 2). We defined mRNA export as partially rescued when the poly(A)⁺ signal was predominantly cytoplasmic or evenly distributed between the nucleoplasm and cytoplasm.

Expression of NXF1-2xUBA partially rescued export in approximately 50% of cells depleted of NXF1 (Table 2; Fig. 6I to L, arrowheads). An indistinguishable restoration of export by NXF1-2xUBA was observed when p15 was depleted (Fig. 6M to O and Table 2). In both cases, the restoration of bulk mRNA export by NXF1-2xUBA was partial, and in most cells a residual nuclear signal was evident. A gallery of various phenotypes is shown in Fig. 7. Cells exhibiting a poly(A)⁺ RNA signal at the nuclear rim were occasionally detected (Fig. 7F and J). Since significant cytoplasmic staining was nevertheless evident in these cells, the accumulation of bulk mRNA at the nuclear periphery suggests that in cells in which mRNA export relies only on NXF1-2xUBA, the translocation step becomes limiting.

The partial restoration of export by NXF1-2xUBA is consistent with the observation that TAP-2xUBA exhibits about 50% of the export activity of wild-type TAP (Table 1). Additionally, the extent of the restoration is likely to depend on the expression levels of the protein, as in a small percentage of cells expressing NXF1-2xUBA, a complete restoration was observed [i.e., the oligo(dT) signal was mainly detected in the cytoplasm] (Fig. 7B and H). Importantly, *D. melanogaster* NXF1-2xUBA did not accumulate within the cytoplasm in cells in which export of bulk mRNA was restored (see, for example, Fig. 7A and G), suggesting that the NTF2-like scaffold is not required for cargo release following export.

The restoration of export appeared to be complete in at least a fraction of cells expressing *D. melanogaster* NXF1-2xUBA, so we investigated whether NXF1-2xUBA could sustain growth in

cytoplasmic (C) fractions were collected 120 min after injection or immediately after injection (t_0 ; lanes 1 to 3 in panel B). RNA samples were analyzed on 8% acrylamide-7 M urea denaturing gels. One oocyte equivalent of RNA, from a pool of 10 oocytes, was loaded per lane. The numbers above the lanes in panel A indicate the concentration (micromolar) of recombinant proteins in the injected samples. The numbers in boxes below the panels represent the percentage of a given RNA in the cytoplasm 120 min after injection in the presence of the proteins indicated above the lanes. Because the nuclear localization of U6 Δ ss RNA and the export of tRNA (>94%) were not affected by any of the injected proteins, the respective values are not included. On the right of panel A, the effects of increasing concentrations of TAP-2xUBA or TAP-3xUBA on the export of U5 Δ Sm RNA and Ftz and Ad mRNAs are compared to those of TAP/p15 heterodimers. For the purpose of comparison, all values were normalized to the export observed in control oocytes. (C) TAP derivatives were expressed in *E. coli* as GST fusions, purified on glutathione-agarose beads, and visualized by Coomassie staining following SDS-polyacrylamide gel electrophoresis. (D) *Xenopus* oocyte nuclei were injected with mixtures of ³²P-labeled RNAs and purified recombinant proteins as indicated. RNA samples from total oocytes (T) and nuclear (N) and cytoplasmic (C) fractions were collected 120 min after injection or immediately after injection (t_0 ; lanes 1 to 3) and analyzed as in panels A and B. DHFR, β -globin, and Ftz mRNAs exhibited similar behavior, so only the quantitation for DHFR mRNA is shown. The nuclear localization of U6 Δ ss RNA was not affected by any of the injected proteins.

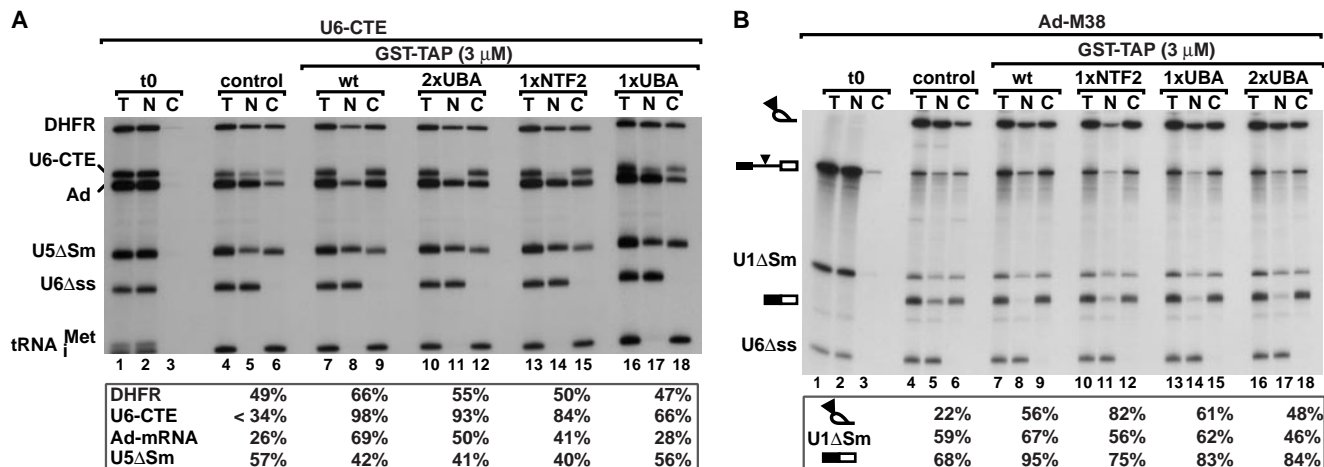


FIG. 5. TAP derivatives having a single nucleoporin-binding domain translocate specific CTE RNA cargoes across the NPC. (A and B) *Xenopus* oocyte nuclei were injected with mixtures of ³²P-labeled RNAs and purified recombinant proteins as indicated. RNA samples from total oocytes (T) and nuclear (N) and cytoplasmic (C) fractions were collected immediately after injection (t₀; lanes 1 to 3) or 90 min after injection in panel A and analyzed as described in the legend to Fig. 4. In panel B, samples were collected 120 min after injection and analyzed in 10% acrylamide-7 M urea denaturing gels. The concentration of recombinant proteins in the injected samples was 3 μM. The numbers below the panels represent the percentage of a given RNA in the cytoplasm in the presence of the proteins indicated above the lanes. The nuclear localization of U6Δss RNA and the export of tRNA (>94%) were not affected by any of the injected proteins, and these values are not included. The mature products and intermediates of the splicing reaction are indicated diagrammatically on the left of panel B. The solid triangle represents the M38 CTE. wt, wild type.

cells depleted of endogenous NXF1 or p15. Cell lines expressing *D. melanogaster* NXF1-2xUBA or GFP constitutively were depleted of endogenous *D. melanogaster* NXF1 or *D. melanogaster* p15. As reported (15), NXF1 or p15 depletion inhibits cell growth as early as 2 days after transfecting the corresponding dsRNAs (Fig. 8A). Cells were kept in culture, and growth was monitored every second day for 10 days and every week for 6 weeks. In the GFP-expressing cell line, no recovery of cell growth was observed within this period (Fig. 8A). Moreover, 32 days after transfecting NXF1 dsRNA, no surviving cells were detected (Fig. 8A). Although a fraction of cells survived p15 depletion, these cells subsequently died (Fig. 8A). In contrast, a higher percentage of cells depleted of *D. melanogaster* NXF1 or p15 but expressing *D. melanogaster* NXF1-2xUBA survived and started to grow exponentially about a month after transfection (Fig. 8B). These results suggest that expression of *D. melanogaster* NXF1-2xUBA allows NXF1- or p15-depleted cells to survive.

In the surviving cell populations, the percentage of cells expressing NXF1-2xUBA increased threefold following *D. melanogaster* NXF1 depletion and 12-fold following p15 depletion. Western blot analysis of samples collected on day 32 revealed that while the levels of endogenous NXF1 had recovered, the expression levels of p15 were about 50% of the levels detected in control cells (data not shown). Thus, expression of *D. melanogaster* NXF1-2xUBA allows NXF1- or p15-depleted cells to survive so that the expression levels of the depleted proteins are progressively restored.

DISCUSSION

Transport receptors promote translocation of cargoes across the central channel of the NPC as a result of their ability to interact with nucleoporins. In particular, the phenylalanine-

glycine (FG) repeats that characterize most nucleoporins are believed to function as docking sites for the receptors moving through the pore (31). The heterodimeric export receptor NXF1/p15 possesses two nucleoporin-binding domains, the UBA-like domain and the NTF2-like scaffold, which results from the heterodimerization of the NTF2-like domain of NXF1 with p15 (10). In this study, we show that although these two nucleoporin-binding domains are unrelated in sequence and structure, they are interchangeable. Indeed, an NXF1 derivative in which the NTF2-like scaffold is replaced by a UBA-like domain (2xUBA) has an export activity similar to that of the converse construct, in which the UBA-like domain is replaced by an NTF2-like scaffold (2xNTF2). These results indicate that the main role of the NTF2-like scaffold is to provide a nucleoporin-binding site. More importantly, although the proteins having two UBA-like domains or two NTF2-like scaffolds in tandem have reduced export activity relative to wild-type NXF1, these proteins are able to promote directional translocation of RNA cargoes across the NPC. We also show that the export activity of NXF1 is not directly related to the number of NPC-binding sites but that a minimum of two sites is required for export of cellular mRNA.

p15 acts as a structural subunit that maintains the proper folding and function of the NTF2-like domain of NXFs. In addition to its essential role in mRNA nuclear export, p15 has been reported to bind RanGTP and nucleoporins directly and to be implicated in the export of tRNA and of substrates exported by CRM1 (5, 6, 23, 28). However, other studies failed to detect a direct interaction between p15 and Ran or nucleoporins (14, 21, 39). A crystallographic analysis of p15 indicates that despite its overall similarity to NTF2, the putative binding site for Ran is occluded in p15 by residues with larger side chains that fill the equivalent hydrophobic pocket in NTF2 (10,

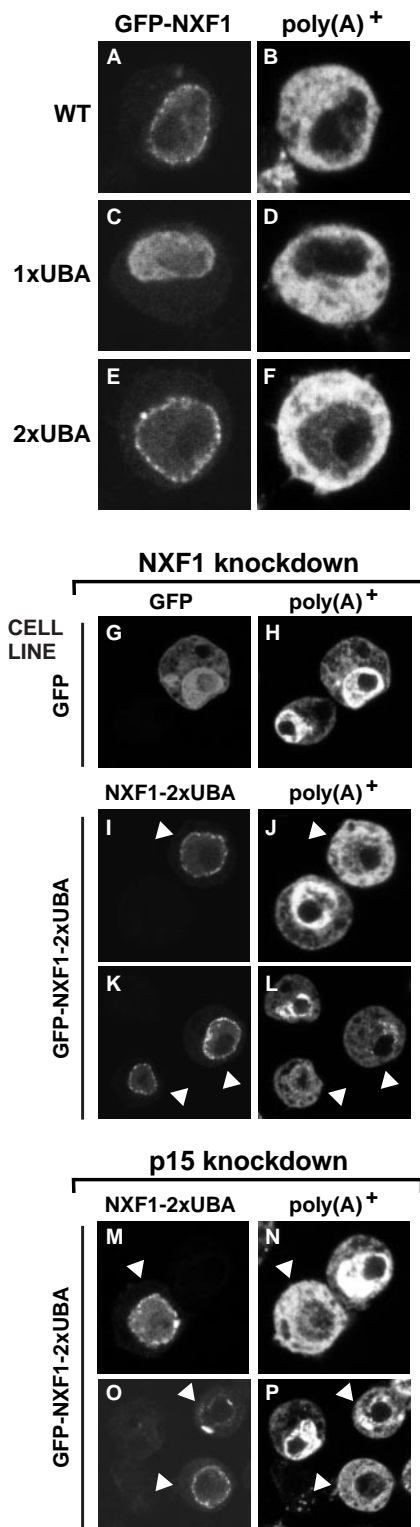


FIG. 6. *D. melanogaster* NXF1-2xUBA partially rescues export in cells depleted of NXF1. (A to F) SL2 cell lines constitutively expressing GFP fusions with wild-type NXF1 (wt), NXF1-1xUBA, or NXF1-2xUBA were fixed in formaldehyde. Bulk poly(A)⁺ RNA was detected by FISH (B, D, and F). (G to P) SL2 cells stably transfected with plasmids expressing GFP or GFP-NXF1-2xUBA were transfected with a dsRNA corresponding to the NTF2-like domain of *D. melanogaster* NXF1 (G to L) or to the coding region of *D. melanogaster* p15

TABLE 2. Percentage of cells accumulating poly(A)⁺ RNA within the nucleus following p15 or NXF1 depletion^a

| Cell line | Poly(A) ⁺ RNA accumulation (% of cells) | | | |
|----------------|--|----|---------------|----|
| | p15 depleted | | NXF1 depleted | |
| GFP | 87 | 86 | 92 | 94 |
| Wild-type NXF1 | 72 | | | |
| NXF1-1xUBA | 60 | | 67 | |
| NXF1-2xUBA | 48 | 50 | 49 | 52 |

^a The SL2 cell lines indicated in the first column were depleted of endogenous p15 or NXF1 by dsRNA interference. At least 100 cells expressing the recombinant proteins were analyzed, and the percentage of cells showing nuclear accumulation of poly(A)⁺ RNA was determined. Values were obtained in two independent experiments.

34). Binding to nucleoporins is also prevented by an additional turn of the N-terminal α -helix of p15, which occludes the hydrophobic pocket present at the equivalent position in TAP and NTF2 (2, 10). Our results, together with available structural data (10), suggest that the essential role of p15 in mRNA export is structural and is to ensure the proper folding and function of the NTF2-like domain of TAP/NXF1, which in turn mediates binding to the NPC.

Because the NTF2-like domain of NXF1 cannot bind to nucleoporins in the absence of p15, p15 offers a possible target for regulating NXF1/NPC interactions. Along these lines, it has been proposed that p15 could impose directionality on the export process by heterodimerizing with TAP in the nucleus and dissociating in the cytoplasm (22, 39). Our data do not rule out a compartment-specific regulation of NXF1/p15 interaction, but they show that if this regulation does exist, it is not strictly or generally required for directional transport. Regulation of NXF1/p15 interaction may nevertheless play a critical role in the overall efficiency of the transport process or the export of specific cargoes. For instance, some cargoes may have the ability to modulate NXF1/p15 dimerization. More generally, by controlling p15 expression levels or its ability to heterodimerize with NXF1, the overall mRNA export activity of the cell could be regulated.

In metazoa, there are multiple NXF proteins that heterodimerize with p15. With the exception of NXF1, it is unclear whether these proteins are involved in mRNA export and whether their NTF2-like domains mediate binding to nucleoporins. In this context, p15 may act as a regulator of NXF activities by functioning as a structural module that maintains the proper folding and function of the NTF2-like domains.

Requirements for NPC translocation are influenced by the cargo transported. The heterodimeric NTF2 scaffold and the UBA-like domain of TAP both feature a single nucleoporin-

(M to P). Five days after transfection, poly(A)⁺ RNA was detected by FISH with an indocarbocyanine-labeled oligo(dT) probe. In the GFP-expressing cell line, depletion of NXF1 causes nuclear accumulation of poly(A)⁺ RNA regardless of whether GFP is expressed (G and H). In the GFP-NXF1-2xUBA cell line, a strong nuclear accumulation of poly(A)⁺ RNA was observed in cells in which the protein was not detected, but when *D. melanogaster* NXF1-2xUBA was expressed at detectable levels, mRNA export was restored (I to L, arrowheads). This restoration of export was also observed when p15 was depleted (M to P).

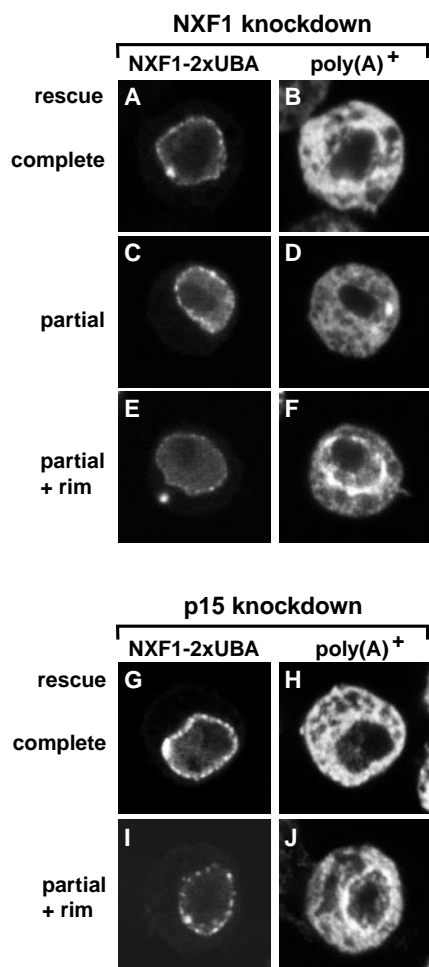


FIG. 7. Patterns of poly(A)⁺ RNA distribution in cells depleted of endogenous NXF1 or p15 but expressing GFP-NXF1-2xUBA. (A to J) Restoration of mRNA export was almost complete (B and H) or partial, with an equal distribution of the oligo(dT) signal between the nucleus and the cytoplasm (D). In panels F and J, cells in which the poly(A)⁺ RNA accumulated at the nuclear rim are shown.

binding site (10, 11). In this study, we show that either of these sites is sufficient to mediate NPC translocation of specific CTE-dependent cargoes in *Xenopus* oocytes. The CTE-bearing RNAs analyzed here are artificial, but the observation that a single nucleoporin-binding domain is sufficient to promote NPC translocation is not without precedent. In *S. cerevisiae*, Mex67p mutants lacking the UBA-like domain can still promote mRNA export when Mtr2p is overexpressed (35). However, these mutants show a conditional growth phenotype and accumulate bulk mRNA within the nucleus at the restrictive temperature (35), suggesting that two NPC-binding sites are required for efficient nuclear mRNA export. In *Drosophila* cells, *D. melanogaster* NXF1-1xUBA partially restores mRNA export in cells depleted of NXF1 or p15, although this restoration occurred only in about 20 to 30% of cells expressing the protein (Table 2). In the case of the specific CTE RNAs shown in Fig. 5, TAP derivatives having a single nucleoporin-binding site were almost as efficient as wild-type TAP in promoting

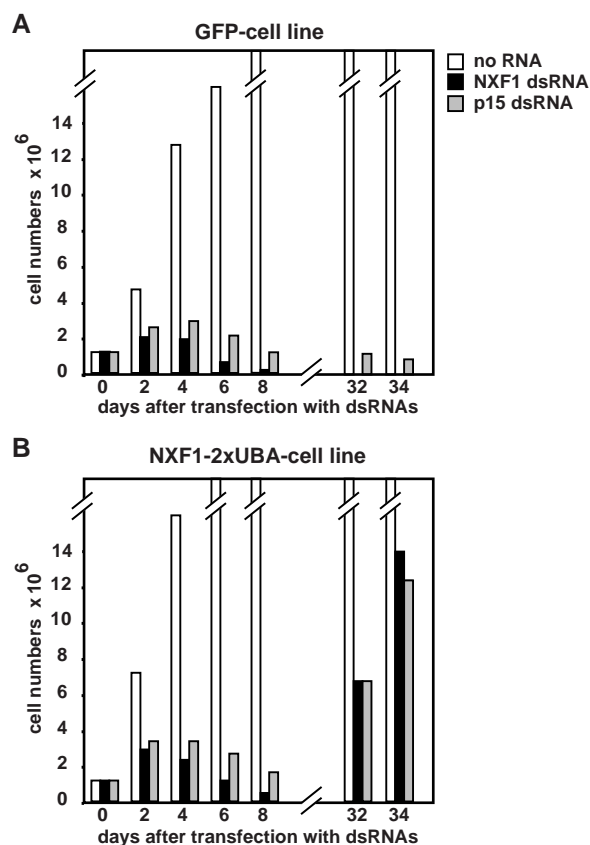


FIG. 8. NXF1-2xUBA sustains growth of cells depleted of endogenous NXF1 or p15. (A and B) SL2 cells stably transfected with plasmids expressing GFP or GFP-NXF1-2xUBA were transfected with NXF1 or p15 dsRNAs as indicated. Cell numbers were determined every second day for 8 days and every week for 6 weeks. In the GFP cell line, no cells survived NXF1 depletion. The surviving cells detected 31 days following p15 depletion died progressively after a few days. Cells expressing NXF1-2xUBA survived NXF1 or p15 depletion and started to grow exponentially 1 month after transfection of the dsRNAs.

export. This suggests that the requirements for NPC translocation are influenced by the nature of the cargo transported.

Two NPC-binding sites are required for TAP-mediated export of cellular mRNA. In contrast to the specific CTE-bearing RNAs described in this study, efficient export of cellular mRNAs requires at least two nucleoporin-binding sites that can be provided by two NTF2-like domains bound to p15 or two UBA-like domains. It can be speculated that the presence of two nucleoporin-binding pockets is a common motif for transport receptors because two binding pockets are also present on the NTF2 homodimer and at the outer surface of the N-terminal half of importin β (3, 34).

The observation that the roles of the UBA-like domain and the NTF2 scaffold are confined to nucleoporin binding raises the question of why the mRNA export receptor has evolved two distinct nucleoporin-binding domains. In vitro binding assays indicate that these domains have different relative affinities for nucleoporins (22). The presence of two nucleoporin-binding sites with different relative affinities rather than a single high-affinity binding site may facilitate a high rate of

translocation, which depends on transient interactions with nucleoporins. Another important difference between these domains is that while the nucleoporin-binding activity of the UBA-like domain is likely to be constitutive, the NTF2-like domain cannot interact with nucleoporins in the absence of p15. Thus, the binding activity of the NTF2 scaffold could be subject to regulation (see above). Finally, two binding sites may bind cooperatively to achieve an optimal affinity for nucleoporins. The NTF2-like scaffold has been reported to increase (39) and to reduce (22) the overall nucleoporin-binding affinity of the UBA-like domain. Our data are consistent with the former possibility; however, the precise mechanism by which these domains influence each other's binding remains to be determined.

Implications for the mechanism underlying directional transport. A comparison of the structures of FG-containing peptides bound to importin β and to the NTF2-like scaffold of TAP has shown similarities in the mode of FG-nucleoporin interactions between these two structurally unrelated transport factors (3, 10). Consistently, the NPC-binding domain of TAP competes with the importin β -like receptors CRM1 and exportin-t for binding sites at the NPC (Fig. 4D) (1). Thus, a similar mechanism of NPC translocation is predicted for these two families of export receptors.

The interactions of importin β -like receptors with nucleoporins and with their cargoes are regulated by Ran. However, NPC passage of these receptors on their own or in association with at least small cargoes is not obligatorily coupled to hydrolysis of GTP by Ran (reviewed in references 26 and 30). It remains to be determined whether NXF1/nucleoporin interactions are regulated (see above), but as for the importin β -like receptors, such regulation may be dispensable for translocation. As in the case of Ran-regulated export complexes, directionality may be achieved by an efficient and irreversible mechanism for cargo release that operates in the cytoplasm or at the cytoplasmic face of the NPC. The mechanism by which NXF1 releases its cargo after translocation is unknown, but it has been proposed that Dbp5, an RNA helicase essential for mRNA export in *S. cerevisiae*, may disrupt mRNA-protein interactions as the mRNP emerges from the NPC (9). Transportin, which is directly involved in TAP nuclear import, may also play a role in this process by coupling cargo release on the cytoplasmic face of the pore with NXF1 recycling back to the nucleus. Clearly, further work is needed to determine the mechanism of mRNP unloading after translocation.

ACKNOWLEDGMENTS

We thank Tom Hope for the kind gift of plasmid pCMV128 and Ann Atzberger for the fluorescence-activated cell sorting. We are grateful to Elena Conti, Jan Ellenberg, Iain Mattaj, and David Thomas for critical reading of the manuscript.

This study was supported by the European Molecular Biology Organization (EMBO) and the Human Frontier Science Program Organization (HFSPO).

REFERENCES

1. Bachi, A., I. C. Braun, J. P. Rodrigues, N. Panté, K. Ribbeck, C. von Kobbe, U. Kutay, M. Wilm, D. Görlich, M. Carmo-Fonseca, and E. Izaurralde. 2000. The C-terminal domain of TAP interacts with the nuclear pore complex and promotes export of specific CTE-bearing RNA substrates. *RNA* **6**:136–158.
2. Bayliss, R., K. Ribbeck, D. Akin, H. M. Kent, C. M. Feldherr, D. Görlich, and M. Stewart. 1999. Interaction between NTF2 and xFG-containing nucleo-

- porins is required to mediate nuclear import of RanGDP. *J. Mol. Biol.* **293**:579–593.
3. Bayliss, R., T. Littlewood, and M. Stewart. 2000. Structural basis for the interaction between FxFG nucleoporin repeats and importin β in nuclear trafficking. *Cell* **102**:99–108.
4. Bear, J., W. Tan, A. S. Zolotukhin, C. Taberero, E. A. Hudson, and B. K. Felber. 1999. Identification of novel import and export signals of human TAP, the protein that binds to the constitutive transport element of the type D retrovirus mRNAs. *Mol. Cell. Biol.* **19**:6306–6317.
5. Black, B. E., L. Lévesque, J. M. Holaska, T. C. Wood, and B. Paschal. 1999. Identification of an NTF2-related factor that binds Ran-GTP and regulates nuclear protein export. *Mol. Cell. Biol.* **19**:8616–8624.
6. Black, B. E., J. M. Holaska, L. Lévesque, B. Ossareh-Nazari, C. Gwizdek, C. Dargemont, and B. M. Paschal. 2001. NXT1 is necessary for the terminal step of Crm1-mediated nuclear export. *J. Cell Biol.* **152**:141–155.
7. Braun, I. C., E. Rohrbach, C. Schmitt, and E. Izaurralde. 1999. TAP binds to the constitutive transport element (CTE) through a novel RNA-binding motif that is sufficient to promote CTE-dependent RNA export from the nucleus. *EMBO J.* **18**:1953–1965.
8. Braun, I. C., A. Herold, M. Rode, E. Conti, and E. Izaurralde. 2001. Overexpression of TAP/p15 heterodimers bypasses nuclear retention and stimulates nuclear mRNA export. *J. Biol. Chem.* **276**:20536–20543.
9. Conti, E., and E. Izaurralde. 2001. Nucleocytoplasmic transport enters the atomic age. *Curr. Opin. Cell Biol.* **3**:310–319.
10. Fribourg, S., I. C. Braun, E. Izaurralde, and E. Conti. 2001. Structural basis for the recognition of a nucleoporin FG repeat by the NTF2-like domain of the TAP/p15 mRNA nuclear export factor. *Mol. Cell* **8**:645–656.
11. Grant, R. P., E. Hurt, D. Neuhaus, and M. Stewart. 2002. Structural basis for the interaction between the Tap C-terminal domain and FG repeat-containing nucleoporins. *Nat. Struct. Biol.* **9**:247–251.
12. Grüter, P., C. Taberero, C. von Kobbe, C. Schmitt, C. Saavedra, A. Bachi, M. Wilm, B. K. Felber, and E. Izaurralde. 1998. TAP, the human homolog of Mex67p, mediates CTE-dependent RNA export from the nucleus. *Mol. Cell* **1**:649–659.
13. Guzik, B. W., L. Lévesque, S. Prasad, Y.-C. Bor, B. E. Black, B. M. Paschal, D. Rekosh, and M.-L. Hammarskjöld. 2001. NXT1 (p15) is a crucial cellular cofactor in TAP-dependent export of intron-containing RNA in mammalian cells. *Mol. Cell. Biol.* **21**:2545–2554.
14. Herold, A., M. Suyama, J. P. Rodrigues, I. C. Braun, U. Kutay, M. Carmo-Fonseca, P. Bork, and E. Izaurralde. 2000. TAP/NXF1 belongs to a multigene family of putative RNA export factors with a conserved modular architecture. *Mol. Cell. Biol.* **20**:8996–9008.
15. Herold, A., T. Klimentko, and E. Izaurralde. 2001. NXF1/p15 heterodimers are essential for mRNA nuclear export in *Drosophila*. *RNA* **7**:1768–1780.
16. Huang, X., T. J. Hope, B. L. Bond, D. McDonald, K. Grahl, and T. G. Parslow. 1991. Minimal Rev-responsive element for type 1 human immunodeficiency virus. *J. Virol.* **65**:2131–2134.
17. Jarmolowski, A., W. C. Boelens, E. Izaurralde, and I. W. Mattaj. 1994. Nuclear export of different classes of RNA is mediated by specific factors. *J. Cell Biol.* **124**:627–635.
18. Jun, L., S. Frints, H. Duhamel, A. Herold, J. Abad-Rodriguez, C. Dotti, E. Izaurralde, P. Marynen, and G. Froyen. 2001. NXF5, a novel member of the nuclear RNA export factor family, is lost in a male patient with a syndromic form of mental retardation. *Curr. Biol.* **11**:1381–1391.
19. Kang, Y., and B. R. Cullen. 1999. The human TAP protein is a nuclear mRNA export factor that contains novel RNA-binding and nucleocytoplasmic transport sequences. *Genes Dev.* **13**:1126–1139.
20. Kang, Y., H. P. Bogerd, and B. R. Cullen. 2000. Analysis of cellular factors that mediate nuclear export of RNAs bearing the Mason-Pfizer monkey virus constitutive transport element. *J. Virol.* **74**:5863–5871.
21. Katahira, J., K. Sträßer, A. Podtelejnikov, M. Mann, J. U. Jung, and E. Hurt. 1999. The Mex67p-mediated nuclear mRNA export pathway is conserved from yeast to human. *EMBO J.* **18**:2593–2609.
22. Katahira, J., K. Sträßer, T. Saiwaki, Y. Yoneda, and E. Hurt. 2001. Complex formation between TAP and p15 affects binding to FG-repeat nucleoporins and nucleocytoplasmic shuttling. *J. Biol. Chem.* **277**:9242–9246.
23. Lévesque, L., B. Guzik, T. Guan, J. Coyle, B. E. Black, D. Rekosh, M. L. Hammarskjöld, and B. M. Paschal. 2001. RNA export mediated by Tap involves NXT1-dependent interactions with the nuclear pore complex. *J. Biol. Chem.* **276**:44953–44962.
24. Liker, E., E. Fernandez, E. Izaurralde, and E. Conti. 2000. The structure of the mRNA nuclear export factor TAP reveals a cis arrangement of a non-canonical RNP domain and a leucine-rich-repeat domain. *EMBO J.* **19**:5587–5598.
25. Luo, M.-J., and R. Reed. 1999. Splicing is required for rapid and efficient mRNA export in metazoans. *Proc. Natl. Acad. Sci. USA* **96**:14937–14942.
26. Mattaj, I. W., and L. Englmeier. 1998. Nucleocytoplasmic transport: the soluble phase. *Annu. Rev. Biochem.* **67**:256–306.
27. Nakiely, S., and G. Dreyfuss. 1999. Transport of proteins and RNAs in and out of the nucleus. *Cell* **99**:677–690.
28. Ossareh-Nazari, B., C. Maison, B. E. Black, L. Lévesque, B. M. Paschal, and

- C. Dargemont. 2000. RanGTP-binding protein NXT1 facilitates nuclear export of different classes of RNA in vitro. *Mol. Cell. Biol.* **20**:4562–4571.
29. Pasquinelli, A. E., R. K. Ernst, E. Lund, C. Grimm, M. L. Zapp, D. Rekosh, M.-L. Hammarskjöld, and J. E. Dahlberg. 1997. The constitutive transport element (CTE) of Mason-Pfizer monkey virus (MPMV) accesses an RNA export pathway utilized by cellular messenger RNAs. *EMBO J.* **16**:7500–7510.
 30. Ribbeck, K., and D. Görlich. 2001. Kinetic analysis of translocation through nuclear pore complexes. *EMBO J.* **20**:1320–1330.
 31. Ryan, K., and S. R. Wenthe. 2000. The nuclear pore complex: a protein machine bridging the nucleus and cytoplasm. *Curr. Opin. Cell Biol.* **12**:361–371.
 32. Saavedra, C. A., B. K. Felber, and E. Izaurralde. 1997. The simian retrovirus-1 constitutive transport element CTE, unlike HIV-1 RRE, utilizes factors required for cellular RNA export. *Curr. Biol.* **7**:619–628.
 33. Segref, A., K. Sharma, V. Doye, A. Hellwig, J. Huber, R. Lührmann, and E. Hurt. 1997. Mex67p, a novel factor for nuclear mRNA export, binds to both poly(A)⁺ RNA and nuclear pores. *EMBO J.* **16**:3256–3271.
 34. Stewart, M., H. M. Kent, and A. J. McCoy. 1998. Structural basis for molecular recognition between nuclear transport factor 2 (NTF2) and the GDP-bound form of the Ras-family GTPase Ran. *J. Mol. Biol.* **277**:635–646.
 35. Strässer, K., J. Basster, and E. Hurt. 2000. Binding of the Mex67p/Mtr2p heterodimer to FXFG, GLFG, and FG repeat nucleoporins is essential for nuclear mRNA export. *J. Cell Biol.* **150**:695–706.
 36. Suyama, M., T. Doerks, I. C. Braun, M. Sattler, E. Izaurralde, and P. Bork. 2000. Prediction of structural domains of TAP reveals details of its interaction with p15 and nucleoporins. *EMBO Rep.* **1**:53–58.
 37. Tan, W., A. S. Zolotukhin, J. Bear, D. J. Patenaude, and B. K. Felber. 2000. The mRNA export in *Caenorhabditis elegans* is mediated by Ce-NXF1, an ortholog of human TAP/NXF1 and *Saccharomyces cerevisiae* Mex67p. *RNA* **6**:1762–1772.
 38. Vankan, P., C. McGuigan, and I. W. Mattaj. 1992. Domains of U4 and U6 snRNAs required for snRNP assembly and splicing complementation in *Xenopus* oocytes. *EMBO J.* **11**:335–342.
 39. Wiegand, H. L., G. A. Coburn, Y. Zeng, Y. Kang, H. P. Bogerd, and B. R. Cullen. 2002. Formation of Tap/NXT1 heterodimers activates Tap-dependent nuclear mRNA export by enhancing recruitment to nuclear pore complexes. *Mol. Cell. Biol.* **22**:245–256.
 40. Wilkie, G. S., V. Zimyanin, R. Kirby, C. A. Korey, H. Francis-Lang, D. Van Vactor, and I. Davis. 2001. Small bristles, the *Drosophila* ortholog of human TAP/NXF1 and yeast Mex67p, is essential for mRNA nuclear export throughout development. *RNA* **7**:1781–1792.
 41. Yang, J., H. P. Bogerd, P. J. Wang, D. C. Page, and B. R. Cullen. 2001. Two closely related human nuclear export factors utilize entirely distinct export pathways. *Mol. Cell* **8**:397–406.
 42. Yoon, J. H., D. C. Love, A. Guhathakurta, J. A. Hanover, and R. Dhar. 2000. Mex67p of *Schizosaccharomyces pombe* interacts with Rae1p in mediating mRNA export. *Mol. Cell. Biol.* **20**:8767–8782.

2.4 Role of Cdc37 in chromosome segregation and cytokinesis

2.4.1 Paper 7:

Cdc37 is essential for chromosome segregation and cytokinesis in higher eukaryotes

Lange, B.M.H., Rebollo, E., Herold, A., and Gonzalez, C. (2002) *EMBO J* **21**, 5364-5374.

Context

The work presented in this paper was mainly carried out in the Gonzalez laboratory at EMBL. They have studied the phenotype of different *Drosophila* strains harboring mutations in the *cdc37* gene. Cdc37 had previously been shown to be required for the activity and stability of protein kinases that regulate cell cycle progression. As our laboratory has successfully applied the RNAi technique to deplete Schneider cells of endogenous proteins, we started a collaboration and performed experiments involving the silencing of *cdc37* in this cell line. The data obtained by depleting Cdc37 from Schneider cells strongly supported and extended the results obtained by studying *Drosophila* mutant strains.

Summary of results and conclusions

The process of spermatogenesis in four different *cdc37* mutant backgrounds was studied in fixed preparations and by time-lapse video microscopy. The mutations in the *cdc37* gene were shown to cause cytokinesis failure in spermatocytes accompanied by defects in chromosome segregation and abnormalities in spindle morphology. To investigate the function of Cdc37 in mitotic cells, we silenced *cdc37* expression in Schneider cells and compared the resulting phenotype with the effects observed after depletion of the Aurora B kinase. We demonstrated that cell proliferation was inhibited in Cdc37- and Aurora B-depleted cells, and that the depleted cells were abnormally large, often with multiple, large and abnormally shaped nuclei. Moreover, the DNA content of these cells was increased, as shown by FACS analysis. These results were consistent with cytokinesis failure and problems in chromosome segregation seen in mutant spermatocytes.

Furthermore, a functional association of endogenous Cdc37 and Aurora B was demonstrated. Cdc37 co-immunoprecipitated with Aurora B in mitotic extracts from mammalian cells. This interaction was disturbed by the drug geldanamycin (GA), an inhibitor of the Hsp90:Cdc37 complex. Consistently, kinase activity of the immunoprecipitated Aurora B kinase was also inhibited by this drug. Importantly, in a cancer line (A549) this functional association of Cdc37 and Aurora B was disturbed.

Western blot experiments demonstrated that the stability of Aurora B was dependent on the Hsp90:Cdc37 complex: first, cells treated with the Hsp90 inhibitor GA had reduced steady levels of Aurora B. Second, *Drosophila cdc37* mutants had diminished Aurora B levels. Third, Schneider cells depleted of Cdc37 by RNAi contained reduced amounts of Aurora B. Consistently, these cells had lower Aurora B levels as judged by immunofluorescence. These cells also exhibited aberrations in spindle morphology.

The association of Cdc37 and Aurora B was further confirmed by immunofluorescence in HeLa cells. Cdc37 was found to colocalize with Aurora B on spindle microtubules and the midbody. A co-sedimentation assay revealed that Cdc37 interacts with microtubules *in vitro*.

Altogether, these data show that Cdc37 and the Cdc37:Hsp90 complex are essential to maintain the stability of Aurora B. Interfering with Cdc37 function leads to the lack of a central spindle, aberrant chromosome segregation and cell cycle arrest.

Contribution

My contribution to this paper was part of a collaboration and mainly technical. I carried out the depletion of Cdc37 from Schneider cells by RNAi including the growth curve and preparation of extracts for Western blotting. I have contributed to Figures 4 and 6. My overall contribution is about 10%.

Cdc37 is essential for chromosome segregation and cytokinesis in higher eukaryotes

Bodo M.H.Lange¹, Elena Rebollo,
Andrea Herold² and Cayetano González

European Molecular Biology Laboratory, Cell Biology and Biophysics Programme and ²Gene Expression Programme, Meyerhofstrasse 1, D-69117 Heidelberg, Germany

¹Corresponding author
e-mail: Blange@EMBL-Heidelberg.de

Cdc37 has been shown to be required for the activity and stability of protein kinases that regulate different stages of cell cycle progression. However, little is known so far regarding interactions of Cdc37 with kinases that play a role in cell division. Here we show that the loss of function of Cdc37 in *Drosophila* leads to defects in mitosis and male meiosis, and that these phenotypes closely resemble those brought about by the inactivation of Aurora B. We provide evidence that Aurora B interacts with and requires the Cdc37/Hsp90 complex for its stability. We conclude that the Cdc37/Hsp90 complex modulates the function of Aurora B and that most of the phenotypes brought about by the loss of Cdc37 function can be explained by the inactivation of this kinase. These observations substantiate the role of Cdc37 as an upstream regulatory element of key cell cycle kinases.

Keywords: Aurora B/Cdc37/cell cycle/cytokinesis/mitosis

Introduction

Cell division in eukaryotes is regulated by mechanisms that are tightly controlled in both time and space (Pines, 1999). This control is exerted by an interplay of mitotic kinases and phosphatases (for an overview, see Nigg, 2001). So far, little is known about the components required to activate and to maintain this regulatory machinery. One such component is Cdc37. Initially isolated in *Saccharomyces cerevisiae* (Reed, 1980), highly conserved homologues of Cdc37 were later identified in *Drosophila* (Cutforth and Rubin, 1994), vertebrates (Stepanova *et al.*, 1996; Huang *et al.*, 1998) and many other organisms (reviewed by Hunter and Poon, 1997; Stepanova *et al.*, 1997). Cdc37 is often associated with members of the Hsp90 heat shock family and interacts with kinases involved in signal transduction, cell growth and differentiation, such as v-src (Dey *et al.*, 1996), Raf (van der Straten *et al.*, 1997; Silverstein *et al.*, 1998; Grammatikakis *et al.*, 1999), sevenless (Cutforth and Rubin, 1994), MPS1 (Schutz *et al.*, 1997), Cdc28 (Gerber *et al.*, 1995), cdk4 (Dai *et al.*, 1996; Stepanova *et al.*, 1996) and others. A genetic interaction has also been described for Cdc37 and cdc2 in *Drosophila* (Cutforth and Rubin, 1994). Cdc37 has, independent of Hsp90, an inherent

chaperon activity, e.g. for casein kinase II (Kimura *et al.*, 1997).

The knowledge we have so far about Cdc37 is limited in several aspects. First, little is known about the function of this protein in mitosis. Secondly, we do not know its spatial and temporal arrangement in the cell and last, but not least, it is likely that we are still missing important Cdc37 substrates (Hunter and Poon, 1997). Here we show that Cdc37 is required for chromosome condensation and segregation, central spindle formation and cytokinesis. We also show that Cdc37 interacts with and is required for the stability of Aurora B (the generic name for AIM-1, Aurora 1, AIR-2, ARK2, Aik2 and AIRK2; see Nigg, 2001), a kinase whose loss of function leads to phenotypes that are very similar to those brought about by inactivation of Cdc37. We propose that inactivation of Aurora B is the main cause of the abnormal phenotypes observed when Cdc37 is abrogated.

Results

Mutations in the Cdc37 gene cause cytokinesis failure in *Drosophila* spermatocytes

To study the function of Cdc37 we used four different mutant alleles, which were originally identified as lethal dominant enhancers of the *sevenless* mutation in *Drosophila* (Cutforth and Rubin, 1994). These alleles include an inversion (e1C), an in-frame deletion of amino acids 26–28 (e1E), a non-sense mutation leading to a stop codon after amino acid 6 (e4D) and a single amino acid replacement at position 338 (e6B). To determine the role of Cdc37 during cell division in *Drosophila*, we studied the phenotype of all three trans-heteroallelic combinations between the strong hypomorphic alleles Cdc37^{e1C}, Cdc37^{e1E} and Cdc37^{e4D} and the weaker hypomorph Cdc37^{e6B} (Cutforth and Rubin, 1994). All these combinations become lethal around the third instar larval stage, thus only allowing for the observation of male meiosis in Cdc37 mutant backgrounds at this stage. All three combinations at this stage have spermatids with a phenotype characteristic of cytokinesis failure. This is apparent in the four nuclei that are associated with a single mitochondrial derivative as the result of two meiotic cycles (Figure 1E and F) without cell division. In addition, the variant size of the nuclei (Figure 1E and F) is evidence for aberrant chromosome distribution between the nuclei in the meiotic division (Gonzalez *et al.*, 1989; Fuller, 1993). Defects were also detected in the spindle morphology of the mutant cells, which were stumpy (Figure 1D) when compared with the control cells (Figure 1A). In spite of these major defects, spermatids with sperm tails are still formed (data not shown). The number and unequal size of the nuclei in the spermatids indicate not only a failure in cytokinesis but also argue for further defects in chromo-

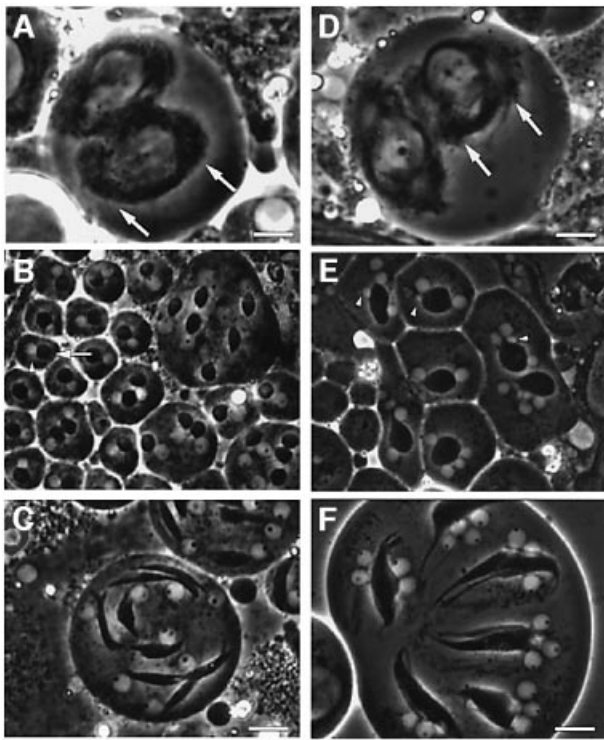


Fig. 1. Mutations in the *Cdc37* gene lead to failure of cytokinesis. Larval testis squash preparations of *Drosophila* visualized by phase microscopy. (A–C) Control heterozygous testis with: (A) normal metaphase spindle morphology (arrows indicate the length of metaphase spindle, scale bar = 8 μ m); (B) single (phase bright) nuclei (arrowhead) attached to single (phase dark) mitochondrial derivatives (arrow) in spermatids; and (C) spermatids with elongating mitochondrial derivatives. Scale bar = 12 μ m. (D–F) Transheterozygous mutant testis show: (D) abnormal stumpy shaped metaphase spindles (arrows indicate the length of metaphase spindle, scale bar = 8 μ m); (E) multiple unequally sized nuclei (arrowheads) attached to mitochondrial derivatives in spermatids (small arrowheads mark micro-nuclei); and (F) four unequally sized nuclei (arrowheads) attached to single elongating mitochondrial derivatives. Scale bar = 12 μ m.

some segregation. This led us to investigate the mechanism of chromosome segregation in live *Drosophila* spermatocytes.

Correct chromosome condensation, central spindle assembly and chromosome segregation in *Drosophila* spermatocytes requires functional *Cdc37*

To further investigate the abnormal phenotypes brought about by mutation in *Cdc37*, we followed meiosis in mutant spermatocytes by time-lapse video microscopy (Rebollo and González, 2000). Heterozygous control larvae show normal chromosome condensation at prometaphase I (Supplementary videos 1 and 2, available at *The EMBO Journal Online*). Bivalents align properly at the metaphase plate during metaphase I (Figure 2A, time point 0') and the homologues separate during anaphase I (Figure 2A, time point 4'). After segregation, the chromatin decondenses (Figure 2A, time point 10') and the two daughter nuclei form at the time the cytokinesis furrow constricts the dividing cell (Figure 2A, time point 20'; Supplementary videos 1 and 2). This is in contrast to the mutants, where at anaphase I chromosomes

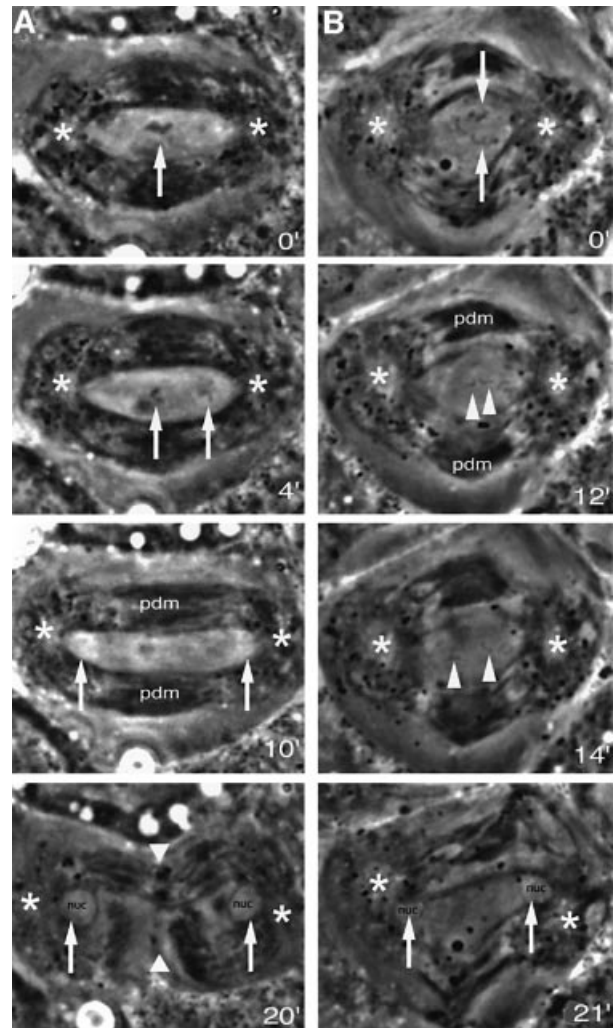


Fig. 2. Chromosome condensation, chromosome segregation and cytokinesis fail in *Cdc37* mutant spermatocytes. Video stills of *Drosophila* primary spermatocytes. The numbers indicate the time points (in minutes) corresponding to each still of the sequence. The full video sequences from which these stills have been taken are attached as Supplementary data (videos 1–4). (A) Control primary spermatocyte tracked from late metaphase I to the completion of cytokinesis. The bivalents (arrows) are fully condensed and aligned at the metaphase plate (time point 0'). At anaphase I (time point 4'), the homologues of each bivalent (arrows) move towards the poles. During anaphase B the chromatin becomes decondensed at the poles (arrows) as the spindle lengthens (time point 10'). Finally, the two daughter nuclei (arrows) are surrounded by the nuclear membrane and the cleavage furrow (arrowheads) has progressed far enough that two daughter cells can be distinguished (time point 20'). (B) *Cdc37* mutant primary spermatocyte tracked from metaphase I to the end of the first meiotic division. At metaphase I the spindle is abnormally stumpy and the chromosomes are not fully condensed (time point 0'). The bivalents (arrows) are not aligned in a normal metaphase plate. After the onset of anaphase I (time point 12') sister chromatid cohesion is released, signalled by the separated sister chromatids of the amphitelic chromosome (arrowheads), while the rest of the chromosomes have already reached the poles. Subsequently, the sister chromatids (arrowheads) move to the poles (time point 14'). The distribution of the parafusorial membranes and mitochondria around the spindle is distorted (time point 21'). The nuclear membrane is reformed around the two daughter nuclei but the cytokinesis furrow invagination is absent. As a result of the cytokinesis failure a binucleated cell is formed. pdm, phase dense parafusorial membranes; nuc, nucleus; *, centrosome.

are poorly condensed and often fail to align in a proper metaphase plate (Figure 2B, time point 0'; Supplementary video 3). The overall distance between the two centro-

somes at metaphase is shorter ($16.8 \mu\text{m} \pm 0.9$) than in control cells ($20.5 \mu\text{m} \pm 1.8$) and the overall shape of the mutant spindle is stumper (compare Figure 1A and D with 2B). During metaphase, the homologues split apart asynchronously and the first signs of splitting are observed 5.9 ± 2.7 min ($N = 6$) before the onset of poleward movement, earlier than in control cells (1.2 ± 0.8 min; $N = 5$). During anaphase, segregation mistakes are obvious. Some chromosomes acquire an amphitelic orientation (Figure 2B, time point 12'), i.e. with both sister kinetochores orientated to opposite poles (Roos, 1976). Premature sister chromatid separation takes place as the amphitelic chromosomes segregate their chromatids during anaphase I (Figure 2B, time point 14'). Single chromatids are also observed at different positions within the anaphase spindle (see Supplementary videos 3 and 4). After segregation the chromatin decondenses and the daughter nuclei are formed (Figure 2B, time point 21'; Supplementary videos 3 and 4). No sign of furrow constriction is detected and cytokinesis does not occur giving rise to binucleated cells (Figure 2B, time point 21') that sometimes might contain additional micronuclei (Figure 1E and F).

To assess the possible involvement of the spindle microtubules in chromosome mis-segregation and cytokinesis failure in *Cdc37* mutants, we examined heteroallelic mutants in a GFP- α -tubulin background. Time-lapse analysis of spermatocytes (Figure 3; Supplementary videos 5 and 6) revealed four major defects. First, in the mutant cells (Figure 3B, time point 0) the kinetochore fibers are reduced both in size and in density compared with wild-type (Figure 3A, time point 0). Secondly, at late anaphase the dense bundles of microtubules that run along the membrane at the area where furrowing will occur in the control (Figure 3A, time point 7) are absent in the mutant cells (Figure 3B, time point 13). Thirdly, in the mutants no central spindle is formed (Figure 3B, time point 38) as opposed to the control cells (Figure 3A, time point 13). Finally, while the midbody can be clearly identified in control cells (Figure 3A, time point 20), it is absent in the *Cdc37* mutant spermatocytes (Figure 3B, time point 44). From these observations, we concluded that several aspects of microtubule organization are severely disrupted in *Cdc37* mutant spermatocytes and that these alterations contribute to the complex phenotype displayed. In particular, since it is well established that the central spindle is critical for cytokinesis (reviewed by Glotzer *et al.*, 2001), its absence in the mutant spermatocytes is likely to be the cause of cytokinesis failure in these cells.

Cdc37 is known to act as a kinase-targeting subunit of the Hsp90 complex, therefore being required for the stability and activity of a number of kinases. It is thus likely that the phenotypes brought about by the inactivation of *Cdc37* are due to the inactivation of one or more of such protein kinases. Interestingly, these phenotypes are very reminiscent of those reported due to loss of Aurora B. (Adams *et al.*, 2001; Giet and Glover, 2001). Therefore, we decided to study whether inactivation of Aurora B was likely to contribute to the alterations observed in *Cdc37* mutant cells.

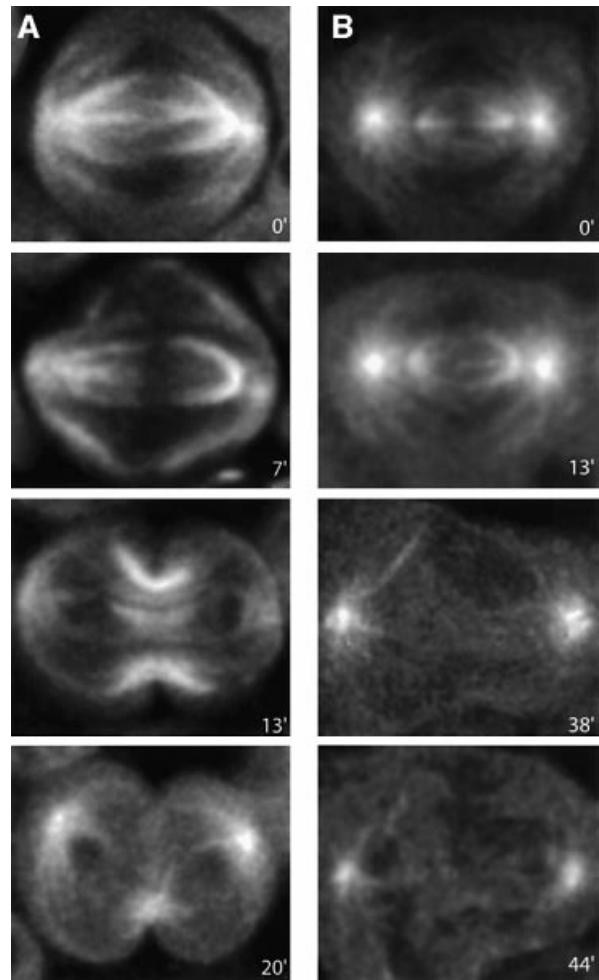


Fig. 3. The central spindle in *Cdc37* mutants fails to be assembled properly. Real-time imaging of α -tubulin-GFP in control (A) and *Cdc37* mutant (B) spermatocytes, followed from late metaphase I until the end of the first meiotic division. The full video sequences from which these stills have been taken are attached as Supplementary data (videos 5 and 6). (A, time point 0) Control spermatocytes show at metaphase I a well defined morphology of astral and kinetochore microtubule bundles. (B, time point 0) In the *Cdc37* spermatocytes asters appear normal, but the spindle is reduced both in size and density of microtubules, especially the kinetochore fibers. (A, time point 7) During wild-type anaphase I, the spindle progressively depolymerizes between the two sets of migrating chromosomes, as microtubule density increases at the spindle poles. Dense bundles of microtubules appear at this stage, which run along the plasma membrane from the asters to the position where the cleavage furrow will be formed. These bundles are not observed in the *Cdc37* mutants (A and B, time point 13) The central spindle becomes evident during the ingression of the cleavage furrow. The two incipient daughter nuclei can be seen as two dark areas at both spindle poles. (B, time point 38) No central spindle is formed in the *Cdc37* spermatocytes. Instead, disorganized bundles of microtubules run from the asters to different positions of the cell surface, at a very delayed time point when compared with the central spindle formation in the control cells. (A, time point 20) At the end of cytokinesis the asters and the midbody can be observed in the control spermatocytes. (B, time point 44) Only the asters are evident in the *Cdc37* spermatocytes at a time at which cytokinesis should have been completed long ago. The lack of a midbody is evident.

RNA interference (RNAi) reveals a functional role of *Cdc37* in cytokinesis and cell cycle progression in *Drosophila* SL2 cells

Having shown that *Cdc37* is essential for chromosome segregation and cytokinesis in meiosis, we investigated the

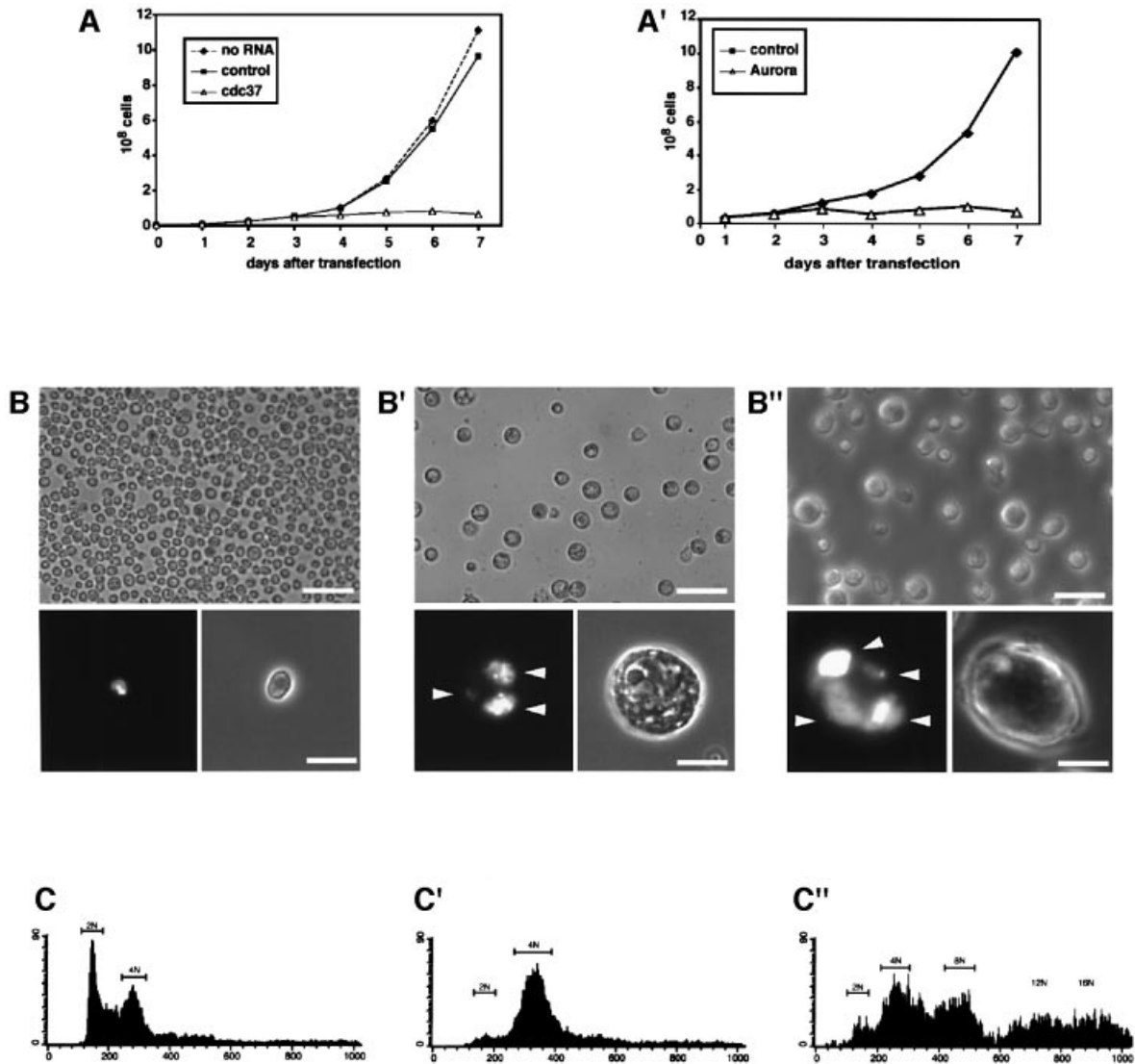


Fig. 4. Cdc37 RNAi leads to cytokinesis failure and blocks cell cycle progression. RNAi with control dsRNA (A, A', B and C), Cdc37 dsRNA (A', B' and C') and Aurora B dsRNA (A', B'' and C'') analysed by cell growth (A and A'), morphology and DNA (B–B'') and cell cycle distribution (C–C''). Cdc37 and Aurora B RNAi lead both to abnormally enlarged cells with multiple unequal sized nuclei. (A) The growth of control cells and cells without treatment is exponential, while Cdc37 dsRNA-treated cells do not increase in number 3 days after transfection. (A') Cells treated with Aurora B dsRNA do not increase in number after 2 days of treatment as compared with control cells. (B) Control cells visualized by phase microscopy display a normal cell size distribution. Lower panel of (B): Examined by fluorescence microscopy, cells have one uniformly shaped nucleus revealed by DAPI staining. (B') Depletion of Cdc37 by RNAi results after 5 days of treatment in large cells with multiple nuclei (lower panel of B', see arrowheads) of unequal size, or cells with abnormally deformed DNA. (B'') Depletion of Aurora B by RNAi results after 3 days of treatment in large cells with multiple nuclei (lower panel of B'', see arrowheads) of unequal size or cells with abnormally deformed DNA. (C) FACS analysis of control cells with apparent G₁ (2N), S and G₂ (4N) DNA content. (C') FACS analysis reveals a cell cycle distribution with the majority of cells possessing a 4N DNA content much different to controls. The cells with 2N DNA content are greatly reduced in number. (C'') FACS analysis reveals a cell cycle distribution with the majority of cells possessing a 4N and 8N DNA content and higher, much different to controls. The cells with 2N DNA content are greatly reduced in number. Scale bar in (B) and (B') top panels = 40 μ m. Scale bar in (B) and (B') lower panels = 10 μ m.

function of Cdc37 via an independent approach in mitotic cells. To this end, we ablated Cdc37 by RNAi (Clemens *et al.*, 2000) in *Drosophila* SL2 cells and compared the results with the phenotypes produced by Aurora B RNAi inactivation in these cells. Depletion of Cdc37 inhibited cell proliferation starting 3 days after transfection (Figure 4A), Aurora B depletion inhibited proliferation already after 2 days (Figure 4A'), while control cells [incubated with GFP double stranded (ds) RNA and without dsRNA] followed exponential growth (Figure 4A and A'). Phase contrast and immunofluorescence micro-

scopy analysis revealed that most Cdc37 dsRNA-treated cells (Figure 4B') had grown abnormally large, i.e. 3–4 times the size of control cells (compare Figure 4B with B') and Aurora B dsRNA-treated cells increased more than 4 times in size (Figure 4B''). Both Cdc37 and Aurora B dsRNA treated cells contained multiple abnormally shaped and unequally sized nuclei (Figure 4B' and B'', lower panels) indicating cytokinesis failure and problems in chromosome segregation. In addition, these cells also had an increased DNA content. Propidium iodide labelling and subsequent FACS analysis (Figure 4C–C'') revealed

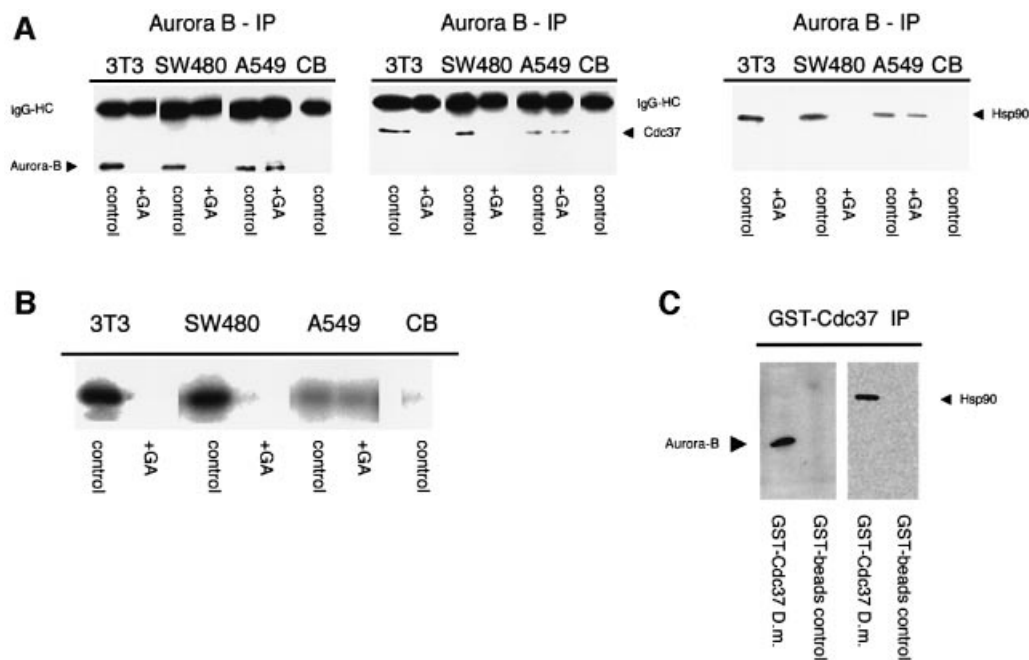


Fig. 5. Aurora B, Cdc37 and Hsp90 are part of the same protein complex in human and *Drosophila* cells but their normal association and kinase activity is disturbed in cancer cells. (A) Cdc37 co-immunoprecipitates with Aurora B from mitotic extracts of NIH 3T3, SW480 and to a lesser extent A549 cells, using the mAb anti-Aurora B. Control beads (CB) exposed to mitotic cell extract carry neither Aurora B nor Cdc37. Hsp90 is also associated with Aurora B in all three different cell lines but not with control beads. There is no Aurora B kinase activity after GA treatment. (B) *In vitro* kinase assay on histone H3 substrate. The kinase activity from immunoprecipitated Aurora B is strongly reduced when isolated from cells treated with GA. The Aurora B activity in A549 is inherently lower in control or GA-treated cells. CB exposed to mitotic cell extract show no kinase activity. The Cdc37/Aurora B protein complex is conserved between humans and *Drosophila*. (C) GST-Cdc37 pulls down Aurora B and Hsp90 from *Drosophila* early embryo extracts, as revealed with an anti-Aurora B rabbit polyclonal antibody and anti-Hsp90 rat mAb.

that the majority of Cdc37 RNAi-treated cells (75%) had a 4N DNA (Figure 4C') content, while Aurora B RNAi-treated cells exhibit an even higher degree of ploidy (Figure 4C''). Thus, Cdc37 RNAi cells had accomplished one round of DNA synthesis but had not undergone further rounds of synthesis as detected in the Aurora B dsRNA-treated cells. These results are consistent with cytokinesis failure and problems in chromosome segregation seen in Cdc37 mutant spermatocytes. They are also consistent with the hypothesis that inactivation of Aurora B might be a major contributing factor to the phenotypes brought about by inactivation of Cdc37. Taken together, these results indicate that Cdc37 function is required for cell cycle progression and cytokinesis in meiotic and mitotic cells.

Cdc37 and Aurora B are part of a molecular complex

To determine whether Cdc37 and Aurora B are part of a molecular complex, we performed co-immunoprecipitation assays in mitotic extracts from mammalian tissue culture cells and in *Drosophila* embryonic extracts. We found that Cdc37 co-immunoprecipitates with Aurora B and Hsp90 (Figure 5A) in a number of different cell lines: NIH 3T3, a mouse fibroblast cell line; SW480, a colorectal adenocarcinoma cell line; and A549, a lung carcinoma cell line. This association is absent in cells that were treated with geldanamycin (GA), an inhibitor of the Hsp90/Cdc37 complex (Pearl and Prodromou, 2000), indicating a functional relationship between Cdc37/Hsp90 and

Aurora B. Interestingly, Aurora B binds less Cdc37 and Hsp90 in A549 cells when compared with the two other cell lines, and moreover, this interaction seems to be independent of GA treatment (Figure 5A).

This raised the question of whether Aurora B in these cells has the same kinase activity as in cells where Aurora B co-immunoprecipitates with higher amounts of Cdc37. We therefore assayed the kinase activity of immunoprecipitated Aurora B on its natural substrate histone H3 *in vitro*. Kinase activity was high of Aurora B immunoprecipitated from NIH 3T3 cells and SW480 cells but lower from A549 cells (Figure 5B). Moreover, GA treatment of NIH 3T3 cells and SW480 cells resulted in strongly reduced kinase activity. In A549 cells the kinase activity was not affected by the GA treatment. These results confirm that a functional association of the endogenous Aurora B and Cdc37 exists, and that this relationship is disturbed in the A549 cells.

Binding assays in extracts of early *Drosophila* embryos showed that bacterially expressed GST-Cdc37 pulls down Aurora B and Hsp90 (Figure 5C), suggesting that the association between Aurora B, Hsp90 and Cdc37 is conserved between *Drosophila* and mammalian cells.

Aurora B stability is maintained by Cdc37 through the Hsp90/Cdc37 complex in wild-type, but not cancer cells

Based on the molecular association between Aurora B and Cdc37, our next approach was to test whether Cdc37 function is required to maintain Aurora B stability.

Initially, we examined whether the stability of Aurora B could be dependent upon the function of the Hsp90/Cdc37 complex. We made use of the Hsp90 inhibitor GA; incubation with this drug leads to the destabilization of Hsp90 substrate proteins (Pratt and Toft, 1997). Following drug treatment, Aurora B levels were reduced in the human primary cell line Hs68, the colorectal adenocarcinoma cell line SW480 and the *Drosophila* cell line SL2, but not in the lung carcinoma A549 cell line (Figure 6A). These results indicate that Aurora B is likely to be a substrate of the Cdc37/Hsp90 complex and that this interaction is conserved between mammals and *Drosophila*. This is not the case in the A549 cell line, where Aurora B is not degraded, suggesting that a normal interaction between Cdc37/Hsp90 and Aurora B is disturbed, supported also by results that comparatively little Cdc37 co-immunoprecipitated with Aurora B from this cell line.

We then investigated the dependency of Aurora B stability on Cdc37 function in *Drosophila* mutants. We found that testis from third instar larval stages of trans-heteroallelic Cdc37 mutants contained reduced levels of Aurora B when compared with the heterozygous control tissue (Figure 6B). α -tubulin was used as a loading control. The same result was obtained from brain tissue (data not shown). Similar results were also obtained when we compared the Aurora B level in SL2 cells depleted of Cdc37 by RNAi (Figure 6C). These results are in good agreement with the inhibition of cell proliferation that occurs 2 days after transfection with Aurora B RNAi and 3 days after transfection with Cdc37 RNAi.

To understand the consequences of the Aurora B destabilization in the RNAi experiment, we analysed the RNAi and control cells by immunofluorescence microscopy with antibodies against tubulin and Aurora B. We looked at cells 2–4 days after dsRNA treatment, and analysed spindle morphology and the distribution of Aurora B. In control cells, we could detect normally organized spindles (Figure 6D, top panel, first column) with the Aurora B kinase localized to the spindle midzone (Figure 6D, top panel, second column and yellow in superimposition). However, in Cdc37 dsRNA-treated cells and in Aurora B dsRNA-treated cells, severe aberrations in spindle morphology were observed. These include a strongly reduced central spindle and reduced labelling of Aurora B (Figure 6D, middle panel, and see arrowheads in the bottom panel, second column). Especially in the midzone, Aurora B was detected only weakly (Figure 6D, middle panel, and see arrowheads in the bottom panel, second column). In addition to the spindle defects, abnormally segregated DNA and DNA bridges were produced (data not shown).

Cdc37 is localized to the spindle and the midbody and associates with microtubules in mitotic cell extracts

A general cytoplasmic and perinuclear localization of Cdc37 has been described previously (Cutforth and Rubin, 1994; Stepanova *et al.*, 1996). Its function in mitosis, however, led us to re-examine its localization throughout the cell cycle. We could confirm the cytoplasmic and perinuclear localization by immunofluorescence microscopy in interphasic mammalian cells (NIH 3T3, SW480

and HeLa) (Figure 7A and B). However, using single labelling with anti-Cdc37 antibodies or double labelling together with an anti- α -tubulin antibody (data not shown), we could detect a distinct labelling in the central spindle and in the midbody. Moreover, Cdc37 co-localizes with Aurora B on the spindle microtubules and midbody (Figure 7D–F). In addition, we performed *in vitro* microtubule-pelleting assays to test whether this localization of Cdc37 could be due to microtubule binding in mitosis. Extracts from mitotically enriched HeLa and SW480 cells were incubated at 37°C in the presence of taxol to polymerize and stabilize microtubules from endogenous tubulin. Control extracts were incubated with nocodazole to depolymerize microtubules. The microtubules and associated proteins were subsequently pelleted. Only the microtubule-containing pellets carried Cdc37 while the pellets of the nocodazole-treated extracts did not, indicating a specific association of Cdc37 with microtubules (Figure 7G). Some of the Cdc37 protein remained in the supernatant in the taxol-treated samples (Figure 7G) indicating that not all the pool of Cdc37 associates with microtubules. Microtubule pelleting was also carried out using interphase extracts, in which Cdc37 did not pellet with microtubules (data not shown).

To further elucidate whether the microtubule association of Cdc37 is direct or indirect, we used pure proteins (*Escherichia coli* expressed GST–Cdc37 and phosphocellulose purified bovine brain tubulin) in an *in vitro* binding assay. From these experiments, we concluded that binding of Cdc37 to microtubules requires additional factors (or modifications), as recombinant GST–Cdc37 only binds microtubules in the presence of a mitotic extract (Figure 7H). Hence, the association with the mitotic spindle and its molecular association with the Aurora B kinase are fully consistent with the role of Cdc37 in cytokinesis.

Altogether, our molecular and cytological data established that the function of Cdc37 and the Cdc37/Hsp90 complex are essential in wild-type cells to maintain stability of Aurora B in diverse tissues and cells of *Drosophila* and humans. Interfering with Cdc37 function leads to lack of a central spindle, aberrant chromosome segregation and cell cycle arrest. Interestingly, the interaction between Aurora B and Cdc37 is defective in certain cancer cells.

Discussion

We have found that loss of Cdc37 function in *Drosophila* results in a series of abnormal phenotypes that affect chromatin condensation, spindle elongation, chromosome pairing and segregation, organization of the central spindle and cytokinesis. Since Cdc37 is known to target kinases to Hsp90, which are stabilized by this chaperone (Dai *et al.*, 1996; Stepanova *et al.*, 1996; Grammatikakis *et al.*, 1999), it was likely that the observed phenotypes could be the result of the inactivation of one or more of these kinases. One possible candidate is Polo, which is known to be stabilized by Hsp90 (Simizu and Osada, 2000; de Carcer *et al.*, 2001) and whose loss of function gives rise to phenotypes (Sunkel and Glover, 1988; Herrmann *et al.*, 1998) that are reminiscent of some of those brought about by loss of Cdc37. However, the correlation is much more

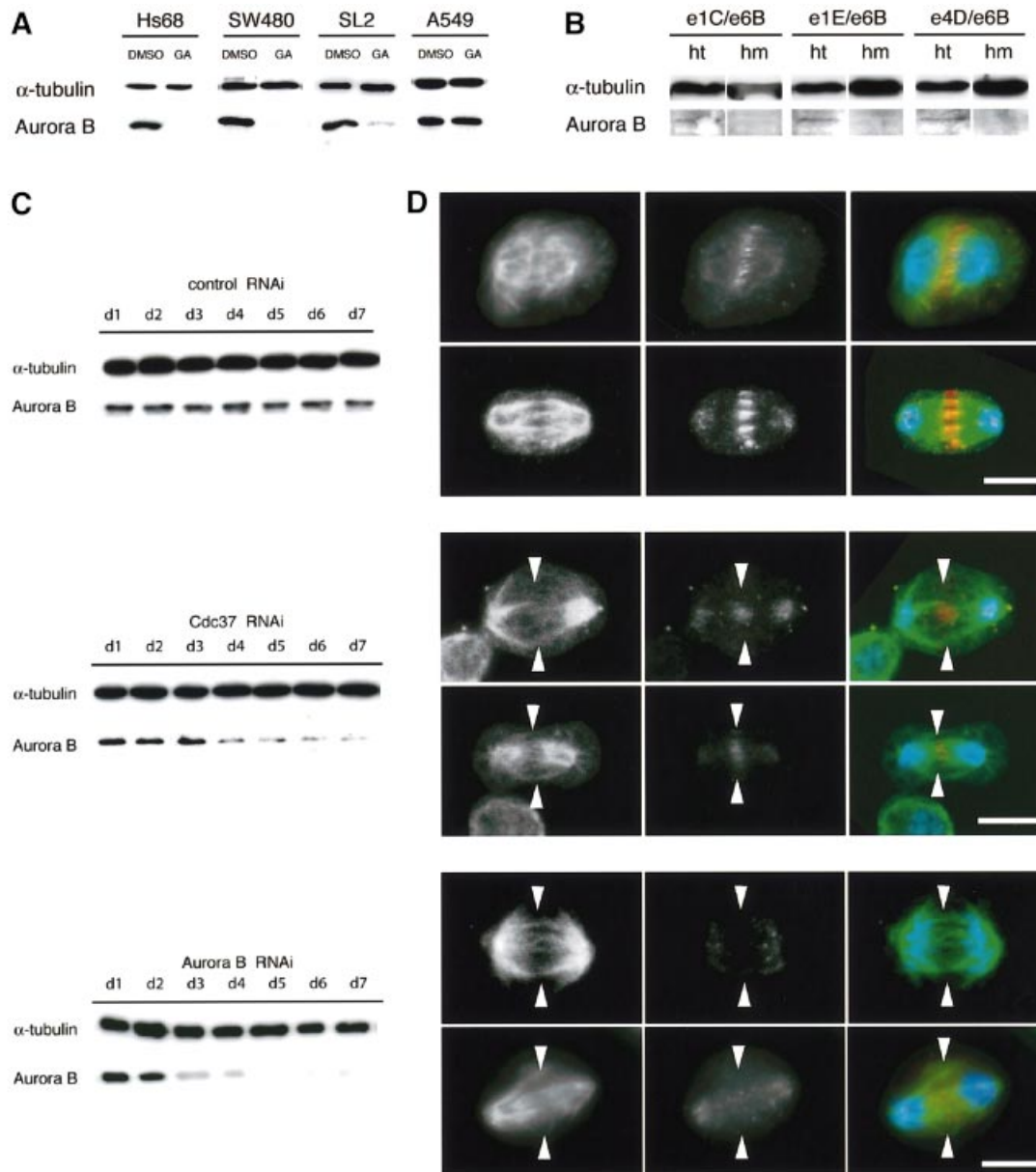


Fig. 6. Aurora B is stabilized by the Cdc37/Hsp90 complex in primary but not in cancer cells. **(A)** Treatment of primary (Hs68), human colon adenocarcinoma (SW480) and *Drosophila* (SL2) cells with the Hsp90 inhibitor GA reduces the levels of the Aurora B kinase, as compared with the control DMSO-treated samples. However, in the human lung carcinoma cell line A549, Aurora B levels remain almost completely unchanged. This indicates that the Hsp90/Cdc37 complex is essential to maintain Aurora B protein levels, while this interaction is disturbed in the A549 cells. α -tubulin is loading control. **(B)** *Drosophila* testis prepared from Cdc37 homozygous mutant larvae (hm) and heterozygous control larvae (ht), analyzed by western blotting with an anti-Aurora B antibody. Homozygous mutant testis contain undetectable levels of Aurora B, indicating that functional Cdc37 is required to maintain Aurora B protein levels. The lanes of the mutant (hm) samples are overloaded, as indicated by the tubulin bands, but still no Aurora B can be detected. **(C)** (Top panel), Aurora B and α -tubulin levels are constant in cells treated with control dsRNA throughout the 7 days of treatment; (middle panel) time course of Cdc37 RNAi in SL2 cells leads to reduced levels of Aurora B after 3 days of treatment, confirming that Cdc37 is required to sustain Aurora B protein levels. α -tubulin is used as loading control; (bottom panel) time course of Aurora B RNAi in SL2 cells leads to reduced levels of Aurora B after 2 days of treatment. Aurora B is not detectable after day 5. **(D)** Top panel, control cells labelled for α -tubulin (first column, green in overlay), Aurora B (second column, red in overlay) and DNA (blue) show a distinct staining at the central spindle in early and late anaphase; (middle panel), 3–4 days after transfection with Cdc37 dsRNA, the central spindles (first column, arrowheads) have almost completely disappeared and cells have low levels of Aurora B (second column); (bottom panel), 2–3 days after transfection with Aurora B dsRNA, the central spindles (first column, arrowheads) have almost completely disappeared and cells have much reduced levels of Aurora B (second column). The phenotype of Cdc37 and Aurora B dsRNA-treated cells both show abnormal organized spindles lacking a dense array of central spindle microtubules. Scale bar in all panels of (D) = 7 μ m.

tight with another protein kinase, Aurora B, to the extent that the phenotypes that result from the inactivation of either Cdc37 or Aurora B are almost indistinguishable (Adams *et al.*, 2001; Giet and Glover, 2001; this paper). The main exception is that inactivation of Aurora B does

not lead to cell cycle arrest as inactivation of Cdc37 does. Given these close similarities, we investigated whether Aurora B function could require the activity of the Hsp90/Cdc37 complex. We indeed found this to be the case; inactivation by different methods of either Cdc37 or

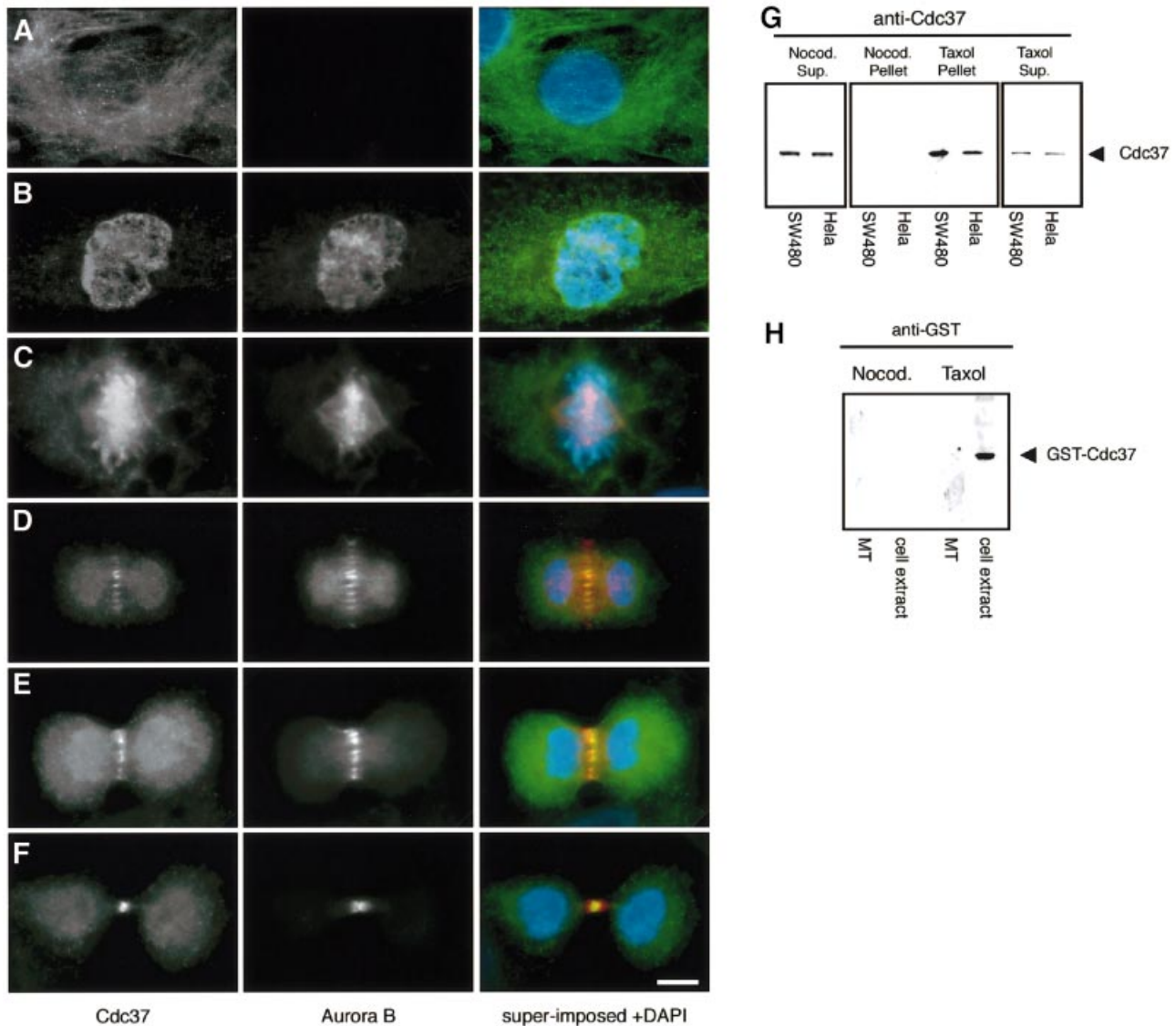


Fig. 7. Cdc37 localizes to the spindle and midbody *in vivo* and binds microtubules *in vitro*. (A–F) Immunofluorescence of HeLa cells, triple-labelled with antibodies against Cdc37 (green and yellow in super-imposed image), Aurora B (red and yellow, in the superimposed image) and the DNA binding dye DAPI (blue). (A) The anti-Cdc37 antibody labels the cytoplasm in interphase. Aurora B labelling is not detectable. (B) In prophase Cdc37 labelling is cytoplasmic and nuclear. Aurora B labels dotted structures in the nucleus. (C) At metaphase, labelling of Cdc37 is predominant at the metaphase chromosomes, while Aurora B labels chromosomes and spindle structure. (D) The anti-Cdc37 antibody labels the cytoplasm and spindle microtubules in telophase. Aurora B co-localizes in the central spindle area with Cdc37 (yellow superimposition). (E) At the beginning of furrow formation, Cdc37 is present in the cytoplasm and central spindle co-localizing with Aurora B (yellow superimposition). (F) In late telophase, Cdc37 is localized to the central midbody structure together with Aurora B (yellow overlay) and the cytoplasm. (G) Microtubule co-sedimentation assay in mitotic cell extracts from two different cell lines (SW480 and HeLa cells). Cdc37 co-sediments with taxol-stabilized microtubules while control pellets of nocodazole treated samples do not contain Cdc37. A fraction of Cdc37 protein remains in the supernatant of taxol-treated extracts indicating that not the whole pool of Cdc37 is associated with microtubules. Cdc37 remains in the supernatant in colcemid-treated cells. (H) This interaction is likely to be indirect as demonstrated using pure recombinant proteins. GST–Cdc37 binds to microtubules in mitotic cell extracts but not to pure phosphocellulose-purified tubulin. Scale bar = 10 μ m.

Hsp90 in flies and mammalian culture cells resulted in a very significant reduction of the levels of Aurora B. In addition, we were able to show that Cdc37, Aurora B and Hsp90 co-immunoprecipitate. Taken altogether, these results show that the Hsp90/Cdc37 complex modulates the function of Aurora B, and strongly suggest that the phenotypes brought about by the loss of Cdc37 function can be largely accounted for by the inactivation of this kinase. However, the partial contribution of the loss of function of Polo and other as yet unidentified protein kinases cannot be ruled out.

It seems likely that the complexity of the abnormal phenotypes brought about by the loss of Cdc37 may reflect a cascade of events in which errors at one particular stage lead to errors in subsequent stages. In fact, most of the abnormal phenotypes that we observe could in principle be traced back to two original ones: impaired chromatin structure and abnormal spindles. One of the essential factors that contribute to the fidelity of chromosome segregation during meiosis is the controlled release of cohesion between homologue chromosomes and sister chromatids. At the onset of anaphase I, cohesion is

released along the arms but maintained at the centromere until anaphase II, thus allowing the bipolar orientation of the sister chromatids in the second meiotic division (Dej and Orr-Weaver, 2000). In *Cdc37* mutant spermatocytes, cohesion along the arms is lost during late prometaphase I, coinciding with the premature and asynchronous splitting of the homologue chromosomes. This, in turn, results in some chromosomes acquiring an amphitelic orientation (with both sister chromatids attached to each pole) during meiosis I, which leads to the segregation of the chromatids and thus to aneuploidy. Therefore, aneuploid gametes, aberrant chromosome orientation and precocious chromosome separation may be accounted for by impaired chromosome cohesion (Goldstein, 1980; Dej and Orr-Weaver, 2000). Moreover, impaired cohesion could be tightly related to the abnormal chromosome condensation displayed by *Cdc37* mutant spermatocytes.

The loss of function of Aurora B also leads to aberrant chromosome orientation and segregation (Kaitna *et al.*, 2002; Kallio *et al.*, 2002; Rogers *et al.*, 2002; Tanaka *et al.*, 2002). Abrogation of Aurora B function leads also to abnormal chromosome condensation and it has been proposed that this could physically interfere with normal chromosome movement in the spindle and result in aneuploidy (Adams *et al.*, 2001; Giet and Glover, 2001).

The other major phenotypes brought about by loss of *Cdc37* are the lack of a central spindle and cytokinesis failure. Here too, it is likely that the latter is a consequence of the former, as the interdependency between the assembly of the central spindle and the contractile ring in *Drosophila* is well established (Giansanti *et al.*, 1998). These two phenotypes have also been observed following the loss of Aurora B function.

The interaction between Aurora B and *Cdc37* that we have observed in flies and primary human cells is disturbed in the lung carcinoma A549 and other cancer cells (data not shown). In these cells, GA treatment does not result in the inactivation of this kinase that still co-immunoprecipitates with *Cdc37*. How these cells can escape the effect of GA we do not know. In the case of Polo, whose stability in these cells has also been shown to be insensitive to GA, it has been proposed that these cells contain a mutant allele of this gene that does not depend upon the Hsp90 complex for its stability (Simizu and Osada, 2000). Interestingly, substrates of *Cdc37* have been implicated in tumorigenesis and are either overexpressed, amplified or mutated in somatic cancer cells. For example, members of the Aurora kinase family are overexpressed in tumour types, such as human colorectal, breast, prostate and ovarian cancer (Bischoff *et al.*, 1998; Tatsuka *et al.*, 1998; Zhou *et al.*, 1998). Moreover, *Cdc37* itself is upregulated in some human prostatic tumours, neoplasias and pre-malignant lesions and, when overexpressed in mice, can induce hyperplasia and dysplasia (Stepanova *et al.*, 2000a,b). Our results provide evidence that functional *Cdc37* is required for the fidelity of chromosome segregation and cell division, and show that a shift in the balance between *Cdc37* and the cell cycle machinery lead to abnormalities that ultimately could result in genomic instability. Future studies will need to show whether mutations in chaperones or their substrates, i.e. mutations that are relevant for chaperone interaction, are critical for the early events that lead to oncogenic transformation.

Materials and methods

Fly stocks

The four mutant alleles of *Cdc37* used in this study (Cutforth and Rubin, 1994) were: *Cdc37^{e1C}*, *Cdc37^{e1E}*, *Cdc37^{e4D}* and *Cdc37^{e6B}*. Except for *Cdc37^{e6B}* these are early lethal mutations, but can reach the stage of third instar larvae as trans-heteroallelic combinations with *Cdc^{e6B}*. The trans-heterozygous combinations *hsp83⁵⁸²/hsp83^{91I}* and *hsp83⁵⁸²/hsp83^{13F3}* of Hsp90 mutant alleles (van der Straten *et al.*, 1997) that allow for larval development were analysed by testis squash techniques with phase microscopy.

Testis squash and live video imaging of spermatocytes

Testis squashes were performed according to Gonzalez and Glover (1993). Live video imaging was performed as described previously by Rebollo and Gonzalez (2000).

Tissue culture cell lines

The human cell lines SW480, SW948 and A549 were obtained from the German tissue culture collection (DSMZ, Braunschweig, Germany), the human newborn foreskin primary cell line Hs68 was obtained from the ECACC (Salisbury, UK).

Immunofluorescence microscopy and image processing

Immunofluorescence microscopy was performed as described previously by Lange and Gull (1995) with the difference that SL2 cells were spun down onto poly-L-lysine-coated glass coverslips in 24-well plates prior to processing for immunofluorescence microscopy. Images were either acquired by laser scanning confocal microscopy using the Leica TCS SP-confocal system or with a 12 bit Hamamatsu Orca C4742-95 CCD camera (Hamamatsu, München, Germany) and the OpenLab software (Improvision, Heidelberg, Germany).

Flow cytometry

DNA content of *Drosophila* SL2 cells was measured after propidium iodide staining using standard methods (Robinson *et al.*, 1999) with a FACS-scan flow cytometer from Becton-Dickinson. Excitation was at 488 nm and fluorescence emitted was collected using a 585 nm/26 bandpass filter.

SL2 cell culture and RNA interference

SL2 cells were propagated at 25°C in Schneider's *Drosophila* medium. dsRNAi was performed essentially as described previously by Clemens *et al.* (2000). SL2 cells were washed twice in serum-free medium, resuspended in serum-free medium and dsRNA was added. After 1.5 h, an equal amount of medium containing 20% FCS was supplemented. GFP-dsRNA was used as a control. *Cdc37* dsRNA and GFP-dsRNA both correspond to the first 650 bp of the coding region. Aurora B dsRNA corresponds to the 650 bp of exon 2. dsRNA-treated cells were counted and then assayed by immunofluorescence microscopy, phase microscopy, FACS analysis and western blotting. Components were purchased from Life Technologies.

Antibodies

We used the following antibodies: anti- α -tubulin DM1A and anti- γ -tubulin (Sigma, München, Germany), anti-*Cdc37* mouse mAb, clone C1 (Dianova, Hamburg, Germany), anti-*Cdc37* mouse mAb clone 15m, anti-AIM-1 mAb (BD Transduction Laboratories, Heidelberg, Germany) and anti-Aurora B rabbit polyclonal antibody (a gift from Drs Giet and Glover).

Microtubule pelleting assay

Mammalian cell lines were grown to ~80% density and extracted in lysis buffer (1% Triton, 25 mM Tris-HCl pH 7.5, 1 mM EGTA, 1 mM EDTA, 0.5% Nonident P-40, 100 mM NaCl, 2 mM ortho-vanadate and proteinase inhibitor mix). Per assay, 500 μ g of protein were used. Microtubule pelleting assays were performed according to Ploubidou *et al.* (2000). Samples were spun through a 15% sucrose cushion. Resulting pellets were resuspended in equal amounts of SDS-PAGE sample buffer and analysed by western blotting techniques.

Cdc37 protein expression

The *Drosophila* *Cdc37* gene was isolated by PCR from a cDNA library (Brown and Kafatos, 1988), subcloned into the pGEX-6-P2 plasmid (Pharmacia) and expressed as a GST fusion protein in XI-I-Blue cells from Stratagene (Amsterdam, Netherlands) at 37°C in liquid cultures.

Resuspended cell pellets were lysed in phosphate buffer (0.05 M PO_4Na , 0.3 M NaCl, 0.5 % Triton X-100 pH 7.5) supplemented with a protease inhibitor mix, sonicated and batch purified using glutathione–Sepharose 4 fast flow according to the manufacturer's instructions (Pharmacia).

Immunoprecipitation and kinase assay

Immunoprecipitation was performed essentially as described previously by Grammatikakis *et al.* (1999). SW480, NIH 3T3 and A549 cells were enriched in mitosis by incubation for 8 h with taxol and nocodazole, then lysed and a post-nuclear high-speed extract was made. This extract was incubated with the anti-Aurora B antibody for 1 h at 4°C and then incubated for an additional 1 h with protein G beads. Beads were pelleted, washed four times and analysed after western blotting by probing with anti-Cdc37 and anti-Aim-1 antibodies. In each immunoprecipitation 2 mg of protein was used. *Drosophila* embryo extract was prepared as described previously by Moritz *et al.* (1995), supplemented with 2 mM sodium ortho-vanadate and centrifuged at 210 000 g for 30 min at 4°C. The GST fusion protein pull-down was performed by adding 2 µg of purified GST–Cdc37 fusion protein to 5 mg of high-speed supernatant of *Drosophila* embryo extract, incubated for 1 h at 4°C followed by addition of 30 µl of glutathione–Sepharose 4 fast-flow beads (Pharmacia, Freiburg, Germany), and incubated for 1 h at 4°C. Then beads were washed four times and processed for western blotting analysis.

For the kinase assay, NIH 3T3, SW480 and A549 cells were mitotically arrested and processed for immunoprecipitation with the anti-AIM-1 antibody as described previously. Equal amounts of beads were washed first three times in immunoprecipitation buffer and then once in high salt buffer to remove non-specific kinase activity. Each sample was incubated with 6 µg of purified histone H3 for 20 min at 37°C and processed according to conditions described previously (Karaiskou *et al.*, 2001).

Supplementary data

Supplementary data are available at *The EMBO Journal* Online.

Acknowledgements

We are grateful to E.Hafen and G.Rubin for mutant fly stocks, to R.Giet and D.Glover for the anti-Aurora B antibody, to A.Atzberger for help with the flow cytometer, to E.Perdiguero and other members of the Nebreda group for help with the kinase assays and the kind gift of histone H3, to S.Llamazares who provided the GFP- α -tubulin-expressing flies, and to all members of the González laboratory and A.Ploubidou for support and discussions. The TCS-SP confocal microscope used here was kindly provided by Leica Microsystems. B.M.H.L. was supported by a research grant from the Deutsche Forschungsgemeinschaft (DFG). Our laboratory is supported by grants from the EU and the Ramon Areces Foundation.

References

- Adams,R.R., Maiato,H., Earnshaw,W.C. and Carmena,M. (2001) Essential roles of *Drosophila* inner centromere protein (INCENP) and Aurora B in histone H3 phosphorylation, metaphase chromosome alignment, kinetochore disjunction, and chromosome segregation. *J. Cell Biol.*, **153**, 865–880.
- Bischoff,J.R. *et al.* (1998) A homologue of *Drosophila* Aurora kinase is oncogenic and amplified in human colorectal cancers. *EMBO J.*, **17**, 3052–3065.
- Brown,N.H., and Kafatos,F.C. (1988) Functional cDNA libraries from *Drosophila* embryos. *J. Mol. Biol.*, **203**, 425–437.
- Clemens,J.C., Worby,C.A., Simonson-Leff,N., Muda,M., Maehama,T., Hemmings,B.A. and Dixon,J.E. (2000) Use of double-stranded RNA interference in *Drosophila* cell lines to dissect signal transduction pathways. *Proc. Natl Acad. Sci. USA.*, **97**, 6499–6503.
- Cutforth,T. and Rubin,G.M. (1994) Mutations in Hsp83 and cdc37 impair signaling by the sevenless receptor tyrosine kinase in *Drosophila*. *Cell*, **77**, 1027–1036.
- Dai,K., Kobayashi,R. and Beach,D. (1996) Physical interaction of mammalian Cdc37 with CDK4. *J. Biol. Chem.*, **271**, 22030–22034.
- Dej,K.J. and Orr-Weaver,T.L. (2000) Separation anxiety at the centromere. *Trends Cell Biol.*, **10**, 392–399.
- Dey,B., Lightbody,J.J. and Boschelli,F. (1996) Cdc37 is required for p60v-src activity in yeast. *Mol. Biol. Cell*, **7**, 1405–1417.
- de Cárcer,G., do Carmo Avides,M., Lallena,M.J., Glover,D.M. and Gonzalez,C. (2001) Requirement of Hsp90 for centrosomal function reflects its regulation of Polo kinase stability. *EMBO J.*, **20**, 2878–2884.
- Fuller,M.T. (1993) Spermatogenesis. In Bate,M. and Arias,A.M. (eds), *The Development of Drosophila melanogaster*. Vol. I. Cold Spring Harbor Laboratory Press, Cold Spring Harbor, NY. pp. 71–147.
- Gerber,M.R., Farrell,A., Deshaies,R.J., Herskowitz,I. and Morgan,D.O. (1995) Cdc37 is required for association of the protein kinase Cdc28 with G₁ and mitotic cyclins. *Proc. Natl Acad. Sci. USA*, **92**, 4651–4655.
- Giansanti,M.G., Bonaccorsi,S., Williams,B., Williams,E.V., Santolamazza,C., Goldberg,M.L. and Gatti,M. (1998) Cooperative interactions between the central spindle and the contractile ring during *Drosophila* cytokinesis. *Genes Dev.*, **12**, 396–410.
- Giet,R. and Glover,D.M. (2001) *Drosophila* Aurora B kinase is required for histone H3 phosphorylation and condensin recruitment during chromosome condensation and to organize the central spindle during cytokinesis. *J. Cell Biol.*, **152**, 669–682.
- Glötzter,M. (2001) Animal cell cytokinesis. *Annu. Rev. Cell Dev. Biol.*, **17**, 351–386.
- Glover,C.V.,III (1998) On the physiological role of casein kinase II in *Saccharomyces cerevisiae*. *Prog. Nucleic Acid Res. Mol. Biol.*, **59**, 95–133.
- Goldstein,L.S. (1980) Mechanisms of chromosome orientation revealed by two meiotic mutants in *Drosophila melanogaster*. *Chromosoma*, **78**, 79–111.
- Gonzalez,C. and Glover,D.M. (1993) Techniques for studying mitosis in *Drosophila*. In Fantes,P. and Brook,R. (eds), *The cell cycle: Practical Approach*. IRL Press at Oxford University Press, pp. 143–175.
- Gonzalez,C., Casal,J. and Ripoll,P. (1989) Relationship between chromosome content and nuclear diameter in early spermatids of *Drosophila melanogaster*. *Genet. Res.*, **54**, 205–212.
- Grammatikakis,N., Lin,J.H., Grammatikakis,A., Tschlis,P.N. and Cochran,B.H. (1999) p50(cdc37) acting in concert with Hsp90 is required for Raf-1 function. *Mol. Cell Biol.*, **19**, 1661–1672.
- Hanna,D.E., Rethinaswamy,A. and Glover,C.V. (1995) Casein kinase II is required for cell cycle progression during G₁ and G₂/M in *Saccharomyces cerevisiae*. *J. Biol. Chem.*, **270**, 25905–25914.
- Herrmann,S., Amorim,I., Sunkel,C.E. (1998) The POLO kinase is required at multiple stages during spermatogenesis in *Drosophila melanogaster*. *Chromosoma*, **107**, 440–451.
- Huang,L., Grammatikakis,N. and Toole,B.P. (1998) Organization of the chick Cdc37 gene. *J. Biol. Chem.*, **273**, 3598–3603.
- Hunter,T. and Poon,R.Y.C. (1997) Cdc37: a protein kinase chaperon. *Trends Cell Biol.*, **7**, 157–161.
- Kaitna,S., Mendoza,M., Jantsch-Plunger,V. and Glötzter,M. (2000) Nucleotide Incenp and an Aurora-like kinase form a complex essential for chromosome segregation and efficient completion of cytokinesis. *Curr. Biol.*, **10**, 1172–1181.
- Kaitna,S., Pasierbek,P., Jantsch,M., Loidl,J. and Glötzter,M. (2002) The aurora B kinase AIR-2 regulates kinetochores during mitosis and is required for separation of homologous chromosomes during meiosis. *Curr. Biol.*, **12**, 798–812.
- Kallio,M.J., McClelland,M.L., Stukenberg,P.T. and Gorbsky,G.J. (2002) Inhibition of aurora B kinase blocks chromosome segregation, overrides the spindle checkpoint, and perturbs microtubule dynamics in mitosis. *Curr. Biol.*, **12**, 900–905.
- Karaiskou,A., Perez,L.H., Ferby,I., Ozon,R., Jesus,C. and Nebreda,A.R. (2001) Differential regulation of Cdc2 and Cdk2 by RINGO and cyclins. *J. Biol. Chem.*, **276**, 36028–36034.
- Kimura,Y., Rutherford,S.L., Miyata,Y., Yahara,I., Freeman,B.C., Yue,L.H., Morimoto,R.I. and Lindquist,S. (1997) Cdc37 is a molecular chaperone with specific functions in signal transduction. *Genes Dev.*, **11**, 1775–1785.
- Lange,B.M.H. and Gull,K. (1995) A molecular marker for centriole maturation in the mammalian cell cycle. *J. Cell Biol.*, **130**, 919–927.
- Moritz,M., Braunfeld,M.B., Fung,J.C., Sedat,J.W., Alberts,B.M. and Agard,D.A. (1995) Three-dimensional structural characterization of centrosomes from early *Drosophila* embryos. *J. Cell Biol.*, **130**, 1149–1159.
- Nigg,E. (2001) Mitotic kinases as regulators of cell division and its checkpoints. *Nat. Rev. Mol. Cell Biol.*, **2**, 21–32.
- Pearl,L.H. and Prodromou,C. (2000) Structure and *in vivo* function of Hsp90. *Curr. Opin. Struct. Biol.* **10**, 46–51.
- Perdew,G., Wiegand,H., Vanden Heuvel,J., Mitchell,C. and Singh.S. (1997) A 50 kiloDalton protein associated with Raf and pp60v-src

- protein kinase is a mammalian homolog of the cell cycle control protein Cdc37. *Biochemistry*, **36**, 3600–3607.
- Pines, J. (1999) Four-dimensional control of the cell cycle. *Nat. Cell Biol.*, **1**, E73–E79.
- Ploubidou, A., Moreau, V., Ashman, K., Reckmann, I., Gonzalez, C. and Way, M. (2000) Vaccinia virus infection disrupts microtubule organization and centrosome function. *EMBO J.*, **19**, 3932–3944.
- Pratt, W.B. and Toft, D.O. (1997) Steroid receptor interactions with heat shock protein and immunophilin chaperones. *Endocr. Rev.*, **18**, 306–360.
- Rebollo, E. and González, C. (2000) Visualizing the spindle checkpoint in *Drosophila* spermatocytes. *EMBO rep.*, **1**, 65–70.
- Reed, S.I. (1980) The selection of *S.cerevisiae* mutants defective in the start event of cell division. *Genetics*, **95**, 561–577.
- Robinson, J.P., Darzynkiewicz, Z., Dean, P., Orfao, A., Rabinovitch, P., Stewart, C., Tanke, H. and Wheelless, L. (eds) (1999) *Current Protocols in Flow Cytometry*, Vol. 1. Wiley, New York, NY.
- Rogers, E., Bishop, J.D., Waddle, J.A., Schumacher, J.M. and Lin, R. (2002) The aurora kinase AIR-2 functions in the release of chromosome cohesion in *Caenorhabditis elegans* meiosis. *J. Cell Biol.*, **157**, 219–229.
- Roos, U.P. (1976) Light and electron microscopy of rat kangaroo cells in mitosis. III. Patterns of chromosome behavior during prometaphase. *Chromosoma*, **54**, 363–385.
- Schutz, A.R., Giddings, T.H., Jr, Steiner, E. and Winey, M. (1997) The yeast Cdc37 gene interacts with MPS1 and is required for proper execution of spindle pole body duplication. *J. Cell Biol.*, **136**, 969–982.
- Silverstein, A.M., Grammatikakis, N., Cochran, B.H., Chinkers, M. and Pratt, W.B. (1998) p50(cdc37) binds directly to the catalytic domain of Raf as well as to a site on hsp90 that is topologically adjacent to the tetratricopeptide repeat binding site. *J. Biol. Chem.*, **273**, 20090–20095.
- Simizu, S. and Osada, H. (2000) Mutations in the Plk gene lead to instability of Plk protein in human tumour cell lines. *Nat. Cell Biol.*, **2**, 852–854.
- Stepanova, L., Leng, X., Parker, S.B. and Harper, J.W. (1996) Mammalian p50Cdc37 is a protein kinase-targeting subunit of Hsp90 that binds and stabilizes Cdk4. *Genes Dev.*, **10**, 1491–502.
- Stepanova, L., Leng, X. and Harper, J.W. (1997) Analysis of mammalian Cdc37, a protein kinase targeting subunit of heat shock protein 90. *Methods Enzymol.*, **283**, 220–229.
- Stepanova, L., Finegold, M., DeMayo, F., Schmidt, E.V. and Harper, J.W. (2000a) The oncoprotein kinase chaperone Cdc37 functions as an oncogene in mice and collaborates with both c-myc and cyclin D1 in transformation of multiple tissues. *Mol. Cell. Biol.*, **20**, 4462–4473.
- Stepanova, L., Yang, G., DeMayo, F., Wheeler, T.M., Finegold, M., Thompson, T.C. and Harper, J.W. (2000b) Induction of human Cdc37 in prostate cancer correlates with the ability of targeted Cdc37 expression to promote prostatic hyperplasia. *Oncogene*, **19**, 2186–2193.
- Sunkel, C.E. and Glover, D.M. (1988) polo, a mitotic mutant of *Drosophila* displaying abnormal spindle poles. *J. Cell Sci.*, **89**, 25–38.
- Tanaka, T.U., Rachidi, N., Janke, C., Pereira, G., Galova, M., Schiebel, E., Stark, M.J. and Nasmyth, K. (2002) Evidence that the Ipl1–Sli15 (Aurora kinase–INCENP) complex promotes chromosome bi-orientation by altering kinetochore–spindle pole connections. *Cell*, **108**, 317–429.
- Tatsuka, M., Katayama, H., Ota, T., Tanaka, T., Odashima, S., Suzuki, F. and Terada, Y. (1998) Multinuclearity and increased ploidy caused by overexpression of the Aurora- and Ipl1-like midbody-associated protein mitotic kinase in human cancer cells. *Cancer Res.*, **58**, 4811–4816.
- Terada, Y., Tatsuka, M., Suzuki, F., Yasuda, Y., Fujita, S. and Otsu, M. (1998) AIM-1: a mammalian midbody-associated protein required for cytokinesis. *EMBO J.*, **17**, 667–676.
- van der Straten, A., Rommel, C., Dickson, B. and Hafen, E. (1997) The heat shock protein 83 (Hsp83) is required for Raf-mediated signalling in *Drosophila*. *EMBO J.*, **16**, 1961–1969.
- Zhou, H., Kuang, J., Zhong, L., Kuo, W.L., Gray, J.W., Sahin, A., Brinkley, B.R. and Sen, S. (1998) Tumour amplified kinase STK15/BTAK induces centrosome amplification, aneuploidy and transformation. *Nat. Genet.*, **20**, 189–193.

Received April 25, 2002; revised August 6, 2002;
accepted August 15, 2002

3 Discussion and Perspectives

3.1 *The NXF:p15 heterodimer acts as a functional unit in mRNA export*

At the time this study was initiated, both human TAP and yeast Mex67p had been proposed to play a role in mRNA export (Gruter *et al.*, 1998; Segref *et al.*, 1997). Results presented in this thesis show that TAP and Mex67p belong to an evolutionarily conserved family of proteins with several members in higher eukaryotes. We called this family nuclear export factor (NXF) family (Herold *et al.*, 2000). The similar domain organization of NXF proteins, together with the presence of at least one *nxf* gene in all eukaryotic genomes analyzed, suggested a conserved function of NXF proteins.

Indeed, results obtained by us and by others showed that *Drosophila* NXF1 and *C. elegans* NXF1 are required for mRNA export, since mutations or the functional knockout (RNAi) of these genes lead to a block of this process (Herold *et al.*, 2001; Tan *et al.*, 2000; Wilkie *et al.*, 2001). Furthermore, similar to TAP, human NXF2 and NXF3 were shown to possess export activity in a reporter gene assay in mammalian cells, providing indirect evidence for their involvement in mRNA export (Herold *et al.*, 2000; Yang *et al.*, 2001). Different functional assays to study mRNA export *in vivo* (e.g. the CAT reporter assay presented in 2.3.1) also allowed us and others to gain insight into the mechanism of TAP-mediated mRNA export (Braun *et al.*, 2001; Braun *et al.*, 2002; Guzik *et al.*, 2001; Wiegand *et al.*, 2002). The ultimate proof that human TAP is required for general mRNA export *in vivo* has been provided by RNAi experiments in human tissue culture cells. In analogy to the situation observed in *Drosophila* cells, HeLa cells depleted of TAP suffer from an mRNA export inhibition, resulting in the nuclear accumulation of poly(A)⁺ RNA, which finally leads to cell death (I. Braun and E. Izaurralde, personal communication).

There is compelling evidence by now that mRNA export in different eukaryotic species requires NXF function. However, the question why genomes of higher eukaryotes encode several NXF proteins has not been answered yet (see 3.4 for a discussion of this issue). This question is obvious since only one NXF protein (TAP in human cells, NXF1 in *C. elegans* and *D. melanogaster*) seems to be essential for general mRNA export in all cases tested so far.

Results presented in this study indicate that NXF proteins in higher eukaryotes can mediate nuclear export of cellular mRNAs only when bound to the small protein p15 (Braun *et al.*, 2001; Herold *et al.*, 2001). When this study was initiated, p15 had just been identified as an interaction partner of human TAP, but its precise role in mRNA export and the significance of this interaction were largely unexplored. The observation that only TAP and p15 together could partially rescue the otherwise lethal *mex67/mtr2* double knockout

strain, already pointed to a conserved and essential role of both proteins in mRNA export (Katahira *et al.*, 1999). The following observations presented in this work and elsewhere supported and extended this hypothesis:

(I) The interaction of NXF proteins with p15 is conserved. All human TAP homologues interact with (human) p15 *in vitro*. Likewise, *Drosophila* NXF1-3 and *C. elegans* NXF1 have been shown to bind to p15 from the respective species (Herold *et al.*, 2001; Herold *et al.*, 2000; Jun *et al.*, 2001; Katahira *et al.*, 1999; Wiegand *et al.*, 2002). The observation that coexpression of human NXF2 or NXF3 with p15 significantly increased their stability in *E. coli* further suggests that p15 might have a chaperone-like activity for NXF proteins. Accordingly, human NXF members can be expressed at higher levels in mammalian cells when p15 is coexpressed (Braun *et al.*, 2001; Herold *et al.*, 2000).

(II) NXF proteins can mediate efficient nuclear export only when bound to p15. Human NXF proteins function with optimal efficiencies in the mammalian reporter assay only when p15 is coexpressed. Accordingly, human NXF mutants which cannot interact with p15, fail to promote mRNA export in reporter assays in mammalian cells and in microinjection experiments in *Xenopus* oocytes (Braun *et al.*, 2001; Herold *et al.*, 2000; Wiegand *et al.*, 2002).

(III) The depletion of either NXF1 or p15 by RNAi in *Drosophila* Schneider cells results in indistinguishable phenotypes. The knockdown of either interaction partner leads to a fast and strong nuclear accumulation of poly(A)⁺ RNA, affecting intron-containing and intronless mRNAs, including heat shock mRNAs. As a consequence of this general block to mRNA export, protein synthesis is strongly inhibited (Herold *et al.*, 2001). Importantly, even when monitoring the nuclear export of about 6000 different transcripts in a large-scale approach, we could not identify any transcript displaying significant differences in between the two knockdowns (Herold *et al.*, 2003). The most likely explanation for these observations is that neither NXF1 nor p15 have a function independent of the other heterodimeric subunit.

These observations indicate that NXFs and p15 function as a heterodimeric unit to mediate mRNA export. But the molecular function of this interaction (and thus of p15 and the domain in TAP interacting with it) was still unclear. Both proteins interact *via* their NTF2-like domains with each other, forming an NTF2-like scaffold. The function of this NTF2-like scaffold was discovered in a recent structural study. Fribourg *et al.* (2001) demonstrated that the NTF2-like scaffold is able to interact with an FG-repeat of a nucleoporin. The heterodimeric surface forms a single structural unit which recognizes the FG-repeat at a hydrophobic pocket present on TAP, but not on p15. Based on the structure and on further functional analysis of TAP and p15 molecules containing selected point mutations, the main function of p15 was suggested to be the stabilization of the correct

folding of the NTF2-like domain in TAP, so that this domain is able to recognize FG-repeats present in NPC components. This hypothesis is in good agreement with a recent report which demonstrates that the binding of p15 activates TAP-dependent mRNA export by enhancing the recruitment of the heterodimer to the NPC (Wiegand *et al.*, 2002).

The NTF2-like domains are related in sequence and structure to the small protein NTF2. NTF2 is a nuclear transport factor mediating the import of Ran into the nucleus which is critical for the maintenance of the RanGTP gradient (Ribbeck *et al.*, 1998). NTF2 acts as a homodimer, interacts with RanGDP and nucleoporins, and mediates the translocation of RanGDP through the NPC. Due to the sequence similarity with NTF2, p15 had previously been proposed interact with Ran (RanGTP in this case) (Black *et al.*, 1999). p15 was also suggested to have a general export activity, being able to stimulate the nuclear export of proteins, U snRNA and tRNA in a Crm1-dependent, and the nuclear export of mRNA in a Crm1-independent manner. All these proposed export activities of p15 were shown to be dependent on its ability to bind RanGTP (Black *et al.*, 1999; Ossareh-Nazari *et al.*, 2000). However, the interaction of p15 with Ran could not be confirmed in other studies (Herold *et al.*, 2001; Katahira *et al.*, 1999). Furthermore, although the interaction of the NTF2-like domains in TAP and p15 results in the formation of a heterodimer with an overall structure similar to the NTF2 homodimer, the structure of the TAP:p15 heterodimeric region is incompatible with Ran-binding in a manner similar to that observed in the RanGDP:NTF2 complex (Fribourg *et al.*, 2001; Stewart *et al.*, 1998). In particular, an insertion loop in TAP and large side chains at the proposed Ran-binding site in p15, occlude the potential Ran binding pocket. These observations make a Ran-dependent export function of p15 which had been suggested to occur independently of NXF proteins rather unlikely.

An autonomous export function of p15 would also require that p15 was able to associate with the NPC independently of NXF1. However, the ability of human p15 to associate with the NPC *in vivo* is clearly mediated through its interaction with TAP (Fribourg *et al.*, 2001). Thus, although other functions of p15 can formally not be ruled out the combination of structural and functional data collected in the last years, reduced the likelihood that p15 has an NXF1-independent export function to a minimum.

Since p15 binding is an essential prerequisite for NXF function, it is formally possible that p15 acts as a molecular switch regulating NXF-dependent mRNA export, e.g. by regulating the association of NXFs with NPC components or influencing NXF/cargo interactions. p15 could thus confer directionality to the mRNA export process similar to the Ran system that provides directionality to most other nucleocytoplasmic transport processes. A prerequisite for this hypothesis is that the heterodimer formation would preferentially occur in the nucleus, but would be reduced in the cytoplasm. However, recent data demonstrate that mutated NXF1 in which the NTF2-like domain was replaced

by a (second) UBA-like domain could promote directional export even in the absence of p15 ([Braun *et al.*, 2002](#)). Thus, p15 is not generally required for the directional export of mRNAs. Nevertheless, p15 could have a regulatory role in affecting the overall efficiency of nuclear mRNA export.

This study also implies that the essential functions of both the NTF2-like and the UBA-like domains in NXF1 are confined to nucleoporin binding, as two copies of either of these domains are sufficient to promote nuclear export of cellular mRNAs ([Braun *et al.*, 2002](#)). These observations, together with available structural data, suggest that the main role of p15 in nuclear mRNA export is to stabilize the NTF2-like domain of NXFs by heterodimerization, thus allowing their interaction with nucleoporins.

3.2 NXF1:p15 and UAP56 define a single mRNA export pathway in *Drosophila*

Depletion of NXF1, p15 or UAP56 from *Drosophila* Schneider cells by RNAi results in the accumulation of poly(A)⁺ RNAs in the nucleus ([Gatfield *et al.*, 2001](#); [Herold *et al.*, 2001](#)). The depletion of NXF1, p15 or UAP56 also inhibits the synthesis of most proteins, suggesting that export of a large proportion of mRNAs is affected. But it was unclear which proportion of mRNAs is affected in any of the knockdowns, and whether some mRNAs could exit the nucleus independently of NXF1, p15 and/or UAP56.

Even though a model, mainly based on data obtained in yeast, suggested that NXF/Mex67p is recruited to mRNAs through the action of UAP56/Sub2p, there was no experimental evidence for this linear pathway in higher eukaryotes, as it was unknown whether mRNAs exported by NXF1:p15 also require UAP56 and *vice versa*.

In a microarray-based analysis of Schneider cells depleted of NXF1, p15 or UAP56, we have examined the expression levels of mRNAs representing nearly half of all predicted *Drosophila* genes ([Herold *et al.*, 2003](#)). As expected, after blocking the export of bulk poly(A)⁺ RNA, the vast majority of transcripts were underrepresented in the cytoplasm of cells depleted of NXF1, p15 or UAP56 as compared to control cells. Moreover, the overall expression profiles obtained in the different knockdowns were extremely similar, indicating that most mRNAs affected by the NXF1 or p15 knockdown were also affected by the depletion of UAP56 and *vice versa*. Thus, most mRNAs which require NXF1:p15 heterodimers for their export, also depend on UAP56 function, suggesting that these three proteins belong to a single pathway through which most transcripts exit the nucleus. Previously, NXF1:p15 or Mex67p:Mtr2p heterodimers had been suggested to be recruited to transcripts through REF, which in turn is recruited by UAP56. However, as REF is dispensable for mRNA export in *Drosophila* ([Gatfield and](#)

Izaurrealde, 2002), the reason for the tight coupling of NXF1:p15 and UAP56 functions is still unknown.

Mammalian UAP56 was initially identified as a spliceosomal component essential for U2 snRNP binding to the pre-mRNA (Fleckner *et al.*, 1997). Likewise, its yeast orthologue has been shown to function during multiple steps of spliceosome assembly (Kistler and Guthrie, 2001; Libri *et al.*, 2001; Zhang and Green, 2001). However, we did not observe an accumulation of precursor mRNAs in *Drosophila* cells depleted of UAP56 (A. Herold and E. Izaurrealde, unpublished results; Gatfield *et al.*, 2001). Thus, the function of UAP56 in splicing is either not essential in *Drosophila* or UAP56 does not participate in this process in this organism. As a third alternative, the residual amount of UAP56 protein that is present in cells after the depletion of UAP56 by RNAi, could be sufficient to fulfill its (essential) function in spliceosome assembly, but not in mRNA export. The fact that *C. tetans* UAP56 is recruited cotranscriptionally to the Balbiani ring RNP, independently of the presence of exonic or intronic sequences, favors the idea that in insects, the main function of UAP56 is not splicing.

Although the vast majority of mRNAs is affected in a similar manner in NXF1:p15 or UAP56 knockdowns, we could identify a small subset of transcripts (32 mRNAs) in our large-scale analysis which behaved differently (Herold *et al.*, 2003). These include mRNAs underrepresented in the cytoplasm of UAP56 knockdowns, but not affected or overrepresented in the NXF1 and p15 knockdowns, and *vice versa*. The first group of these mRNAs could either point to an additional role of UAP56 in the transcription/stabilization of these mRNAs, or represent transcripts which are exported through UAP56, but with the help of an export receptor other than NXF1:p15. Conversely, the second class of transcripts could represent mRNAs which are exported by NXF1:p15 heterodimers independently of UAP56. Altogether, despite the existence of such exceptional subgroups, our large-scale analysis suggested that most mRNAs are exported through a single pathway, requiring both UAP56 and NXF1:p15 function.

A recent genome-wide analysis investigated the interactions between export factors and their mRNA substrates in yeast (Hieronymus and Silver, 2003). The authors demonstrated by co-immunoprecipitation that less than 40% of transcripts were stably associated with Mex67p (although the nuclear accumulation of poly(A)⁺ RNA seen in *mex67* mutant strains is also very strong). While 40% is still a large fraction of the transcriptome, it is significantly less than the up to 75% of mRNAs, which were underrepresented in the cytoplasm of Schneider cells depleted of NXF1 in our analysis (Herold *et al.*, 2003). This difference is most likely a result of the different methodology applied in the two studies as the approach in yeast monitors stable interactions between export factors and mRNAs, while our approach in *Drosophila* cells monitors the effects of depleting export factors. Both approaches have their caveats: the depletion by RNAi is a

gradual process requiring some time (usually days) to reduce the amount of the targeted export factor in the cell. For this reason, the time period for which the targeted export factor had been "inactive" at the time when the resulting effects are observed is difficult to estimate. The normal half-life of most transcripts in *Drosophila* lies in the range of 6-7 hours, but can be much shorter or longer for a specific transcript (Lengyel *et al.*, 1977). Thus, a possible export effect could be masked for some transcripts with a very high stability. But the most striking disadvantage concerning the RNAi approach is that it is also virtually impossible to distinguish direct effects from indirect effects. Such indirect effects are likely to appear after the export of mRNAs encoding essential cellular proteins has been blocked. Thus, the number of mRNAs, which are directly exported by NXF1, could be significantly lower than the 75% of observed underrepresented transcripts.

In contrast, the immunoprecipitation method can only observe stable interactions between an export factor and its substrate mRNAs. However, some of the interactions which occur during nuclear export could be transient and thus might not be detectable with this method. Therefore, the number of mRNAs, which depend on an export factor for export, is likely to be much higher than the number of transcripts that is stably associated with it.

Despite these caveats, the authors who present the large-scale analysis in yeast propose that there are several parallel export pathways, which are defined by the specificity of different export factors for transcript subpopulations (combinatorial model). In contrast, our data rather suggest the presence of one major, linear pathway (linear model), as the vast majority of mRNAs is affected by the depletion of NXF1, p15 or UAP56. Only future investigations will answer which of the two models is correct.

3.3 Cotranscriptional surveillance might account for decreased mRNA levels after export inhibition

When nuclear mRNA export is inhibited, the levels of those transcripts that cannot exit the nucleus are expected to decrease in the cytoplasm. A decrease of total levels of the affected mRNAs is not necessarily expected *a priori*. However, Northern blots analyzing the levels of a few selected mRNAs in Schneider cells depleted of NXF1 or p15 revealed that the steady-state (total) levels of these mRNAs were reduced in these cells as compared to control cells (Herold *et al.*, 2001). The genome-wide analysis of effects caused by the depletion of NXF1, p15 or UAP56 presented in paper 4 (section 2.2.2) demonstrated that this overall decrease of mRNA levels is a general phenomenon in cells in which nuclear mRNA export has been blocked (Herold *et al.*, 2003). Several possible mechanisms could account for this general reduction of steady-state levels: (I) mRNAs accumulating inside the nucleus might be less stable in this compartment (posttranscriptional degradation).

(II) Transcription of many genes might be less active. (III) Genes might be transcribed with normal frequencies, but mRNAs could be degraded cotranscriptionally.

(I) We have tested the stability of several mRNAs which displayed decreased total mRNA levels after an export block, but none of them displayed a higher turnover rate in cells depleted of NXF1, suggesting that posttranscriptional degradation is not responsible for the decreased levels in the cases tested.

(II) We have not measured the overall transcriptional activity of cells depleted of NXF1, p15 or UAP56, but the observation that heat shock mRNA synthesis can be induced to normal levels in depleted cells, indicates that the transcription machinery is functional in these cells (Gatfield *et al.*, 2001; Herold *et al.*, 2001). This does not exclude that many genes are transcribed with lower frequencies.

(III) mRNA degradation has been observed in yeast strains in which mRNA export has been inhibited as a consequence of mutations in genes encoding export factors, including Sub2p and Yra1p (Zenklusen *et al.*, 2002). This decrease is overcome in a genetic background in which components of the exosome are inactivated. These data suggested that in yeast cells, following an export block mRNAs are degraded by the exosome. The observation that Yra1p physically and genetically interacts with exosomal components, provides another link between nuclear export and degradation (Zenklusen *et al.*, 2002). The exosome is a multiprotein-complex of 3'→5' nucleases involved in processing of rRNA, snoRNAs and snRNAs and is also implicated in the degradation of pre-mRNAs. It has been proposed that the observed degradation might be part of a cotranscriptional surveillance mechanism which monitors proper mRNP assembly, and assures that only mature mRNPs leave the nucleus (reviewed by Jensen and Rosbash, 2003).

Proper 3' end formation is one example for a processing event that is disturbed after export inhibition and may therefore generate aberrant mRNPs that are targeted for degradation. In many yeast strains carrying mutations in genes encoding export factors (e.g. Gle1p, Mex67p or Dbp5p) RNA polymerase II transcripts are hyperadenylated and/or have extended 3' ends (Hammell *et al.*, 2002; Hilleren and Parker, 2001; Jensen *et al.*, 2001b). These aberrant transcripts are retained at the site of transcription (Hilleren *et al.*, 2001; Jensen *et al.*, 2001b; Libri *et al.*, 2002), a process which requires a functional exosome. These observations indicate that the exosome might be responsible not only for the degradation of aberrant transcripts, but also for their retention (Hilleren *et al.*, 2001; Jensen *et al.*, 2001b; Libri *et al.*, 2002). But even without any obvious defects (like improperly processed 3' ends) mRNAs accumulated in the nuclear compartment might compete for nuclear RNA-binding proteins resulting in the formation of "incomplete" mRNPs which are targeted for degradation.

Although there is no direct evidence that such a surveillance mechanism exists in *Drosophila*, an interaction between the exosome and two transcription factors, dSpt5 and dSpt6, has been recently described (Andrulis *et al.*, 2002). The same study has also shown that, similar to dSpt5 and dSpt6, exosomal components are recruited to actively transcribed genes, suggesting that the quality of a transcript might already be controlled during its synthesis.

We do not have any experimental evidence to date that the decreased total levels of most mRNAs observed after depletion of NXF1, p15 or UAP56 are indeed caused by such a cotranscriptional surveillance mechanism. Attempts to restore normal levels by codepletion of some exosomal components and the export factor failed, although we cannot rule out that in these experiments the exosome was not completely inactivated (A. Herold and E. Izaurralde, unpublished observations).

Determining which processes cause the reduced steady-state levels of most mRNAs after a block to nuclear mRNA export is a challenging question for future investigations. Possibly, all three suggested mechanisms (decreased stability of mRNAs accumulating within the nucleus, reduction of the transcriptional activity in depleted cells, and cotranscriptional degradation of newly synthesized mRNAs) contribute to the observed effects.

3.4 A role for Crm1 and NXF proteins in mediating alternative mRNA export pathways?

As discussed above, the genome-wide analysis of mRNA export pathways in *Drosophila* Schneider cells revealed that the vast majority of transcripts use a common pathway to exit the nucleus. This "standard" export pathway involves the export factors UAP56 and NXF1:p15 (Herold *et al.*, 2003).

However, we could also identify a small group of mRNAs in our genome-wide analysis which were apparently not affected by the knockdown of NXF1, p15 or UAP56. As many of the transcripts belonging to this group are known not to be extremely stable, their unchanged levels in the cytoplasm indicate that they were still able to exit the nucleus despite the general export block. There are two possible explanations for this observation: (I) These transcripts could harbor high affinity binding sites for the depleted proteins, enabling them to very efficiently recruit the residual amounts of NXF1:p15 or UAP56 that are still present after depletion by RNAi. This would allow these mRNAs to be exported preferentially over other transcripts containing lower affinity binding sites for these export factors. (II) Alternatively, this group of mRNAs could represent transcripts, which are exported through alternative mRNA export pathways, i.e. independently of NXF1:p15 and UAP56.

It has previously been suggested that specialized mRNA export pathways exist which could be used to regulate the nuclear export of specific mRNAs independently of bulk mRNA export. This has been shown to occur e.g. when mammalian cells are subjected to heat stress. Upon heat shock, mRNAs encoding heat shock proteins are efficiently exported while the nuclear export of bulk mRNA is inhibited. Other cases of regulated mRNA export events could also involve such alternative export pathways (see also Introduction, section 1.2.4).

A protein which has been implicated in such alternative mRNA export events in mammals is the importin β -like family member Crm1. Other candidate factors which could serve as alternative mRNA export receptors for specific mRNAs include the members of the NXF family which do not act as general export receptors, e.g. human NXF2-5, *D. melanogaster* NXF2-4 or *C. elegans* NXF2.

Crm1

Crm1 is involved in the nuclear export of a variety of RNA and protein substrates (e.g. U snRNAs, rRNAs and proteins carrying leucine-rich NESs), but is thought not to be a general mRNA export receptor in mammals (Bogerd *et al.*, 1998, Gallouzi and Steitz, 2001; Guzik *et al.*, 2001; Wolff *et al.*, 1997). Nevertheless, human Crm1 was shown to be essential for the nuclear export of mRNAs carrying AU-rich elements (AREs) (Brennan *et al.*, 2000; Gallouzi *et al.*, 2001). These mRNAs often encode proteins whose expression needs to be shut-off or induced rapidly (such as heat shock factors, cytokines, lymphokines, and protooncogenes). Thus, mammalian Crm1 seems to be a specialized export factor for mRNAs for certain subclasses of mRNAs. Whether Crm1 plays a similar role in *Drosophila* was unknown at the time this study was initiated.

We have tested whether the transcripts which were still exported in cells depleted of NXF1, p15 or UAP56, used the Crm1 pathway to exit the nucleus (Herold *et al.*, 2003). To this end, we analyzed whether these mRNAs were still able to reach the cytoplasm in *Drosophila* cells in which endogenous Crm1 had been inactivated with the drug leptomycin B (LMB). However, the cytoplasmic levels of none of the candidate mRNAs changed significantly. Thus, most - if not all - mRNAs of this group do not reach the cytoplasm by recruiting CRM1. We cannot exclude that a few mRNAs of this group could also be extremely stable so that an export block would not be visible after the 12-hour treatment.

Overall, less than 0.5% of all detectable mRNAs were underrepresented in the cytoplasm of cells treated with LMB. This indicates that in *Drosophila*, like in mammals, Crm1 is not a major mRNA export receptor. Furthermore, all candidate mRNAs underrepresented in the cytoplasm after LMB treatment were also underrepresented in the cytoplasm of NXF1 knockdowns. Hence, in this genome-wide analysis, we could not

identify mRNAs which are exported by Crm1, independently of the default mRNA export machinery.

NXF proteins

The genomes of all higher eukaryotes analyzed so far encode more than one NXF protein. We have shown that the multiplication of *nxf* genes occurred independently in several eukaryotic lineages, suggesting that the selective advantage of having several NXF proteins was high. Only one NXF member in all species tested so far seems to fulfill a general role in the export of bulk mRNA (e.g. NXF1 in *C. elegans* or *Drosophila*) while the function of the other NXF proteins from the same species is largely unknown. As many of these NXF proteins were shown to possess features required to export mRNAs, they were suggested to possibly serve as "alternative" export receptors.

Drosophila NXFs

Of the four *Drosophila* NXF members, three were found to be expressed in Schneider cells (NXF1-3), but only NXF1 plays an essential role in general mRNA export (Herold *et al.*, 2001). The depletion of NXF2 and NXF3 by RNAi does not result in any obvious growth phenotype suggesting that, if they participated in mRNA export, their cargoes are not essential in cultured cells (Herold *et al.*, 2001). To identify potential export substrates of NXF2 and NXF3, we depleted these proteins from Schneider cells and monitored the effects by microarray analysis (Herold *et al.*, 2003). But despite monitoring the relative cytoplasmic expression levels of about 6000 different mRNAs we have not been able to identify any potential mRNA export substrate for NXF2 or NXF3. The only mRNAs which were changed significantly in NXF2 or NXF3 knockdowns, were the mRNAs encoding the targeted export factors themselves. We cannot rule out that NXF2 or NXF3 do nevertheless participate in the export of specific mRNAs, but play a redundant or non-essential role. In this context it should be noted that codepletion of both NXF2 and NXF3 does not lead to a growth defect or any other obvious phenotype (A. Herold and E. Izaurralde, unpublished observations). It is also possible that potential substrate mRNAs were not represented on the microarray, since the *Drosophila* genome is predicted to contain approximately 14,000 genes, with only ~ 6000 represented on our array. Despite these caveats, our data argue against a role for NXF2 and NXF3 in mRNA export in S2 cells.

It is possible that *Drosophila* NXF2 and NXF3 play a role in the export of transcripts which are not expressed in S2 cells. One could for example imagine a tissue- or stage-specific expression of the different NXF proteins to direct the regulated export of selected mRNAs. Currently, we do not have any indication for a tissue-specific expression of NXF members in *Drosophila*. The transcripts encoding NXF1-3 were found to be

expressed in embryos and in all cell lines tested including two embryonic and one imaginal disc cell line (Herold *et al.*, 2001). *In situ* hybridization to detect endogenous *nxf1*, *nxf2* and *nxf3* mRNA in embryos revealed a uniform staining, although a tissue-specific expression pattern in larvae or adult flies cannot be ruled out (A. Herold and E. Izaurralde, unpublished results; C. Korey and D. Van Vactor, personal communication). Also, tissue-specific distribution or activation of NXF proteins cannot be excluded, as the presence of a specific mRNA does not always lead to (active) protein. We have not investigated whether the expression of NXF2-4 is regulated during specific stages of development.

C. elegans NXFs

The *C. elegans* genome encodes two *nxf* genes (*nxf1* and *nxf2*). CeNXF1 is a shuttling protein that can interact with RNA and nucleoporins. Its functional knockout by RNAi is lethal and results in the nuclear accumulation of poly(A)⁺ RNA, suggesting that it functions as a general mRNA export receptor. In contrast, silencing of Ce *nxf2* by RNAi does not result in nuclear accumulation of poly(A)⁺ RNA or any other obvious phenotype (Tan *et al.*, 2000). CeNXF2 is therefore another candidate protein which could be involved in very specific (non-essential) export processes. Indeed, CeNXF2 has recently been implicated in a regulated mRNA transport event.

As mentioned in the Introduction, the terminal steps of sex determination in *C. elegans* require the activity of two genes: *tra-1* and *tra-2*. *tra-2* mRNA is retained in the nucleus in the absence of TRA-1 protein. Only when TRA-1 binds the *tra-2* transcript, it is exported to the cytoplasm. This export was shown to depend on Crm1 (Graves *et al.*, 1999; Segal *et al.*, 2001). The nuclear retention seen in the absence of TRA-1 depends on the activity of at least three proteins: CeNXF2, REF-1 and REF-2. Depletion of any of these three proteins by RNAi switches the *tra-2* mRNA export to the "default" CeNXF1 pathway (S. Kuersten and E. Goodwin, personal communication).

Thus, the "alternative" NXF protein (= CeNXF2) in *C. elegans* participates in repressing the normal nuclear export of an mRNA rather than promoting it. CeNXF2 is the only "alternative" NXF protein to date with a clearly assigned function. This example demonstrates that the existence of more than one NXF protein can be used to modulate the "default" mRNA export pathway, and hence provide another posttranscriptional mechanism to regulate gene expression. Several cases of mRNAs whose export is developmentally regulated have been reported in the literature (see section 1.2.4). In most cases, the mechanisms underlying these regulated transport events are only poorly characterized and the export receptors involved remain to be identified. It will be an interesting goal for the future to investigate if in some of these cases "alternative" NXF proteins might be involved.

Human NXFs

While there is no indication for a tissue-specific expression pattern of *D. melanogaster* or *C. elegans* NXF members, work presented in this thesis ([Herold *et al.*, 2001](#); [Jun *et al.*, 2001](#)) and by Yang *et al.* (2001) revealed that mammalian *nxf* transcripts are expressed in a tissue-specific manner. For example, transcripts encoding human NXF2 and NXF3 are mainly found in testis, and the mRNAs encoding mouse NXF-a and NXF-b show especially high levels in brain. In contrast, human *tap* mRNA is expressed at high levels in all tissues tested. These data (in combination with all the functional data implicating TAP in bulk mRNA export) suggest that TAP acts as a general export receptor for mRNAs, while the other human NXF members may have more specialized functions.

We and others have shown that (I), like TAP, human NXF2 and NXF3 also have the ability to promote the nuclear export of reporter mRNAs in mammalian cells, albeit NXF3 only when directly tethered to the reporter ([Herold *et al.*, 2000](#); Yang *et al.*, 2001; and A. Herold, I. Braun and E. Izaurralde, unpublished results). (II) TAP and NXF2 were also shown to directly interact with RNA, with several RNA-binding proteins and with nucleoporins, this latter interaction resulting in a fraction of the proteins being localized to the nuclear envelope ([Herold *et al.*, 2000](#)). (III) TAP and NXF3 associate with mRNAs *in vivo*, as both proteins can be crosslinked with poly(A)⁺ RNA in transfected cells (Yang *et al.*, 2001).

Thus, human NXF2 and NXF3 fulfill many of the basic requirements to act as mRNA export receptors. Due to the abundance of their mRNAs in testis, they have been suggested to play a role in male germ cell development, possibly acting as tissue-specific nuclear RNA export factors (Yang *et al.*, 2001). Such mRNA export factors could participate in the export of bulk mRNA in tissues in which they are expressed, maybe enhancing the overall efficiency of mRNA export. Alternatively, they could participate in the tissue-specific export of selected mRNAs.

Human NXF3 lacks most of the UBA-like domain implicated in nucleoporin binding and fails to directly interact with nucleoporins ([Herold *et al.*, 2000](#)). A TAP mutant carrying the equivalent deletion of the UBA-like domain cannot stimulate nuclear export of a tethered reporter mRNA. Nevertheless, NXF3 is able to promote the nuclear export of such mRNAs (Yang *et al.*, 2001; A. Herold, I. Braun and E. Izaurralde, unpublished results). This apparent contradiction can be explained by the fact that NXF3 (but not TAP) contains a leucine-rich NES allowing the interaction with Crm1. Accordingly, the export and shuttling activity of NXF3 depends on Crm1, and can be blocked by LMB, while TAP-mediated export occurs independently of Crm1 (Yang *et al.*, 2001). In that sense, human NXF3 seems to serve as an adapter protein rather than as an actual transport receptor, since it is Crm1 that mediates the interaction with the components of the NPC. In this scenario, the export of specific mRNAs could be regulated independently of bulk

mRNA export. This situation is somehow reminiscent of the regulated export of *tra-2* mRNA in *C. elegans* which also involves an NXF protein and Crm1 (see above).

Interestingly, we have observed that *Drosophila* NXF3 also shuttles in a Crm1-dependent manner. Transiently expressed HA-tagged DmNXF3 localizes to the cytoplasm of Schneider cells at steady state. When Crm1-dependent export is blocked with LMB, the protein accumulates in the nuclear compartment, indicating that DmNXF3 is actively exported to the cytoplasm by Crm1 (A. Herold and E. Izaurralde, unpublished results). Along these lines, it is important to note that the UBA-like domain in DmNXF3 has diverged substantially from the typical UBA-like domain present in TAP, and lacks residues that are believed to be critical for nucleoporin-binding. It is therefore possible, that NXF members that acquired the ability to interact with Crm1 (or possibly with other transport factors) have lost their intrinsic competence to contact components of the NPC. In this case, domains which were thought to be essential for NXF function are dispensable. Thus, the lack of such "essential" domains does not always result in non-functional proteins.

As reported in paper 2 of this thesis (section 2.1.2), human NXF5 has been linked to a syndromic form of X-linked mental retardation, as the *nxf5* gene was mutated in a patient carrying this disease, resulting in a functional nullisomy. Since NXF5 exhibits some of the features critical for an mRNA export factor (RNA binding, heterodimerization with p15) and transcripts encoding the closest mouse orthologues of NXF5 are mainly expressed in the neural system, NXF5 was suggested to play a role in nuclear mRNA export in neurons. Similar to other human NXF homologues, NXF5 might be involved in the export of only a few mRNA species which might be only expressed/exported in neuronal cells. Alternatively, NXF5 could fulfill a more general function in modulating bulk mRNA export in these cells.

Altogether, even though some of the "non-default" NXF proteins have been shown to fulfill many of the requirements to act as mRNA export receptors, the nature of their potential endogenous cargoes is - apart from *tra2* mRNA as a target of *C. elegans* NXF2 - still unknown. Attempts to find export substrates of *Drosophila* NXF2 and NXF3 in Schneider cells failed (Herold *et al.*, 2003). The identification of NXF targets therefore remains a challenging task for future investigations.

In principle, the possible functions of NXF proteins are not restricted to nuclear mRNA export or repression of this process. Whether a specific NXF protein is implicated in mRNA export or not, should therefore be investigated for each NXF member experimentally, as NXF proteins may also be involved in other aspects of mRNA metabolism, or in unrelated cellular processes. This might especially be true for the *Drosophila* NXF members whose sequences have diverged considerably from each other, resulting in only about 20% identical amino acids when compared amongst each other.

Therefore, DmNXF1 shares more identical amino acids with human TAP (~ 30%) than with the other *Drosophila* NXF members (Herold *et al.*, 2001).

3.5 RNAi and microarrays: novel approaches to study mRNA export *in vivo*

At the time this Ph.D. thesis was initiated, the two main systems used in the functional analysis of nuclear mRNA export in higher eukaryotes were microinjection in *Xenopus* oocytes and transfection assays in mammalian cells (e.g. mRNA export reporter assays or overexpression studies using dominant negative mutants). Albeit both systems have been proven to be powerful tools for the analysis of this pathway *in vivo*, they limited the analysis to selected "representative" mRNAs or bulk poly(A)⁺ RNA. Moreover, microinjection experiments require that the potential export factors to be analyzed are available in a purified form, thus largely restricting the analysis to proteins which can be expressed and/or purified in a functional form. Alternatively, specific antibodies or drugs inactivating the protein of interest could be injected. The reporter assays available for mammalian cells were largely designed for the analysis of viral transcripts, and only some recent modifications also allowed the analysis of cellular mRNA export. And although these systems allow to investigate whether a protein of interest stimulates or inhibits nuclear export of a specific mRNA, the natural role of the protein cannot be analyzed. For example, none of the above systems allows to analyze whether a protein is essential or dispensable for the export of endogenous mRNAs. Knockout approaches that could address this issue were available (e.g. in mouse), but technically difficult and time-consuming. Analysis of mRNA export in yeast does not suffer from these limitations as targeted mutagenesis by homologous recombination allows the straightforward inactivation of the protein of interest. In addition, the functional analysis is facilitated by the availability of temperature-sensitive mutants. This, in combination with a large variety of biochemical and other screening methods (such as TAP-tagging and synthetic lethal screens etc.) still makes yeast one of the most powerful systems to study nuclear export.

The recent discovery of RNAi provides an efficient tool to generate functional knockouts ("knockdowns") in higher eukaryotes. This method involves the specific degradation of an endogenous mRNA species triggered by the presence of double-stranded RNA (dsRNA) which contains the mRNA sequence to be targeted. As the degraded mRNA cannot direct protein synthesis anymore, the protein of interest is subsequently depleted from the cell. RNAi therefore allows the transient silencing of specific genes. The successful use of RNAi has been described for many different eukaryotic species, including *C. elegans*, *D. melanogaster* and human tissue culture cells. The advantage of *Drosophila* tissue culture cells is that long dsRNA molecules synthesized *in vitro* can be used. These are readily taken up by the cells without the need for a specific transfection

reagent which ensures that virtually all cells in the population are targeted. The homogeneity of the treated cell population facilitates subsequent biochemical analysis, e.g. fractionation of nuclear and cytoplasmic components, and is a prerequisite for large-scale approaches such as microarray analysis. This is in contrast to human cells in which the targeting efficiency depends on the successful transfection of siRNAs mediated by special transfection reagents, usually resulting in only a fraction of the cells being targeted.

Using a combination of RNAi and subsequent microarray analysis we have monitored the cytoplasmic abundance of nearly half of the predicted *Drosophila* transcriptome after depleting five different potential export factors (Herold *et al.*, 2003). This approach led to important discoveries (e.g. that NXF1, p15 and UAP56 belong to a single major pathway in *Drosophila*) but also raised some interesting questions that should be addressed in the future. We have identified a set of mRNAs which are exported despite the general mRNA export block, and some which require NXF1:p15 but not UAP56. It would be interesting to investigate which features allow these particular transcripts to behave differently than bulk poly(A)⁺ RNA. In addition, our analysis revealed a feedback loop by which a block to mRNA export triggers the upregulation of genes implicated in this process. The mechanisms that are responsible for sensing the export block and for the subsequent response are completely unexplored and should be investigated in the future. It is also possible that unknown components of the nuclear export pathway will be identified amongst the upregulated mRNAs. We have already provided some experimental evidence that Ssrp, encoded by one of the upregulated mRNAs, might play a role in the export of poly(A)⁺ RNA. Several of the upregulated mRNAs encode ABC class ATPases. Interestingly, a recent report described Elf1p, another member of this family of ATPases, as an mRNA export factor in *S. pombe* (Kozak *et al.*, 2002). These results suggest that the data obtained in the large-scale analysis could serve as a starting point to identify unknown components of the mRNA export machinery.

Other interesting issues that should be investigated in the future are: At which step in the export pathway does UAP56 act? How does it recruit NXF1:p15 heterodimers? As REF proteins and other components of the EJC are dispensable for mRNA export in *Drosophila*, other adapters must exist which link UAP56 to NXF1:p15 heterodimers (Gatfield and Izaurralde, 2002). The identification of these adapters is an important goal for the future.

Since the RNAi technology also has some clear disadvantages (the depletion is never 100% effective and only transient; the reduction of the protein level is gradual and dependent on the stability of the targeted mRNA and the protein; many effects observed can be indirect etc.) only the combination of all available methods, including "classical" (biochemical and cell biological) and RNAi-based approaches can give us conclusive answers to how mRNA export works.

References

- Aitchison, J.D. and Rout, M.P. (2000) The road to ribosomes. Filling potholes in the export pathway. *J Cell Biol* **151**, F23-26.
- Amberg, D.C., Fleischmann, M., Stagljar, I., Cole, C.N. and Aebi, M. (1993) Nuclear PRP20 protein is required for mRNA export. *EMBO J* **12**, 233-241.
- Amberg, D.C., Goldstein, A.L. and Cole, C.N. (1992) Isolation and characterization of RAT1: an essential gene of *Saccharomyces cerevisiae* required for the efficient nucleocytoplasmic trafficking of mRNA. *Genes Dev* **6**, 1173-1189.
- Andrulis, E.D., Werner, J., Nazarian, A., Erdjument-Bromage, H., Tempst, P. and Lis, J.T. (2002) The RNA processing exosome is linked to elongating RNA polymerase II in *Drosophila*. *Nature* **420**, 837-841.
- Arts, G.J., Fornerod, M. and Mattaj, I.W. (1998a) Identification of a nuclear export receptor for tRNAs. *Curr Biol* **8**, 305-314.
- Arts, G.J., Kuersten, S., Romby, P., Ehresmann, B. and Mattaj, I.W. (1998b) The role of exportin-t in selective nuclear export of mature tRNAs. *EMBO J* **17**, 7430-7441.
- Bachi, A., Braun, I.C., Rodrigues, J.P., Pante, N., Ribbeck, K., von Kobbe, C., Kutay, U., Wilm, M., Gorlich, D., Carmo-Fonseca, M. and Izaurralde, E. (2000) The C-terminal domain of TAP interacts with the nuclear pore complex and promotes export of specific CTE-bearing RNA substrates. *RNA* **6**, 136-158.
- Bailer, S.M., Sinioglou, S., Podtelejnikov, A., Hellwig, A., Mann, M. and Hurt, E. (1998) Nup116p and nup100p are interchangeable through a conserved motif which constitutes a docking site for the mRNA transport factor gle2p. *EMBO J* **17**, 1107-1119.
- Bassler, J., Grandi, P., Gadal, O., Lessmann, T., Petfalski, E., Tollervey, D., Lechner, J. and Hurt, E. (2001) Identification of a 60S preribosomal particle that is closely linked to nuclear export. *Mol Cell* **8**, 517-529.
- Bear, J., Tan, W., Zolotukhin, A.S., Tabernero, C., Hudson, E.A. and Felber, B.K. (1999) Identification of novel import and export signals of human TAP, the protein that binds to the constitutive transport element of the type D retrovirus mRNAs. *Mol Cell Biol* **19**, 6306-6317.
- Bischoff, F.R., Scheffzek, K. and Ponstingl, H. (2002) How Ran is regulated. *Results Probl Cell Differ* **35**, 49-66.
- Black, B.E., Levesque, L., Holaska, J.M., Wood, T.C. and Paschal, B.M. (1999) Identification of an NTF2-related factor that binds Ran-GTP and regulates nuclear protein export. *Mol Cell Biol* **19**, 8616-8624.
- Blencowe, B.J., Issner, R., Nickerson, J.A. and Sharp, P.A. (1998) A coactivator of pre-mRNA splicing. *Genes Dev* **12**, 996-1009.
- Bogerd, H.P., Echarri, A., Ross, T.M. and Cullen, B.R. (1998) Inhibition of human immunodeficiency virus Rev and human T-cell leukemia virus Rex function, but not Mason-Pfizer monkey virus constitutive transport element activity, by a mutant human nucleoporin targeted to Crm1. *J Virol* **72**, 8627-8635.
- Bohnsack, M.T., Regener, K., Schwappach, B., Saffrich, R., Paraskeva, E., Hartmann, E. and Gorlich, D. (2002) Exp5 exports eEF1A via tRNA from nuclei and synergizes with other transport pathways to confine translation to the cytoplasm. *EMBO J* **21**, 6205-6215.
- Braun, I.C., Herold, A., Rode, M., Conti, E. and Izaurralde, E. (2001) Overexpression of TAP/p15 heterodimers bypasses nuclear retention and stimulates nuclear mRNA export. *J Biol Chem* **276**, 19.
- Braun, I.C., Herold, A., Rode, M. and Izaurralde, E. (2002) Nuclear export of mRNA by TAP/NXF1 requires two nucleoporin-binding sites but not p15. *Mol Cell Biol* **22**, 5405-5418.
- Braun, I.C., Rohrbach, E., Schmitt, C. and Izaurralde, E. (1999) TAP binds to the constitutive transport element (CTE) through a novel RNA-binding motif that is sufficient to promote CTE-dependent RNA export from the nucleus. *EMBO J* **18**, 1953-1965.

- Brennan, C.M., Gallouzi, I.E. and Steitz, J.A. (2000) Protein ligands to HuR modulate its interaction with target mRNAs *in vivo*. *J Cell Biol* **151**, 1-14.
- Brodsky, A.S. and Silver, P.A. (2000) Pre-mRNA processing factors are required for nuclear export. *RNA* **6**, 1737-1749.
- Brown, J.A., Bharathi, A., Ghosh, A., Whalen, W., Fitzgerald, E. and Dhar, R. (1995) A mutation in the *Schizosaccharomyces pombe* rae1 gene causes defects in poly(A)⁺ RNA export and in the cytoskeleton. *J Biol Chem* **270**, 7411-7419.
- Chang, D.D. and Sharp, P.A. (1989) Regulation by HIV Rev depends upon recognition of splice sites. *Cell* **59**, 789-795.
- Cheng, Y., Dahlberg, J.E. and Lund, E. (1995) Diverse effects of the guanine nucleotide exchange factor RCC1 on RNA transport. *Science* **267**, 1807-1810.
- Clouse, K.N., Luo, M.J., Zhou, Z. and Reed, R. (2001) A Ran-independent pathway for export of spliced mRNA. *Nat Cell Biol* **3**, 97-99.
- Cramer, P., Srebrow, A., Kadener, S., Werbajh, S., de la Mata, M., Melen, G., Nogues, G. and Kornblihtt, A.R. (2001) Coordination between transcription and pre-mRNA processing. *FEBS* **498**, 179-182.
- Cullen, B.R. (1998) Retroviruses as model systems for the study of nuclear RNA export pathways. *Virology* **249**, 203-210.
- Cullen, B.R. (2000) Nuclear RNA export pathways. *Mol Cell Biol* **20**, 4181-4187.
- Cullen, B.R. (2003) Nuclear RNA export. *J Cell Sci* **116**, 587-597.
- Custodio, N., Carmo-Fonseca, M., Geraghty, F., Pereira, H.S., Grosveld, F. and Antoniou, M. (1999) Inefficient processing impairs release of RNA from the site of transcription. *EMBO J* **18**, 2855-2866.
- Daneholt, B. (1997) A look at messenger RNP moving through the nuclear pore. *Cell* **88**, 585-588.
- De Robertis, E.M., Black, P. and Nishikura, K. (1981) Intranuclear location of the tRNA splicing enzymes. *Cell* **23**, 89-93.
- Del Priore, V., Snay, C.A., Bahr, A. and Cole, C.N. (1996) The product of the *Saccharomyces cerevisiae* RSS1 gene, identified as a high-copy suppressor of the rat7-1 temperature-sensitive allele of the RAT7/NUP159 nucleoporin, is required for efficient mRNA export. *Mol Biol Cell* **7**, 1601-1621.
- Dower, K. and Rosbash, M. (2002) T7 RNA polymerase-directed transcripts are processed in yeast and link 3' end formation to mRNA nuclear export. *RNA* **8**, 686-697.
- Dreyfuss, G., Matunis, M.J., Pinol-Roma, S. and Burd, C.G. (1993) hnRNP proteins and the biogenesis of mRNA. *Annu Rev Biochem* **62**, 289-321.
- Eckner, R., Ellmeier, W. and Birnstiel, M.L. (1991) Mature mRNA 3' end formation stimulates RNA export from the nucleus. *EMBO J* **10**, 3513-3522.
- Fahrenkrog, B. and Aebi, U. (2002) The vertebrate nuclear pore complex: from structure to function. *Results Probl Cell Differ* **35**, 25-48.
- Fischer, U., Huber, J., Boelens, W.C., Mattaj, I.W. and Luhrmann, R. (1995) The HIV-1 Rev activation domain is a nuclear export signal that accesses an export pathway used by specific cellular RNAs. *Cell* **82**, 475-483.
- Fleckner, J., Zhang, M., Valcarcel, J. and Green, M.R. (1997) U2AF65 recruits a novel human DEAD box protein required for the U2 snRNP-branchpoint interaction. *Genes Dev* **11**, 1864-1872.
- Fornerod, M. and Ohno, M. (2002) Exportin-mediated nuclear export of proteins and ribonucleoproteins. *Results Probl Cell Differ* **35**, 67-91.
- Fornerod, M., Ohno, M., Yoshida, M. and Mattaj, I.W. (1997) CRM1 is an export receptor for leucine-rich nuclear export signals. *Cell* **90**, 1051-1060.
- Forrester, W., Stutz, F., Rosbash, M. and Wickens, M. (1992) Defects in mRNA 3'-end formation, transcription initiation, and mRNA transport associated with the yeast mutation prp20: possible coupling of mRNA processing and chromatin structure. *Genes Dev* **6**, 1914-1926.
- Fribourg, S., Braun, I.C., Izaurrealde, E. and Conti, E. (2001) Structural basis for the recognition of a nucleoporin FG repeat by the NTF2-like domain of the TAP/p15 mRNA nuclear export factor. *Mol Cell* **8**, 645-656.

- Gadal, O., Strauss, D., Braspenning, J., Hoepfner, D., Petfalski, E., Philippsen, P., Tollervey, D. and Hurt, E. (2001a) A nuclear AAA-type ATPase (Rix7p) is required for biogenesis and nuclear export of 60S ribosomal subunits. *EMBO J* **20**, 3695-3704.
- Gadal, O., Strauss, D., Kessler, J., Trumpower, B., Tollervey, D. and Hurt, E. (2001b) Nuclear export of 60s ribosomal subunits depends on Xpo1p and requires a nuclear export sequence-containing factor, Nmd3p, that associates with the large subunit protein Rpl10p. *Mol Cell Biol* **21**, 3405-3415.
- Gallouzi, I.E., Brennan, C.M. and Steitz, J.A. (2001) Protein ligands mediate the CRM1-dependent export of HuR in response to heat shock. *RNA* **7**, 1348-1361.
- Gallouzi, I.E., Brennan, C.M., Stenberg, M.G., Swanson, M.S., Eversole, A., Maizels, N. and Steitz, J.A. (2000) HuR binding to cytoplasmic mRNA is perturbed by heat shock. *Proc Natl Acad Sci U S A* **97**, 3073-3078.
- Gallouzi, I.E. and Steitz, J.A. (2001) Delineation of mRNA export pathways by the use of cell-permeable peptides. *Science* **294**, 1895-1901.
- Gatfield, D. and Izaurralde, E. (2002) REF1/Aly and the additional exon junction complex proteins are dispensable for nuclear export. *J Cell Biol* **159**, 579-88.
- Gatfield, D., Le Hir, H., Schmitt, C., Braun, I.C., Kocher, T., Wilm, M. and Izaurralde, E. (2001) The DEXH/D box protein HEL/UAP56 is essential for mRNA nuclear export in *Drosophila*. *Curr Biol* **11**, 1716-1721.
- Gorlich, D. and Kutay, U. (1999) Transport between the cell nucleus and the cytoplasm. *Annu Rev Cell Dev Biol* **15**, 607-660.
- Grant, R.P., Hurt, E., Neuhaus, D. and Stewart, M. (2002) Structure of the C-terminal FG-nucleoporin binding domain of Tap/NXF1. *Nat Struct Biol* **9**, 247-251.
- Graves, L.E., Segal, S. and Goodwin, E.B. (1999) TRA-1 regulates the cellular distribution of the *tra-2* mRNA in *C. elegans*. *Nature* **399**, 802-805.
- Grosshans, H., Hurt, E. and Simos, G. (2000) An aminoacylation-dependent nuclear tRNA export pathway in yeast. *Genes Dev* **14**, 830-840.
- Gruter, P., Taberner, C., von Kobbe, C., Schmitt, C., Saavedra, C., Bachi, A., Wilm, M., Felber, B.K. and Izaurralde, E. (1998) TAP, the human homolog of Mex67p, mediates CTE-dependent RNA export from the nucleus. *Mol Cell* **1**, 649-659.
- Guzik, B.W., Levesque, L., Prasad, S., Bor, Y.C., Black, B.E., Paschal, B.M., Rekosh, D. and Hammarskjold, M.L. (2001) NXT1 (p15) is a crucial cellular cofactor in TAP-dependent export of intron-containing RNA in mammalian cells. *Mol Cell Biol* **21**, 2545-2554.
- Hamm, J. and Mattaj, I.W. (1990) Monomethylated cap structures facilitate RNA export from the nucleus. *Cell* **63**, 109-118.
- Hammell, C.M., Gross, S., Zenklusen, D., Heath, C.V., Stutz, F., Moore, C. and Cole, C.N. (2002) Coupling of termination, 3' processing, and mRNA export. *Mol Cell Biol* **22**, 6441-6457.
- Herold, A., Klymenko, T. and Izaurralde, E. (2001) NXF1/p15 heterodimers are essential for mRNA nuclear export in *Drosophila*. *RNA* **7**, 1768-1780.
- Herold, A., Suyama, M., Rodrigues, J.P., Braun, I.C., Kutay, U., Carmo-Fonseca, M., Bork, P. and Izaurralde, E. (2000) TAP (NXF1) belongs to a multigene family of putative RNA export factors with a conserved modular architecture. *Mol Cell Biol* **20**, 8996-9008.
- Herold, A., Teixeira, L. and Izaurralde, E. (2003) Genome-wide analysis of mRNA nuclear export pathways in *Drosophila*. *Submitted*.
- Hieronimus, H. and Silver, P. (2003) Genome-wide analysis of RNA-protein interactions illustrates specificity of the mRNA export machinery. *Nat Gen*.
- Hilleren, P., McCarthy, T., Rosbash, M., Parker, R. and Jensen, T.H. (2001) Quality control of mRNA 3'-end processing is linked to the nuclear exosome. *Nature* **413**, 538-542.
- Hilleren, P. and Parker, R. (2001) Defects in the mRNA export factors Rat7p, Gle1p, Mex67p, and Rat8p cause hyperadenylation during 3'-end formation of nascent transcripts. *RNA* **7**, 753-764.
- Ho, D.N., Coburn, G.A., Kang, Y., Cullen, B.R. and Georgiadis, M.M. (2002) The crystal structure and mutational analysis of a novel RNA-binding domain found in the human Tap nuclear mRNA export factor. *Proc Natl Acad Sci U S A* **99**, 1888-1893.

- Ho, J.H., Kallstrom, G. and Johnson, A.W. (2000) Nmd3p is a Crm1p-dependent adapter protein for nuclear export of the large ribosomal subunit. *J Cell Biol* **151**, 1057-1066.
- Hodge, C.A., Colot, H.V., Stafford, P. and Cole, C.N. (1999) Rat8p/Dbp5p is a shuttling transport factor that interacts with Rat7p/Nup159p and Gle1p and suppresses the mRNA export defect of xpo1-1 cells. *EMBO J* **18**, 5778-5788.
- Huang, Y. and Carmichael, G.C. (1996) Role of polyadenylation in nucleocytoplasmic transport of mRNA. *Mol Cell Biol* **16**, 1534-1542.
- Hurt, D.J., Wang, S.S., Lin, Y.H. and Hopper, A.K. (1987) Cloning and characterization of LOS1, a *Saccharomyces cerevisiae* gene that affects tRNA splicing. *Mol Cell Biol* **7**, 1208-1216.
- Hurt, E., Hannus, S., Schmelzl, B., Lau, D., Tollervey, D. and Simos, G. (1999) A novel *in vivo* assay reveals inhibition of ribosomal nuclear export in ran-cycle and nucleoporin mutants. *J Cell Biol* **144**, 389-401.
- Izaurrealde, E. (2002) A novel family of nuclear transport receptors mediates the export of messenger RNA to the cytoplasm. *Eur J Cell Biol* **81**, 577-584.
- Izaurrealde, E., Jarmolowski, A., Beisel, C., Mattaj, I.W., Dreyfuss, G. and Fischer, U. (1997a) A role for the M9 transport signal of hnRNP A1 in mRNA nuclear export. *J Cell Biol* **137**, 27-35.
- Izaurrealde, E., Kutay, U., von Kobbe, C., Mattaj, I.W. and Gorlich, D. (1997b) The asymmetric distribution of the constituents of the Ran system is essential for transport into and out of the nucleus. *EMBO J* **16**, 6535-6547.
- Izaurrealde, E., Lewis, J., Gamberi, C., Jarmolowski, A., McGuigan, C. and Mattaj, I.W. (1995) A cap-binding protein complex mediating U snRNA export. *Nature* **376**, 709-712.
- Izaurrealde, E., Lewis, J., McGuigan, C., Jankowska, M., Darzynkiewicz, E. and Mattaj, I.W. (1994) A nuclear cap binding protein complex involved in pre-mRNA splicing. *Cell* **78**, 657-668.
- Jang, B.C., Munoz-Najar, U., Paik, J.H., Claffey, K., Yoshida, M. and Hla, T. (2002) Leptomycin B, an inhibitor of the nuclear export receptor CRM1, inhibits COX-2 expression. *J Biol Chem* **4**, 4.
- Jarmolowski, A., Boelens, W.C., Izaurrealde, E. and Mattaj, I.W. (1994) Nuclear export of different classes of RNA is mediated by specific factors. *J Cell Biol* **124**, 627-635.
- Jensen, T.H., Boulay, J., Rosbash, M. and Libri, D. (2001a) The DECD box putative ATPase Sub2p is an early mRNA export factor. *Curr Biol* **11**, 1711-1715.
- Jensen, T.H., Patricio, K., McCarthy, T. and Rosbash, M. (2001b) A Block to mRNA Nuclear Export in *S. cerevisiae* Leads to Hyperadenylation of Transcripts that Accumulate at the Site of Transcription. *Mol Cell* **7**, 887-898.
- Jensen, T.H. and Rosbash, M. (2003) Co-transcriptional monitoring of mRNP formation. *Nat Struct Biol* **10**, 10-11.
- Jimeno, S., Rondon, A.G., Luna, R. and Aguilera, A. (2002) The yeast THO complex and mRNA export factors link RNA metabolism with transcription and genome instability. *EMBO J* **21**, 3526-3535.
- Jun, L., Frints, S., Duhamel, H., Herold, A., Abad-Rodrigues, J., Dotti, C., Izaurrealde, E., Marynen, P. and Froyen, G. (2001) *NXF5*, a novel member of the nuclear RNA export factor family, is lost in a male patient with a syndromic form of mental retardation. *Curr Biol* **11**, 1381-1391.
- Kadowaki, T., Chen, S., Hitomi, M., Jacobs, E., Kumagai, C., Liang, S., Schneiter, R., Singleton, D., Wisniewska, J. and Tartakoff, A.M. (1994) Isolation and characterization of *Saccharomyces cerevisiae* mRNA transport-defective (mtr) mutants. *J Cell Biol* **126**, 649-659.
- Kadowaki, T., Goldfarb, D., Spitz, L.M., Tartakoff, A.M. and Ohno, M. (1993) Regulation of RNA processing and transport by a nuclear guanine nucleotide release protein and members of the Ras superfamily. *EMBO J* **12**, 2929-2937.
- Kadowaki, T., Zhao, Y. and Tartakoff, A.M. (1992) A conditional yeast mutant deficient in mRNA transport from nucleus to cytoplasm. *Proc Natl Acad Sci U S A* **89**, 2312-2316.
- Kang, Y., Bogerd, H.P. and Cullen, B.R. (2000) Analysis of cellular factors that mediate nuclear export of RNAs bearing the Mason-Pfizer monkey virus constitutive transport element. *J Virol* **74**, 5863-5871.
- Kang, Y. and Cullen, B.R. (1999) The human Tap protein is a nuclear mRNA export factor that contains novel RNA-binding and nucleocytoplasmic transport sequences. *Genes Dev* **13**, 1126-1139.

- Katahira, J., Strasser, K., Podtelejnikov, A., Mann, M., Jung, J.U. and Hurt, E. (1999) The Mex67p-mediated nuclear mRNA export pathway is conserved from yeast to human. *EMBO J* **18**, 2593-2609.
- Kataoka, N., Diem, M.D., Kim, V.N., Yong, J. and Dreyfuss, G. (2001) Magoh, a human homolog of *Drosophila mago nashi* protein, is a component of the splicing-dependent exon-exon junction complex. *EMBO J* **20**, 6424-6433.
- Kataoka, N., Yong, J., Kim, V.N., Velazquez, F., Perkinson, R.A., Wang, F. and Dreyfuss, G. (2000) Pre-mRNA splicing imprints mRNA in the nucleus with a novel RNA-binding protein that persists in the cytoplasm. *Mol Cell* **6**, 673-682.
- Kiesler, E., Miralles, F. and Visa, N. (2002) HEL/UAP56 binds cotranscriptionally to the Balbiani ring pre-mRNA in an intron-independent manner and accompanies the BR mRNP to the nuclear pore. *Curr Biol* **12**, 859-862.
- Kim, V.N., Yong, J., Kataoka, N., Abel, L., Diem, M.D. and Dreyfuss, G. (2001) The Y14 protein communicates to the cytoplasm the position of exon-exon junctions. *EMBO J* **20**, 2062-2068.
- Kistler, A.L. and Guthrie, C. (2001) Deletion of MUD2, the yeast homolog of U2AF65, can bypass the requirement for sub2, an essential spliceosomal ATPase. *Genes Dev* **15**, 42-49.
- Kozak, L., Gopal, G., Yoon, J.H., Sauna, Z.E., Ambudkar, S.V., Thakurta, A.G. and Dhar, R. (2002) Elf1p, a member of the ABC class of ATPases, functions as a mRNA export factor in *Schizosaccharomyces pombe*. *J Biol Chem* **277**, 33580-33589.
- Kraemer, D. and Blobel, G. (1997) mRNA binding protein mrnp 41 localizes to both nucleus and cytoplasm. *Proc Natl Acad Sci U S A* **94**, 9119-9124.
- Krebber, H., Taura, T., Lee, M.S. and Silver, P.A. (1999) Uncoupling of the hnRNP Npl3p from mRNAs during the stress-induced block in mRNA export. *Genes Dev* **13**, 1994-2004.
- Kuersten, S., Ohno, M. and Mattaj, I.W. (2001) Nucleocytoplasmic transport: Ran, beta and beyond. *Trends Cell Biol* **11**, 497-503.
- Kutay, U., Lipowsky, G., Izaurralde, E., Bischoff, F.R., Schwarzmaier, P., Hartmann, E. and Gorlich, D. (1998) Identification of a tRNA-specific nuclear export receptor. *Mol Cell* **1**, 359-369.
- Labeit, S., Kolmerer, B. and Linke, W.A. (1997) The giant protein titin. Emerging roles in physiology and pathophysiology. *Circ Res* **80**, 290-294.
- Larocque, D., Pilotte, J., Chen, T., Cloutier, F., Massie, B., Pedraza, L., Couture, R., Lasko, P., Almazan, G. and Richard, S. (2002) Nuclear retention of MBP mRNAs in the *quaking* viable mice. *Neuron* **36**, 815-829.
- Le Hir, H., Gatfield, D., Braun, I.C., Forler, D. and Izaurralde, E. (2001a) The protein Mago provides a link between splicing and mRNA localization. *EMBO Rep* **2**, 1119-1124.
- Le Hir, H., Gatfield, D., Izaurralde, E. and Moore, M.J. (2001b) The exon-exon junction complex provides a binding platform for factors involved in mRNA export and nonsense-mediated mRNA decay. *EMBO J* **20**, 4987-4997.
- Le Hir, H., Izaurralde, E., Maquat, L.E. and Moore, M.J. (2000a) The spliceosome deposits multiple proteins 20-24 nucleotides upstream of mRNA exon-exon junctions. *EMBO J* **19**, 6860-6869.
- Le Hir, H., Moore, M.J. and Maquat, L.E. (2000b) Pre-mRNA splicing alters mRNP composition: evidence for stable association of proteins at exon-exon junctions. *Genes Dev* **14**, 1098-1108.
- Lee, M.S., Henry, M. and Silver, P.A. (1996) A protein that shuttles between the nucleus and the cytoplasm is an important mediator of RNA export. *Genes Dev* **10**, 1233-1246.
- Legrain, P. and Rosbash, M. (1989) Some cis- and trans-acting mutants for splicing target pre-mRNA to the cytoplasm. *Cell* **57**, 573-583.
- Lei, E.P., Krebber, H. and Silver, P.A. (2001) Messenger RNAs are recruited for nuclear export during transcription. *Genes Dev* **15**, 1771-1782.
- Lei, E.P. and Silver, P.A. (2002a) Intron status and 3'-end formation control cotranscriptional export of mRNA. *Genes Dev* **16**, 2761-2766.
- Lei, E.P. and Silver, P.A. (2002b) Protein and RNA export from the nucleus. *Dev Cell* **2**, 261-272.
- Lengyel, J.A., and Penman, S. (1977) Differential stability of cytoplasmic RNA in a *Drosophila* cell line. *Dev Biol* **57**, 243-253.

- Levesque, L., Guzik, B., Guan, T., Coyle, J., Black, B.E., Rekosh, D., Hammarskjold, M.L. and Paschal, B.M. (2001) RNA export mediated by tap involves NXT1-dependent interactions with the nuclear pore complex. *J Biol Chem* **276**, 44953-44962.
- Libri, D., Dower, K., Boulay, J., Thomsen, R., Rosbash, M. and Jensen, T.H. (2002) Interactions between mRNA export commitment, 3'-end quality control, and nuclear degradation. *Mol Cell Biol* **22**, 8254-8266.
- Libri, D., Graziani, N., Saguez, C. and Boulay, J. (2001) Multiple roles for the yeast SUB2/yUAP56 gene in splicing. *Genes Dev* **15**, 36-41.
- Liker, E., Fernandez, E., Izaurralde, E. and Conti, E. (2000) The structure of the mRNA export factor TAP reveals a cis arrangement of a non-canonical RNP domain and an LRR domain. *EMBO J* **19**, 5587-5598.
- Lipowsky, G., Bischoff, F.R., Izaurralde, E., Kutay, U., Schafer, S., Gross, H.J., Beier, H. and Gorlich, D. (1999) Coordination of tRNA nuclear export with processing of tRNA. *RNA* **5**, 539-549.
- Long, R.M., Elliott, D.J., Stutz, F., Rosbash, M. and Singer, R.H. (1995) Spatial consequences of defective processing of specific yeast mRNAs revealed by fluorescent *in situ* hybridization. *RNA* **1**, 1071-1078.
- Lund, E. and Dahlberg, J.E. (1998) Proofreading and aminoacylation of tRNAs before export from the nucleus. *Science* **282**, 2082-2085.
- Luo, M.J. and Reed, R. (1999) Splicing is required for rapid and efficient mRNA export in metazoans. *Proc Natl Acad Sci U S A* **96**, 14937-14942.
- Luo, M.L., Zhou, Z., Magni, K., Christoforides, C., Rappsilber, J., Mann, M. and Reed, R. (2001) Pre-mRNA splicing and mRNA export linked by direct interactions between UAP56 and Aly. *Nature* **413**, 644-647.
- Maniatis, T. and Reed, R. (2002) An extensive network of coupling among gene expression machines. *Nature* **416**, 499-506.
- Mattaj, I.W. and Englmeier, L. (1998) Nucleocytoplasmic transport: the soluble phase. *Annu Rev Biochem* **67**, 265-306.
- Mayeda, A., Badolato, J., Kobayashi, R., Zhang, M.Q., Gardiner, E.M. and Krainer, A.R. (1999) Purification and characterization of human RNPS1: a general activator of pre-mRNA splicing. *EMBO J* **18**, 4560-4570.
- McGarvey, T., Rosonina, E., McCracken, S., Li, Q., Arnaout, R., Mientjes, E., Nickerson, J.A., Awrey, D., Greenblatt, J., Grosveld, G. and Blencowe, B.J. (2000) The acute myeloid leukemia-associated protein, DEK, forms a splicing-dependent interaction with exon-product complexes. *J Cell Biol* **150**, 309-320.
- Melton, D.A., De Robertis, E.M. and Cortese, R. (1980) Order and intracellular location of the events involved in the maturation of a spliced tRNA. *Nature* **284**, 143-148.
- Michael, W.M., Eder, P.S. and Dreyfuss, G. (1997) The K nuclear shuttling domain: a novel signal for nuclear import and nuclear export in the hnRNP K protein. *EMBO J* **16**, 3587-3598.
- Mili, S., Shu, H.J., Zhao, Y. and Pinol-Roma, S. (2001) Distinct RNP complexes of shuttling hnRNP proteins with pre-mRNA and mRNA: candidate intermediates in formation and export of mRNA. *Mol Cell Biol* **21**, 7307-7319.
- Milkereit, P., Gadal, O., Podtelejnikov, A., Trumtel, S., Gas, N., Petfalski, E., Tollervey, D., Mann, M., Hurt, E. and Tschochner, H. (2001) Maturation and intranuclear transport of pre-ribosomes requires Noc proteins. *Cell* **105**, 499-509.
- Milkereit, P., Strauss, D., Bassler, J., Gadal, O., Kuhn, H., Schutz, S., Gas, N., Lechner, J., Hurt, E. and Tschochner, H. (2002) A Noc-complex specifically involved in the formation and nuclear export of ribosomal 40S subunits. *J Biol Chem* **20**, 20.
- Moy, T.I. and Silver, P.A. (1999) Nuclear export of the small ribosomal subunit requires the ran-GTPase cycle and certain nucleoporins. *Genes Dev* **13**, 2118-2133.
- Moy, T.I. and Silver, P.A. (2002) Requirements for the nuclear export of the small ribosomal subunit. *J Cell Sci* **115**, 2985-2995.

- Murphy, R., Watkins, J.L. and Wentz, S.R. (1996) GLE2, a *Saccharomyces cerevisiae* homologue of the *Schizosaccharomyces pombe* export factor RAE1, is required for nuclear pore complex structure and function. *Mol Biol Cell* **7**, 1921-1937.
- Murphy, R. and Wentz, S.R. (1996) An RNA-export mediator with an essential nuclear export signal. *Nature* **383**, 357-360.
- Nabel-Rosen, H., Dorevitch, N., Reuveny, A. and Volk, T. (1999) The balance between two isoforms of the *Drosophila* RNA-binding protein how controls tendon cell differentiation. *Mol Cell* **4**, 573-584.
- Nabel-Rosen, H., Volohonsky, G., Reuveny, A., Zaidel-Bar, R. and Volk, T. (2002) Two isoforms of the *Drosophila* RNA binding protein, how, act in opposing directions to regulate tendon cell differentiation. *Dev Cell* **2**, 183-193.
- Nakielnny, S. and Dreyfuss, G. (1996) The hnRNP C proteins contain a nuclear retention sequence that can override nuclear export signals. *J Cell Biol* **134**, 1365-1373.
- Neville, M. and Rosbash, M. (1999) The NES-Crm1p export pathway is not a major mRNA export route in *Saccharomyces cerevisiae*. *EMBO J* **18**, 3746-3756.
- Ohno, M., Fornerod, M. and Mattaj, I.W. (1998) Nucleocytoplasmic transport: the last 200 nanometers. *Cell* **92**, 327-336.
- Ohno, M., Segref, A., Bachi, A., Wilm, M. and Mattaj, I.W. (2000) PHAX, a mediator of U snRNA nuclear export whose activity is regulated by phosphorylation. *Cell* **101**, 187-198.
- Ohno, M., Segref, A., Kuersten, S. and Mattaj, I.W. (2002) Identity elements used in export of mRNAs. *Mol Cell* **9**, 659-671.
- Ossareh-Nazari, B., Maison, C., Black, B.E., Levesque, L., Paschal, B.M. and Dargemont, C. (2000) RanGTP-binding protein NXT1 facilitates nuclear export of different classes of RNA *in vitro*. *Mol Cell Biol* **20**, 4562-4571.
- Pasquinelli, A.E., Ernst, R.K., Lund, E., Grimm, C., Zapp, M.L., Rekosh, D., Hammarskjold, M.L. and Dahlberg, J.E. (1997) The constitutive transport element (CTE) of Mason-Pfizer monkey virus (MPMV) accesses a cellular mRNA export pathway. *EMBO J* **16**, 7500-7510.
- Petersen, N.S. and Nierlich, D.P. (1978) Yeast mutant, rna 1, affects the entry into polysomes of ribosomal RNA as well as messenger RNA. *Mol Gen Genet* **162**, 319-322.
- Pinol-Roma, S. and Dreyfuss, G. (1992) Shuttling of pre-mRNA binding proteins between nucleus and cytoplasm. *Nature* **355**, 730-732.
- Pokrywka, N.J. and Goldfarb, D.S. (1995) Nuclear export pathways of tRNA and 40 S ribosomes include both common and specific intermediates. *J Biol Chem* **270**, 3619-3624.
- Portman, D.S., O'Connor, J.P. and Dreyfuss, G. (1997) YRA1, an essential *Saccharomyces cerevisiae* gene, encodes a novel nuclear protein with RNA annealing activity. *RNA* **3**, 527-537.
- Pritchard, C.E., Fornerod, M., Kasper, L.H. and van Deursen, J.M. (1999) RAE1 is a shuttling mRNA export factor that binds to a GLEBS-like NUP98 motif at the nuclear pore complex through multiple domains. *J Cell Biol* **145**, 237-254.
- Proudfoot, N.J., Furger, A. and Dye, M.J. (2002) Integrating mRNA processing with transcription. *Cell* **108**, 501-512.
- Ribbeck, K. and Gorlich, D. (2001) Kinetic analysis of translocation through nuclear pore complexes. *EMBO J* **20**, 1320-1330.
- Ribbeck, K., Lipowsky, G., Kent, H.M., Stewart, M. and Gorlich, D. (1998) NTF2 mediates nuclear import of Ran. *EMBO J* **17**, 6587-6598.
- Rodrigues, J.P., Rode, M., Gatfield, D., Blencowe, B., Carmo-Fonseca, M. and Izaurralde, E. (2001) REF proteins mediate the export of spliced and unspliced mRNAs from the nucleus. *Proc Natl Acad Sci U S A* **98**, 1030-1035.
- Rout, M.P. and Aitchison, J.D. (2001) The nuclear pore complex as a transport machine. *J Biol Chem* **276**, 16593-16596.
- Saavedra, C., Felber, B. and Izaurralde, E. (1997a) The simian retrovirus-1 constitutive transport element, unlike the HIV-1 RRE, uses factors required for cellular mRNA export. *Curr Biol* **7**, 619-628.

- Saavedra, C., Tung, K.S., Amberg, D.C., Hopper, A.K. and Cole, C.N. (1996) Regulation of mRNA export in response to stress in *Saccharomyces cerevisiae*. *Genes Dev* **10**, 1608-1620.
- Saavedra, C.A., Hammell, C.M., Heath, C.V. and Cole, C.N. (1997b) Yeast heat shock mRNAs are exported through a distinct pathway defined by Rip1p. *Genes Dev* **11**, 2845-2856.
- Sadis, S., Hickey, E. and Weber, L.A. (1988) Effect of heat shock on RNA metabolism in HeLa cells. *J Cell Physiol* **135**, 377-386.
- Santos-Rosa, H., Moreno, H., Simos, G., Segref, A., Fahrenkrog, B., Pante, N. and Hurt, E. (1998) Nuclear mRNA export requires complex formation between Mex67p and Mtr2p at the nuclear pores. *Mol Cell Biol* **18**, 6826-6838.
- Sarkar, S., Azad, A.K. and Hopper, A.K. (1999) Nuclear tRNA aminoacylation and its role in nuclear export of endogenous tRNAs in *Saccharomyces cerevisiae*. *Proc Natl Acad Sci U S A* **96**, 14366-14371.
- Schlenstedt, G., Saavedra, C., Loeb, J.D., Cole, C.N. and Silver, P.A. (1995a) The GTP-bound form of the yeast Ran/TC4 homologue blocks nuclear protein import and appearance of poly(A)⁺ RNA in the cytoplasm. *Proc Natl Acad Sci U S A* **92**, 225-229.
- Schlenstedt, G., Wong, D.H., Koepp, D.M. and Silver, P.A. (1995b) Mutants in a yeast Ran binding protein are defective in nuclear transport. *EMBO J* **14**, 5367-5378.
- Schmitt, C., von Kobbe, C., Bachi, A., Pante, N., Rodrigues, J.P., Boscheron, C., Rigaut, G., Wilm, M., Seraphin, B., Carmo-Fonseca, M. and Izaurralde, E. (1999) Dbp5, a DEAD-box protein required for mRNA export, is recruited to the cytoplasmic fibrils of nuclear pore complex *via* a conserved interaction with CAN/Nup159p. *EMBO J* **18**, 4332-4347.
- Seedorf, M. and Silver, P.A. (1997) Importin/karyopherin protein family members required for mRNA export from the nucleus. *Proc Natl Acad Sci U S A* **94**, 8590-8595.
- Segal, S.P., Graves, L.E., Verheyden, J. and Goodwin, E.B. (2001) RNA-Regulated TRA-1 nuclear export controls sexual fate. *Dev Cell* **1**, 539-551.
- Segref, A., Sharma, K., Doye, V., Hellwig, A., Huber, J., Luhrmann, R. and Hurt, E. (1997) Mex67p, a novel factor for nuclear mRNA export, binds to both poly(A)⁺ RNA and nuclear pores. *EMBO J* **16**, 3256-3271.
- Shamsher, M.K., Ploski, J. and Radu, A. (2002) Karyopherin beta 2B participates in mRNA export from the nucleus. *Proc Natl Acad Sci U S A* **99**, 14195-14199.
- Simos, G., Grosshans, H. and Hurt, E. (2002) Nuclear export of tRNA. *Results Probl Cell Differ* **35**, 115-131.
- Snay-Hodge, C.A., Colot, H.V., Goldstein, A.L. and Cole, C.N. (1998) Dbp5p/Rat8p is a yeast nuclear pore-associated DEAD-box protein essential for RNA export. *EMBO J* **17**, 2663-2676.
- Stade, K., Ford, C.S., Guthrie, C. and Weis, K. (1997) Exportin 1 (Crm1p) is an essential nuclear export factor. *Cell* **90**, 1041-1050.
- Stage-Zimmermann, T., Schmidt, U. and Silver, P.A. (2000) Factors affecting nuclear export of the 60S ribosomal subunit *in vivo*. *Mol Biol Cell* **11**, 3777-3789.
- Stewart, M., Kent, H.M. and McCoy, A.J. (1998) Structural basis for molecular recognition between nuclear transport factor 2 (NTF2) and the GDP-bound form of the Ras-family GTPase Ran. *J Mol Biol* **277**, 635-646.
- Strahm, Y., Fahrenkrog, B., Zenklusen, D., Rychner, E., Kantor, J., Rosbach, M. and Stutz, F. (1999) The RNA export factor Gle1p is located on the cytoplasmic fibrils of the NPC and physically interacts with the FG-nucleoporin Rip1p, the DEAD-box protein Rat8p/Dbp5p and a new protein Ymr 255p. *EMBO J* **18**, 5761-5777.
- Strasser, K., Bassler, J. and Hurt, E. (2000) Binding of the Mex67p/Mtr2p heterodimer to FXFG, GLFG, and FG repeat nucleoporins is essential for nuclear mRNA export. *J Cell Biol* **150**, 695-706.
- Strasser, K. and Hurt, E. (2000) Yra1p, a conserved nuclear RNA-binding protein, interacts directly with Mex67p and is required for mRNA export. *EMBO J* **19**, 410-420.
- Strasser, K. and Hurt, E. (2001) Splicing factor Sub2p is required for nuclear mRNA export through its interaction with Yra1p. *Nature* **413**, 648-652.

- Strasser, K., Masuda, S., Mason, P., Pfannstiel, J., Oppizzi, M., Rodriguez-Navarro, S., Rondon, A.G., Aguilera, A., Struhl, K., Reed, R. and Hurt, E. (2002) TREX is a conserved complex coupling transcription with messenger RNA export. *Nature* **417**, 304-308.
- Strawn, L.A., Shen, T. and Wente, S.R. (2001) The GLFG regions of Nup116p and Nup100p serve as binding sites for both Kap95p and Mex67p at the nuclear pore complex. *J Biol Chem* **276**, 6445-6452.
- Stutz, F., Bachi, A., Doerks, T., Braun, I.C., Seraphin, B., Wilm, M., Bork, P. and Izaurralde, E. (2000) REF, an evolutionary conserved family of hnRNP-like proteins, interacts with TAP/Mex67p and participates in mRNA nuclear export. *RNA* **6**, 638-650.
- Stutz, F., Kantor, J., Zhang, D., McCarthy, T., Neville, M. and Rosbash, M. (1997) The yeast nucleoporin rip1p contributes to multiple export pathways with no essential role for its FG-repeat region. *Genes Dev* **11**, 2857-2868.
- Sun, X., Alzhanova-Ericsson, A.T., Visa, N., Aissouni, Y., Zhao, J. and Daneholt, B. (1998) The hrp23 protein in the balbiani ring pre-mRNP particles is released just before or at the binding of the particles to the nuclear pore complex. *J Cell Biol* **142**, 1181-1193.
- Tan, W., Zolotukhin, A.S., Bear, J., Patenaude, D.J. and Felber, B.K. (2000) The mRNA export in *Caenorhabditis elegans* is mediated by Ce-NXF-1, an ortholog of human TAP/NXF and *Saccharomyces cerevisiae* Mex67p. *RNA* **6**, 1762-1772.
- Truant, R., Kang, Y. and Cullen, B.R. (1999) The human tap nuclear RNA export factor contains a novel transportin- dependent nuclear localization signal that lacks nuclear export signal function. *J Biol Chem* **274**, 32167-32171.
- Tseng, S.S., Weaver, P.L., Liu, Y., Hitomi, M., Tartakoff, A.M. and Chang, T.H. (1998) Dbp5p, a cytosolic RNA helicase, is required for poly(A)⁺ RNA export. *EMBO J* **17**, 2651-2662.
- Vainberg, I.E., Dower, K. and Rosbash, M. (2000) Nuclear export of heat shock and non-heat-shock mRNA occurs via similar pathways. *Mol Cell Biol* **20**, 3996-4005.
- Vasu, S., Shah, S., Orjalo, A., Park, M., Fischer, W.H. and Forbes, D.J. (2001) Novel vertebrate nucleoporins Nup133 and Nup160 play a role in mRNA export. *J Cell Biol* **155**, 339-354.
- Vasu, S.K. and Forbes, D.J. (2001) Nuclear pores and nuclear assembly. *Curr Opin Cell Biol* **13**, 363-375.
- Visa, N., Alzhanova-Ericsson, A.T., Sun, X., Kiseleva, E., Bjorkroth, B., Wurtz, T. and Daneholt, B. (1996) A pre-mRNA-binding protein accompanies the RNA from the gene through the nuclear pores and into polysomes. *Cell* **84**, 253-264.
- Watkins, J.L., Murphy, R., Emtage, J.L. and Wente, S.R. (1998) The human homologue of *Saccharomyces cerevisiae* Gle1p is required for poly(A)⁺ RNA export. *Proc Natl Acad Sci U S A* **95**, 6779-6784.
- Wiegand, H.L., Coburn, G.A., Zeng, Y., Kang, Y., Bogerd, H.P. and Cullen, B.R. (2002) Formation of Tap/NXT1 heterodimers activates Tap-dependent nuclear mRNA export by enhancing recruitment to nuclear pore complexes. *Mol Cell Biol* **22**, 245-256.
- Wilkie, G.S., Zimyanin, V., Kirby, R., Korey, C., Francis-Lang, H., Van Vactor, D. and Davis, I. (2001) Small bristles, the *Drosophila* ortholog of NXF-1, is essential for mRNA export throughout development. *RNA* **7**, 1781-1792.
- Wolff, B., Sanglier, J.J. and Wang, Y. (1997) Leptomycin B is an inhibitor of nuclear export: inhibition of nucleocytoplasmic translocation of the human immunodeficiency virus type 1 (HIV-1) Rev protein and Rev-dependent mRNA. *Chem Biol* **4**, 139-147.
- Wolin, S.L. and Matera, A.G. (1999) The trials and travels of tRNA. *Genes Dev* **13**, 1-10.
- Yang, J., Bogerd, H.P., Wang, P.J., Page, D.C. and Cullen, B.R. (2001) Two closely related human nuclear export factors utilize entirely distinct export pathways. *Mol Cell* **8**, 397-406.
- Yoon, J.H., Love, D.C., Guhathakurta, A., Hanover, J.A. and Dhar, R. (2000) Mex67p of *Schizosaccharomyces pombe* interacts with Rae1p in mediating mRNA export. *Mol Cell Biol* **20**, 8767-8782.
- Zenklusen, D., Vinciguerra, P., Strahm, Y. and Stutz, F. (2001) The yeast hnRNP-Like proteins Yra1p and Yra2p participate in mRNA export through interaction with Mex67p. *Mol Cell Biol* **21**, 4219-4232.

-
- Zenklusen, D., Vinciguerra, P., Wyss, J.C. and Stutz, F. (2002) Stable mRNP formation and export require cotranscriptional recruitment of the mRNA export factors Yra1p and Sub2p by Hpr1p. *Mol Cell Biol* **22**, 8241-8253.
- Zhang, M. and Green, M.R. (2001) Identification and characterization of yUAP/Sub2p, a yeast homolog of the essential human pre-mRNA splicing factor hUAP56. *Genes Dev* **15**, 30-35.
- Zhou, Z., Luo, M.J., Straesser, K., Katahira, J., Hurt, E. and Reed, R. (2000) The protein Aly links pre-messenger-RNA splicing to nuclear export in metazoans. *Nature* **407**, 401-405.
- Zolotukhin, A.S., Tan, W., Bear, J., Smulevitch, S. and Felber, B.K. (2002) U2AF participates in the binding of TAP (NXF1) to mRNA. *J Biol Chem* **277**, 3935-3942.

Abbreviations

| | |
|--------------------------|---|
| ARE | AU-rich element |
| ATP | adenosine triphosphate |
| CAT | chloramphenicol acetyl transferase |
| CBC | cap-binding complex |
| CBP | cap-binding protein |
| Ce | <i>Caenorhabditis elegans</i> |
| CTE | constitutive transport element |
| Da | Dalton |
| Dm | <i>Drosophila melanogaster</i> |
| DNA | deoxyribonucleic acid |
| dsRNA | double-stranded RNA |
| EJC | exon-exon junction complex |
| FG | phenylalanine, glycine |
| FISH | fluorescence <i>in situ</i> hybridization |
| GAP | GTPase activating protein |
| GDP | guanosine diphosphate |
| GEF | guanine nucleotide exchange factor |
| GTP | guanosine triphosphate |
| hnRNP | heterogenous nuclear ribonucleoprotein |
| LMB | leptomycin B |
| LRR | leucine-rich repeat |
| m ⁷ G | monomethylguanosine |
| mRNA | messenger RNA |
| NES | nuclear export signal |
| NLS | nuclear localization signal |
| NPC | nuclear pore complex |
| NTF2 | nuclear transport factor 2 |
| NXF | nuclear export factor (sometimes also: nuclear RNA export factor) |
| PHAX | phosphorylated adapter for RNA export |
| poly(A) ⁺ RNA | polyadenylated RNA |
| RBD | RNA-binding domain |
| REF | RNA and export factor-binding |
| RNA | ribonucleic acid |
| RNAi | double-stranded RNA interference |
| RNP | ribonucleoprotein |

| | |
|--------|---|
| RRE | Rev response element |
| rRNA | ribosomal RNA |
| S | Svedberg unit |
| S2 | <i>Drosophila</i> Schneider cell line 2 |
| siRNA | small interfering RNA |
| snoRNA | small nucleolar RNA |
| snRNA | small nuclear RNA |
| SRV-1 | simian retrovirus-1 |
| TAP | Tip associated protein |
| tRNA | transfer RNA |
| UBA | ubiquitin-associated |

Gene names

The rules how to indicate genes and gene products are different for each organism. To avoid using many different styles, I have applied the following simplified rules in this thesis:

All organisms except for yeast:

genes and mRNAs: italicized, all lower case letters (e.g. *nxf*)

proteins: not italicized, first letter capital (e.g. NXF1, Crm1)

Yeast (standard nomenclature for yeast):

dominant allele (most often wild-type): italicized, all capital letters (e.g. *MEX67*)

recessive allele (mutants): italicized, all lower case letters (e.g. *mex67-5*)

protein: not italicized, only first letter capital, additional p as last letter (e.g. Mex67p)

The paper publications in the Results section of this thesis are excluded from this simplified nomenclature.

Curriculum vitae

Personal Details

Name: Andrea Herold
Date of birth: 10 September 1974
Place of birth: Würzburg, Germany
Marital status: Single
Nationality: German

Education

09/81 - 07/85 Eichendorff-Grundschule (elementary school) in Gerbrunn, Germany
09/85 - 07/94 Matthias-Grünwald-Gymnasium (grammar school) in Würzburg, Germany
1 July 1994 Degree "Allgemeine Hochschulreife"
11/94 - 04/99 Studies in Biology (Diplom) at the Bayerische Julius-Maximilians-Universität Würzburg, Germany
09/96 - 10/96 Intermediate examinations (Diplomvorprüfungen)
08/97 - 05/98 Advanced Studies at Duke University, NC, USA (DAAD program "Integrated Studies Abroad")
Status: non-degree graduate student
11/98 - 12/98 Final examinations (Diplomhauptprüfungen) in Biochemistry (major subject), Zoology (Cell and Developmental Biology) and Genetics
01/99 - 04/99 Diploma thesis: "Characterization of the functional domain organization of the importin α nuclear transport factor" in the laboratory of Prof. Dr Bryan Cullen, Duke University, Department of Genetics, Durham, NC, USA
14 April 1999 University degree "Diplom-Biologin Univ."
since 09/99 Ph.D. thesis: "The role of human and *Drosophila* NXF proteins in nuclear mRNA export" in the laboratory of Dr Elisa Izaurralde (Gene Expression Program, EMBL Heidelberg, Germany) under the supervision of Prof. Dr Ulrich Scheer (Department of Cell and Developmental Biology, University of Würzburg, Germany)

Further Research Experience

06/99 - 08/99 Visiting scientist in the laboratory of Dr Elisa Izaurralde (Department of Molecular Biology, University of Geneva, Switzerland)

Heidelberg, 17 February 2003

Publications¹

1. Herold, A., Truant, R., Wiegand, H., and Cullen, B.R. (1998) Determination of the functional domain organization of the importin alpha nuclear import factor. *J Cell Biol* **143**, 309-318.
2. Truant, R., Fridell, R.A., Benson, E.R., Herold, A., and Cullen, B.R. (1998) Nucleocytoplasmic shuttling by protein nuclear import factors. *Eur J Cell Biol* **77**, 269-275.
3. Bogerd, H.P., Benson, R.E., Truant, R., Herold, A., Phingbodhipakkiya, M., and Cullen, B.R. (1999) Definition of a consensus transportin-specific nucleocytoplasmic transport signal. *J Biol Chem* **274**, 9771-9777.
4. Herold, A., Suyama, M., Rodrigues, J. P., Braun, I.C., Kutay, U., Carmo-Fonseca, M., Bork, P., and Izaurralde, E. (2000) TAP (NXF1) belongs to a multigene family of putative RNA export factors with a conserved modular architecture. *Mol Cell Biol* **20**, 8996-9008.
5. Braun, I.C., Herold, A., Rode, M., Conti, E., and Izaurralde, E. (2001) Overexpression of TAP/p15 heterodimers bypasses nuclear retention and stimulates nuclear mRNA export. *J Biol Chem* **276**, 20536-20543.
6. Jun, L., Frints, S., Duhamel, H., Herold, A., Abad-Rodrigues, J., Dotti, C., Izaurralde, E., Marynen, P., Froyen, G. (2001) NXF5, a novel member of the nuclear RNA export factor family, is lost in a male patient with a syndromic form of mental retardation. *Curr Biol* **11**, 1381-1391.
7. Herold, A., Klymenko, T., and Izaurralde, E. (2001) NXF1/p15 heterodimers are essential for mRNA nuclear export in *Drosophila*. *RNA* **7**, 1768-1780.
8. Braun, I. C., Herold, A., Rode, M., and Izaurralde, E. (2002) Nuclear export of mRNA by TAP/NXF1 requires two nucleoporin binding sites but not p15. *Mol Cell Biol* **22**, 5405-5418.
9. Lange, B.M.H., Rebollo, E., Herold, A., and Gonzalez, C. (2002) Cdc37 is essential for chromosome segregation and cytokinesis in higher eukaryotes. *EMBO J* **21**, 5364-5374.
10. Herold, A., Teixeira L., and Izaurralde, E. (2003) Genome-wide analysis of mRNA nuclear export pathways in *Drosophila*. *Submitted*.

Poster presentations (meetings)

Herold, A., Suyama, M., Bork, P., and Izaurralde, E. (2000) Identification and characterization of human TAP homologues. *Fifth Annual Meeting of the RNA Society (Madison, USA)*.

Herold, A., Klymenko, T., and Izaurralde, E. (2001) NXF1 and p15 mediate the nuclear export of mRNA in *D. melanogaster*. *Sixth Annual Meeting of the RNA Society (Banff, Canada)*.

Herold, A., Klymenko, T., and Izaurralde, E. (2002) NXF1/p15 heterodimers are essential for mRNA nuclear export in *Drosophila*. *Symposium on "Structure of the Nucleus and Trafficking of RNPs in the Cell" (Göttingen, Germany)*.

Oral presentations (meetings)

Herold, A., and Izaurralde, E. (2002) Genome-wide analysis of mRNA nuclear export pathways. *Meeting on "Dynamic Organization of Nuclear Function", Cold Spring Harbor Laboratories (Cold Spring Harbor, NY, USA)*.

¹ The results presented in papers 4-10 were obtained during my time as a graduate student. These papers are part of the Results section of this thesis.

Erklärung

Hiermit erkläre ich ehrenwörtlich, dass ich die vorliegende Arbeit selbständig angefertigt und keine anderen als die angegebenen Quellen und Hilfsmittel benutzt habe.

Diese Dissertation hat weder in gleicher noch in ähnlicher Form in einem anderen Prüfungsverfahren vorgelegen.

Ich habe bisher außer den mit dem Zulassungsgesuch urkundlich vorgelegten Graden keine weiteren akademischen Grade erworben oder zu erwerben versucht.

Heidelberg, den 17.02.03